Complexity and Entanglement for Pure and Mixed States in Quantum Field Theories

Dissertation

zur Erlangung des Grades eines

Doktors der Naturwissenschaften

am

Fachbereich Physik

der

Freien Universität Berlin

vorgelegt von

Hugo Antonio Camargo Montero

Berlin, August 2021

Betreuer	Dr. Michal P. Heller
Hochschullehrer am Fachbereich	Prof. Felix von Oppen, PhD
Zweitgutachter	Prof. Dr. Jens Eisert
Datum der Disputation	6. Dezember 2021

Selbstständigkeitserklärung

Name: Camargo Montero
Vorname: Hugo Antonio

Ich erkläre gegenüber der Freien Universität Berlin, dass ich die vorliegende Dissertation selbstständig und ohne Benutzung anderer als der angegebenen Quellen und Hilfsmittel angefertigt habe. Die vorliegende Arbeit ist frei von Plagiaten. Alle Ausführungen, die wörtlich oder inhaltlich aus anderen Schriften entnommen sind, habe ich als solche kenntlich gemacht. Diese Dissertation wurde in gleicher oder ähnlicher Form noch in keinem früheren Promotionsverfahren eingereicht.

Mit einer Prüfung meiner Arbeit durch ein Plagiatsprüfungsprogramm erkläre ich mich einverstanden.

Datum: 18.08.21 Unterschrift: _____

Abstract

Over the past two decades, ideas coming from quantum information science have substantially influenced the research carried out in the field of high-energy physics. This is particularly evident in the AdS/CFT correspondence, a framework which postulates a duality between certain gravitational theories on negatively-curved anti-de Sitter (AdS) spacetimes and conformal field theories (CFTs).

In this thesis we take a close look at quantities associated with two quantum information theoretic notions which have led to novel insights into quantum gravity within the AdS/CFT correspondence: entanglement and complexity. Entanglement entropy (EE) is a well studied quantity that quantifies the pure state entanglement between a subregion and its complement, whose study has lead to outstanding results in the field. Complexity, on the other hand, appeared recently in the context of quantum field theories (QFTs) motivated by the aim of understanding the interior of black holes in the AdS/CFT and whose study in QFTs represents a very promising research direction.

Particularly compelling open problems in our understanding of these quantities include the time-dependence of complexity and the interplay between complexity and entanglement both in non-equilibrium systems and for subregions in QFTs corresponding to mixed states. In this work we explore these problems in scenarios which allow us to make tractable computations and extract their universal properties.

Within the former context, the study of quantum quenches is one of the most active areas of research into non-equilibrium quantum dynamics. In this regard, we explore the pure state complexity of exact time-dependent solutions for free scalar theories undergoing a quench through a critical point, finding evidence for universal scaling behaviour dominated by the zero mode.

An intimately connected problem is the study of quantum information-theoretic properties of mixed states in QFTs. In this context, we study complexity of purification (CoP), entanglement of purification (EoP) and reflected entropy (RE). For set-ups in free QFTs on a lattice which lead to Gaussian mixed states, we consider the most general Gaussian purifications and find universal properties using the mathematical machinery of covariance matrices. In settings which lead to genuinely non-Gaussian settings, we find a general proof valid for a CFT in any dimension with a gap in the operator spectrum, that EoP and RE exhibit an enhancement with respect to the known power-law decay of mutual information measuring the correlations of a mixed state consisting of two subregions which are largely separated. These result open a new avenue of research to study the properties of these quantities from the perspective of CFT data.

Collectively, these findings set the stage to a better understanding of complexity and entanglement in QFTs by providing insights into their universal properties. This is paramount to elucidating the mechanism which connects gravity and quantum theories within the AdS/CFT correspondence. Consequently, we believe that these can lead to a better understanding of quantum gravity and quite possibly to new tools in the study of quantum many-body systems.

Zusammenfassung

Ideen aus der Quanteninformation haben die Forschung auf dem Gebiet der Hochenergiephysik in den letzten zwei Jahrzehnten wesentlich beeinflusst. Dies zeigt sich insbesondere in der AdS/CFT-Korrespondenz, einer vorgeschlagenen Dualität zwischen bestimmten Gravitationstheorien auf negativ gekrümmten Anti-De-Sitter (AdS)-Raumzeiten und konformen Feldtheorien (CFTs).

In dieser Arbeit studieren wir detailliert zwei Konzepte der Quanteninformation, welche zu neuen Einsichten in die Quantengravitation innerhalb der AdS/CFT-Korrespondenz geführt haben: Verschränkung und Komplexität. Die Verschränkungsentropie als eine bereits vielfach untersuchte physikalische Größe quantifiziert die Verschränkung reiner Zustände zwischen einem Teilgebiet und seinem Komplement. Ihre Untersuchung hat zu herausragenden Ergebnissen auf diesem Gebiet geführt. Andererseits tauchte Komplexität erst kürzlich im Kontext von Quantenfeldtheorien (QFTs) auf, motiviert durch das Ziel, das Innere von Schwarzen Löchern mittels der AdS/CFT-Korrespondenz zu verstehen. Die damit einhergehenden Untersuchungen entwickeln sich zu einer sehr vielversprechenden neuen Forschungsrichtung.

Die Zeitabhängigkeit der Komplexität und das Zusammenspiel zwischen Komplexität und Verschränkung sowohl in Nicht-Gleichgewichtssystemen als auch in gemischten Zuständen in QFTs sind offene Probleme in unserem Verständnis dieser Größen. In dieser Arbeit erforschen wir diese Fragestellungen in Szenarien, die es uns erlauben, nachvollziehbare Berechnungen durchzuführen, um deren universelle Eigenschaften zu extrahieren.

Im ersteren Kontext ist das Studium von sogenannten *Quantenquenchen* eines der aktivsten Forschungsgebiete der Nicht-Gleichgewichts-Quantendynamik. Hier untersuchen wir die reine Zustandskomplexität von exakten zeitabhängigen Lösungen für freie Skalartheorien, die einen Quench durch einen kritischen Punkt durchlaufen. Wir finden Beweise für ein universelles Skalierungsverhalten, das durch den Nullmodus dominiert wird.

Eine eng damit verbundene Problemstellung ist die Untersuchung der quanteninformationstheoretischen Eigenschaften von Mischzuständen in QFTs. In diesem Zusammenhang untersuchen wir die sogenannte *Komplexität der Reinigung* (CoP), die *Verschränkung der Reinigung* (EoP) und die *reflektierte Entropie* (RE). Wir betrachten die allgemeinsten Gaußschen Reinigungen für freie QFTs auf einem Gitter, die zu Gaußschen Mischzuständen führen, und finden universelle Eigenschaften unter Verwendung mathematischer Methoden basierend auf Kovarianzmatrizen. Für echte nicht-Gaußsche Szenarien beweisen wir, dass EoP und RE eine Verstärkung gegenüber dem bekannten Potenzgesetz-Abfall der sogenannten *gegenseitigen Information* aufweisen, welche die Korrelationen gemischter Zustände misst, die aus zwei weit voneinander entfernten Teilbereichen bestehen. Dieses Ergebnis gilt für eine CFT in beliebiger Dimension mit einer Lücke im Operatorspektrum und eröffnet einen neuen Forschungszweig, um die Eigenschaften dieser Größen aus der Perspektive von CFT-Daten zu untersuchen.

Zusammengenommen stellen diese Ergebnisse die Weichen für ein besseres Verständnis von Komplexität und Verschränkung in QFTs, indem sie Einblicke in deren universelle Eigenschaften geben. Dies ist von entscheidender Bedeutung, um Aufschluss darüber zu erlangen, welche Mechanismen Gravitations- und Quantentheorien innerhalb der AdS/CFT-Korrespondenz miteinander verbinden. Folglich glauben wir, dass diese zu einem besseren Verständnis der Quantengravitation und möglicherweise zu neuen methodischen Werkzeugen bei der Untersuchung von Quanten-Vielkörpersystemen führen können.

List of Contributions

This dissertation is based on the journal publications and preprint listed below. Chapter 4 is based on [**CamH03**]. Chapter 5 is based on [**CamH02**] and [**CamH03**]. Chapter 6 is based on [**CamH02**] and [**CamH01**].

[**CamH01**] H. A. Camargo, L. Hackl, M. P. Heller, A. Jahn and B. Windt, "Long-distance entanglement of purification and reflected entropy in conformal field theory", arXiv:2102.00013 [hep-th] , *Phys. Rev. Lett.*, vol. 127, p. 141604, 2021, **DOI:** https://doi.org/10.1103/PhysRevLett.127.141604 . **Note:** The preprint (arXiv) version of this publication, as published on arXiv, was reviewed and approved by the Doctoral Thesis Committee.

My main contributions in this work involved performing numerical computations for entanglement of purification and reflected entropy as well as writing sections of the manuscript, producing figures and managing the journal submission.

[**CamH02**] H. A. Camargo, L. Hackl, M. P. Heller, A. Jahn, T. Takayanagi and B. Windt, "Entanglement and Complexity of Purification in (1+1)-dimensional free Conformal Field Theories", *Phys. Rev. Res.*, vol. 3, p. 013248, 2019, **DOI:** https://doi.org/10.1103/PhysRevResearch.3.013248 .

My main contributions in this work involved the initial formulation and early development of the numerical algorithm used throughout this work and its implementation in the study of complexity of purification as well as writing sections of the manuscript, producing figures and managing the journal submission.

[**CamH03**] H. A. Camargo, P. Caputa, D. Das, M. P. Heller and R. Jefferson, "Complexity as a novel probe of quantum quenches: universal scalings and purifications", *Phys. Rev. Lett.* vol **122**, no. 8, p. 081601, 2019, **DOI:** https://doi.org/10.1103/PhysRevLett.122.081601 .

My main contributions in this work involved performing analytical and numerical computations particularly in the context of complexity of purification as well as writing the section of the appendix where details of this quantity are provided.

The following publications, not included in this thesis, were also produced during the course of doctoral research.

- H. A. Camargo, P. Caputa and P. Nandy, "Q-curvature and Path Integral Complexity", (2022), arXiv:2201.00562 [hep-th] .
- H. A. Camargo, M. P. Heller, R. Jefferson and J. Knaute, "Path integral optimization as circuit complexity," *Phys. Rev. Lett.*, vol. **123**, no. 1, p. 011601, 2019, **DOI:** https://doi.org/10.1103/PhysRevLett.123.011601 .

Acknowledgments

I would like to begin by expressing my gratitude to my supervisor Michal P. Heller. I want to thank him for his patience, tireless support and scientific advice throughout these past four years. His commitment to hard work and passion for science are lessons that I will carry with me to the future. I am privileged to have been able to grow as scientist under his supervision.

I would also like to thank my fellow GQFI-ers, past and present, for many interesting physics discussions, conversations, collaborations and advice. Thank you Nishan C J, Diptarka Das, Ro Jefferson, Eivind Jørstad, Johannes Knaute, Fernando Pastawski, Ignacio Reyes, Leo Shaposhnik, Sukhi Singh and Viktor Svensson. I am also grateful to Jens Eisert for welcoming me into his group at FU and for our brief yet stimulating physics discussions.

My special gratitude also to my amazing collaborators throughout these years; Pawel Caputa, Lucas Hackl, Alexander Jahn, Pratik Nandy, Tadashi Takayanagi and Bennet Windt. I am thankful for the privilege of working with you and for all the inspiring discussions about physics that we had during the course of our collaborations.

I am indebted to the Konrad-Adenauer-Stiftung for giving me the opportunity to study in Germany. I would like to express my special gratitude to Simon Backovsky, Diego Cuadra, Maike Ender, Berthold Gees, Stefan Jost, Kerim Kudo and Andrea Stüdemann for their support and for allowing me to participate in many fascinating seminars about Germany's history, society and complex political reality.

I am also grateful to all the marvelous people that I met at the Max Planck Institute for Gravitational Physics (the Albert Einstein Institute). I would like to thank my friends at the AEI for all the great times throughout these years. Andrea Antonelli, Ana Alonso, Teresa Bautista, Enrico Brehm, Matteo Broccoli, Lorenzo Casarin, Franz Ciceri, Roberto Cotesta, Alice Di Tucci, Shane Farnsworth, Marco Finocchiaro, Jan Gerken, Serena Giardino, Hadi Godazgar, Alex Goeßmann, Caroline Jonas, Isha Kotecha, Lars Kreutzer, Hannes Malcha, Matin Mojaza, Alejandro Peñuela, Tung Tran, and Adriano Viganò. My special gratitude to Matthias Blittersdorf, Axel Kleinschmidt, Darya Niakhaichyk, Hermann Nicolai, Anika Rast and the IT Department for all their kind help.

Being far away from home can be a challenging experience. I am grateful for my family and friends back home for their support throughout these past four years and specially in recent times. I am especially thankful to my endless source of love, my mom. I would not have reached this point without her continuous encouragement. Finally, I am deeply grateful to Penelope for teaching me to smile again.

Contents

List of Figures

List of Tables

1. Introduction

In the past ten years we have witnessed three historical events that stand out as landmarks in humanity's scientific enterprise. In 2012 the ATLAS and CMS experiments at the Large Hadron Collider (LHC) found experimental evidence for the existence of the Higgs boson [1, 2]; a key ingredient of the Standard Model of particle physics predicted over fifty years ago by Engler, Brout and Higgs [3, 4]. A few years later, the Laser Interferometer Gravitational-Wave Observatory (LIGO) detected gravitational waves [5, 6]; originally predicted by Einstein himself over a hundred years ago [7] and produced by the coalescence of compact binary objects such as black holes. More recently, in 2019, the Event Horizon Telescope (EHT) collaboration obtained the first images of a black hole at the center of the Galaxy Messier 87 (M87) [8], cementing our view that black holes are astrophysical objects that not only exist as mathematical constructions and opening new avenues for studying their astrophysical properties.

These unprecedented achievements are based on our two most successful physical theories to date: the Standard Model of particle physics, and Einstein's general theory of relativity (GR). The former is based on quantum field theory (QFT) and is the framework with which we describe three of the fundamental interactions in nature [9, 10]. The latter, on the other hand, is a geometric theory of the fundamental interaction between space, time and matter which has allowed us to tackle questions about gravity and the large-scale structure of the Universe [11–13].

Together, these theories make up the foundation of our most basic understanding of nature. As a consequence, there exists a long-standing hope that these two distinct approaches can be reconciled within a single framework. However, attempts to carry out this task have so far been either unsuccessful, or beyond our abilities to test them. Indeed, in certain cases these two theories even provide different and irreconcilable predictions for the same phenomena and this fact is nowhere more evident than in the study of black holes.

Classically, black holes are perfect traps in time and space from which nothing can escape. As astrophysical objects they represent the last stage of stellar evolution and can even be found at galactic nuclei. From a mathematical perspective, these fascinating objects were found to have mechanical properties which are analogous to the laws of thermodynamics [14, 15]. Completing the thermodynamical picture of black holes was Hawking's realisation that by taking into account quantum effects near the event horizon of a black hole, it could be shown that these objects in fact produce radiation in a black-body-like fashion at a given temperature [16, 17], leading to their eventual and complete evaporation as they radiate their energy away.

This inevitable evaporation of a black hole raises a profound question about the fate of the information contained in it once it completely evaporates. After all, a basic

principle of quantum mechanics is that the unitary evolution of a pure quantum state into another one preserves the information contained therein. To put differently, a pure state cannot evolve in time via a unitary operation into a mixed one, thereby losing information. As a consequence, an evident contradiction arises when attempting to reconcile a black hole's inevitable evaporation and the preservation of any in-falling information in the form of the unitary evolution of a quantum state.

This so-called black hole *information paradox*, whose detailed explanation is beyond the scope of this work, has stood as one of theoretical physics' most puzzling open questions for almost fifty years. Quite remarkably however, recent developments involving novel semi-classical computations [18, 19] have been used to reproduce the Page curve [20, 21], a necessary feature of unitary black hole evaporation, leading to a new phase in our understanding of the information paradox. See [22] for a review of such developments. Nevertheless, work remains to be done in order to claim its complete resolution. One can even argue that this would either require a more precise understanding of the quantum properties of gravity beyond semi-classical approaches [23, 24] or provide it.

At the same time, the black hole interior presents another outstanding puzzle. In our classical understanding of black holes, nothing which travels through a black hole horizon can ever get out. As a consequence, it is not possible to know whether any unfortunate astronauts who attempt to take a closer look at a black hole will smoothly traverse the horizon and continue to their inexorable death at a singularity, if they will instead violently combust at a firewall [25], or something completely different all together.

Fortunately, over the past twenty years it has become increasingly clear that a very fruitful tool to tackle these and other pressing issues in our understanding of gravity and its relation to the other fundamental interactions is to bring in quantum information science [26–28] into the equation.

Indeed a framework which has become the main stage for the convergence of ideas coming from different areas of physics is the anti-de Sitter/conformal field theory (AdS/CFT) correspondence [29–31]; a conjectured *duality* between certain quantum gravity and quantum field theories. Though arising from within the realm of string theory [32–37], over the past twenty years the correspondence has become a bridge between several disciplines ranging from condensed matter, to high-energy physics and quantum information.

In particular, by looking at gravity through the lens of quantum information via the AdS/CFT correspondence, we are uncovering deep connections between spacetime, entanglement, tensor networks and quantum error correcting codes. The powerful dual description of physical quantities enabled by the correspondence linking gravity and physics in negatively-curved spaces to quantum theory on a flat geometry is arguably the reason why it is one of the most active areas of research in theoretical physics, allowing us to tackle some of quantum gravity's most challenging and pressing issues while at the same time providing useful tools for understanding quantum systems in regimes where it would otherwise be an insurmountable task.

In this thesis we take a close look at quantities associated with two quantum information theoretic notions which have led to novel insights into quantum gravity within the AdS/CFT correspondence: entanglement and complexity. Entanglement entropy (EE) is a well studied quantity that quantifies the pure state entanglement between a subregion and its complement, whose study has lead to outstanding results in the field. Complexity, on the other hand, appeared recently in the context of quantum field theories (QFTs) motivated by the aim of understanding the interior of black holes in the AdS/CFT and whose study in QFTs represents a very promising research direction.

Within the AdS/CFT correspondence, entanglement entropy (EE) and complexity acquire a geometric realization in terms of properties of certain hypersurfaces characterized by their codimension. This term refers to the complementary dimension of geometric objects and can be understood as follows: a hypersurface corresponding to a time-slice of a $(D+1)$-dimensional spacetime is be a codimension-1 object, while a region such as the causal development of said time-slice $D(\Sigma_t)$ is a codimension-0 object, regardless of the dimension $(D+1)$ of the spacetime which contains them.

To be precise, holographic entanglement entropy (EE) acquires a natural geometric description as a generalization of the Bekenstein–Hawking entropy obtained from the area of codimension-2 surfaces in AdS and its connection to EE in CFTs has already been established for several years. Complexity, on the other hand, appears as a conjectured realization of the observation that codimension-1 maximal volumes and codimension-0 causal developments which penetrate the event horizon of AdS black holes have properties expected from the "difficulty" of preparing states in random quantum many-body systems.

Indeed a vast effort in the field has been devoted to understanding the properties of the holographic realization of complexity and to uncovering its field-theoretic properties. The main reason being that understanding complexity within QFTs presents computational challenges surmounted by remaining within the field of free theories or by exploiting the symmetries of CFTs, making a connection with its holographic counterpart(s) beyond our reach for the moment.

At the same time, the quantum information-theoretic properties of mixed states corresponding to spatial subregions in AdS are much less understood than their enlarged, pure-state counterparts. In particular, both the geometric and field-theoretic properties of correlations between components of subregions and the complexity of mixed states have not been completely understood despite their key roles within the AdS/CFT correspondence.

As a consequence, it is an essential task to improve our understanding of these quantities both from the perspective of the AdS/CFT correspondence and of QFTs. Particularly compelling open problems in this direction include the time-dependence of complexity and the interplay between complexity and entanglement both in non-equilibrium systems and for subregions in QFTs corresponding to mixed states. In this work we explore these problems in scenarios which allow us to make tractable computations and extract their universal properties in QFTs.

Within the former context, the study of quantum quenches is one of the most act-

ive areas of research into non-equilibrium quantum dynamics. In this regard, we will explore the pure state complexity of exact time-dependent solutions for free scalar theories undergoing a quench through a critical point, with the goal of finding evidence for universal scalings. It has been proven, in fact, that EE exhibits universal behaviour and it will be therefore interesting to contrast these findings with complexity.

In the context of quantum information-theoretic properties of mixed states, our objective will be to study mixed-state generalizations of pure state complexity and EE, as well as another interesting correlation measure in mixed states called reflected entropy (RE). Our aim is to find properties of these quantities which are universal in CFTs and a natural stage for this exercise will be provided by lattice realizations of said theories.

Collectively, our goal is to set the stage to a better understanding of complexity and entanglement in QFTs by providing insights into their universal properties. This is paramount to elucidating the mechanism which connects gravity and quantum theories within the AdS/CFT correspondence. As argued above, this would lead to a better understanding of quantum gravity and quite possibly to new tools in the study of quantum many-body systems.

1.1. The Holographic Principle and the AdS/CFT Correspondence

The *Anti-de Sitter/Conformal Field Theory* (AdS/CFT) correspondence [38] is a powerful framework which posits an equivalence between two distinct physical theories; one which describes gravitational phenomena on an asymptotically anti-de Sitter spacetime in $D+1$ dimensions and another one which describes quantum many-body phenomena at the D-dimensional conformal boundary of said negatively-curved spacetime.

It is also a realization of the *holographic principle* [39–41]: a proposed tenet of quantum gravity which roughly states that the physical information contained in a spacetime volume $\mathscr{V}_{D+1}$ can be thought of as encoded in its boundary $(\partial\mathscr{V})_D$. The name of the principle alludes to an analogy with optical holograms: the gravitational theory is the extra-dimensional image which emerges from the quantum theory living on its lower-dimensional boundary. Originally discussed by 't Hooft in the context of black holes, this observation was elevated to the status of principle through an analysis of entropy bounds for matter in gravitational systems.

The origin of the holographic principle dates back to the studies of black hole thermodynamics and in particular to the statement that the entropy of a black hole is proportional to the area of its event horizon $\mathscr{H}$ via the Bekenstein–Hawking entropy formula

$$S_{\mathrm{BH}} = \frac{\mathrm{Area}(\mathscr{H})}{4G_N} \,, \tag{1.1}$$

where G_N is Newton's constant [42]. This property of black holes is in contrast with other thermodynamical systems whose entropy scales with the volume enclosing the system rather than its area. Since one typically associates the number of degrees of

freedom, or microstates, with the exponential of the entropy $N \sim e^{S_{\rm BH}}$, this suggests that the microstates describing a black hole with temperature $T_{\rm BH}$ given by

$$T_{\rm BH} = \frac{\kappa}{2\pi} \ , \tag{1.2}$$

where κ is the event horizon's surface gravity, are *holographically encoded* in its event horizon $\mathscr{H}$. For example, for a Schwarzschild black hole of mass M the surface gravity κ and area of the event horizon $\mathscr{H}$ are given respectively by $\kappa = 1/4G_N M$ and $\text{Area}(\mathscr{H}) = 16\,\pi\, G_N^2 M^2$ leading to a temperature and entropy given by $T_{\rm BH} = 1/(8\pi G_N M)$ and $S_{\rm BH} = 4\,\pi\, G_N M^2$.

Following the generalized second law of black hole thermodynamics [43], Bekenstein argued that the entropy of in-falling matter into a black hole via a "Geroch process", a thought experiment proposed by Robert Geroch during a 1970 Princeton colloquium in which a small thermodynamic system is moved from infinity into a black hole, must be bounded from above by

$$S_{\rm Matter} \leq 2\pi E R \ , \tag{1.3}$$

where E is the energy of the in-falling matter contained in a sphere of radius R [44]. This entropy bound was proven for quantum field theories in [45] based on the positivity of relative entropy. Considering a matter system which instead of falling into a black hole collapses to form one, Susskind further argued [40] that the entropy of such a system is bounded by the area of the smallest sphere $\mathbb{S}$ that can contain it

$$S_{\rm Matter} \leq \frac{\text{Area}(\mathbb{S})}{4G_N} \ . \tag{1.4}$$

A drawback of Susskind's spherical entropy bound (1.4) is that it is not generally valid in cosmological spacetimes. However, in 1999 Bousso [46] proposed a covariant generalization of it, formalized in terms of the area of the *light-sheet* $L(B)$ of a surface B

$$S(L(B)) \leq \frac{\text{Area}(B)}{4G_N} \ , \tag{1.5}$$

which was found to be valid for all physically reasonable systems, including cosmological spacetimes. A light-sheet $L(B)$ of a surface B is in general a null hypersurface generated by null rays emanating orthogonally from B and which do not expand with respect to B. That is, their cross-section decreases moving outward from B, as can be seen in Fig.1.1.

The entropy bound (1.5) naturally leads to a covariant version of the holographic principle which states that a consistent quantum theory of gravity and matter must be such that the number of degrees of freedom necessary to describe the physics on a light sheet $L(B)$ must not exceed $\text{Area}(B)/4G_N$. This can be heuristically interpreted as stating that the number of degrees of freedom in a given region of spacetime $\mathscr{V}_{D+1}$ cannot exceed $\text{Area}(\partial\mathscr{V}_D)/4G_N$. Systems contained in $\mathscr{V}_{D+1}$ which saturate the bound (1.5) can hence be thought of as having all their information holographically encoded in $\partial\mathscr{V}_D$; one degree of freedom per Planck area.

While conceptually profound, the limitation of the holographic principle is that it does not specify which theory of quantum gravity is behind the holographic mapping between the systems living in the different dimensions, or even in what way is

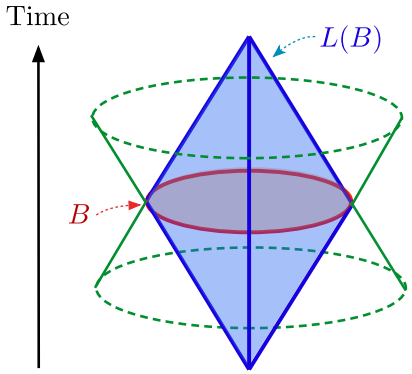

Figure 1.1.: Diagram of the light-sheet $L(B)$ constructed from the non-expanding light rays emanating from a closed surface B. In this picture, the spherical surface B has four null hypersurfaces which are orthogonal to it. From these only two have a negative expansion and correspond to the future and past cones of the light-sheet $L(B)$.

it implemented. This is why the AdS/CFT correspondence was not only rapidly embraced by the community, but it was also met with an incredible amount of research activity: it provides a specific holographic mapping between two theories.

The most prominent example of the AdS/CFT correspondence is the dynamical equivalence between $\mathcal{N} = 4$ Super Yang–Mills (SYM) theory in $(3+1)$-dimensional Minkoswki spacetime $\mathbb{R}^{3,1}$ and type IIB superstring theory on $\mathrm{AdS}_5 \times S^5$. This is in fact the original form of the conjecture and is sometimes also referred to as Maldacena's $\mathrm{AdS}_5/\mathrm{CFT}_4$ correspondence.

$\mathcal{N} = 4$ SYM is a non-Abelian gauge theory with gauge group $\mathrm{SU}(N)$ and Yang–Mills coupling constant g_{YM}. It is also a maximally supersymmetric theory that is also invariant under transformations of the conformal group $\mathrm{SO}(4,2)$ and it is hence a conformal field theory (CFT). It corresponds to the "CFT" side of the correspondence.

Type IIB superstring theory, on the other hand, is a proposed quantum theory of gravity characterized by two parameters; the string length $l_s = \sqrt{\alpha'}$ and the string coupling g_s. It is defined on the product spacetime $\mathrm{AdS}_5 \times S^5$, which involves anti-de Sitter space of radius of curvature L and N units of Ramond-Ramond flux through the five-sphere S^5. The dimensionless ratio $L/\sqrt{\alpha'}$ and the coupling g_s are the independent parameters of the theory, which corresponds to the "AdS" side of the correspondence.

The free parameters on both sides of the correspondence are identified in the following way

$$g^2_{\mathrm{YM}} = 2\pi g_s \ , \ 2g^2_{\mathrm{YM}} N = L^4/(\alpha')^2 \ . \tag{1.6}$$

The second identification can be also be written in terms of the *'t Hooft coupling* $\lambda := g^2_{\mathrm{YM}} N$ as

$$\lambda = \frac{1}{2}\left(\frac{L}{l_s}\right)^4 \ . \tag{1.7}$$

The conjectured dynamical equivalence between these two theories implies that they describe the same physics from two different perspectives. The remarkable consequence of this is that we can describe a theory of quantum gravity, type IIB superstring theory, in terms of a gauge theory without any gravitational degrees of freedom, $\mathcal{N} = 4$ SYM, and vice-versa. This interpretation of the correspondence is the reason why it is also sometimes referred to as the *gauge/gravity duality*.

In its strongest form, the $\mathrm{AdS}_5/\mathrm{CFT}_4$ correspondence deals with arbitrary values of the dimension N of the gauge group $\mathrm{SU}(N)$ and the 't Hooft coupling λ, leading to a full quantum description of the superstring theory on the gravitational side. However, since string theory is better understood perturbatively, one can consider the weak string-coupling regime $g_s \ll 1$ while keeping the ratio L/l_s constant. At leading order in g_s, this corresponds to classical string theory. On the CFT side, this leads to the large-N limit $N \to \infty$ for fixed λ; known as the *'t Hooft limit*. This is known as the strong form of Maldacena's $\mathrm{AdS}_5/\mathrm{CFT}_4$ correspondence and is a realization of 't Hooft's observation that a quantum field theory in the large-N limit has a perturbation series similar to that of a string theory in terms of planar diagrams [47].

In the limit where the string length $\alpha' = l_s^2$ is taken to be small compared to the AdS radius L, *i.e.*, $l_s/L \to 0$, this equivalence leads to the strong/weak duality between *strongly-coupled* $\mathcal{N} = 4$ SYM with $\lambda \to \infty$ and type IIB supergravity on *weakly curved* $AdS_5 \times S^5$. Hence in this regime classical gravity on a weakly negatively-curved background is equivalent to a strongly-coupled quantum field theory. This is one of the main reasons why the AdS/CFT correspondence became a very promising approach to study strongly-coupled quantum field theories, an otherwise monumental and in some cases even unfeasible task.

Indeed, one of the first successes of the correspondence was the computation of the ratio between the shear viscosity η and the entropy density s of the deconfined phase of $\mathcal{N} = 4$ SYM [48] as a model for the quark-gluon plasma (QGP) of quantum chromodynamics (QCD). The expression for η/s which was found to be universal in the $\lambda \to \infty$ limit [49], is in remarkable semi-quantative agreement with estimations arising from experimental data obtained at the Relativistic Heavy Ion Collider (RHIC) laboratory in Brookhaven and the Large Hadron Collider (LHC) at CERN, where heavy-ion collisions are performed to study systems such as the QGP.

Nonetheless and as alluded to earlier in this section, the applicability of the AdS/CFT correspondence can be thought of as being broader than this particular example. That is, other $\mathrm{AdS}_{D+1}/\mathrm{CFT}_D$ correspondences can in principle be constructed between different theories for different dimensions D. Indeed, even in Maldacena's original work [38] other examples were proposed.

This observation is also consistent with the symmetries on both sides of the correspondence. AdS_{D+1} is a maximally symmetric $(D+1)$-dimensional spacetime with symmetry group $\mathrm{SO}(D,2)$ which can be embedded in flat $\mathbb{R}^{D,2}$ spacetime as a hyperboloid. The symmetries of AdS_{D+1} precisely match the conformal and spacetime symmetries of CFT_D, also given by the conformal group $\mathrm{SO}(D,2)$. A remarkable example is the case of $\mathrm{AdS}_3/\mathrm{CFT}_2$ where it was found years prior to the original proposal, that the algebra of AdS_3 generators turns into the $\mathrm{SO}(2,2)$ conformal algebra

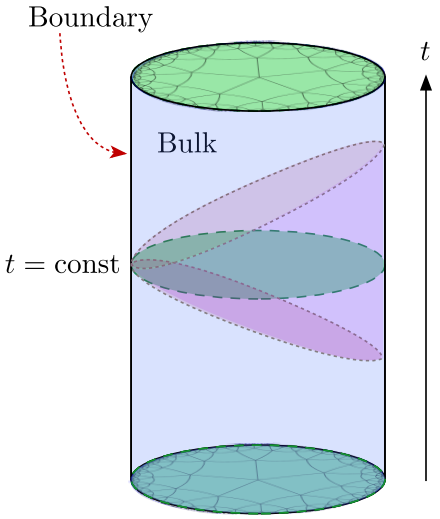

Figure 1.2.: Diagram of the bulk/boundary correspondence in AdS/CFT. The AdS_{D+1} spacetime is represented by the interior (bulk) of the cylinder, with its conformal boundary located represented by the boundary of said cylinder. A time slice t =const of AdS_{D+1} is a negatively-curved hyperbolic space. The pink shaded region corresponds to the Poincaré patch characterized by the metric (1.8).

at the conformal boundary of AdS_3 [50].

Moreover, it can be seen that the supersymmetries of the field theory are related to the compact symmetries of the gravitational theory. In Maldacena's $\text{AdS}_5/\text{CFT}_4$ case, the isometry group of S^5 is SO(6), which coincides with part of the bosonic subgroup of the supergroup of $\mathcal{N} = 4$ SYM given by $\text{SU}(4) \sim \text{SO}(6)$. Together with the spacetime symmetries discussed above, there is a full agreement between the symmetries of both theories. A natural question, however, in this case is whether supersymmetries are a necessary ingredient of the correspondence. Since these can be argued to be related to the compact dimensions in the case of $\text{AdS}_5 \times S^5$, it is perhaps reasonable to suspect the validity of a non-supersymmetric type of duality.

1.1.1. The AdS/CFT Dictionary

The AdS/CFT correspondence is a duality between two theories. As such, it provides a one-to-one mapping between objects such as operators and fields on both sides. This mapping is collectively called the *AdS/CFT dictionary*.

The first entry in the dictionary is the identification of the flat background spacetime $\mathbb{R}^{D-1,1}$ of the CFT_D with the conformal boundary of the AdS_{D+1} spacetime, which is consistent with the analysis of symmetries from the previous section. In this regard, one often refers to the interior of the AdS_{D+1} spacetime as the *bulk* and to the asymptotic $\mathbb{R}^{D-1,1}$ spacetime where the CFT_D "lives", as the *boundary*. This can be seen in Fig. 1.2.

To be precise, consider the Euclidean AdS_{D+1} spacetime whose metric in local *Poincaré coordinates* $\{z, \tau, \vec{x}\}$ is given by

$$\mathrm{d}s^2 = \frac{L^2}{z^2}\left(\mathrm{d}z^2 + \mathrm{d}\tau^2 + \mathrm{d}\vec{x}^2\right) \ , \tag{1.8}$$

which has constant negative curvature $R = -D(D+1)/L^2$ and satisfies the vacuum Einstein equations with cosmological constant $\Lambda = -D(D-1)/(2L^2)$. This coordinate system covers only a portion of global ADS called the *Poincaré patch*. In this case, the conformal boundary of AdS_{D+1} is located at $z = 0$, while the Poincaré horizon is located at $z \to \infty$. In Fig. 1.2, t is a global time coordinate while z extends from the boundary of the cylinder towards its central axis bounded by the Poincaré horizon. Furthermore, in these coordinates, each z =const. slice corresponds to a flat $\mathbb{R}^{D-1,1}$ spacetime.

The bulk/boundary mapping between the two theories relates objects on both sides, such as fields ϕ on the AdS side with operators $\hat{O}$ on the holographic CFT side. It is based on the identification of partition functions $\mathcal{Z}$ on both sides of the correspondence

$$\mathcal{Z}_{\mathrm{CFT}}[\hat{O}] \equiv \mathcal{Z}_{\mathrm{AdS}}[\phi] \ , \tag{1.9}$$

as proposed in the Gubser-Klebanov-Polyakov-Witten (GKPW) method [51, 52]. To be precise, boundary configurations of sources, as encoded in the path-integrals, specify gravitational problems whose solution in semi-classical configurations provide an approximation to the evaluation of the path-integral in the holographically dual CFT.

Consider, for example, a CFT operator $\hat{O}$ with scaling dimension Δ, whose two-point correlation function in the vacuum is

$$\langle \hat{O}(\vec{x})\hat{O}(\vec{y})\rangle \propto \frac{1}{|\vec{x}-\vec{y}|^{2\Delta}} \ , \tag{1.10}$$

and where $\vec{x}$ and $\vec{y}$ are two points at the boundary. The GKPW method relates the boundary operator $\hat{O}$ with a dual field ϕ in the bulk, with boundary value $\phi^{(0)}$, that is

$$\lim_{z\to 0}\phi(z,\mathbf{x}) = z^{\Delta_\pm}\phi^{(0)}(\mathbf{x}) := \phi^{\pm}(\mathbf{x}) \ , \tag{1.11}$$

where the coefficient $\Delta_+ \equiv \Delta$ leads to a so-called *leading mode* ϕ^+, $\Delta_- = D - \Delta$ leads to a *sub-leading mode* ϕ^- and where Δ coincides with the scaling dimension of the CFT operator $\hat{O}$ dual to the field ϕ. Focusing on the sub-leading mode in the standard quantisation allows us to compute the partition function (1.9) which takes the form

$$\mathcal{Z}_{\mathrm{AdS}}[\phi]\Big|_{\phi^{(0)}(\mathbf{x})=\lim_{z\to 0}(z^{\Delta-D}\phi(z,\mathbf{x}))} = \left\langle \exp\left(\int \mathrm{d}^D x\, \hat{O}\,\phi^{(0)}\right)\right\rangle_{\mathrm{CFT}} \ , \tag{1.12}$$

where one typically takes the *saddle-point approximation* on the left hand side. That is, the boundary value $\phi^{(0)}$ of the field ϕ is interpreted as a source of the dual CFT operator $\hat{O}$. This relation has been used, for example, to compute the relation between the mass m of a bulk scalar field and the scaling dimension Δ of its

dual operator [52], showing how indeed the AdS/CFT dictionary provides a precise mapping between asymptotic bulk fields and boundary CFT operators.

Despite the fact that there is not a formal proof of the AdS/CFT correspondence, several entries of the AdS/CFT dictionary have been found both in the original example as well as in several others, providing evidence that the conjecture is correct and applicable in more general scenarios.[1] Furthermore, Maldacena's $\text{AdS}_5/\text{CFT}_4$ conjecture has been extremely well tested at the planar level using integrability techniques (see *e.g.*, [55–57] for some reviews). Such entries have applications ranging from high energy physics to condensed matter physics. Indeed, since the inception of the AdS/CFT correspondence there has been an extraordinary amount of exchange of ideas between these disciplines which are reshaping the way we approach different phenomena in various areas of physics. For a review of applications of AdS/CFT to condensed matter physics see [30, 58–60]. Other resources for its applications to the study of QCD are [61–63]and we further refer the reader to the earlier discussion of the ratio η/s of the deconfined phase of $\mathcal{N} = 4$ SYM as a model for the QGP of QCD.

Despite the successes of the AdS/CFT correspondence there are still outstanding questions about the mechanism behind it. For example, how are the spacetime geometry and other local gravitational observables encoded in a CFT state, or what are the necessary and sufficient conditions for a QFT to have a dual gravitational theory.

However, over the past fifteen years it has become increasingly clear that a very useful way to tackle these questions and other related ones, is to think about the CFT from the perspective of quantum information science. For example, a considerable amount of evidence has arisen which shows that the entanglement structure of CFT states is directly related to the geometrical structure of the dual spacetime. Quantum information-theoretic quantities such as *entanglement entropy* and relative entropy have been shown to have natural gravitational duals. At the same time, *complexity* has emerged as a quantum information-theoretic quantity conjectured to encode information about black hole interiors. This thesis deals with the field-theoretic properties of mixed-state generalizations of these notions.

Further evidence for this intimate relation has also emerged from tensor networks (TN), a powerful computational tool used in quantum many-body systems, and also from associated quantum error-correcting codes. In the following Section we give a brief review of the former, while a discussion of the latter is beyond the scope of this thesis, but the reader can refer to [64, 65] for a review on the topic.

[1] While this claim is conjectured to hold between any CFT on $\mathbb{R} \times S^{D-1}$ and a quantum theory on gravity in asymptotically $\text{AdS}_{D+1} \times M$, where M is some compact manifold, in practice one assumes that the gravitational dual of the CFT is a semicalssical theory of gravity described by an effective action with a UV cutoff Λ such that $1/L \ll \Lambda \leq 1/G_N^{\frac{1}{(D-1)}}$. This implies in particular that gapped large-N CFTs are expected have a semiclassical dual [53, 54].

1.2. Tensor Networks

Tensor network (TN) states are variational wavefunction ansätze for states in quantum many-body systems whose coefficients can be written as a contraction of "fundamental" tensors which encode correlations between different subsystems. Their construction usually takes place within lattice models although some TNs have a continuous counterpart. They are useful for representing ground states of local Hamiltonians and they have also been used as toy models for holographic error-correcting codes. See [66, 67] for recent reviews.

Consider a pure state $|\Psi\rangle$ in a Hilbert space $\mathcal{H}$ with N degrees of freedom, where each one of them corresponds to an M-level system. That is, each degree of freedom can take M different values. In a basis of $\mathcal{H}$ given by

$$|j_1, \ldots, j_N\rangle = |j_1\rangle \otimes \ldots \otimes |j_N\rangle \ , \tag{1.13}$$

we can represent the state $|\Psi\rangle$ as

$$|\Psi\rangle = \sum_{j_1,\ldots,j_N=1}^{M} \Psi_{j_1,\ldots,j_N} |j_1, \ldots, j_N\rangle \ , \tag{1.14}$$

where the M^N coefficients $\Psi_{j_1,\ldots,j_N} \in \mathbb{C}$ define a complex-valued tensor Ψ of rank N. In general, the dimension of the indices $\{j_i\}$ is called the *physical dimension* $\chi_j = M$, since it describes the dimension of local Hilbert spaces. The question which lies at the foundation of TN is whether all the information encoded in the coefficients $\Psi_{j_1,\ldots,j_N}$ is useful or needed to study specific properties of the state $|\Psi\rangle$.

Hence, the TN representation of $|\Psi\rangle$ consists in writing the coefficients $\Psi_{j_1,\ldots,j_N}$ as contractions of more fundamental tensors which accurately capture said correlations between different subsystems in $\mathcal{H}$. For example, in the case $N = 4$ we can write

$$\Psi_{j_1,j_2,j_3,j_4} = \sum_{k_1,k_2,k_3,k_4=1}^{\chi_k} T_{j_1,k_4,k_1} U_{j_2,k_1,k_2} V_{j_3,k_2,k_3} W_{j_4,k_3,k_4} \ , \tag{1.15}$$

where T, U, V, W, are tensors of rank 3 and where χ_k is the bond dimension of the k indices.

TN states are usually represented as networks or graphs, where nodes represent tensors and their legs represent indices. For example, the tensor T in (1.15) can be represented as

$T_{j,k_4,k_1} =$ 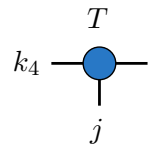

, (1.16)

while the coefficients Ψ_{j_1,j_2,j_3,j_4} (1.15) are represented by

$\Psi_{j_1,j_2,j_3,j_4} =$ 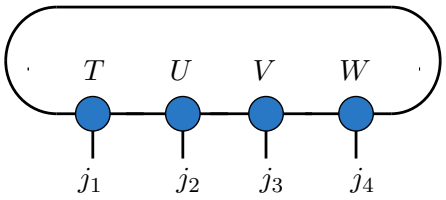

, (1.17)

where the connected legs between the nodes are represented by the contracted indices k_1, k_2, k_3, k_4. In (1.17) the un-contracted legs labelled by j_1, j_2, j_3, j_4 are called open legs or free indices.

The graphical representation of TN states bares resemblance to Penrose's "abstract tensor system" (ATS) [68, 69] used in spin networks [70]; representations of particles and their interactions in loop quantum gravity (LQG) [71]. While inspiration may have indeed been drawn from Penrose's ideas, it is clear that the implementation of the graphical notation in the context presented here occurred decades later. See *e.g.*, [72–75] for some of the earliest implementations of these ideas in quantum many-body systems, and in particular for the *density matrix renormalization group* (DMRG), a key technique in the development of TNs.

The advantage of the TN ansatz becomes evident when we consider large tensor networks. For example, the generalization of (1.16) and (1.17) to $N \gg 1$ degrees of freedom is known as a *matrix product state* (MPS), and consists of a chain of N 3-legged tensors where each one of them is contracted with two neighbouring nodes.

The usefulness of the MPS tensor network lies on the fact that it uses $N\chi_j\chi_k^2$ parameters to describe a state with χ_j^N coefficients, allowing for an exponentially smaller representation of $|\Psi\rangle$ in N. Note that unless χ_k depends exponentially on N, the MPS ansatz can only represent a subset of the full Hilbert space $\mathcal{H}$. However, it can be shown that the MPS ansatz is sufficient to describe ground states of gapped local Hamiltonians in $(1+1)$-dimensions [76–79], which implies that correlations in MPS decay exponentially [80], which in turn implies an area law for *entanglement entropy*.

Entanglement entropy S_A is a measure of pure state entanglement defined for a subsystem A of a bipartite Hilbert space $\mathcal{H} = \mathcal{H}_A \otimes \mathcal{H}_{\bar{A}}$, where $\bar{A}$ is the complement of A. If the system is in a pure state determined by a density matrix ρ, then the entanglement entropy S_A is defined as the von Neumann entropy of the reduced density matrix of the subsystem A, $\rho_A = \mathrm{tr}_{\bar{A}}(\rho)$, via

$$S_A = -\mathrm{tr}_A(\rho_A \log(\rho_A)) \ . \tag{1.18}$$

S_A characterizes the pure state entanglement of degrees of freedom in subsystem A given the pure state ρ.

It is usually said that the entanglement entropy S_A of a system follows an *area law* if S_A scales with the size of the boundary of A: ∂A. In $(1+1)$-dimensions, where A corresponds to a spatial subregion, S_A satisfies an area law if it is constant. In

general, area laws are characteristic of ground states of gapped local Hamiltonians, and have been proven rigorously in $(1+1)$-dimensions [76] and for non-interacting systems in arbitrary dimensions [81, 82]. For example, the entanglement entropy of connected subsystems in an MPS is constant in their size. See [83] for a review. We will discuss entanglement entropy and other correlation measures in detail in Chapter 6 of this thesis.

For TN states of arbitrary geometry it can be shown that the entanglement entropy S_A of a subregion A is generally bounded from above as

$$S_A \leq |\gamma_A| \log(\chi_k) \ , \tag{1.19}$$

where χ_k is the bond dimension of all internal contracted legs in the network and where $|\gamma_A|$ is the length of the *minimal cut* γ_A as counted by the number of legs it cuts; *i.e.*, γ_A is the line that divides the tensor network into two pieces corresponding to A and $\bar{A}$ and which cuts through the smallest number of legs between tensors in the network. This bound can be derived by a careful analysis of the Schmidt and *singular value decompositions* (SVD) of a bipartite quantum state. The entanglement entropy S_A will be maximal if all the Schmidt coefficients of the state are equal to the reciprocal of the bond dimension.

Not all TN represent states whose entanglement satisfies an area law. States that arise from critical or gapless Hamiltonians, as in the case for conformal field theories (CFTs), have a more complicated entanglement structure. In $(1+1)$-dimensional CFTs, the entanglement entropy S_A of a subsystem A of size $\ell = |A|$ has a logarithmic scaling [84–86]

$$S_A = \frac{c}{3} \log\left(\frac{\ell}{\delta}\right) \ , \tag{1.20}$$

where c is the central charge of the CFT and δ is a lattice (UV) regulator.

A class of tensor networks which reproduces a relation $|\gamma_A| \propto \log(\ell/\delta)$ for arbitrary subsystem sizes ℓ is the *multi-scale entanglement renormalization ansatz* (MERA) [87]. It consists of a multi-layered structure built two different types of tensors: *isometries* w and *disentanglers* u. The latter are unitary operators which account for the entanglement between neighbouring sites in the lattice. The tree-like structure of the TN leads a logarithmic scaling of the minimal cut γ_A with the size of a subregion A.

The MERA can also be interpreted as an *entanglement renormalization* procedure [88], transforming a fine-grained state into a coarse-grained one, or viceversa, by the action of the isometries w, as displayed in Fig. 1.3. As can be seen, the MERA consists of different layers, each one corresponding to a different coarse-grained state with a characteristic energy scale $E \sim 1/l$, where l is a characteristic length scale.

These properties of the MERA led Brian Swingle to propose it as a toy model of the AdS/CFT correspondence [89]. In particular, he suggested that the MERA tensor network could be interpreted as a time-slice of an AdS spacetime, as represented in Fig. 1.4. The reason being that, just as the MERA implements an entanglement renormalization at different scales, so does a time-slice of AdS at a fixed $z > 0$

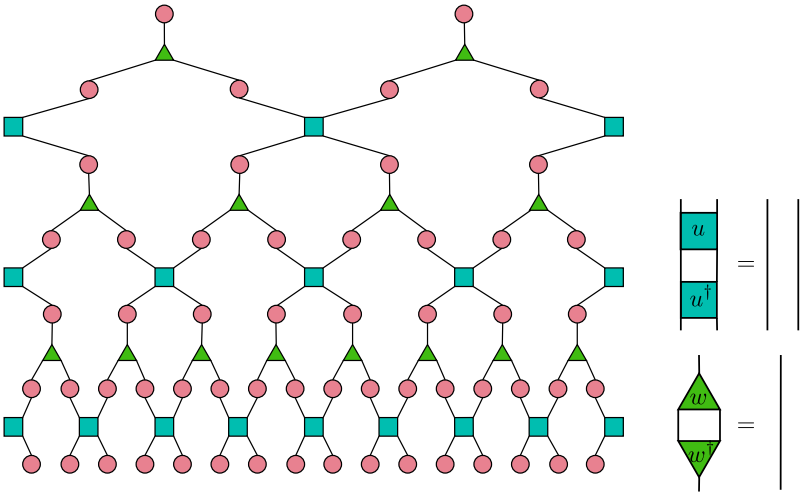

Figure 1.3.: A MERA tensor network composed of disentanglers u (squares) and isometries w (triangles). On the left, the entanglement renormalization of MERA on lattice sites (circles) at various coarse-grained scales. The vertical direction corresponds to the depth of the network, increasingly coarse-graining the state as it moves upward. On the right, the identities of disentanglers and isometries for contractions with their Hermitian conjugates.

describes an increasingly coarse-grained state. Moreover, the critical states that are produced by the MERA resemble those of conformal field theories.

However, the network geometry does not exactly match that of a time-slice of AdS, leading to inconsistencies [90]. Alternative proposals have also interpreted the MERA network geometry as a path integral discretization of a null cone in AdS [91], as a time-like surface in de Sitter [92], and as a discretization of the kinematic space of AdS [93].

In [91], authors also proposed an extension of MERA which incorporates Euclidean time-evolution in $(1+1)$-dimensional CFTs through operators known as *euclideons* e, leading to a TN known as *Euclidean MERA*. Such operators are inserted between the output of isometries w and the input of disentanglers u and implement an infinitesimal Euclidean time evolution given by $e^{-\delta\tau\hat{H}}$ where $\hat{H}$ is the CFT Hamiltonian and $\delta\tau$ is a time-step in Euclidean time τ. That is, each layer of euclideons implements a one-step Euclidean time evolution.[2] Furthermore, the eMERA has been argued to correspond to hyperbolic space $\mathbb{H}^2$ from a path-integral perspective, perhaps realizing a toy model of the AdS/CFT correspondence though this idea has yet to be formalized. More concrete toy models include the well-known *Harlow-Pastawski-Preskill-Yoshida (HaPPY)* quantum error-correcting code [94].

Though TN are highly efficient numerical tools in discretized theories, a natural ques-

[2] A similar extension of the MERA based on operators which implement real-time evolution was also conjectured to represent two-dimensional de Sitter space dS_2 from the path-integral perspective.

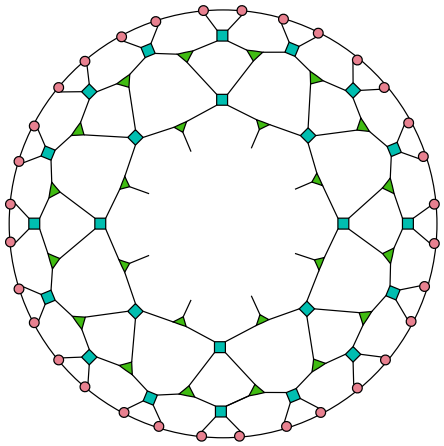

Figure 1.4.: MERA as a toy model of the AdS/CFT Correspondence. The fine-grained discretized state at the conformal boundary of AdS space in the UV is coarse-grained as the networks peers deeper into the bulk of AdS in the z-direction.

tion is whether these can be generalized to continuous settings. In the case of MERA, this generalization is achieved by the continuous MERA (cMERA) [95].[3] Just as MERA implements a discrete entanglement renormalization, cMERA implements a renormalization group flow of quantum field theories in real space, leading to a variational class of wavefunctions that are both translationally invariant and which also exhibit an area-law for gapped Hamiltonians and logarithmic divergence for critical ones.

The cMERA ansatz in its original formulation has so far only been understood for free theories [97, 98], particularly in the case of Gaussian cMERA, and to the leading order in perturbation theory [99, 100]. In this framework, one starts with a Hamiltonian $\hat{H}$ in a QFT and a UV cut-off $\Lambda \sim 1/\delta$. where δ is identified with a lattice spacing in a discretized setting. The Hilbert space defined by the fields with UV cut-off Λ is denoted by $\mathcal{H}_\Lambda$. Similarly to MERA, one performs a coarse-graining procedure on states in $\mathcal{H}_\Lambda$. Consider a one-parameter family of states

$$|\Psi(u)\rangle \in \mathcal{H}_\Lambda \ , \tag{1.21}$$

where $u \in (-\infty, 0)$ is a scale parameter, labelling the layer of coarse-graining. In momentum space, the parameter u is taken in such a way that the k modes are cut-off by $|k| \leq \Lambda e^u$. One can take the UV and IR limits defined by $u \to u_{\mathrm{UV}} = 0$, $u \to u_{\mathrm{IR}} = -\infty$. The states in the UV and IR limits are then labelled as

$$|\Psi(u_{\mathrm{UV}})\rangle \equiv |\Psi^\Lambda\rangle \ , \tag{1.22a}$$

$$|\Psi(u_{\mathrm{IR}})\rangle \equiv |\Omega\rangle \ , \tag{1.22b}$$

where the UV state (1.22a) typically acts as a variational ansatz for the ground state $|\Psi\rangle$ of the QFT. The IR state (1.22b) is usually taken to be a spatially-disentangled

[3] There also exists a continuous generalization of MPS called cMPS [96].

product state, such that the entanglement entropy vanishes $S_A = 0$ for any subsystem bipartition in the IR state.

The crucial point is that the one-parameter family of states (1.21) can be obtained from the IR state (1.22b) via a *quantum circuit* defined through a unitary transformation

$$|\Psi(u)\rangle := \hat{U}(u, u_{\mathrm{IR}})\,|\Omega\rangle \equiv \overleftarrow{\mathcal{P}}\left\{\exp\left(-\mathrm{i}\int_{-\infty}^{u} \mathrm{d}u'\,(\hat{L} + \hat{\mathcal{K}}(u'))\right)\right\}|\Omega\rangle \ , \tag{1.23}$$

where $\overleftarrow{\mathcal{P}}$ denote a path-ordered exponential, the operators $\hat{L}$ and $\hat{\mathcal{K}}(u')$ are respectively the generator of scale transformations (coarse-graining) and the *entangler*. In other words, $\hat{L}$ and $\hat{\mathcal{K}}$ are the continuum analogues of the disentanglers u and isometries w in the MERA. Note that the unitaries $\hat{\mathcal{K}}$ and u can be thought of as entanglers or disentanglers depending on the direction of the entanglement renormalization, just as the scalings $\hat{L}$ and w can be thought of as performing a coarse- or fine-graining. While the scaling operator $\hat{L}$ is independent of u' and only depends on the generic properties of the QFT, the entangler $\hat{\mathcal{K}}(u')$ is theory-dependent and is the basis for the variational ansatz.

The UV state (1.22a) can also be obtained from the on-parameter family (1.21) as $|\Psi^{\Lambda}\rangle := \hat{U}(u_{\mathrm{UV}}, u)\,|\Psi(u)\rangle$, where $|\Psi(u)\rangle$ is given by (1.23). In this framework, the IR state $|\Omega\rangle$ is invariant under re-scalings $\hat{L}$, $\hat{L}\,|\Omega\rangle = 0$, since it is a completely spatially disentangled state. On the other hand, the operator $\hat{\mathcal{K}}(u)$ generates entanglement for modes $|k| \leq \Lambda e^{u}$. One can then see from (1.23) that the UV state $|\Psi^{\Lambda}\rangle$ is obtained from the disentangled state $|\Omega\rangle$ by a continuous generation of entanglement as the scale parameter varies from $-\infty$ to 0. As mentioned before, this process can be reverted, starting from the UV state and flowing to the IR in which case the operator $\hat{\mathcal{K}}(u)$ disentangles the system as the operator $\hat{L}$ coarse-grains it.

The cMERA circuit (1.23) was central to early efforts in defining a notion of *complexity* in quantum field theories [101, 102]. The reason being that it is natural to ask what is the minimal number of tensors needed to produce a state. On one hand, if a state is simple, then it should be possible, at least in principle, to produce it using fewer tensors than a more "complex" state. In this sense, one can heuristically associate a notion of complexity to the number of tensors needed to produce a given state. This applies in particular to MERA and cMERA states and is the origin of complexity in quantum-many body systems and quantum fields as studied in the course of the past four years.

We review the general notion of complexity arising from quantum circuits for QFTs in Chapter 3. Other proposals to realize an AdS/TN correspondence include the path-integral optimization approach [103, 104]. More recent efforts to construct TN states in the AdS/CFT correspondence include [105–107].

1.3. Organization of this thesis

This thesis is organized as follows: Chapter 2 is dedicated to presenting the notions of entanglement entropy, complexity and related quantities from the perspective of

the AdS/CFT correspondence. The goal of this Chapter is to provide a conceptual background for the developments presented in this thesis.

In Chapter 3 we present the mathematical techniques and tools necessary for describing the computation of circuit complexity of vacuum states of free bosonic and fermionic QFTs. We also describe the motivation and geometrical tools developed by Michael Nielsen and collaborators used to study circuit complexity in quantum mechanics and which led to the recent implementation of the concept of complexity geometry in QFTs. The aim of this Chapter is to present the necessary mathematical and physical background that will be used in the subsequent chapters of the thesis.

Chapter 4 deals with the study of complexity in a time-dependent setting and is based on [**CamH03**]. We do this by considering a smooth quench through a critical point in a free bosonic CFT. We analyse the complexity of the time-dependent ground state and study the universal scalings. We show that complexity, like entanglement entropy, can be used as a probe of phase transitions in quantum-many body systems providing a foundation for further studies in this direction.

In Chapter 5 we present the study of complexity of purification, a measure of complexity which generalizes the notion from pure to mixed quantum states, based on [**CamH03**, **CamH02**]. We study complexity of purification for vacuum subregions of free QFTs and show that complexity of purification captures the divergence structure of pure state complexity. In the case of two adjacent intervals we show that complexity of purification exhibits a logarithmic divergence akin to the holographic subregion complexity proposals. We also compare our bosonic complexity of purification results with two other approaches present in the literature.

In Chapter 6, based on [**CamH02**, **CamH01**], we present the study of entanglement of purification, a correlation measure which generalizes the notion of entanglement entropy to mixed states, and of reflected entropy, another correlation measure built from the so-called canonical purification We first focus on entanglement of purification, and discuss its behaviour for vacuum subregions of free CFT consisting of two adjacent intervals. We show that it behaves in agreement both with holographic and CFT expectations. We then compare our results for entanglement of purification and reflected entropy for subregions of free CFTs consisting of two disjoint intervals which are largely separated from each other. Here we focus specifically on the $c = 1/2$ Ising CFT and show that both entanglement of purification and reflected entropy present a logarithmic enhancement with respect to the leading power-law divergence in the separation, a feature which provides new insights into the large distance behaviour of these correlation measures.

Finally, in Chapter 7 we discuss the developments presented in this thesis, their significance in the current state of research in this field and future directions.

2. Quantum Information Aspects of the AdS/CFT Correspondence

In this Chapter we review recent developments in the AdS/CFT correspondence that have been motivated by connections between quantum gravity and quantum information. We start with a discussion of holographic entanglement entropy and the Ryu–Takayanagi formula in Sec. 2.1.1. We follow this discussion by a review of entanglement wedge reconstruction and the holographic interpretation of its cross section in Sec. 2.2. Finally, we present the holographic complexity proposals in Sec. 2.3 as well as the holographic subregion complexity proposals. By the end of this Chapter, we will have motivated the study of quantum information-theoretic quantities such as complexity, entanglement of purification and reflected entropy in the context of quantum field theories.

2.1. Holographic Entanglement Entropy

Entanglement is a fundamental property of quantum systems that distinguishes them from classical ones. A particular notion of it, *entanglement entropy* (EE) (1.18), has played a key role in recent developments in quantum field theory (QFT) and in gravity through the AdS/CFT correspondence for more than two decades. This has been motivated on one hand by the study of black hole entropy (1.1) and quantum gravity, and on the other by the study of quantum many-body systems in condensed matter physics.

In the former case, it was understood that the leading UV divergent term in the entropy of a region is proportional to its surface area [108–111] and therefore black hole entropy S_{BH} must be understood, at least to some extent, as arising from the entanglement of quantum fields across its horizon $\mathscr{H}$. This in turn inspired a deeper study of EE in QFTs, where useful techniques such as the replica trick were developed [85, 112] and which led to a variety of results in $(1+1)$-dimensional conformal field theories (CFTs) [86, 113], in gapped systems [114], topological set-ups [115, 116], and related to the quantum Hall effect [117].

In the context of high-energy physics and particularly within the AdS/CFT community, the proposal of Shinsei Ryu and Tadashi Takayanagi [118, 119] represents arguably the most groundbreaking discovery since Maldacena's conjecture. It is also one of the first and most representative connections between AdS/CFT and quantum-information, together with Swingle's description of MERA as a toy model of AdS (see Fig. 1.4).

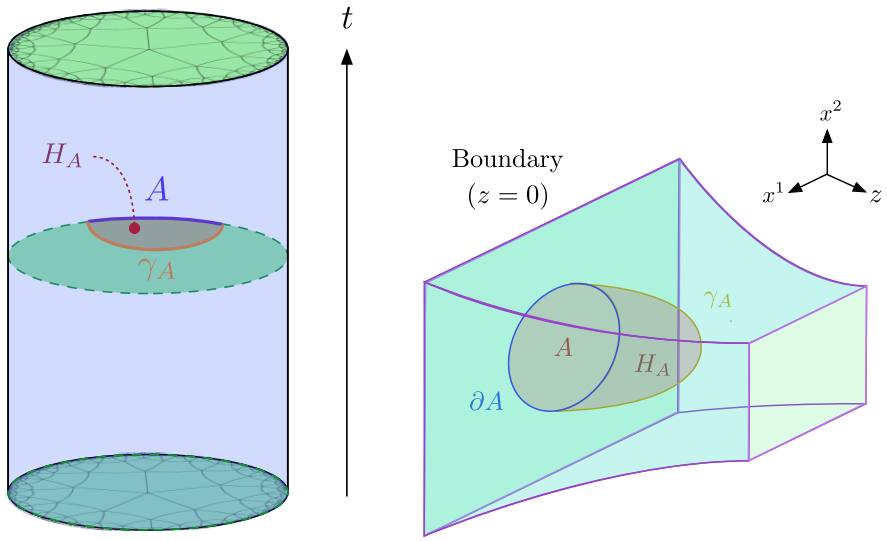

Figure 2.1.: Diagrams of a Ryu–Takayanagi (RT) surface in the bulk of anti-de Sitter space. On the left, the RT surface γ_A of a boundary subregion A in a time-slice of global AdS_3. On the right, the RT surface γ_A of a spherical boundary subregion A in a time-slice of planar AdS_4.

2.1.1. The Ryu–Takayanagi Formula

Inspired by the connections between black hole entropy and EE, Ryu and Takayanagi tackled the following question: What is the bulk gravitational dual in AdS_{D+1} of the entanglement entropy S_A of a boundary spatial subregion A in a holographic CFT_D? They proposed the answer to be given in terms of the area of a $(D-1)$-dimensional (or equivalently codimension-2) bulk minimal-area surface γ_A *homologous* to the boundary subregion A. See Fig. 2.1.

Given a spatial subregion A in the boundary CFT_D, there exist in principle infinitely many codimension-2 spatial submanifolds γ in the bulk which are homologous to A. Of these, however, we must find the one which minimizes the area functional, since this one provides the measure for the gravitational dual of S_A, as given by the *Ryu–Takayanagi* (RT) *formula*

$$S_A := \frac{1}{4G_N^{(D+1)}} \min_{\partial\gamma\sim\partial A} [\text{Area}(\gamma)] \equiv \frac{\text{Area}(\gamma_A)}{4G_N^{(D+1)}} , \tag{2.1}$$

where $G_N^{(D+1)}$ is the $(D+1)$-dimensional Newton's constant. In this context, γ_A is usually called the *RT surface*.

In the construction of the RT surface, the boundary of the surface γ_A must coincide with the boundary of the subregion A, and in this sense, one typically says that the RT surface is *boundary-anchored*. Furthermore, note that γ_A being homologous to A implies that there exists a spatial codimension-1 submanifold with boundary, H_A, usually called a *homology hypersurface*, such that $\partial H_A = \gamma_A \cup A$.

The power of the RT formula (2.1) is that it is a general entry in the AdS/CFT dic-

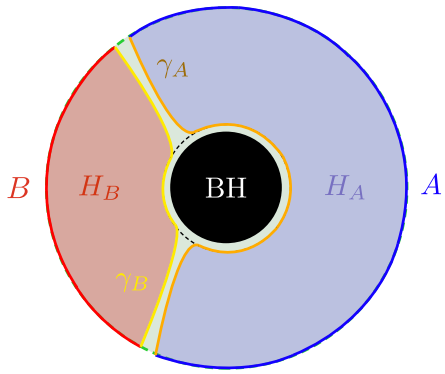

Figure 2.2.: Diagram of RT surfaces in the bulk of a time-slice of an AdS_3 Black Hole. The RT surfaces γ_A and γ_B associated with the boundary subregions A and B wrap around the black hole horizon, increasing their area as the size of the subregions increases. Note that the RT surfaces do not pierce through the horizon.

tionary and hence independent of the particular aspects of the holographic theories. The only requirement on the AdS side is that the bulk corresponds to an asymptotically anti-de Sitter (aAdS) spacetime (with time-reflection symmetry) satisfying Einstein's equations. It in fact agrees with computations of EE performed starting from first principles in QFT, including for example the well-known expression for S_A of a boundary spatial subregion A of size ℓ in $(1+1)$-dimensional CFTs (1.20). It has also been found to obey highly non-trivial properties of EE, such as strong subadditivity [120, 121], in fact obeying all known properties of EE in QFT [122].

Moreover, the RT formula can be interpreted as a generalization of the Bekenstein–Hawking entropy formula (1.1). This can be seen by considering a thermal state ρ_β on the CFT_D, which is holographically dual to an AdS_{D+1} black hole geometry. Considering a boundary region A and its associated RT surface γ_A, as in Fig. 2.2, this RT surface is deformed with respect to the RT surface obtained in an empty AdS_{D+1} geometry corresponding to the vacuum state of the CFT_D. In the former case, the RT surface wraps around the black hole horizon, increasing its area and and acquiring a contribution proportional to the thermal entanglement S_{Thermal} associated with a thermal state ρ_β with finite temperature $T = 1/\beta$ on the CFT [118]. As the size of A increases, the RT surface γ_A wraps more around the black hole horizon though it never fully encapsulates it. This also shows that a black hole horizon is an extremal surface and that (2.1) is a Bekenstein–Hawking entropy of such class of surfaces. For a critical size of the boundary subregion A there is a phase-transition in the RT surface, where the complementary configuration corresponding to the complementary boundary subregion $\bar{A}$ becomes the dominant one, as it leads to a lower area.

For general asymptotically AdS spacetimes that are not necessarily time-symmetric, and for general boundary spatial subregions A, the RT formula (2.1) is generalized by the *Hubeny–Rangamani–Takayanagi* (HRT) *formula*, where the entropy S_A of the subregion A is obtained via the area of the minimal bulk extremal spacelike

hypersurface homologous to A [123]. In this context, the area of γ_A is taken to be extremal under small variations of its position in spacetime [124], provided $\partial\gamma_A = \partial A$. In this case, γ_A is said to be minimal in the sense that there is no other hypersurface with a strictly smaller area which satisfies these conditions.

The RT formula was proven within the AdS/CFT correspondence for $(1+1)$-dimensional CFTs in [125, 126] and subsequently for more general scenarios in [127]. In particular, the HRT formula was proven in [128] by implementing the Schwinger-Keldysh construction [129–131] on the bulk side in order to compute the reduced density matrix of a boundary subregion. In the context of spherical vacuum subregions for arbitrary dimensions, the RT formula was proven in [132]. However, the RT formula and its covariant generalization, the HRT formula, hold only for classical bulk spacetimes satisfying Einstein's equations.

Beyond Einstein gravity, there are generalizations of these formulas for classical bulk geometries arising from higher-derivative gravitational theories [133] such as Lovelock theories [134, 135]. There also exist conjectured generalizations for 3-dimensional Chern–Simons theories [136] and higher-spin gravity [137].

Beyond classical gravitational theories, there must to be quantum corrections to the RT formula appearing as a perturbative expansion in G_N. At order G_N^0 such correction is given by a semiclassical treatment of the bulk fields,*i.e.*, by treating them as quantum fields on a fixed classical background and computing S_A for the homology hypersurface H_A. The expression containing this quantum correction is known as the *Faulkner–Lewkowycz–Maldacena* (FLM) *formula* [138], for which there exists a conjectured generalization to all-orders in $\mathcal{O}(1/G_N)$ [139]. Precious little is known beyond such perturbative quantum corrections to RT, but they are thought to be relevant for smoothening phase transitions of RT surfaces *e.g.*, in the presence of a black hole.

In this regard, it was further argued in [139] that in the presence of quantum fields, the RT prescription needs to be modified in order to account for the entropy arising from the entanglement of the quantum fields across the minimal (or extremal) surface γ_A. This observation is the natural holographic analogue of the generalized second law of black hole thermodynamics [43]. In this construction, one has that the holographic entanglement entropy of a boundary subregion A is given by

$$S_A := \min\left\{\text{ext}(S_{\text{gen}}(\gamma))\right\} = \min_{\partial\gamma\sim\partial A}\left\{\text{ext}\left(\frac{\text{Area}(\gamma)}{4G_N^{(D+1)}} + S_{\text{bulk}}(\gamma)\right)\right\}\,, \tag{2.2}$$

where γ is the bulk surface homologous to the boundary subregion A, and where $S_{\text{bulk}}(\gamma)$ is the entropy of quantum fields in the homology hypersurface H_A. The surface γ which extremizes the generalized entropy is called a *quantum extremal surface* (QES) [139]. In formula (2.2) one first needs to find the surface γ which extremizes the generalized entropy $S_{\text{gen}}(\gamma)$ and in case there is more than one surface which does this, then one needs to choose the one yielding the minimum value of $S_{\text{gen}}(\gamma)$.

This approach has led to novel insights in holographic models of black hole evaporation and in particular it has been used to compute the Page curve in a controlled

manner [18, 19, 140]. The surprising aspect, as we mentioned in the Introduction 1, is that the Page curve can be obtained from semi-classical gravity computations involving saddle points for the QES. In this case, the computation of the EE of the Hawking radiation is encapsulated by the *island formula* [140]. While we will not explore the details of this construction and the consequences of the island formula, we would be remiss not to mention its relevance in understanding this crucial aspect of unitary black hole evaporation. Despite this significant breakthrough, however, we cannot claim that the black hole information paradox has been resolved. In fact, as we will discuss in the later sections of this chapter, it can be argued that one requires additional information about the quantum state involved int he black hole evaporation process beyond what can be captured by entanglement entropy.

2.2. The Entanglement Wedge

Perhaps the most fascinating aspect of the AdS/CFT correspondence is that it relates a quantum theory of gravity to a theory without it. In the regime where the quantum theory is strongly-coupled this duality relates such a theory with a classical theory of gravity. This, as we have mentioned, has led to new insights into the properties of strongly-coupled theories. However from a fundamental perspective, the correspondence has also opened the path to understand gravity from a different perspective; that of a quantum theory without gravitational degrees of freedom.

Indeed, an idea which has taken a central role in recent investigations of the AdS/CFT correspondence is that gravity, at least when it pertains to the physics on negatively-curved spaces, is an *emergent phenomenon*. This idea was argued by Mark Van Raamsdonk, stating that an essential ingredient in the emergence of spacetime is quantum entanglement [141]. Van Raamsdonk's claim was that the connectivity between different regions in spacetime could be seen as a consequence of the entanglement between them. This proposal was motivated by Maldacena's observation that the eternal AdS black hole geometry is obtained by maximally-entangling two spatially-separated copies of a CFT in a thermal state which are initially unentangled form each other [142], see Fig. 2.3. In said entangled state of two copies of the CFT, entanglement is measured by the *mutual information* (MI)

$$I(A:B) := S_A + S_B - S_{A\cup B} \ , \tag{2.3}$$

where here A and B represent spatial subregions on the entangled CFT states. In the context of the AdS/CFT correspondence, the behaviour of MI has been understood as a function of the distance between subsystems A and B [143, 144]. Furthermore, it is also an upper-bound to two-point correlation functions [145], which are expected to decay exponentially with the bulk geodesic distance [144]. This means that an increment in the entanglement implies a shorter bulk distance between the subsystems and viceversa. This observation was then taken as heuristically implying that entanglement between the subregions is responsible for binding the bulk spacetime between them.

Though the precise connection between entanglement and the emergence of gravity has not been rigorously established or even understood, it has led to new in-

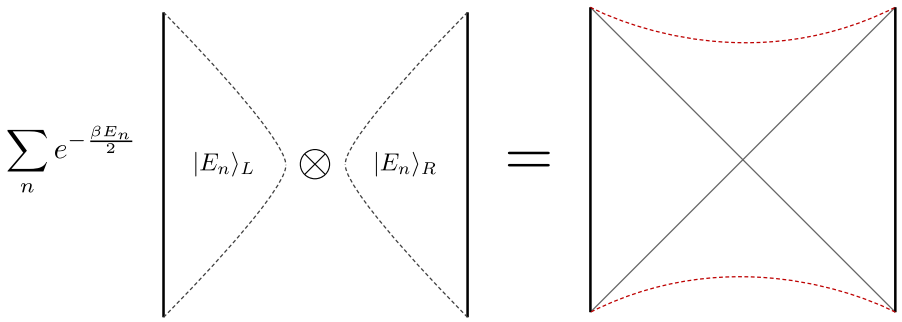

Figure 2.3.: Heuristic interpretation of the construction of the thermofield double (TFD) state. A weighted sum over the geometries corresponding to two disjoint copies of a CFT on a thermal state gives rise to the geometry dual to the TFD state: the eternal AdS black hole.

sights.[1] One can ask, for example, how is the physical information of a certain local bulk region encoded in the boundary, or what is the bulk region which can be reconstructed from the information contained in a given boundary subregion. In other words, what happens when we focus on boundary subregions corresponding to mixed states instead of a pure state. More concretely: what is the bulk region in AdS which can be "reconstructed" from the information contained in a subregion on the boundary characterized by a mixed state in the CFT?

A decade ago it was realized that the geometric object to consider in this case is the *entanglement wedge* [147–150]. This bulk region can be constructed from a boundary region A via its RT (or more generally its HRT) surface γ_A and the associated homology hypersurface H_A. Essentially, the entanglement wedge $\mathcal{E}_A$ is defined as the codimension-0 bulk domain of dependence of H_A, $\mathcal{E}_A := D(H_A)$, as in Fig. 2.4. Given a well-posed initial value problem defined on H_A, the entanglement wedge $\mathcal{E}_A$ is the bulk region which is fully determined by said initial data on H_A, as any causal curve passing through a point in $\mathcal{E}_A$ will intersect H_A.

This implies, for example, that any field ϕ contained in $\mathcal{E}_A$ can effectively be reconstructed from data contained in A. This can in fact be done perturbatively in $1/N$ by solving a non-standard Cauchy problem via the so-called *Hamilton–Kabat–Lifschytz–Lowe* (HKLL) *procedure* [151]. An example of which is the work [152] by *Jafferis–Lewkowycz–Maldacena–Suh* (JLMS), where the authors propose a bulk formula for the modular Hamiltonian $\mathfrak{H}_A$ defined via $\mathfrak{H}_A \sim -\log(\rho_A)$ for a mixed state ρ_A, effectively relating the relative entropy $S(\rho||\sigma) := \mathrm{tr}(\rho\log(\rho)) - \mathrm{tr}(\rho\log(\sigma))$ between two boundary states ρ, σ in A with the relative entropy between states in $\mathcal{E}_A$.

[1] A particularly controversial idea is the so-called *ER=EPR* conjecture by Susskind and Maldacena [146], which states that entangled pairs of black holes (or particles) are connected by a non-traversable wormhole. The name of the conjecture, which also provides a resolution to the firewall paradox [25], is an acronym of *Einstein-Rosen=Einstein-Podolsky-Rosen*, implying that wormholes, Einstein-Rosen (ER) bridges, are a manifestation of the quantum entanglement between Einstein-Podolsky-Rosen (EPR) pairs of black holes, or particles.

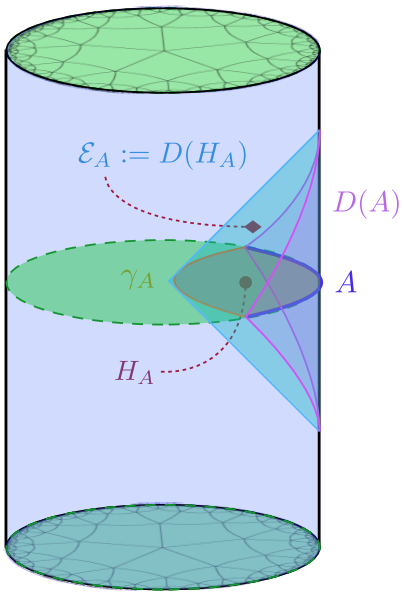

Figure 2.4.: Diagram of the Entanglement Wedge in anti-de Sitter space. Given a boundary subregion A, its RT surface γ_A and its homology hypersurface H_A, the entanglement wedge $\mathcal{E}_A$ is defined as the bulk domain of dependence of H_A: $D(H_A)$. At the boundary, $D(H_A)$ coincides with the domain of dependence of A: $D(A)$.

The entanglement wedge $\mathcal{E}_A$ was realized to be a more suitable geometric dual to the spatial subregion A than the *causal wedge* C_A [153], which is instead defined as the bulk region connected via causal curves to the boundary domain of dependence $D(A)$, and which under reasonable assumptions is in fact contained in the former: $C_A \subseteq \mathcal{E}_A$.

Understanding how the dual gravitational spacetime in the entanglement wedge $\mathcal{E}_A$ emerges from the subregion A at the boundary led to the programme in AdS/CFT known as *entanglement wedge reconstruction*, which has understood to be intimately connected with error-correcting codes in the form of a *subregion duality* [154]. See [54, 67] for a detailed review of these ideas. However the aspect of the entanglement wedge that we are interested in at the moment, is the way it encodes correlations between bipartite boundary subsystems via the area of its minimal cross section, as we will discuss in the following section.

2.2.1. The Entanglement Wedge Cross-Section

As mentioned previously, given a bipartite Hilbert space $\mathcal{H}_{AB}$, pure state entanglement between two subsystems A and B is accurately captured by MI (2.3). This correlation measure acquires a natural geometric meaning in the AdS/CFT correspondence via the area of extremal surfaces as prescribed by the RT formula (2.1). However, from the perspective of the quantum theory it is assumed that there is a pure state $\rho = |\psi\rangle\langle\psi|$ from which the reduced density matrices of the mixed states ρ_A

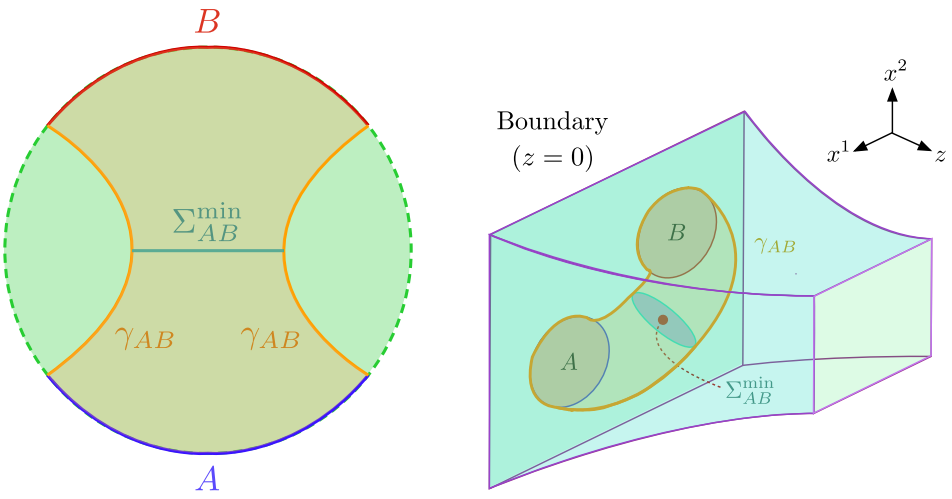

Figure 2.5.: Diagrams of the entanglement wedge cross-section in anti-de Sitter space. Given two boundary spatial subregions A and B, the RT surface(s) γ_{AB}, and the homology hypersurface H_{AB}, the cross-section $\Sigma_{AB}^{\min}$ is defined as the hypersurface which splits H_{AB} into two disjoint components each one containing only one of the boundary subregions, and which has the minimal area.

and ρ_B describing subregions A and B are obtained. It is natural then to ask about correlation measures which can be defined *a priori* for mixed states and explore their geometric interpretation and properties via the AdS/CFT correspondence.

Assuming we only had access to the information contained in the spatial subregions A and B at the boundary, it is plausible to expect that whatever geometric object captures correlations between them, to be contained in the entanglement wedge $\mathcal{E}_{AB}$, constructed from the homology hypersurface H_{AB} obtained via the RT surface(s) γ_{AB}.

A geometric object which naturally stands out in this case is the *minimal cross section* $\Sigma_{AB}^{\min}$ of $\mathcal{E}_{AB}$. Given the entanglement wedge $\mathcal{E}_{AB}$, there are in principle infinitely many codimension-2 hypersurfaces Σ_{AB} which separate the wedge into two parts: one containing A and the other one B. However, there is a special cross section which has a minimal area with respect to all others, and that is $\Sigma_{AB}^{\min}$.

The *entanglement wedge cross-section* $E_W(A:B)$ is then defined as

$$E_W(A:B) := \frac{1}{4G_N^{(D+1)}} \min_{\Sigma_{AB}} [\text{Area}(\Sigma_{AB})] = \frac{\text{Area}(\Sigma_{AB}^{\min})}{4G_N^{(D+1)}} , \tag{2.4}$$

where $\Sigma_{AB}^{\min}$ is the minimal cross section of the entanglement wedge $\mathcal{E}_{AB}$, as in Fig. 2.5.

Purely from a geometric perspective, this quantity can be argued to measure the strength of correlations between subsystems A and B within the entanglement

wedge, since it reduces to EE if the total system ρ_{AB} is in a pure state $E_W(A:B) = S_A = S_B$ and because it also satisfies the following bounds [155]

$$\frac{1}{2}I(A:B) \leq E_W(A:B) \leq \min[S_A, S_B] \ , \tag{2.5}$$

as well as strong subadditivity

$$E_W(\rho_{AB} \otimes \rho_{CD}) \geq E_W(\rho_{AB}) + E_W(\rho_{CD}) \ . \tag{2.6}$$

However in [156, 157] authors went beyond this general connection and conjectured the entanglement wedge cross-section E_W to be dual to a mixed state generalization of EE known as the *entanglement of purification* (EoP)

$$E_W(A:B) \equiv E_P(A:B) \ , \tag{2.7}$$

where this expression holds to the leading order in N and for all CFTs with a holographic dual. EoP is a measure of total correlations between two subsystems that includes both classical and quantum correlations [158, 159], and which is well known in the quantum information community.

Given a mixed state in a bipartite Hilbert space $\mathcal{H}_{AB}$ with reduced density matrix $\rho_{AB} : \mathcal{H}_{AB} \to \mathcal{H}_{AB}$, one can construct a purification $|\psi\rangle \in \mathcal{H}$ of ρ_{AB} by extending the Hilbert space $\mathcal{H}_{AB}$ according to $\mathcal{H}_{AB} \to \mathcal{H}_{AB} \otimes \mathcal{H}_{A'B'}$, such that $\rho_{AB} = \mathrm{tr}_{A'B'}(|\psi\rangle\langle\psi|)$. The EoP, $E_P(\rho_{AB}) \equiv E_P(A:B)$, is then defined as the minimum of the entanglement entropy $S(A \cup A') = S_{AA'} = -\mathrm{tr}_{AA'}(\rho_{AA'}\log(\rho_{AA'}))$ for the reduced density matrix $\rho_{AA'} = \mathrm{tr}_{BB'}(|\psi\rangle\langle\psi|)$ with respect to all possible purifications $|\psi\rangle \in \mathcal{H}$.

The conjecture (2.7) was based on tensor network interpretations of the AdS/CFT correspondence, supported by CFT techniques in specific examples [160] and has since been an active topic of research [161–168], which strongly motivates its study in QFTs, being one of the main objectives of this thesis.

The main obstacle, or perhaps the unsatisfactory aspect of EoP, is that it intrinsically requires to solve a challenging minimization procedure, in principle over all possible purifications of the given mixed state. This makes any efforts to test the conjecture (2.7) equally challenging.

Because of this, authors in [169] proposed a "simpler" holographic dual to the entanglement wedge cross section E_W which does not require any minimization like EoP. They argued that in QFTs with a holographic dual, a quantity known as *reflected entropy* S_R is also dual to E_W. They proposed the identification

$$E_W(A:B) \equiv \frac{1}{2}S_R(A:B) \ , \tag{2.8}$$

which they conjectured to be valid to leading order in N and also for all CFTs with a holographic dual.

For a bipartite quantum system $\mathcal{H}_{AB}$, the *reflected entropy* (RE) S_R of a mixed state ρ_{AB} is defined as the von-Neumann entropy

$$S_R(\rho_{AB}) := S\left(\mathrm{tr}_{BB'}\left(|\sqrt{\rho_{AB}}\rangle\langle\sqrt{\rho_{AB}}|\right)\right) \ , \tag{2.9}$$

computed from the so-called *canonical purification* $|\sqrt{\rho_{AB}}\rangle$ of ρ_{AB}, constructed by a "doubling" of the Hilbert space in a manner reminiscent of the TFD state. We will give a more detailed description of both S_R and $|\sqrt{\rho_{AB}}\rangle$ of ρ_{AB} in Chapter 6, but for the moment it suffices to say that $|\sqrt{\rho_{AB}}\rangle$ is the unique purification which is symmetric under the exchange $A \leftrightarrow A'$ and $B \leftrightarrow B'$.

Authors in [169] backed the conjecture (2.8) by performing computations of reflected entropy based on the replica trick and by studying the properties of the so-called reflected minimal surfaces, which they use to connect the holographic dual of reflected entropy with the entanglement wedge cross-section E_W.

Much like EoP, RE is a measure of correlations between subsystems A and B which contains both classical and quantum contributions. However, unlike E_P, S_R does not have a direct operational interpretation but instead stands out among other correlation measures as the EE entropy corresponding to the unique canonical purification.

Note that the conjectures (2.8) and (2.7) imply the following relation between EoP, RE and E_W in the AdS/CFT correspondence

$$E_P(A:B) = E_W(A:B) = \frac{S_R(A:B)}{2} \ . \tag{2.10}$$

One of the main motivations of this thesis is to deepen our understanding of quantities such as EoP and RE and test their conjectured holographic properties such as (2.10) from the perspective of CFTs. We will do this in Chapter 6, where we will study their propreties in CFTs with a gap in the operator spectrum that can be represented as a lattice model. It suffices to say, for the moment, that understanding the role of these quantities within the entanglement reconstruction would allow us to gain more insight into the deep connection between quantum information and gravity on negatively-curved, asymptotically AdS spaces.

2.3. The Holographic Complexity Proposals

A basic ingredient in the reconstruction of the bulk spacetime within the AdS/CFT correspondence is entanglement. In this context, HRT surfaces not only encode information about the entanglement entropy S_A of the mixed state ρ_A associated with a spatial boundary subregion A, but they also define a larger bulk region, the entanglement wedge $\mathcal{E}_A$, whose information we expect to be completely reconstructible from the information contained in A.

However, in the presence of a black hole, the HRT surfaces "wrap" around the horizon as the size of the subregion increases, making them incapable of probing the interior of the black hole. This raises the interesting question of whether there exists a quantity on the boundary CFT which has information about the interior of the black hole.

Consider the TFD state $|\text{TFD}\rangle$, which is constructed by entangling two copies of a CFT in a thermal state. In an energy eigenbasis $\{|E_n\rangle_{L,R}\}$, and for times $t_{L,R}$ of

the "left/right" CFTs, this state can be written as

$$|\mathrm{TFD}(t_L, t_R)\rangle = \frac{1}{\sqrt{\mathcal{Z}}} \sum_n e^{-\frac{\beta E_n}{2}} e^{-\mathrm{i}\, E_n (t_L + t_R)} \, |E_n\rangle_L \otimes |E_n\rangle_R \ , \tag{2.11}$$

where $\mathcal{Z} = \mathrm{tr}(e^{-\beta \hat{H}}) = \sum_n e^{-\beta E_n}$ is the partition function in the canonical ensemble. This state is holographically dual to the eternal AdS black hole [142], as displayed in Fig. 2.3, where each copy of the CFT is defined on the left and right timelike asymptotic boundaries of the spacetime.

The two CFTs are connected by a codimension-1 spatial hypersurface: a wormhole or Einstein-Rosen bridge (ERB) Σ_{ERB}, which penetrates the black hole horizon $\mathscr{H}$ and into the black hole region as the left and right times $t_{L,R}$ increase. As a consequence, the ERB can be seen to probe the black hole interior for arbitrarily large times $t_{L,R}$. Moreover, its volume $\mathrm{Vol}(\Sigma_{\mathrm{ERB}})$ classically grows indefinitely for a time which is found to be exponential in the number of degrees of freedom K of the boundary state [170].

This exponential growth of the volume of the ERB is much larger than other characteristic time scales such as the thermalization time, which is instead polynomial in the number of degrees of freedom. This implies that "entanglement (entropy) is not enough" [171] to capture the physics behind the black hole horizon, which means that there should be another quantity on the boundary CFT which encodes this exponential growth of $\mathrm{Vol}(\Sigma_{\mathrm{ERB}})$.

Susskind and collaborators conjectured the growth of the $\mathrm{Vol}(\Sigma_{\mathrm{ERB}})$ to be dual to a quantity called the *computational complexity* of the boundary state [172, 173]. We will discuss the notion of circuit complexity in detail in Sec. 3.1. For the moment, complexity can be thought of intuitively as measure of the "hardness" of preparing states or the "difficulty" of implementing a given operation that transforms a state into another.

Suppose a system is in a given state, and one would like to map it to a different one. Complexity is then a measure of how difficult it is to achieve this task, typically measured in the number of times a unitary operator needs to be applied to the state in order to reach the other one. Interestingly, complexity has been conjectured to increase for times exponential in the number of degrees of freedom of the system [174]. This can be thought of as a reflection of the fact that Hilbert spaces for quantum many-body systems are exponentially large.

In the context of chaotic systems, one can think that states obtained by time evolution can look approximately thermal after a few steps of time evolution. This means that when considering a small subsystem of a pure state and computing its entanglement entropy with respect to its complement, one would find that it will be approximately thermal if the entanglement entropy approaches its maximum. If every subsystem which is smaller than half of the whole system has a maximum entanglement entropy, then the whole system has "scrambled" enough information so that one would need to access at least half of the system in order to recover any information about it.

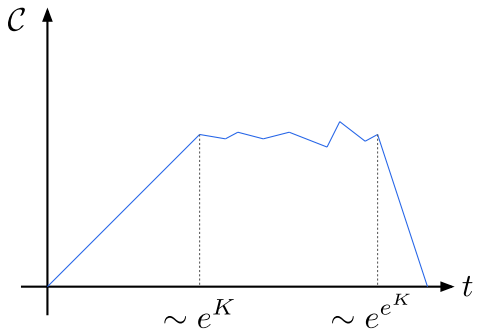

Figure 2.6.: Pictorial representation of the time evolution of complexity in strongly-coupled system, conjectured in [174] and recently proven in [176] for random quantum circuits. Quantum circuit complexity exhibits a linear growth for times of the order $\mathcal{O}(e^K)$ where K is the number of degrees of freedom of the quantum state. Quantum recurrences are expected to occur at double exponential times e^{e^K} bringing the complexity down to its initial value.

One typically expects that the so-called *scrambling time* in a system described by an interacting Hamiltonian scales as the logarithm of the degrees of freedom of the system, while complexity still increases for exponentially large times. In this sense, one typically expects the complexity of a state in a chaotic system to increase for long times, even after the thermalization of perturbations. For longer times, doubly exponential in the number of degrees of freedom, one typically expects quantum recurrences to occur so that the system returns to its initial state [175].

In the regime of linear growth, complexity $\mathcal{C}$ is conjectured to increase proportionally to the energy E of the system

$$\left.\frac{\mathrm{d}\mathcal{C}}{\mathrm{d}t}\right|_{t\leq e^K} \sim E \ , \tag{2.12}$$

where K is the number of degrees of freedom of the system, see Fig. 2.6. It is important to mention that this linear growth of complexity conjectured in [174] has recently been proven in [176] for random quantum circuits.

Returnig to the discussion regarding the volume of the ERB; the fact that there is a property of the bulk geometry that keeps increasing for much longer times even though the entanglement has thermalized is what motivated Susskind and collaborators to argue that the growth of the volume of the ERB captures properties of the complexity of the time evolution of the TFD state.

2.3.1. Actions and Volumes

Motivated by the analogy between the growth of the black hole interior as measured by the volume of the ERB and the growth of computational complexity, Susskind

proposed the notion of *holographic complexity* as the quantity which encodes this evolution of the ERB from the perspective of the boundary CFT.

Together with collaborators, he proposed two gravitational observables which accurately capture the late time growth of the ERB. The first one of these is known as the "complexity=volume" (CV) proposal [170, 173], which postulates that the complexity of the boundary state is proportional to the volume of a maximal codimension-1 bulk hypersurface $\mathcal{B}$ that extends to the asymptotic boundary and which asymptotes to the time slice Σ where the boundary state is defined

$$\mathcal{C}_{\mathrm{V}}[\Sigma] := \frac{1}{\ell_{\mathrm{bulk}}\, G_N^{(D+1)}} \max_{\Sigma=\partial\mathcal{B}} [\mathrm{Vol}(\mathcal{B})] = \frac{\mathrm{Vol}(\Sigma^{\mathrm{max}})}{\ell_{\mathrm{bulk}}\, G_N^{(D+1)}} \ , \tag{2.13}$$

where ℓ_{bulk} is an arbitrary length scale needed to make complexity dimensionless and which is typically chosen to be the AdS radius L, though certain authors [177] proposed a sophisticated approach in order to determine this length scale. In the case of the eternal AdS black hole, this bulk surface connects the time slices at times $t_{L,R}$ through the ERB, as shown on the left side in Fig. 2.7.

The second conjecture goes by the name of "complexity=action" (CA) proposal [178, 179] and identifies the complexity of the boundary state with the gravitational action I_{G} evaluated on a codimension-0 bulk region known as the *Wheeler-De Witt* (WDW) *patch*

$$\mathcal{C}_{\mathrm{A}}[\Sigma] := \frac{I_{\mathrm{G}}[\mathcal{W}_{\mathrm{WDW}}]}{\pi} = \frac{I_{\mathrm{WDW}}}{\pi} \ , \tag{2.14}$$

where the WDW patch $\mathcal{W}_{\mathrm{WDW}}$ is defined as the causal development of the spacelike hypersurface Σ^{max} singled out by the CV construction, as shown on the right side in Fig. 2.7. The factor of $1/\pi$ was a chosen by authors of [178, 179] in an attempt to connect to a suggestion that computation rates are bounded, a conjecture known as *Lloyd's bound* [180]. However, that this bound is generically violated in the CA proposal [181].

This gravitational action I_{G} consists of various terms which include the bulk action I_{Bulk}, proportional to the spacetime volume of the WDW patch $\mathrm{Vol}(\mathcal{W}_{\mathrm{WDW}})$, as well as a Gibbons–Hawking–York term defined on the timelike and spacelike boundaries, as well as other terms arising from the null boundaries [182, 183], Hayward (joint) terms [184, 185] and counter-terms. A third conjecture, the "complexity=volume 2.0" (CV2) proposal [186] was proposed some years later stating that the complexity of the boundary state is instead identified with the spacetime volume of the WDW patch

$$\mathcal{C}_{\mathrm{V}_{2.0}}[\Sigma] := \frac{\widetilde{\mathrm{Vol}}(\mathcal{W}_{\mathrm{WDW}})}{L^2\, G_N^{(D+1)}} \ . \tag{2.15}$$

The properties of these holographic complexity conjectures have been studied in a variety of settings and the structure of their UV divergences has been understood in several asymptotically AdS spacetimes [181, 187–192].

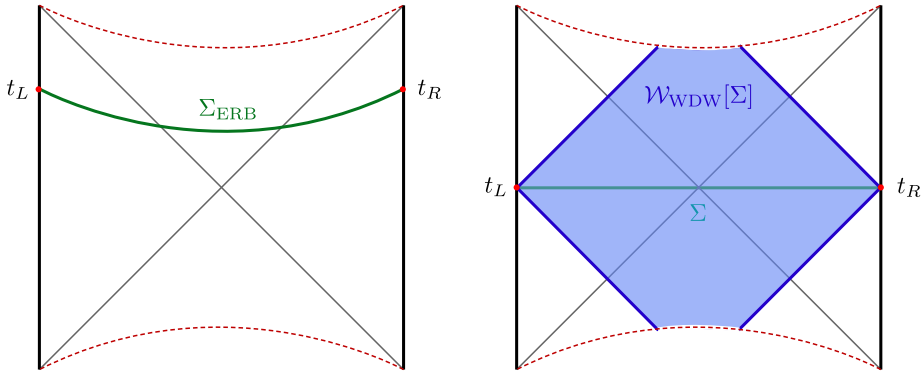

Figure 2.7.: Diagrams of the holographic complexity proposals defined on an eternal AdS black hole, dual to the thermofield-double (TFD) state. On the left, the "complexity=volume" (CV) proposal, where the complexity of the TFD state is given by the volume of the Einstein-Rosen bridge (green line) connecting the asymptotic boundaries where the entangled CFT thermal states live, at times t_L and t_R, $\mathcal{C}_{\mathrm{V}} \sim \mathrm{Vol}(\Sigma_{\mathrm{ERB}})$. On the right, the "complexity=action" (CA) proposal, in which the complexity of the TFD state is given by the gravitational action evaluated on the Wheeler-De Witt patch (WDW) (shaded blue region), defined as the domain of dependence of the hypersurface Σ connecting the two boundaries at times t_L and t_R, $\mathcal{C}_{\mathrm{A}} \sim I_{\mathrm{G}}[\mathcal{W}_{\mathrm{WDW}}] := I_{\mathrm{WDW}}$. The third holographic complexity proposal "complexity=volume 2.0" ($\mathrm{CV}_{2.0}$) posits that the complexity of the TFD state is defined as the spacetime volume of the WDW patch, $\mathcal{C}_{\mathrm{V}_{2.0}} \sim \widetilde{\mathrm{Vol}}(\mathcal{W}_{\mathrm{WDW}})$.

2.3.2. The Subregion Complexity Proposals

A natural question is how to apply the holographic complexity proposals to boundary subregions corresponding to mixed states. The motivation for this is that one of the main goals of the present thesis is to understand the behaviour of subregion complexity in QFTs, whose natural holographic counterparts are the subregion complexity proposals. As such, it is crucial to understand the universal properties of said proposals in scenarios where we can make direct comparisons with the QFT results that will be presented in Sec. 5.2.

The subregion complexity proposals are defined as generalizations of the holographic complexity proposals applicable to finite boundary spatial subregions corresponding to mixed states on the CFT [193–195]. These are constructed by taking into account the existence of the entangelement wedge determined by the boundary subregion. As generalizations of the original proposals, it is possible to recover them in the limit where the subregion is taken to be the full spatial boundary.

Given a spacelike hypersurface Σ_t defining a timeslice of $\mathrm{AdS}_{(D+1)}$, a spatial boundary subregion A on Σ_t, its HRT surface γ_A and entanglement wedge $\mathcal{E}_A$, the holographic subgregion complexity proposals are defined with respect to the intersection of the Wheeler-De Witt patch $\mathcal{W}_{\mathrm{WDW}}(\Sigma_t)$ and the entanglement wedge: $\tilde{\mathcal{W}} :=$

$\mathcal{E}_A \cap \mathcal{W}_{\rm WDW}[\Sigma_t]$. See Fig. 2.8 for details. These are given by

$$\mathcal{C}_{\rm V}(A) := \frac{1}{L\, G_N^{(D+1)}} \max_{\partial R_A = A \cup \gamma_A} [{\rm Vol}(R_A)] = \frac{{\rm Vol}(R_A^{\rm max})}{L\, G_N^{(D+1)}} \ , \tag{2.16a}$$

$$\mathcal{C}_{\rm A}(A) := \frac{I_{\rm G}[\tilde{\mathcal{W}}_A]}{\pi} = \frac{I_{\tilde{\mathcal{W}}_A}}{\pi} \ , \tag{2.16b}$$

$$\mathcal{C}_{\rm V_{2.0}}(A) := \frac{\widetilde{\rm Vol}(\tilde{\mathcal{W}}_A)}{L^2\, G_N^{(D+1)}} \ . \tag{2.16c}$$

The hypersurfaces R_A in (2.16a) are codimension-1 surfaces bounded by A and its HRT surface γ_A. On the other hand, the gravitational action $I_{\rm G}$ in (2.16b) contains various terms including boundary contributions such as a Gibbons–Hawking–York term $I_{\rm GHY}$ for timelike and spacelike boundaries, as well as an analogous term for null boundaries for which one must include an *ad hoc* counter-term $I_{\rm CT}$ to restore reparametrization invariance. That is, in order to evaluate $\mathcal{C}_{\rm A}$ (2.16b) one must compute the following terms

$$I_{\rm G} = I_{\rm Bulk} + I_{\rm GHY} + I_{\rm Null} + I_{\rm CT} + I_{\rm Joints} \ . \tag{2.17}$$

Particularly interesting is the counter-term $I_{\rm CT}$, which requires an introduction of an arbitrary length scale $\ell_{\rm ct}$, which directly influences aspects of complexity.

The subregion $\rm CV_{2.0}$ proposal (2.16c) can be seen to be directly related to the bulk contribution of the gravitational action (2.17), as it evaluates the spacetime volume $\widetilde{\rm Vol}$ of the codimension-0 region $\tilde{\mathcal{W}}_A$

$$\mathcal{C}_{\rm V_{2.0}}(A) = -\frac{8\pi}{D} I_{\rm Bulk}(\tilde{\mathcal{W}}_A) \ . \tag{2.18}$$

The holographic subregion complexity proposals have been studied in a variey of settings [193, 194], which include multiple subregions [196], subregions with defects [197], and subregions in black hole geometries [198, 199].

Of particular interest to us in the context of this thesis are the expressions for the holographic subergion complexity proposals for vacuum subregions of $\rm AdS_3$. Using Poincaré coordinates one finds the following expressions for the subregion complexity proposals for a single boundary spatial interval of size w [196, 200–202]

$$\mathcal{C}_{\rm V} = \frac{2c}{3}\left(\frac{w}{\delta} - \pi\right) \ , \tag{2.19a}$$

$$\mathcal{C}_{\rm A} = \frac{c}{3\pi^2}\left(\frac{w}{2\delta}\log\left(\frac{\ell_{\rm ct}}{L}\right) - \log\left(\frac{2\ell_{ct}}{L}\right)\log\left(\frac{w}{\delta}\right) + \frac{\pi^2}{8}\right) \ , \tag{2.19b}$$

$$\mathcal{C}_{\rm V_{2.0}} = \frac{4c}{3}\left(\frac{w}{2\delta} - \log\left(\frac{w}{\delta}\right) - \frac{\pi^2}{8}\right) \ , \tag{2.19c}$$

where δ is a UV regulator, c is the central charge of the holographic CFT, L is the AdS radius, and the parameter $\ell_{\rm ct}$ in (2.19b) is an arbitrary constant associated with the freedom of defining a counter-term in the computation of the gravitational

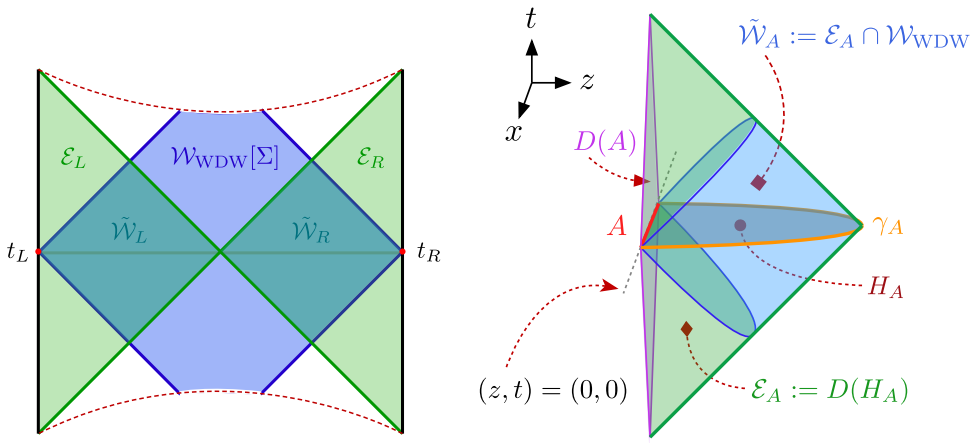

Figure 2.8.: Diagrams of the holographic subregion complexity proposals. On the left, a diagram of an eternal AdS black hole showing the entanglement wedges $\mathcal{E}_{L,R}$ (shaded green regions) of the left and right CFTs, the Wheeler-De Witt (WDW) patch $\mathcal{W}_{\text{WDW}}$ (shaded blue) and their intersections $\tilde{\mathcal{W}}_{L,R} := \mathcal{E}_{L,R} \cap \mathcal{W}_{\text{WDW}}$. On the right, a detail of one such intersections for a spatial subregion A on AdS_3. The subregion CV proposal posits the equivalence of the complexity of the mixed state ρ_A defined on A to be given by the volume (area in this case) of H_A, $\mathcal{C}_{\text{V}} \sim \text{Vol}(H_A)$. The subregion CA and $\text{CV}_{2.0}$ proposals posit instead that the complexity of ρ_A is given respectively by the evaluation of the gravitational action on, and by the spacetime volume of $\tilde{\mathcal{W}}_A := \mathcal{E}_A \cap \mathcal{W}_{\text{WDW}}$, namely $\mathcal{C}_{\text{A}} \sim I_{\text{G}}[\tilde{\mathcal{W}}_A]$ and $\mathcal{C}_{\text{V}_{2.0}} \sim \widetilde{\text{Vol}}(\tilde{\mathcal{W}}_A)$.

action, as we mentioned previously. The central charge c of the CFT enters the expressions via the *Brown–Henneaux formula* [50]

$$c = \frac{3\,L}{2\,G_N^{(3)}} \ . \tag{2.20}$$

Note the general structure of the UV divergences in the expressions (2.19)

$$\mathcal{C}^{\text{holo}}(w) \equiv a_2 \frac{w}{\delta} + a_1 \log\left(\frac{w}{\delta}\right) + a_0 \ , \tag{2.21}$$

where the coefficients a_i can be directly identified by comparing with each individual result. In particular, note that the CV result (2.19a) does not have a subleading logarithmic UV divergence in contrast with the other two results (2.19b), (2.19c).

It is natural to ask whether these results can be generalized to boundary subregions consisting of more than one interval. In particular, considering a set-up where the boundary subregion consists of two components $A \cup B$ naturally leads to a notion which is adequate for studying complexity of multi-component boundary subregions, akin to how mutual information (MI) $I(A:B)$ is an adequate correlation measure for bipartite Hilbert spaces. Such notion is *mutual complexity* (MC) $\Delta\mathcal{C}$ [203].

MC disposes of (some of) the UV divergences inherent to complexity and is therefore regarded as an appropriate quantity for studying subregion complexity. This

quantity can hence be thought of as a "UV-regularised" measure of complexity between subsystems. For general boundary spatial subregions A and B, $\Delta\mathcal{C}$ is defined as:

$$\Delta\mathcal{C}(A:B) := \mathcal{C}(A) + \mathcal{C}(B) - \mathcal{C}(A\cup B)\ . \tag{2.22}$$

In particular, MC can be used to study the complexity of two spatial intervals in the vacuum of AdS_3 characterized by expressions (2.19). A direct computation shows that the MC of *adjacent* boundary spatial intervals A and B of sizes w_A and w_B respectively are given by

$$\Delta\mathcal{C}_{\rm V}(A:B) = -\frac{2\pi\, c}{3}\ , \tag{2.23a}$$

$$\Delta\mathcal{C}_{\rm A}(A:B) = -\frac{c}{3\pi^2}\log\left(\frac{2L}{\ell_{ct}}\right)\log\left(\frac{w_A w_B}{(w_A+w_B)\delta}\right) + \frac{c}{24}\ , \tag{2.23b}$$

$$\Delta\mathcal{C}_{\rm V_{2.0}}(A:B) = -\frac{4c}{3}\log\left(\frac{w_A w_B}{(w_A+w_B)\delta}\right) - \frac{\pi^2 c}{6}\ . \tag{2.23c}$$

From these expressions we find the general structure of their UV divergences to be given by

$$\Delta\mathcal{C}^{\rm holo}(A:B) \equiv a_1\log\left(\frac{w_A w_B}{(w_A+w_B)\delta}\right) + a_0\ , \tag{2.24}$$

where it can be seen that in all three cases the leading UV divergence proportional to the sizes of the individual intervals directly cancels out, leaving the logarithmic divergence as the leading one, except for the CV expression (2.23a) which is constant. Furthermore, it can be seen that in all three cases (2.23) the mutual complexity is negative $\Delta\mathcal{C}(A:B) < 0$ since $a_1, a_0 < 0$, which implies that the complexity of vacuum subregions in AdS_3 is *superadditive*. Of course in the case of the subregion-CA proposal this is mediated by the relation between the constant $\ell_{\rm ct}$ and the AdS radius L.

It can also be seen that if the adjacent intervals are taken to be of sizes $w_A = w_B = \ell/2$, then one can see that the mutual complexity is proportional to the EE, $S_{A\cup B}$, of an interval of size ℓ

$$\Delta\mathcal{C}^{\rm holo} \sim a_1\log\left(\frac{\ell}{\delta}\right) \propto -S_{A\cup B}\ . \tag{2.25}$$

A natural and fundamental question arises when one seeks to establish a concrete connection between the gravitational observables defined by the original and subregion holographic complexity proposals, and a specific quantity on the boundary CFT. Can one go beyond the qualitative analogy provided by Susskind and compute a notion of "complexity" on the CFT side of the AdS/CFT correspondence?

Though we currently do not have a complete understanding of complexity in CFTs, by now there exist two main approaches at characterizing the so-called pure state complexity of a quantum state. The first one is based on a notion of circuit complexity arising from minimizations of *unitary quantum circuits*. We will review this construction, apply it to $(1+1)$-dimensional free theories in Chapter 3 and we will study its time-dependent behaviour in the context of non-equilibrium quantum dynamics in Chapter 4. The other approach is based on the optimization of Euclidean

path-integrals which evaluate CFT wavefunctionals, and is known as *path-integral complexity*.

In the context of spatial subregions, there exist a few proposals for characterizing the complexity of mixed states from the perspective of CFTs. One of these notions, *complexity of purification* (CoP) will be the main focus of Chapter 5 of this thesis. We will show how this notion is capable of characterizing the mixed-state complexity of spatial intervals in $(1+1)$-dimensional free CFTs, displaying a behaviour in remarkable agreement with expressions (2.19) though satisfying the opposite inequality.

We should remark the study of circuit complexity in CFTs and more generally in QFTs has remained within the realm of free theories [101, 102, 204, 205] and of circuits constructed from the stress-energy tensor in 2-dimensional CFTs [206–209]. We currently do not have an understanding of how to compute the complexity of states in interacting theories. Nevertheless, the results that will be presented in the later Chapters of this thesis are intended to lay a foundation for further investigations that will hopefully lead to a better understanding of complexity in more general settings and ultimately to understanding the connection between the conjecture holographic complexity proposals and a concrete notion of complexity in QFTs. The expectation is undoubtedly that by understanding complexity in strongly interacting theories and for states whose holographic dual corresponds to an AdS black hole geometry, we will gain insights into the physics behind the black hole horizon.

3. Complexity in Quantum Field Theory

In this chapter we present the mathematical techniques and tools necessary for describing the computation of circuit complexity of vacuum states of free bosonic and fermionic quantum field theories (QFTs). In Sec. 3.1 we discuss the notion of circuit complexity in quantum information as well as the geometrical tools developed by Michael Nielsen and collaborators which allow this notion to be successfully implemented in free QFTs on a lattice. We then discuss the mathematical structure of the Lie algebras associated with symplectic and orthogonal transformations of bosonic and fermionic Gaussian states and the covariance matrix formalism in Sec. 3.2. We then use these tools to study the complexity of bosonic and fermionic vacuum states in Sec. 3.3, which are Gaussian. By the end of this chapter we will have the necessary mathematical and physical background that will be used in the subsequent chapters of the thesis which discuss complexity in non-equilibrium quantum dynamics and subregion complexity in QFTs.

3.1. Complexity in Quantum Information

The concept of circuit complexity has its origins in computer science and is associated with the process of preparing quantum states in a quantum circuit. Suppose that we are given an initial (*reference*) state $|\psi_{\mathrm{R}}\rangle$, which could consist on, say, n-qubits $|0,\ldots,0\rangle$, and a set of discrete operations $\mathcal{G}=\{\hat{U}_{g_1},\ldots,\hat{U}_{g_N}\}$ which we can apply to said state. Such a set of discrete operations, called *gates*, could incorporate quantum versions of logical gates which act locally on a discrete set of qubits, such as the Pauli, Hadamard, Toffoli, CNOT, and SWAP gates.

Suppose we are asked what is the optimal way that we can produce a final (*target*) state $|\psi_{\mathrm{T}}\rangle$ by applying gates belonging to the set $\mathcal{G}$ to $|\psi_{\mathrm{R}}\rangle$. In this context we can think of the target state being a different n-qubit state, *e.g.*, $|1,0,1,1,\ldots,0\rangle$. There are in principle an infinite number of ways in which we can produce the state $|\psi_{\mathrm{T}}\rangle$ by acting successively on $|\psi_{\mathrm{R}}\rangle$ with the gates $\hat{U}_{g_i}\in\mathcal{G}$ via a quantum circuit

$$|\psi_{\mathrm{T}}\rangle=\hat{U}\,|\psi_{\mathrm{R}}\rangle=\hat{U}_{g_{i_N}}\cdots\hat{U}_{g_{i_1}}\,|\psi_{\mathrm{R}}\rangle\ , \tag{3.1}$$

and different combinations and permutations of the same operations can also yield the same final sate, or at least come close to producing it. That is, one may need to consider a tolerance ϵ such tat even if it is not possible to produce the desired state exactly, the transformation $\hat{U}$ still brings the reference state close to the target state, according to some distance measure $||\,|\psi_{\mathrm{T}}\rangle-\hat{U}\,|\psi_{\mathrm{R}}\rangle\,||^2\leq\epsilon$.

The notion of complexity then arises when we ask if there is an *optimal* way in which we can apply the desired transformation on $|\psi_{\mathrm{R}}\rangle$, *i.e.*, with a minimal number of operations. In other words: is there an optimal quantum circuit which allows

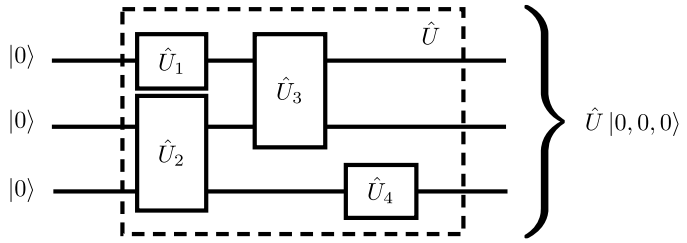

Figure 3.1.: A quantum circuit $|\psi_{\mathrm{T}}\rangle = \hat{U}\,|\psi_{\mathrm{R}}\rangle = \hat{U}\,|0,0,0\rangle$. The unitary $\hat{U}$ is built from unitaries $\hat{U}_i$ which act locally on the three qubits acting from left to right.

us to produce the target state from the reference state: $|\psi_{\mathrm{T}}\rangle = \hat{U}_{g_{\alpha_M}} \cdots \hat{U}_{g_{\alpha_1}}\,|\psi_{\mathrm{R}}\rangle$? *Complexity* is then defined as the size or *length* of this optimal quantum circuit.

In essence, complexity is a measure of how many (typically unitary) transformations we need to apply to a state in order to obtain another one. That is, how much more "complex" is this target state with respect to the original reference state. In this sense, complexity can be associated with a notion of distance between quantum states, albeit a special one, and which differs from the usual inner product in Hilbert space.

A clear argument that provides an intuitive explanation of this fact can be found in [210] and is as follows: consider a very complicated highly-entangled state $|\Psi\rangle$ and two other states constructed from taking its tensor product with a single qubit: $|\Psi\rangle \otimes |0\rangle$ and $|\Psi\rangle \otimes |1\rangle$. If we compute the usual inner product on Hilbert space we would find that these states are orthogonal, because $\langle 0\,|\,1\rangle = 0$, and hence infinitely far away from each other; since orthogonal states cannot be more different, or far away, from each other. But as we can also note, a single operation acting on the qubit would suffice to transform one state into the other; and in this sense these states are not so different from each other. This operation would simply be given by $\hat{\mathbb{1}} \otimes \hat{X}$, where $\hat{X}$ is the Pauli X-gate, which satisfies $\hat{X}\,|0\rangle = |1\rangle$ and vice versa. This means that there is another way besides the usual inner product in which we can quantify how close these two states are to each other. This special notion of distance between states is the one captured by complexity.

It is also important to note that complexity, as a particular measure of distance between states, is dependent on the choice of reference and target state, as well as on the set of allowed operations and on a notion of distance associated with the length of the quantum circuit connecting such states. Formally speaking, this is referred to as *state complexity* and quantifies how difficult it is to produce one state using a set of universal gates $\mathcal{G}$, given another one. There is also a notion of *gate complexity*, which instead quantifies the minimum number of discrete operations that one needs in order to implement a given transformation. In the limit where there is a continuous implementation of transformations defining a unitary operator of this type, complexity is referred to as *unitary complexity*. While distinct, we will usually focus on the first one, and simply refer to it as *circuit complexity*.

These are intimately connected with another concept commonly used in computer science called computational complexity. This notion refers to the hardness of computational problems and is often formalized in terms of number of steps required by deterministic Turing machines to solve given computational problems [28, 211, 212]. In computational complexity theory one studies different classes of promise problems and attempts to classify whether they are solvable and under which conditions. While this concept does not enter the main discussion of this work, it is still relevant to establish a connection between the notion of complexity that we are interested in, and other ones which are also used in computer science, and which are central to the efforts of realizing quantum computers.

Coming back to quantum circuits such as (3.1), it's not too difficult to convince oneself that it is in general a complicated question to ask what is the optimal choice of gates that produces a desired target state. Or what is the most efficient way to implement a desired operation on a given reference state. This is in fact a central problem of quantum computing and apart from certain known examples, it is in general not known how to efficiently, *i.e.*, in polynomial time, implement unitary operations on quantum systems comprised of many qubits.

3.1.1. The Geometric Approach to Circuit Complexity

It is because of this, that the ideas developed by Michael Nielsen and collaborators on how to tackle the construction of quantum circuits using geometric tools [213–215] became relevant and even crossed the border of quantum computing and into the high-energy physics community. Over such series of works, they systematically translated the problem of finding optimal quantum circuits that efficiently implement a unitary operation $\hat{U}$, into the problem of finding geodesics in Riemannian manifolds. Initially Nielsen intended his computations to serve as a lower bound on the minimal size of a quantum circuit that exactly implements an n-qubit operation, as can be seen in [214].

In order to do this, they used the theory of optimal quantum control [216–218] to construct a time-dependent Hamiltonian $\hat{H}(t)$ that generates the desired unitary $\hat{U}$ in (3.1) via

$$\hat{U} = \overleftarrow{\mathcal{P}} \left\{ \exp\left(-\mathrm{i} \int_0^1 \mathrm{d}t\, \hat{H}(t) \right) \right\} \ , \tag{3.2}$$

where the *control Hamiltonian* $\hat{H}(t)$ is expanded in terms of elementary operations $\hat{K}_\mathrm{I}$ as[1]

$$\hat{H}(t) = \sum_\mathrm{I} Y^\mathrm{I}(t) \hat{K}_\mathrm{I} \ , \tag{3.3}$$

where the symbol $\overleftarrow{\mathcal{P}}$ in (3.2) denotes a path-ordering such that the operations at earlier time-steps are applied to the reference state first, *i.e.*, the quantum circuit is built from right to left. The $Y^\mathrm{I}(t)$ are *control functions* which are responsible for

[1] In Nielsen's original works the elementary operations $\hat{K}_\mathrm{I}$ corresponded to Pauli matrices, given that he was interested in studying the action of $\mathrm{SU}(2^n)$ gates on quantum circuits comprised of n-qubit states.

"activating" a particular gate $\hat{K}_{\mathrm{I}}$ at time t. Note that in order for $\hat{U}$ in (3.2) to be unitary, the generators $\hat{K}_{\mathrm{I}}$ in (3.3) must be Hermitian.

Note that (3.2) defines *path* in the space of unitaries $\mathcal{G}$ via

$$\hat{U}(\tau) = \overleftarrow{\mathcal{P}} \left\{ \exp\left(-\mathrm{i} \int_0^\tau \mathrm{d}t\, \hat{H}(t) \right) \right\} \ , \tag{3.4}$$

with boundary conditions: $\hat{U}(\tau = 1) = \hat{U}$, as in (3.2), and $\hat{U}(\tau = 0) = \hat{\mathbb{1}}$. Then, for every value of $\tau \in [0, 1]$, the action of the unitary $\hat{U}(\tau)$ on the reference state $|\psi_{\mathrm{R}}\rangle$ defines a state $|\psi(\tau)\rangle$ which is constructed from the successive application of gates $\hat{K}_{\mathrm{I}}$ activated by functions $Y^{\mathrm{I}}(t)$. From (3.4) we can also see that the control functions Y^{I} define in general a tangent vector to the trajectory $\hat{U}(\tau)$ with

$$\sum_{\mathrm{I}} Y^{\mathrm{I}}(\tau)\hat{K}_I = \frac{\mathrm{d}\hat{U}(\tau)}{\mathrm{d}\tau}\hat{U}^{-1}(\tau) \ . \tag{3.5}$$

The idea is then to associate a *cost* for different circuits associated with paths in Hilbert space defined by unitaries (3.4). This is done by considering a *cost function* $F(\hat{U}(\tau), \partial_\tau \hat{U}(\tau))$, such that

$$\mathcal{D}_F(\hat{U}) = \int_0^1 \mathrm{d}\tau\, F(\hat{U}(\tau), \partial_\tau \hat{U}(\tau)) \ , \tag{3.6}$$

defines the *depth*, or length $l_F(\hat{U})$, of the circuit. In order to identify the optimal circuit one should find the minimum of $\mathcal{D}_F(\hat{U})$ for a choice of cost function F.

The authors of [213–215] identified the properties that cost functions $F(U, v)$ with $U \in \mathcal{G}$ and $v \in T_U(\mathcal{G})$ should have in order to by physically reasonable. These properties include continuity, positivity, (positive) homogeneity and subadditivity. If one further imposes the condition of smoothness, then (3.6) defines a distance or length functional for a class of smooth manifolds called *Finsler manifolds* [219]. Essentially, a Finsler manifold is a manifold where each tangent space is equipped with a norm that is not necessarily induced by an inner product.

In such a way, the authors of [213–215] translated the problem of finding optimal circuits into the problem of finding geodesics in Finsler geometries, where the complexity of the circuit is identified with the length of the geodesic joining the reference and target states. In other words

$$\mathcal{C}_F := \min[\mathcal{D}_F] \ . \tag{3.7}$$

Regarding the cost functions F (3.6), the authors of [213–215] the properties of possibilities such as

$$F_1^p(U, \vec{Y}) = \sum_{\mathrm{I}} p_{\mathrm{I}}(U) \left| Y^{\mathrm{I}} \right| \ , \tag{3.8a}$$

$$F_2^q(U, \vec{Y}) = \sqrt{\sum_{\mathrm{IJ}} q_{\mathrm{IJ}}(U) Y^{\mathrm{I}} Y^{\mathrm{J}}} \ , \tag{3.8b}$$

where the functions $\{p_{\mathrm{I}}(U), q_{\mathrm{IJ}}(U)\}$ are *penalty factors*, *i.e.*, numbers or functions which are meant to penalize certain functions Y^{I} in order to control how much

a particular operator $\hat{K}_{\mathrm{I}}$ contributes to the circuit depth at given points of the path $\hat{U}(\tau)$ thus providing a way of distinguishing between gates which are "easy" to implement, and gates which are "hard" to implement. That is, penalty factors are used to "penalize" certain gates in the quantum circuit. In the case in which there are no penalty factors, *i.e.*, $p_{\mathrm{I}} \propto 1$ and $q_{\mathrm{IJ}} \propto \mathbb{1}_2$, these cost functions are simply denoted respectively by F_1 and F_2, and define the known L^1 and L^2 norms in finite-dimensional vector spaces.

The authors of [213–215] were particularly interested in the first one of these, namely (3.8a), since its associated circuit depth (3.6) can be interpreted as the time needed to implement the unitary (3.4). However its main disadvantage is that it is not smooth. As a consequence, the cost function (3.8a) does not define a Finsler metric and one cannot directly apply the calculus of variations to find its minimal-length curves. In other words, minimizing such cost function is in general a challenging task.

This is not the case for (3.8b). Here, the positive-definite functions $\{q_{\mathrm{IJ}}(U)\}$ can be thought of as defining a *local metric* on the tangent space $T_Y(U)$. In this sense, this cost function induces the known L^2-type norm or distance, used to characterize the length of curves in Riemannian geometry, and which allows for a minimization of the circuit depth $\mathcal{D}_2$ (3.6) using the known techniques of calculus of variations and differential geometry.

Apart from these two, one could in principle consider other cost functions which incorporate sums of products of p control functions with an appropriate power of $1/p$. Such functions would be of the form $F_p \sim (\sum_{\mathrm{I}} |Y^{\mathrm{I}}|^p)^{1/p}$ and would lead to L^p norms. While mathematically interesting, these kinds of norms are less studied in the context of complexity.

Even though in the context of [213–215] only the F_1 cost function appeared to have interesting properties, it is *a priori* not clear which one of these would be "appropriate" in a different scenario. Of course, the advantage of the F_2 cost function is that it is in principle possible to minimize its associated circuit depth $\mathcal{D}_2$, while the physical interpretation of the F_1 cost function is closer to the original motivation of understanding how to efficiently implement an n-qubit operation as in the case of [213–215]. As we will see in Sec. 3.3.1 and Sec. 3.3.2, the geometric approach put forth by the authors of [213–215] will allow us to study the complexity of vacuum states of free quantum field theories. In these cases, the spaces of unitaries will consist of symplectic and orthogonal transformations allowing for an elegant description using the covariance matrix formalism, which will be the focus of the following section.

3.2. Gaussian Techniques

Given a quantum field theory (QFT) in D-dimensions, one is typically interested in computing n-point correlation functions, such as $\langle 0|\hat{O}_1(x_1)\cdots\hat{O}_n(x_n)|0\rangle$ for a set of operators $\hat{O}_i$ associated with physical observables, as these are directly related to the probability amplitude of physical processes in said theory. In momentum

space, such correlators give rise to scattering amplitudes which yield the probability amplitude of scattering processes of particles in the theory.

In essence, knowing the n-point correlation functions of a state in a quantum field theory amounts to having access to all its relevant physical information. However, it is in practice a difficult task to actually compute these n-point functions, although crucial results such as Wick's theorem allows us to reduce the problem of computing higher-point functions to lower-point functions. At the same time, in conformal field theories in D-dimensions, two and three-point functions of primary fields are completely fixed, up to normalization, by conformal symmetry [220]. In contrast, higher-point functions are not fully determined by conformal symmetry and are in general functions of cross-ratios of spacetime coordinates and are theory-dependent.

The choice of a quantum state is also implicit in the computation of the correlation functions. Typically one considers ground states of free theories or primary states in the case of conformal field theories. Of special interest in this work, however, are the ground states of free Hamiltonians in quantum field theories, as these have the property of being completely characterised by their two-point functions. While at first glance this fact could be interpreted as signaling the mathematical triviality of such states, they are in fact used extensively in quantum information and quantum field theory. The fact that Gaussian states are completely characterized by their two-point functions also allows us to use the mathematical machinery of symplectic and orthogonal transformations and their associated Lie groups to describe them. As we will show in the following chapters, this will in turn allow to study the complexity and entanglement of vacuum states of free quantum field theories in a compact and elegant way, providing also a clear picture of how the physical information of such states is encoded in these quantities.

3.2.1. The Covariance Matrix Approach

In the following sections and chapters, we will be interested in studying the complexity of Gaussian states in free bosonic QFTs on a lattice. As a consequence, it will be useful to have a complete description of their mathematical properties. We will do this in this section.

A bosonic or fermionic system with N degrees of freedom can be described by $2N$ observables $\hat{\xi}^a \equiv \{\hat{q}^1, \hat{p}^1, \ldots, \hat{q}^N, \hat{p}^N\}$ which correspond to canonical coordinates in a classical phase space. Such phase space coordinates satisfy canonical commutation or anticommutation relations

$$[\hat{\xi}^a, \hat{\xi}^b] = \mathrm{i}\,\Omega^{ab} \ , \tag{3.9a}$$

$$\{\hat{\xi}^a, \hat{\xi}^b\} = G^{ab} \ , \tag{3.9b}$$

where G^{ab} is a symmetric positive definite metric and Ω^{ab} is a non-degenerate anti-symmetric symplectic form.

A normalized Gaussian quantum state $|\psi\rangle$ with vanishing one-point functions $\langle\psi|\hat{\xi}^a|\psi\rangle = 0$ is completely characterised by its two-point function C_2^{ab} with entries defined by

$$C_2^{ab} := \langle\psi|\, \hat{\xi}^a \hat{\xi}^b \,|\psi\rangle \ . \tag{3.10}$$

We can also decompose it into a symmetric and an antisymmetric part

$$C_2^{ab} = \frac{1}{2}\left(G^{ab} + \mathrm{i}\Omega^{ab}\right) \ . \tag{3.11}$$

It can be shown that due to the commutation and anticommutation relations (3.9) and up to basis' transformations, G^{ab} is fixed for fermions while Ω^{ab} is fixed for bosons, which implies that only the other piece of the two-point function (3.11), namely G^{ab} for bosons and Ω^{ab} for fermions, will depend on the state $|\psi\rangle$. By this we mean that for a given choice of basis $\hat{\xi}^a$, the expressions for Ω^{ab} and G^{ab} are fixed. For example, in canonical coordinates $\hat{\xi}^a = (\hat{q}^1, \hat{p}^1, \ldots, \hat{q}^N, \hat{p}^N)$

$$\Omega = \begin{pmatrix} 0 & \mathbb{1}_N \\ -\mathbb{1}_N & 0 \end{pmatrix} \ , \ G = \begin{pmatrix} \mathbb{1}_N & 0 \\ 0 & \mathbb{1}_N \end{pmatrix} \ , \tag{3.12}$$

where $\mathbb{1}_N$ is the identity matrix in N dimensions. As a consequence, Ω^{ab} and G^{ab} completely characterize Gaussian states and are respectively called the fermionic and bosonic *covariance matrices*.

Consider, for example, a pure Gaussian state $|\psi\rangle$ corresponding to the ground state of a single harmonic oscillator in a bosonic free quantum field theory, *i.e.*, $|\psi\rangle$ describes a single bosonic mode. Such a state can be characterized by its wavefunction

$$\langle q|\psi\rangle = \psi(q) = \left(\frac{a}{\pi}\right)^{1/4} \exp\left\{-\frac{1}{2}(a + \mathrm{i}b)q^2\right\} \ , \tag{3.13}$$

where $a, b \in \mathbb{R}$, and $a > 0$. In this case, the covariance matrix

$$G^{ab} := \langle\psi| \left(\hat{\xi}^a\hat{\xi}^b + \hat{\xi}^b\hat{\xi}^a\right) |\psi\rangle \ , \tag{3.14}$$

can be computed directly using canonical coordinates $\hat{\xi}^a = \{\hat{q}, \hat{p}\}$ and is given by

$$G = \begin{pmatrix} \frac{1}{a} & \frac{-b}{a} \\ \frac{-b}{a} & \frac{a^2+b^2}{a} \end{pmatrix} \ . \tag{3.15}$$

In the wavefunction (3.13), the functions a and b completely characterize the Gaussian state. Equivalently, one can think of these as given in terms of the covariance matrix entries (3.15), which are related to the 2-point correlation functions via

$$a = \frac{1}{G^{11}} = \frac{1}{\langle\psi| 2\hat{q}^2 |\psi\rangle} \ , \tag{3.16a}$$

$$b = \frac{-G^{21}}{G^{11}} = \frac{-\langle\psi| (\hat{q}\hat{p} + \hat{p}\hat{q}) |\psi\rangle}{\langle\psi| 2\hat{q}^2 |\psi\rangle} \ , \tag{3.16b}$$

where $G^{11} = \langle\psi| 2\hat{q}^2 |\psi\rangle > 0$, thus showing that the covariance matrix (3.15) contains the same physical information about the state as the wavefunction (3.13). There are other equivalent ways of representing Gaussian states which are not covered in this present work, such as the characteristic function and the quasi-probability distribution. The reader can refer to [221] for a detailed description of them.

One can further check that in this case $\det(G) = 1$ and therefore the entry G^{22} of (3.15) doesn't carry additional information about the state. The fact that the

determinant of the covariance matrix of state (3.13) is the unity is a general property of pure Gaussian states.

This can be made more precise by the definition of a linear map called the *linear complex structure* J^{ab} defined via

$$J^a{}_b := -G^{ac}\Omega^{-1}_{cb} = \Omega^{ac}G^{-1}_{cb} \ . \tag{3.17}$$

It can be shown that $|\psi\rangle$ is a pure Gaussian state, if and only if $J^2 = -\mathbb{1}$, which implies that the eigenvalues of J, called *symplectic eigenvalues*, which in general come in pairs, are given in this case by $\pm\mathrm{i}$ [222, 223].

It is also important to note that the complex structure J provides a unified way of denoting both bosonic and fermionic Gaussian states simply by $|J\rangle$, as it integrates both the symmetric and antisymmetric part of the 2-point function (3.11). It also allows to define a notion of creation and annihilation operators [224] and on the mathematical level, it endows the phase space of Gaussian states with a Käler structure, a full description of which escapes the scope of this work. However, the reader can refer to the elegant discussion of this aspect of Gaussian states in [221].

Of course, not only pure Gaussian states can be described in terms of their complex linear structure. Mixed Gaussian states described by a density matrix ρ are also uniquely characterized by their covariance matrix, computed in this case via

$$G^{ab}_\rho = \mathrm{tr}\left(\rho\left(\hat{\xi}^a\hat{\xi}^b + \hat{\xi}^b\hat{\xi}^a\right)\right) \ , \tag{3.18a}$$

$$\Omega^{ab}_\rho = \mathrm{tr}\left(\rho\left(\hat{\xi}^a\hat{\xi}^b - \hat{\xi}^b\hat{\xi}^a\right)\right) \ , \tag{3.18b}$$

in which case, their complex structures now satisfies the inequalities: $\mathbb{1} \leq -J^2$ for bosons, and $0 \leq -J^2 \leq \mathbb{1}$ for fermions. Additionally, in order for a mixed state ρ to be Gaussian, there should exist a positive-definite bilinear form q_{ab} and a constant c_0 such that

$$\rho = \begin{cases} e^{-q_{ab}\hat{\xi}^a\hat{\xi}^b - c_0} \ , \\ e^{-\mathrm{i}\,q_{ab}\hat{\xi}^a\hat{\xi}^b - c_0} \ , \end{cases} \tag{3.19}$$

where the top expression corresponds to bosons, and the bottom one to fermions. We will return to mixed Gaussian states when we discuss complexity and entanglement of purification, in Ch. 5 and 6.

3.2.2. The Symplectic and Orthogonal Groups

The usefulness of the covariance matrix approach, however, becomes manifest when one studies trajectories of states within the subspace of Gaussian states. By considering only such a class of states one gets restricted to transformations belonging to the symplectic group $\mathrm{Sp}(2N,\mathbb{R})$ in the case of bosons, and to the orthogonal group $\mathrm{O}(2N,\mathbb{R})$ in the case of fermions. The reason being that these Lie groups preserve the symplectic form Ω^{ab} and the metric G^{ab} respectively, allowing us to remain within the subspace of Gaussian states. These Lie groups are formally defined in the following way

$$\mathrm{Sp}(2N,\mathbb{R}) := \{M^a{}_b \in \mathrm{GL}(2N,\mathbb{R}) \,|\, M\Omega M^\intercal = \Omega\} \ , \tag{3.20a}$$

$$\mathrm{O}(2N,\mathbb{R}) := \{M^a{}_b \in \mathrm{GL}(2N,\mathbb{R}) \,|\, MGM^\intercal = G\} \ , \tag{3.20b}$$

while their associated Lie algebras are defined by

$$\mathfrak{sp}(2N,\mathbb{R}) := \{K^a{}_b \in \mathfrak{gl}(2N,\mathbb{R}) \,|\, K\Omega + \Omega K^\intercal = 0\} \ , \tag{3.21a}$$

$$\mathfrak{so}(2N,\mathbb{R}) := \{K^a{}_b \in \mathfrak{gl}(2N,\mathbb{R}) \,|\, KG + GK^\intercal = 0\} \ , \tag{3.21b}$$

It should be noted that the Lie algebras of $\mathrm{O}(2N,\mathbb{R})$ and $\mathrm{SO}(2N,\mathbb{R})$ coincide and correspond to $\mathfrak{so}(2N,\mathbb{R})$. In this context, it is common to denote with $\mathcal{G}$ the Lie groups $\mathrm{Sp}(2N,\mathbb{R})$ and $\mathrm{O}(2N,\mathbb{R})$ and with $\mathfrak{g}$ the Lie algebras $\mathfrak{sp}(2N,\mathbb{R})$ and $\mathfrak{so}(2N,\mathbb{R})$ when discussing the covariance matrix approach to Gaussian states from a general perspective. In the same vein, it is also common to generically denote the covariance matrix of bosonic and fermionic Gaussian states with Γ.

It is possible to construct representations of the Lie groups (3.20) as unitary operators $\mathcal{R}(M)$ acting on Hilbert space by exponentiating quadratic operators. To do this, elements of the Lie algebras $K \in \mathfrak{g}$ can be identified with quadratic anti-Hermitian operators $\hat{K}$ via

$$K^a{}_b \iff \hat{K} = \begin{cases} -\frac{\mathrm{i}}{2}\Omega^{-1}_{ac} K^c{}_b \hat{\xi}^a \hat{\xi}^b \ , \\ \frac{1}{2} G^{-1}_{ac} K^c{}_b \hat{\xi}^a \hat{\xi}^b \ , \end{cases} \tag{3.22}$$

where the top expression corresponds to bosons and the lower one to fermions, such that for any $M = e^K \in \mathcal{G}$ and up to a complex phase, one can define the following operator

$$\mathcal{R}(M) = \mathcal{R}(e^K) = e^{\hat{K}} \ . \tag{3.23}$$

For bosons, this identification immediately defines a unitary operator which maps Gaussian states into Gaussian states. For example, the unitary $\mathcal{R}(M(\sigma)) = e^{\sigma \hat{K}}$, for $K \in \mathfrak{sp}(2N,\mathbb{R})$ maps a Gaussian state $|G_{\mathrm{R}}\rangle$ into a one-parameter family of Gaussian states via $|G_\sigma\rangle = \mathcal{R}(M(\sigma))\,|G_{\mathrm{R}}\rangle = |\left(e^{\sigma K}\right) G_{\mathrm{R}} \left(e^{\sigma K}\right)^\intercal\rangle$ [221, 225].

However in the case of fermions one needs to be more careful, as considering the exponential map of elements of $\mathfrak{so}(2N,\mathbb{R})$ would generate only the subgroup of $\mathrm{O}(2N,\mathbb{R})$ connected to the identity map, namely $\mathrm{SO}(2N,\mathbb{R})$. By considering a dual vector v_a satisfying $v_a G^{ab} v_b = 2$, one can define a representation $\mathcal{R}(M_v) = v_a \hat{\xi}^a$ of the matrix $(M_v)^a{}_b = v_c G^{ca} v_b - \delta^a{}_b$ with $\det(M_v) = -1$ leading to a projective representation $\mathcal{R}(e^K)\mathcal{R}(M_v) = \pm\mathcal{R}(e^K M_v)$ of the elements of $\mathrm{O}(2N,\mathbb{R})$ not connected to the identity. Together with (3.23) for $K \in \mathfrak{so}(2N,\mathbb{R})$, this representation is capable of generating the full $\mathrm{O}(2N,\mathbb{R})$ group.

3.2.3. The Relative Complex Structure and its Spectrum

Transformations that preserve both the symplectic form Ω^{ab} and metric G^{ab}, which are given by the intersection of $\mathrm{Sp}(2N,\mathbb{R})$ and $\mathrm{O}(2N,\mathbb{R})$, belong to the unitary group

$$\begin{aligned} \mathrm{U}(N) :&= \{M \in \mathcal{G} \,|\, M\Gamma M^\intercal = \Gamma\} \\ &= \left\{M \in \mathcal{G} \,|\, MJM^{-1} = J\right\} \ , \end{aligned} \tag{3.24}$$

which is also the stabilizer subgroup of Gaussian states $|J\rangle$, since it preserves both J and Γ. To be more precise, the stabilizer subgroups depend on the state $|J\rangle$

$$\mathrm{Sta}_{\mathrm{Sp}(2N,\mathbb{R})} = \{\mathcal{U} \in \mathrm{Sp}(2N,\mathbb{R}) \,|\, \mathcal{U}G\mathcal{U}^{\intercal} = G\} \cong \mathrm{U}_G(N) \ , \tag{3.25a}$$

$$\mathrm{Sta}_{\mathrm{O}(2N,\mathbb{R})} = \{\mathcal{U} \in \mathrm{O}(2N,\mathbb{R}) \,|\, \mathcal{U}\Omega\mathcal{U}^{\intercal} = \Omega\} \cong \mathrm{U}_\Omega(N) \ . \tag{3.25b}$$

The associated unitary operator $\mathcal{R}(\mathcal{U})$ preserves the state $|J\rangle$ up to a complex phase: $\mathcal{R}(\mathcal{U})\,|J\rangle = |J\rangle$ for all $\mathcal{U} \in \mathrm{U}(N)$. This defines the Lie subalgebra

$$\begin{aligned} \mathfrak{u}(N) :&= \{K \in \mathfrak{g} \,|\, K\Gamma + \Gamma K^{\intercal} = 0\} \\ &= \{K \in \mathfrak{g} \,|\, [K, J] = 0\} \ , \end{aligned} \tag{3.26}$$

which also preserves the state: $\hat{K}\,|J\rangle \propto |K\rangle$ for $K \in \mathfrak{u}(N)$.

In general, given a Gaussian reference state $|J_{\mathrm{R}}\rangle$, it is possible to reach any other Gaussian target state $|J\rangle$ via

$$|J\rangle = \mathcal{R}(M)\,|J_{\mathrm{R}}\rangle = |M\Gamma_{\mathrm{R}}M^{\intercal}\rangle \ , \tag{3.27}$$

for $M \in \mathcal{G}$. For bosons, the generator $K \in \mathfrak{g}$ of the transformation $M \in \mathcal{G}$ can be found simply by taking $K = \log(M)$, while for fermions one finds it by taking $K = \log(MM_v^{-1})$. However, there is no unique solution to the condition $M\Gamma_{\mathrm{R}}M^{\intercal} = \Gamma$, as one can always multiply by $u \in \mathrm{U}_{J_{\mathrm{R}}}(N)$ in such a way that $(Mu)\Gamma_{\mathrm{R}}(Mu)^{\intercal} = Mu\Gamma_{\mathrm{R}}u^{\intercal}M^{\intercal} = M\Gamma_{\mathrm{R}}M^{\intercal}$. Nevertheless, one can find a specific solution T by imposing the constraint $T\Gamma_{\mathrm{R}} = \Gamma_{\mathrm{R}}T^{\intercal}$, which leads to an equation $J = TJ_{\mathrm{R}}T^{-1} = T^2J_{\mathrm{R}}$ which can be solved by $T^2 = -JJ_{\mathrm{R}}$. This leads to the definition of *relative complex structure*, or *relative covariance matrix*

$$\mathscr{G}^a{}_b := -J^a{}_c(J_{\mathrm{R}})^c{}_b = \Gamma^{ac}(\Gamma_{\mathrm{R}}^{-1})_{cb} \ , \tag{3.28}$$

a notion which captures the full information about the relation between two Gaussian states $|J\rangle$, and $|J_{\mathrm{R}}\rangle$, in a basis invariant way. In other words, any function which is invariant under the action of $\mathcal{G}$ is a function only of the spectrum of $\mathscr{G}$. As we will see in Sec. 3.3.1 and Sec. 3.3.2, this powerful observation will allow to define a notion of circuit complexity for bosonic and fermionic Gaussian states invariant under transformations belonging to $\mathcal{G}$.

For bosons, the spectrum of $\mathscr{G}$ consists of pairs (e^{2r_i}, e^{-2r_i}) with $r_i \in [0,\infty)$, such that $T = \sqrt{\mathscr{G}}$ has eigenvalues (e^{r_i}, e^{-r_i}), where the r_i are called *squeezing parameters*. This means that $\mathscr{G}$ is an element of $\mathrm{Sp}(2N,\mathbb{R})$ and is diagonalizable. Consider for example, a single bosonic mode and the canonical basis $\hat{\xi} = (\hat{q}, \hat{p})$. The most general Gaussian state $|J\rangle$ (see *e.g.*, [226]) can be written with respect to number eigenstates $|n\rangle$ as

$$|J\rangle = \frac{1}{\sqrt{\cosh(r)}} \sum_{n=0}^{\infty} \frac{\sqrt{(2n)!}}{2^n n!} \left(-e^{\mathrm{i}\,\phi}\,\tanh(r)\right)^n |2n\rangle \ , \tag{3.29}$$

where $\phi \in [0, 2\pi)$ and $r \in [0,\infty)$. In this case, the covariance matrix G^{ab} and complex structure $J^a{}_b$ can be written with respect to the basis $\hat{\xi}$ as

$$G = \begin{pmatrix} \cosh(2r) + \cos(\phi)\sinh(2r) & \sin(\phi)\sinh(2r) \\ \sin(\phi)\sinh(2r) & \cosh(2r) - \cos(\phi)\sinh(2r) \end{pmatrix} \ , \tag{3.30a}$$

$$J = \begin{pmatrix} -\sin(\phi)\sinh(2r) & \cos(\phi)\sinh(2r)+\cosh(2r) \\ \cos(\phi)\sinh(2r)-\cosh(2r) & \sin(\phi)\sinh(2r) \end{pmatrix} , \tag{3.30b}$$

from which it can be seen that single bosonic modes form a two-dimensional subspace and can be parametrized by polar coordinates (r, ϕ). If we now consider a reference state $|J_{\mathrm{R}}\rangle$ with

$$G_{\mathrm{R}} = \begin{pmatrix} 1 & 0 \\ 0 & 1 \end{pmatrix} \quad , \quad J_{\mathrm{R}} = \begin{pmatrix} 0 & 1 \\ -1 & 0 \end{pmatrix} , \tag{3.31}$$

then from the relative complex structure $\mathscr{G} = -JJ_{\mathrm{R}}$ we can compute the generator

$$K = \frac{1}{2}\log(\mathscr{G}) = r \begin{pmatrix} \sin(\phi) & \cos(\phi) \\ \cos(\phi) & -\sin(\phi) \end{pmatrix} , \tag{3.32}$$

of the transformation $\mathcal{R}(e^K) = e^{\hat{K}}$ such that $|J\rangle = e^{\hat{K}}|J_{\mathrm{R}}\rangle$. By transforming to a basis for which $\phi = \pi/2$, we can read-off the spectrum (e^{2r}, e^{-2r}) of $\mathscr{G}$. In general, for a Gaussian state of N bosonic modes, we are able to decompose it into 2×2 one-mode blocks, where each of the blocks will be parametrized by (r_i, ϕ_i) as in (3.30), and in which case the relative covariance matrix with respect to a state $|J_{\mathrm{R}}\rangle$ with at 2×2 block structure given by (3.31) satisfies $\mathscr{G} = \oplus_i \mathscr{G}^i$ with $\mathscr{G}^i$ having a spectrum, like shown above, given by (e^{2r_i}, e^{-2r_i}).

In the case of fermions, the spectrum of $\mathscr{G}$ is richer [221, 226]. Its eigenvalues consist of quadruples $(e^{\mathrm{i}\,2r_i}, e^{\mathrm{i}\,2r_i}, e^{-\mathrm{i}\,2r_i}, e^{-\mathrm{i}\,2r_i})$ with $r_i \in (0, \pi/2)$ or of pairs $(1,1)$ or $(-1,-1)$, corresponding to $r_i \in \{0, \pi/2\}$. If the number of pairs $(-1,-1)$ appearing in the spectrum of $\mathscr{G}$ is even, then J and J_{R} belong to the same topological component of fermionic Gaussian states, meaning that they can be continuously transformed into each other, and in this case $T = \sqrt{\mathscr{G}}$ will exist but will not be unique. If the number of pairs $(-1,-1)$ in the spectrum is odd, then then J and J_{R} belong to separate topological components and there will not exist any T which satisfies $T^2 = \mathscr{G}$ and $TJ = JT^{-1}$ simultaneously. $T = \sqrt{\mathscr{G}}$ will only be uniquely defined if -1 is not an eigenvalue of $\mathscr{G}$, in which case there exists a unique T such that $TJ = JT^{-1}$ with eigenvalues $(e^{\mathrm{i}\,r_i}, e^{\mathrm{i}\,r_i}, e^{-\mathrm{i}\,r_i}, e^{-\mathrm{i}\,r_i})$ with $r_i \in (0, \pi/2)$. In this case, $\mathscr{G}$, T, and K can be brought to a block-diagonal form, where there will be 4×4 two-mode blocks.

Consider, for example, a single fermionic mode and canonical coordinates $\hat{\xi} = (\hat{q}, \hat{p})$. In this case, there are only two distinct pure Gaussian states, rather than a family of states, characterized by

$$|J_+\rangle = |0\rangle \quad , \quad |J_-\rangle = |1\rangle \ , \tag{3.33}$$

whose covariance matrix and complex structure are given by

$$\Omega_\pm = \begin{pmatrix} 0 & \pm 1 \\ \mp 1 & 0 \end{pmatrix} = J_\pm \ . \tag{3.34}$$

We can now consider a reference fermionic state $|J_R\rangle$ with

$$\Omega_{\mathrm{R}} = \begin{pmatrix} 0 & 1 \\ -1 & 0 \end{pmatrix} = J_{\mathrm{R}} \ . \tag{3.35}$$

The stabilizer subgroup $U(1)$ coincides with $\mathrm{SO}(2,\mathbb{R})$ and as a consequence, only group elements which transform $|J_{\mathrm{R}}\rangle = |J_+\rangle$ into $|J_-\rangle$ belongs to the disconnected component.

A more interesting case, which generalizes to states with more fermionic modes, is the two-fermionic mode case. Consider canonical coordinates $\hat{\xi} = (\hat{q}^1, \hat{p}^1, \hat{q}^2, \hat{p}^2)$. IN this case, the most general Gaussian states can be written in terms of tensor products of the single fermionic modes as

$$|J_+\rangle = \cos(r)\,|0,0\rangle + e^{\mathrm{i}\,\phi}\sin(r)\,|1,1\rangle \ , \tag{3.36a}$$

$$|J_-\rangle = \cos(r)\,|1,0\rangle + e^{\mathrm{i}\,\phi}\sin(r)\,|1,1\rangle \ , \tag{3.36b}$$

where $r \in [0, \pi/2]$ and $\phi \in [0, 2\pi]$. In this case, the covariance matrix and complex structure are given by

$$\Omega_\pm = \begin{pmatrix} 0 & \mp\sin(2r)\sin(\phi) & \pm\cos(2r) & \pm\sin(2r)\cos(\phi) \\ \pm\sin(2r)\sin(\phi) & 0 & -\sin(2r)\cos(\phi) & \cos(2r) \\ \mp\cos(2r) & \sin(2r)\cos(\phi) & 0 & \sin(2r)\sin(\phi) \\ \mp\sin(2r)\cos(\phi) & -\cos(2r) & -\sin(2r)\sin(\phi) & 0 \end{pmatrix} = J_\pm \ . \tag{3.37}$$

One should be careful and note that the fact that $(\Omega_\pm)^{ab}$ and $(J_\pm)^a{}_b$ coincide in (3.37) is due to the choice of basis. If one chooses a different basis, such as one in terms of creation and annihilation operators, then these matrices are no longer equal.

From this it can be seen that Gaussian states of two fermionic modes can be split in two disconnected spaces parametrized by (r, ϕ), which separate Gaussian states of type $|J_+\rangle$ and $|J_-\rangle$. It is also worth pointing out that these two spaces are distinguished by the parity operator $\hat{P} = \exp(\mathrm{i}\,\pi\,\hat{N})$ with total number operator $\hat{N} = \sum_i \hat{a}_i^\dagger \hat{a}_i$ which is even for $|J_+\rangle$ and odd for $|J_-\rangle$.

If we now consider a two-mode fermionic reference state $|J_{\mathrm{R}}\rangle$ in a basis $\hat{\xi} = (\hat{q}^1, \hat{p}^1, \hat{q}^2, \hat{p}^2)$ given by

$$\Omega_{\mathrm{R}} = \begin{pmatrix} 0 & \mathbb{1}_2 \\ -\mathbb{1}_2 & 0 \end{pmatrix} = J_{\mathrm{R}} \ , \tag{3.38}$$

then one can find a 4-dimensional subspace of generators satisfying $[k, J_{\mathrm{R}}] = 0$ which generates the stabilizer subgroup $\mathrm{U}(2) \subset \mathrm{O}(4,\mathbb{R})$. The state $|J_+\rangle$ can be reached by a continuous path generated by

$$K = \frac{1}{2}\log(\mathscr{G}) = r \begin{pmatrix} 0 & \cos(\phi) & 0 & \sin(\phi) \\ -\cos(\phi) & 0 & -\sin(\phi) & 0 \\ 0 & \sin(\phi) & 0 & -\cos(\phi) \\ -\sin(\phi) & 0 & \cos(\phi) & 0 \end{pmatrix} \ , \tag{3.39}$$

for $\mathscr{G} = -J_+ J_{\mathrm{R}}$. On the other hand, in order to reach the state $|J_-\rangle$ we need to apply and additional transformation $\mathcal{R}(M_v)$ with $v = (\sqrt{2}, 0, 0, 0)$ such that $|J_-\rangle = \mathcal{R}(M_v)\,|J_+\rangle$. By a change of basis such that $\phi = 0$, it is possible to read-off the spectrum of $\mathscr{G}$ given by $(e^{\mathrm{i}\,2r}, e^{\mathrm{i}\,2r}, e^{-\mathrm{i}\,2r}, e^{-\mathrm{i}\,2r})$. Just like in the bosonic case, for a fermionic Gaussian state of $2N$ degrees of freedom, we can find a 4×4 and 2×2 block decomposition of the form (3.38) such that $\mathscr{G} = \oplus_i \mathscr{G}^i$ where the eigenvalues of the $\mathscr{G}^i$ are $(e^{\mathrm{i}\,2r}, e^{\mathrm{i}\,2r}, e^{-\mathrm{i}\,2r}, e^{-\mathrm{i}\,2r})$.

3.3. Complexity in Quantum Field Theories

The holographic complexity proposals discussed in Sec. 2.3 raised a challenge on our understanding the black hole interior, provided a definition of its volume in a covariant way and made a conjecture relating it to complexity, opening a new perspective into the study of the holographic black holes. The fact that these gravitational quantities capable of probing the interior of AdS black holes are conjectured to be related to the difficulty of preparing states in chaotic quantum many-body systems provides another prime example of how deeply intertwined ideas from quantum information are with gravity in negatively curved spaces.

Of course, the prototypical example of this intimate relation between quantum information and gravity is encapsulated by the notion of entanglement entropy, which has played a key role in the development of the field over the past fifteen years. The Ryu–Takayanagi formula [118, 227], discussed in Sec. 2.1.1, and its covariant generalization [123] provided a stepping stone for understanding the way that gravitational quantities are encoded in the boundary quantum field theories.

However a key aspect of the development of the study of entanglement entropy in holographic theories, and particularly in the AdS/CFT correspondence, is that prior to the Ryu–Takayanagi conjecture in the AdS/CFT Correspondence, the concept of entanglement entropy had already been established in quantum field theories by pioneering works such as [109, 111] (see Sec. 2.1 for more details). Afterwards and through a series of pivotal works [127, 128, 132, 138, 228, 229] the validity of the duality of descriptions of entanglement entropy was strengthened. One could even argue that a significant amount of the "success" of the Ryu–Takayanagi formula is due to the possibility of matching its predictions from both sides of the holographic duality.

In stark contrast, the notion of complexity in the AdS/CFT correspondence entered through the holographic proposals (see Sec. 2.3.1 and Sec. 2.3.2) without a preexisting notion of complexity in quantum field theory. While the arguments in the original holographic proposals [170, 173, 178, 179] indeed connect a notion of complexity arising from tensor network arguments with such gravitational observables, the lack of a concrete definition of it on the quantum field theory side hinders the possibility of reconciling their proposals with any computation of complexity arising from first-principles.

As a consequence of this, a significant amount of effort in the community over the past five years has been devoted to bringing the notion of complexity on a similar footing to entanglement entropy in quantum field theories. Two fundamental works in this direction [101, 102] were inspired by the geometric approach developed by authors of [213–215] (see Sec. 3.1.1) and by the continuous multi-scale entanglement renormalization ansatz (cMERA) [95] (see Sec. 1.2). The first of these relied on a lattice approach to study the complexity of the vacuum state of a free scalar field theory, where the measure of complexity was defined via the geodesic distance of a Riemannian metric defined through the generators of unitaries belonging to the general linear group $\mathrm{GL}(N, \mathbb{R})$, in a manner akin to the geometric approach. The second one was based on the cMERA approach to quantum field theories, and the

authors obtained complexity as a geodesic distance of the Fubini-Study metric for the $\mathrm{SU}(1,1)^{\otimes N}$ group of Gaussian states generated by the action of this group.

In a subsequent works such techniques were applied to study the circuit complexity of free fermions [204] with an approach based on the notion of geodesic distance on the $\mathrm{SO}(2N,\mathbb{R})$ group. One should also mention [205], where the cMERA approach was used to study complexity once again in fermionic field theories. Similar methods have also been applied in other relevant set-ups, such as thermofield double (TDF) states [230] and conformal field theories [206, 208, 209, 231].

In this section we review the construction and results for circuit complexity for the vacuum states of two free quantum field theories in $(1+1)$-dimensions: the Klein–Gordon field and the critical transverse field Ising model. This section lays the foundation for subsequent chapters in this thesis, in particular to Chap 5, where we discuss a notion of complexity for mixed states called complexity of purification. At the same time, the models that we are considering will also appear in Chap 4 where we study the time-dependence of complexity and also in Chap 6 where we instead study entanglement of purification and reflected entropy.

Vacuum states of two free quantum field theories in $(1+1)$-dimensions have the property of being Gaussian and we will hence be able to use the machinery described in Sec. 3.2 to study the complexity of their vacuum states. In order to regularize the UV divergences, we will consider lattice representations of such theories, even though one could also regularise it by placing a cut-off Λ_{UV} in momentum space.

The approach that we will follow is based on the geometrization of complexity as described in Sec. 3.1.1 where circuits are built from a continuous representation of unitaries, which in the case of bosons will correspond to unitaries built from symplectic transformations and for fermions from orthogonal ones. Furthermore, we will focus on the F_2 cost function (3.8b) as derived originally in [204, 230], which is based on a natural metric on the group manifold and which coincides with the geodesic distance on the Gaussian state manifold, *i.e.*, with the Fubini-Study metric, studied originally in [101]. The main reason for this is that such cost function allows for an analytical minimization, in contrast with other cost functions, such as F_1. One should mention, nonetheless, that the latter one is expected to have properties which more closely resemble the holographic complexity proposals. The following sections will also serve as the basis for the content of chapters 4 and 5, where we will study complexity in the context of quantum quenches and complexity of purification.

3.3.1. Complexity of the Klein–Gordon Vacuum

Consider the Hamiltonian of a free massive scalar field in $(1+1)$- spacetime dimensions

$$\hat{H} = \frac{1}{2}\int \mathrm{d}x \left(\hat{\pi}(x)^2 + \hat{\varphi}'(x)^2 + m^2\hat{\varphi}(x)^2\right) \ , \tag{3.40}$$

where $\hat{\varphi}(x)$ and $\hat{\pi}(x)$ are the field and conjugate momentum operators, respectively. This theory describes the well known Klein–Gordon field with mass m.

We now introduce a lattice spacing δ and discretize the Hamiltonian (3.40) on a

circular lattice with N sites and circumference $L = N\delta$

$$\hat{H} = \frac{\delta}{2} \sum_{i=0}^{N-1} \left(\hat{\pi}_i^2 + \frac{m^2}{\delta^2} \hat{\varphi}_i^2 + \frac{1}{\delta^4} (\hat{\varphi}_i - \hat{\varphi}_{i+1})^2 \right) , \tag{3.41}$$

where $\hat{\varphi}_i := \hat{\varphi}(x_i)$ and $\hat{\pi}_i := \hat{\pi}(x_i)$ correspond to our choice of canonical variables $\hat{\xi}_i^a = (\hat{\varphi}_i, \hat{\pi}_i)$, and where $a = 1, 2$. Positions x_i label the lattice site i, with $i \in \{0, \dots, N-1\}$ with periodic boundary condition: $x_{N+i} = x_i \; \forall \, i$.

The Hamiltonian (3.41) can be diagonalized via a discrete Fourier transform

$$\hat{\varphi}_j = \frac{1}{\sqrt{N}} \sum_{k=0}^{N-1} \exp\left(2\pi \mathrm{i}\, k\, j/N\right) \tilde{\varphi}_k \ , \tag{3.42a}$$

$$\hat{\pi}_j = \frac{1}{\sqrt{N}} \sum_{k=0}^{N-1} \exp\left(-2\pi \mathrm{i}\, k\, j/N\right) \tilde{\pi}_k \ , \tag{3.42b}$$

leading to

$$\hat{H} = \frac{1}{2} \sum_{k=0}^{N-1} \left(\delta |\tilde{\pi}_k|^2 + \frac{\omega_k^2}{\delta} |\tilde{\varphi}_k|^2 \right) \ , \tag{3.43}$$

which describes a system of N decoupled harmonic oscillators with frequencies

$$\omega_k = \sqrt{m^2 + \frac{4}{\delta^2} \sin^2\left(\frac{\pi k}{N}\right)} \ . \tag{3.44}$$

The ground state $|0\rangle$ of the Hamiltonian (3.43) is Gaussian, and hence fully characterized by its covariance matrix (3.14), written in a momentum basis $\hat{\xi}_i^a = (\tilde{\varphi}_k, \tilde{\pi}_k)$ as

$$\begin{aligned} G_{ij}^{ab} :&= \langle \psi | \left(\hat{\xi}^a \hat{\xi}^b + \hat{\xi}^b \hat{\xi}^a \right) | \psi \rangle \\ &= \frac{1}{N} \sum_{k=0}^{N-1} e^{\mathrm{i} \frac{2\pi k}{N} (i-j)} \begin{pmatrix} \frac{1}{\omega_k} & 0 \\ 0 & \omega_k \end{pmatrix} \ , \end{aligned} \tag{3.45}$$

where a, b labels the entries of G_{ij} for sites i and j of the lattice. Note that the full covariance matrix can be decomposed in 2×2 blocks

$$G = \bigoplus_{k=0}^{N-1} \begin{pmatrix} \frac{1}{\omega_k} & 0 \\ 0 & \omega_k \end{pmatrix} = \bigoplus_{k=0}^{N-1} G_k \ , \tag{3.46}$$

which is just a consequence of the fact that we have decoupled the system by performing a normal mode decomposition.

Considering the continuum limit on a circle of circumference $L = N\delta$ requires to take the limit $N \to \infty$ while keeping the product of meaningful combinations such as $mL = mN\delta$ fixed. Strictly speaking, each value of this combination corresponds to a different QFT in the continuum limit within the class of Klein–Gordon theories. In Chap. 5 we will be interested in considering subsystems and in this case the continuum limit will further require that as N is increased, quantities such as the

mutual information stabilize to a value in the vicinity of their QFT expectations. If $w\delta$ is the size of the subsystem, then the results of numerical computations should be indistinguishable from the set-up when the spatial direction is a line. In this case, the mass of the field $m \ll 1/\delta$ becomes the only dimensionful parameter of the theory in the continuum limit. Furthermore, in this case the discrete k associated with different momentum modes in (3.44) become a continuum variable and the discrete sum in (3.45) must be replaced by an integral.

Before proceeding to the discussion of the reference state and complexity, it is worth pointing out a known subtlety of this discretized model, namely the zero-mode problem: The frequency of the oscillator with zero momentum mode $k = 0$ is given by $\omega_0 = m$, which vanishes in the massless limit $m \to 0$. This entails a divergence of the $\tilde{\varphi}\tilde{\varphi}$ two-point function

$$\langle 0|\tilde{\varphi}_0(x_i)\tilde{\varphi}_0(x_j)|0\rangle \sim \frac{1}{m} \xrightarrow{m\to 0} \infty \ , \tag{3.47}$$

leading to divergences in the covariance matrix (3.45), implying that in this limit the ground state $|0\rangle$ approaches a delta distribution. This means that in this limit the ground state of the theory (3.43) is only defined distributionally, and does not lie in Hilbert space, since it is not square integrable, *i.e.*, it is not in $L^2(\mathbb{C})$.

If there is a problem with the zero-mode in the massless limit, then why bother taking it at all? Because the massless limit of the Klein–Gordon model (3.40) is a free conformal field theory in $(1+1)$-dimensions with *central charge* $c = 1$, and it will be the focus of Sec. 5.2.2.

To be precise, the $c = 1$ CFT with the periodic boundary conditions that we imposed previously can be regarded as a 1-parameter family of theories which arise in the path-integral language from the compactification of the bosonic field φ with periodicity

$$\varphi + 2\pi R = \varphi \ , \tag{3.48}$$

where R here is a dimensionless parameter corresponding to the *compactification radius* in field space and that plays the role of a moduli which specifies a particular $c = 1$ CFT [232]. In this case, the scaling dimension of the lowest lying operator is given by

$$\Delta_{\text{min}} = \min\left(\frac{1}{R^2}, \frac{R^2}{4}\right) \ . \tag{3.49}$$

Note that this expression is the same for a theory with a compactification radius given by $2/R$, which shows an underlying duality between theories with compatification radii R and $2/R$ [232].

The massless limit of the discretized Klein–Gordon theory (3.41) corresponds to the decompactification limit, $R \to \infty$ of free compact bosonic CFTs, which as we just mentioned, is a subtle limit since in this case the gap in the operator spectrum approaches zero (3.49). This limit leads to the correct correlation functions of vertex operators and single interval entanglement entropy. However, for other quantities this limit is more complicated. Particularly for the partition function of the theory.

The modular invariant partition function of the free boson [232] given by

$$Z_{\text{mod-inv}} \sim \frac{1}{(\beta/L)^{1/2}\eta(\mathrm{i}\,\beta/L)^2} \ , \tag{3.50}$$

while the partition function of the free massive boson in the regime $mL \ll 1$ obtained by maintaining the wero-point energy is

$$Z_{mL\ll 1} \sim \frac{1}{(\beta m)\eta(\mathrm{i}\,\beta/L)^2} \ , \tag{3.51}$$

where in both cases η is the *Dedekind eta function* defined by

$$\eta(\mathrm{i}\,\beta/L) = e^{-\frac{\pi}{12}\frac{\beta}{L}} \prod_{n=1}^{\infty}\left(1 - e^{-2\pi n\beta/L}\right) \ . \tag{3.52}$$

These two partition functions are not equivalent, and the mismatch between them can be understood by looking at the representation of the partition function on a circle as the Euclidean path-integral on a torus. For (3.51), the contribution coming from the zero mode is neglected, since including it would lead to an infinite volume term arising from the field-space integration. On the other hand, for (3.52), the zero mode contribution ϕ to the path-integral is included but it remains finite, as it can be seen as originating from a term

$$\int_{-\infty}^{+\infty} \mathrm{d}\phi\, e^{-\frac{1}{2}\beta L m^2\phi^2} \sim \frac{1}{m\sqrt{\beta L}} \ , \tag{3.53}$$

where βL is the spatial volume of the torus. Multiplying the modular invariant partition function (3.50) by the zero-mode contribution (3.53) leads to the free massive partition function (3.51), which explicitly shows how these two are related.

In our numerical studies we will use the free massive boson theory to extract the properties of the modular invariant $c = 1$ free boson CFT in the limit $R \to \infty$. In this regard, we can recover the modular invariant partition function (3.50) from the free massive boson partition function (3.51) by dividing it by the zero-mode contribution (3.53). However, for certain quantities it is not straightforward to isolate the effect of the zero-mode contribution when performing computations with a non-vanishing mass. Nevertheless, there exist numerical studies which show that Gaussian computations with a small but finite mass in fact reproduce the universal entanglement entropy of a single interval [228]. Moreover, one can expect that one can trust the free massive boson calculations in cases where the higher-momentum modes dominate over the zero-mode, as is the case for short-, or UV-, distance physics. This will be the case, for example, when we consider two disjoint intervals at small separations, as will be the focus of Chap. 5 and parts of Chap 6.

We will return to a discussion of the continuum and conformal limits for this model when we discuss bosonic complexity of purification in Sec. 5.2.2. In short, the conformal limit $m \to 0$ of (3.43) is subtle, due to the presence of the zero-mode, and one should bear this in mind when performing numerical computations, as isolating the contribution of the zero-mode is non trivial. Nonetheless, one can

trust short distance computations since the zero-mode affects primarily long-distance physics.

Suppose now that the vacuum state $|0\rangle$ with covariance matrix (3.46) corresponds to our *target state* $|J_{\mathrm{T}}\rangle$

$$J_{\mathrm{T}} = \bigoplus_{k=0}^{N-1} \begin{pmatrix} 0 & \frac{1}{\omega_k} \\ -\omega_k & 0 \end{pmatrix} . \tag{3.54}$$

As a reference state $|J_{\mathrm{R}}\rangle$, a natural choice is a spatially disentangled state due to its interesting properties in connection with divergences present in the holographic complexity proposals as with cMERA. To be precise, this choice of reference state will allow us to study the structure of divergences of circuit complexity and to compare it with the holographic complexity proposals (see Sec. 2.3). From the perspective of cMERA, this state corresponds to the IR state,*i.e.*, a state in Hilbert space which has a vanishing entanglement entropy for any subsystem bipartition (see Sec. 1.2 and particularly (1.22)). In this way, the state $|J_{\mathrm{R}}\rangle$ is defined by

$$J_{\mathrm{R}} = \bigoplus_{i=0}^{N-1} \begin{pmatrix} 0 & \frac{1}{\mu} \\ -\mu & 0 \end{pmatrix} , \tag{3.55}$$

where μ plays the role of a *reference state scale*. That is, the reference state that we will consider is simply a tensor product of N disentangled single harmonic oscillators, all of which are characterized by the same frequency μ. One should also note that the reference state covariance matrix G_{R} is invariant under $\mathrm{U}(N)$ transformations, that is, it is invariant under the action of the stabilizer group.

Following the geometric approach, we ask what is the optimal circuit defined via the unitary $\hat{U}$

$$\hat{U} = \overleftarrow{\mathcal{P}} \left\{ e^{\int_0^1 \mathrm{d}t\, \hat{K}(t)} \right\} , \tag{3.56}$$

with $\hat{K}(t)$ given by the bottom expression in (3.22), such that the target state $|J_{\mathrm{T}}\rangle$ (3.54) can be reached/generated from the reference state $|J_{\mathrm{R}}\rangle$ (3.55)

$$|J_{\mathrm{T}}\rangle = \overleftarrow{\mathcal{P}} \left\{ e^{\int_0^1 \mathrm{d}t\, \hat{K}(t)} \right\} |J_{\mathrm{R}}\rangle \ . \tag{3.57}$$

In order to measure the optimality of the circuit (3.57) we consider a cost function based on an L^2 norm, usually called a F_2 cost function, given by

$$\mathcal{C}_2^b(J_{\mathrm{R}}, J_{\mathrm{T}}) := \frac{1}{2\sqrt{2}} \sqrt{\mathrm{tr}\left(\log(-J_{\mathrm{T}} J_{\mathrm{R}})^2\right)} = \frac{1}{2\sqrt{2}} \sqrt{\mathrm{tr}\left(\log(\mathscr{G})^2\right)} , \tag{3.58}$$

where here $\mathscr{G}^a{}_b = -(J_{\mathrm{T}})^a{}_c (J_{\mathrm{R}})^c{}_b$ is given by

$$\mathscr{G} = \bigoplus_{k=0}^{N-1} \begin{pmatrix} \frac{\mu}{\omega_k} & 0 \\ 0 & \frac{\omega_k}{\mu} \end{pmatrix} = \bigoplus_{k=0}^{N-1} \mathscr{G}^k \ . \tag{3.59}$$

This cost function arises from a right-invariant metric on the manifold $\mathrm{Sp}(2N, \mathbb{R})$ constructed in terms of the generators $K \in \mathfrak{sp}(2N, \mathbb{R})$ via

$$F_2(K) = \sqrt{\mathrm{tr}\left(K G K^{\intercal} G^{-1}\right)}/\sqrt{2} , \tag{3.60}$$

and coincides with the norm induced by the Frobenius inner product $\langle K, \tilde{K} \rangle = \mathrm{tr}\left(KG\tilde{K}^{\intercal}G^{-1}\right)/2$ defined on $\mathfrak{sp}(2N, \mathbb{R})$ for a positive-definite matrix G, which in this case corresponds to the bosonic covariance matrix.

The decomposition (3.59) is consistent with the observation following (3.32), where we note that the spectrum of a bosonic relative complex structure $\mathscr{G} = \oplus_k \mathscr{G}^k$ consists of pairs (e^{2r_k}, e^{-2r_k}), where in this case $r_k = \log(\omega_k/\mu)/2$.

With this we are able to evaluate the complexity $\mathcal{C}_2(J_{\mathrm{R}}, J_{\mathrm{T}})$ (3.58) which is given by

$$\mathcal{C}_2^{\mathrm{Scalar}}(\omega_k, \mu) = \frac{1}{2}\sqrt{\sum_{k=0}^{N-1} \log^2\left(\frac{\omega_k}{\mu}\right)}\,, \tag{3.61}$$

and where we assume $\omega_k/\mu > 0$ so that the logarithm is well-defined. In terms of dimensionless ratios of the mass m, circumference L, reference scale μ and lattice spacing δ (via (4.15)) this expression becomes

$$\mathcal{C}_2^{\mathrm{Scalar}}(m/\mu, \mu\delta, \mu L) = \frac{1}{2}\left(\sum_{k=0}^{N-1} \log^2\left(\sqrt{\left(\frac{m}{\mu}\right)^2 + \left(\frac{2}{\mu\delta}\right)^2 \sin^2\left(\frac{k\pi\mu\delta}{\mu L}\right)}\right)\right)^{1/2}. \tag{3.62}$$

This is the complexity of the vacuum state of the discretized $(1+1)$-dimensional free scalar quantum field theory with respect to a spatially disentangled reference state. Note that this expression is divergent in the continuum limit $N \to \infty$. However, as we mentioned previously, we want to keep the values of meaningful combinations such as mL fixed as we take this limit. As can also be seen, the reference state scale introduces another relevant scale in the system which also takes an important role in the continuum limit besides the mass of the field m. This fact will be relevant when we discuss the bosonic Gaussian complexity of purification in Sec. 5.2.2. We will see that in fact a combination which we will keep fixed as we take the continuum limit is m/μ as well as the sizes of the subsystems in consideration. This will allow us to extract the divergent properties of complexity in this limit.

We can see from this expression that in the continuum limit we can expect the sum over modes to be replaced by an integral over continuous momenta. Furthermore, this expression allows us to gain an intuition of the contribution to complexity 3.62 both from the high-energy modes $\omega_k \approx \Lambda_{\mathrm{UV}} \sim 1/\delta$ and in particular from the zero-mode $\omega_0 = m$. In the first case, we simply replace $\omega_k \to 1/\delta$ in (3.61) from which we obtain the behaviour

$$\mathcal{C}_2^{\mathrm{UV}} \approx \frac{L^{1/2}}{2\delta^{1/2}} \log\left(\frac{1}{\mu\delta}\right) \sim \left(\frac{L}{\delta}\right)^{1/2} = \left(\frac{\mathrm{Vol}}{\delta}\right)^{1/2}. \tag{3.63}$$

This not only shows that the complexity of the UV modes is insensitive to the mass m of the field, but also that in general we could expect a behaviour proportional to the square root of the volume from the high-energy modes in higher-dimensional versions of the model (3.40).

It should be remarked that it was also found in [101, 102] that in general L_1 cost functions have a divergent structure which closely resembles the holographic com-

plexity proposals. In general, an L_1 complexity will have a structure reminiscent of the CA proposal

$$\mathcal{C}_1^{\mathrm{UV}} \approx \frac{\mathrm{Vol}}{\delta} \log\left(\frac{1}{\mu\delta}\right) \ . \tag{3.64}$$

This, however, is usually interpreted as an upper bound on complexity rather than its true value, since it's obtained by evaluating the L_1 cost function using optimal circuit obtained for the L_2 cost function. Other works which provide evidence that L_1 cost functions have a closer agreement with the holographic proposals comes from the thermofield double (TFD) states and complexity of formation [181, 230].

An equivalent result in higher dimensions was found in [102], where it was compared to the holographic "complexity=volume" proposal (2.13). The authors noted a difference in the power with which the volume contributes to the complexity. To be precise, the authors found $\mathcal{C}_2 \sim (\mathrm{Vol}/\delta^{D-1})^{1/2}$ and $\mathcal{C}_V \sim \mathrm{Vol}/\delta^{D-1}$, where D is the spacetime dimension. Authors in [101] arrived at similar results based on a regularization scheme dependent on the introduction of a UV cut-off in momentum-space.

In the case of the zero-mode contribution, we simply neglect all contributions coming from the other modes ω_k with $k > 0$, and obtain

$$\mathcal{C}_2^{k=0} = \frac{1}{2} \log\left(\frac{m}{\mu}\right) \ , \tag{3.65}$$

which diverges in the $m \to 0$ limit. It can be shown, see *e.g.*, [102], that the IR contributions to complexity take the form $\mathcal{C}_2^{\mathrm{IR}} \sim L\, m \log(m/\mu)$.

Expressions (3.58), (3.61) will be the basis for our subsequent discussions of complexity, both in the context of quantum quenches (see Sec. 4.2) and complexity of purification (see Sec. 5.2.2).

3.3.2. Complexity of the Ising CFT Vacuum

Consider the transverse field Ising model [233, 234] on a 1-dimensional circular lattice of N sites, where the sites are denoted by $i = 1, \ldots, N$ and where we assume periodic boundary conditions $N + i = i$. Here we also implicitly consider a lattice spacing set to unity $\delta = 1$ and so the size of the periodic lattice L is equal to the number of lattice sites N. Suppose for simplicity that N is an even integer. The Hamiltonian of this model is given by

$$\hat{H} = -\sum_{i=1}^{N} \left(2J \hat{S}_i^x \hat{S}_{i+1}^x + J_z\, \hat{S}_i^z\right) \ , \tag{3.66}$$

where the $\hat{S}_i^\alpha$ with $\alpha \in \{x, y, z\}$ are spin-1/2 operators defined in terms of the known 2×2 Pauli matrices σ_α

$$\sigma_x = \begin{pmatrix} 0 & 1 \\ 1 & 0 \end{pmatrix} , \sigma_y = \begin{pmatrix} 0 & -\mathrm{i} \\ \mathrm{i} & 0 \end{pmatrix} , \sigma_z = \begin{pmatrix} 1 & 0 \\ 0 & -1 \end{pmatrix} \ , \tag{3.67}$$

via

$$\hat{S}_i^\alpha := (\mathbb{1}_2)^{\otimes(i-1)} \otimes \frac{\sigma_\alpha}{2} \otimes (\mathbb{1}_2)^{\otimes(N-i)} \ . \tag{3.68}$$

In other words, the spin operators $\hat{S}_i^\alpha$ are *local* insertions of a Pauli matrix $\sigma_\alpha/2$ on the site i of the periodic lattice. These also satisfy the identification $\hat{S}_{N+1}^\alpha = \hat{S}_1^\alpha$ imposed by the periodic boundary conditions. It is also common to consider operators $\hat{X}_i$, $\hat{Y}_i$ and $\hat{Z}_i$ defined similarly to (3.68) with respect to σ_α instead of $\sigma_\alpha/2$.

This model can be diagonalized by following a procedure which involves the Jordan–Wigner transform [235] and a decomposition of the Hilbert space into odd and even sectors of the parity operator. To start, we construct the spin-1/2 ladder operators $\hat{S}_i^\pm := \hat{S}_i^x \pm \mathrm{i}\,\hat{S}_i^y$, which can be written in terms of the Pauli matrices σ_α simply as

$$\hat{S}_i^\pm := (\mathbb{1}_2)^{\otimes(i-1)} \otimes \frac{\sigma_x \pm \mathrm{i}\,\sigma_y}{2} \otimes (\mathbb{1}_2)^{\otimes(N-i)} \ , \tag{3.69}$$

which is basically an insertion of the usual $\mathfrak{su}(2)$ ladder operators $\sigma_\pm = (\sigma_x \pm \mathrm{i}\,\sigma_y)/2$ on site i of the lattice. We now consider fermionic creation and annihilation operators $\hat{f}_i$ and $\hat{f}_i^\dagger$ related to the ladder operators $\hat{S}_i^\pm$ via the *Jordan–Wigner transformation*

$$\hat{S}_i^+ = \hat{f}_i^\dagger \exp\left(\mathrm{i}\,\pi \sum_{j=1}^{i-1} \hat{f}_j^\dagger \hat{f}_j\right) \ . \tag{3.70}$$

Note that the exponential in (3.70), which contains the *fermionic number operator* at site j, namely $\hat{n}_j := \hat{f}_j^\dagger \hat{f}_j$, is a fermionic *string operator*, meaning that it acts on all sites of the lattice $j < i$ in a *non-local* way. This is because the *number operator* $\hat{\mathcal{N}}_k$ defined as

$$\hat{\mathcal{N}}_k := \sum_{j=1}^{k} \hat{n}_j \ , \tag{3.71}$$

contains a sum over all fermion occupancies at the left of site i. Note that for $k = N$ this becomes the total number operator $\hat{\mathcal{N}} := \hat{\mathcal{N}}_N$. Furthermore, the exponential in (3.70) containing the number operator is also referred to as the *parity operator* $\hat{P}_k$

$$\hat{P}_k = \exp\left(\mathrm{i}\,\pi \sum_{j=1}^{k} \hat{f}_j^\dagger \hat{f} j\right) \ , \tag{3.72}$$

with $\hat{P}_{\mathrm{tot}} := \hat{P}_N$ called the *total parity operator*. As we will see below, this operator is called the parity operator as its action on a state is determined by the number of occupied fermionic modes in modes $j = 1, \ldots, k$ of the field. It is equal to $+1$ if the number of occupied modes is even and -1 if the number of occupied modes is odd.

We then arrive at the same realization that Jordan and Wigner arrived, namely that in this 1-dimensional lattice

$$\text{spin} = \text{fermion} \times \text{string} \ . \tag{3.73}$$

In other words, in a 1-dimensional lattice a spin-1/2 operator acting on site i is equivalent to a fermionic string operator counting the number of fermions on sites $j < i$ followed by a fermionic operator inserted on site i [236], as shown in Fig. 3.2.

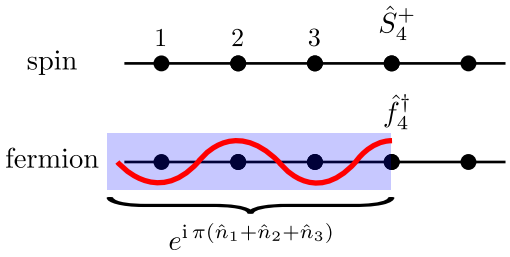

Figure 3.2.: Representation of the Jordan–Wigner transformation on a lattice. the ladder spin operator $\hat{S}_4^+$ is written as the product of the fermionic creation operator $\hat{f}_4^\dagger$ and the string (parity) operator $e^{\mathrm{i}\pi(\hat{n}_1+\hat{n}_2+\hat{n}_3)}$.

This observation (3.73) has profound implications on the notion of *locality*, particularly when splitting the lattice into two spatial subregions and tracing out the degrees of freedom of one of them. *A partial trace which is local on the spin picture is non-local in the fermionic picture.* This non-locality has unavoidable consequences when computing the entanglement entropy of a spatial subregion, and therefore also quantities obtained thereof, such as mutual information. One should mention the interesting series of papers [237–240] investigating dualities in spin systems and the notion of locality from the perspective of the algebraic approach to quantum field theory, based on operator algebras. We will return to this discussion in 6 when we study entanglement of purification for adjacent and disjoint subregions. This can also be seen more clearly be considering the inverse transformations to (3.70), which following our conventions (3.68) are given by

$$\hat{f}_i = \left(\prod_{j=1}^{i-1} \hat{Z}_j\right) \frac{(\hat{X}_i - \mathrm{i}\,\hat{Y}_i)}{2} \,, \tag{3.74a}$$

$$\hat{f}_i^\dagger = \left(\prod_{j=1}^{i-1} \hat{Z}_j\right) \frac{(\hat{X}_i + \mathrm{i}\,\hat{Y}_i)}{2} \,. \tag{3.74b}$$

which shows that the transformation between spins and fermions inevitably requires an insertion of $\hat{Z}_i$, acting as a string of operators. Let us now return to the diagonalization of the Hamiltonian (3.66).

We can also introduce $2N$ Majorana modes by

$$\gamma_{2k-1} := \sigma_z^{\otimes(k-1)} \otimes \sigma_x \otimes \mathbb{1}^{\otimes(N-k)} = \left(\prod_{j=1}^{k-1} \hat{Z}_j\right) \hat{X}_k \,, \tag{3.75a}$$

$$\gamma_{2k} := \sigma_z^{\otimes(k-1)} \otimes \sigma_y \otimes \mathbb{1}^{\otimes(N-k)} = \left(\prod_{j=1}^{k-1} \hat{Z}_j\right) \hat{Y}_k \,. \tag{3.75b}$$

That is, on every site $i = k/2$ of the lattice, we have two Majorana modes: $\{\gamma_{2k-1}, \gamma_{2k}\}$. These are related to the fermionic operators via $\hat{f}_k = (\gamma_{2k-1} - \mathrm{i}\,\gamma_{2k})/2$. In terms

of Majorana modes, the total parity operator $\hat{P}_N$ can be written as $\prod_{k=1}^{N} \hat{Z}_k = \prod_{k=1}^{N} (-\mathrm{i}\,\gamma_{2k-1}\gamma_{2k})$.

We can now write the Hamiltonian (3.66) in terms of fermionic creation and annihilation operators. By using (3.69) we arrive at the Hamiltonian

$$\begin{aligned} \hat{H} = -\sum_{i=1}^{N} \left(\frac{J}{2} \left[\hat{f}_i^\dagger (\hat{f}_{i+1} + \hat{f}_{i+1}^\dagger) + \text{h.c.} \right] + J_z\, \hat{f}_i^\dagger \hat{f}_i \right) \\ + \frac{J}{2} \left[\hat{f}_N^\dagger (\hat{f}_1 + \hat{f}_1^\dagger) + \text{h.c.} \right] (\hat{P}_N + 1) + \frac{N\, J_z}{2} \ , \end{aligned} \tag{3.76}$$

where the last term, namely $N\, J_z/2$ corresponds to a boundary term.

The total parity operator $\hat{P}_N$ in (3.76) makes the Hamiltonian not exactly quadratic in $\hat{f}_i^\dagger$ and $\hat{f}_i$. Moreover, the presence of the term containing it makes the Hamiltonian distinguish between sectors of even and odd eigenvalues of the total number operator $\hat{\mathcal{N}}$. As a consequence, the Hilbert space of the theory can be decomposed as a direct sum

$$\mathcal{H} = \mathcal{H}^+ \oplus \mathcal{H}^- \ , \tag{3.77}$$

where $\mathcal{H}^+$ and $\mathcal{H}^-$ are eigenspaces of the total parity operator $\hat{P}_N$ associated with eigenvalues ± 1. This means that the fermionic Hamiltonian (3.76) can be written as a sum of two Hamiltonians $\hat{H}^\pm$

$$\hat{H} = \hat{H}_+ \hat{\mathcal{P}}_+ + \hat{H}_- \hat{\mathcal{P}}_+ \ , \tag{3.78}$$

with $\hat{\mathcal{P}}_\pm = (\hat{\mathbb{1}} \pm \hat{P}_N)/2$ the orthogonal projectors on each of the eigenspaces

$$\mathcal{H}^\pm = \text{Span} \left\{ |n_1, \ldots, n_N\rangle \in \mathcal{H} \,|\, \hat{P}_N\, |n_1, \ldots, n_N\rangle = \pm\, |n_1, \ldots, n_N\rangle \right\} \ , \tag{3.79}$$

where $\hat{n}_i\, |n_1, \ldots, n_N\rangle = n_i\, |n_1, \ldots, n_N\rangle$. The even sector $\mathcal{H}^+$ is usually referred to as the Neveu-Schwarz (NS) sector, while the odd sector $\mathcal{H}^-$ is referred to as the Ramond (R) sector.

We can also write the Hamiltonian (3.76) in terms of Majorana modes $\hat{\xi}_k^a = \{\gamma_{2k-1}, \gamma_{2k}\}$ as

$$\hat{H} = \frac{\mathrm{i}}{2} \left(\gamma_1 \gamma_{2N} \hat{P}_N + J \sum_{k=1}^{N-1} \gamma_{2k}\gamma_{2k+1} + J_z \sum_{k=1}^{N} \gamma_{2k-1}\gamma_{2k} \right) \ . \tag{3.80}$$

We are interested in the ground state $|0\rangle$ of the critical model $J = J_z = 1$ whose Hamiltonian is

$$\hat{H} = \frac{\mathrm{i}}{2} \left(\gamma_1 \gamma_{2N} \hat{P}_N + \sum_{k=1}^{2N-1} \gamma_k \gamma_{k+1} \right) \ . \tag{3.81}$$

which in terms of canonical coordinates $\hat{\xi}_i^a = \{\hat{q}_i, \hat{p}_i\}$ with $\hat{q}_i = \gamma_{2i-1}$ and $\hat{p}_i = \gamma_{2i}$ can be written as

$$\hat{H} = \frac{\mathrm{i}}{2} \left(\sum_{i=1}^{N} (\hat{p}_i \hat{q}_{i+1} - \hat{q}_i \hat{p}_i) - \hat{p}_N \hat{q}_1 (\hat{P}_N + 1) \right) \ . \tag{3.82}$$

In the limit $N \to \infty$ this leads to a lattice model of the $c = 1/2$ Ising CFT.

We will now focus on the even-parity sector of the theory (consistent with of choice of even N), as it corresponds to the true ground state.[2] The ground state $|0\rangle$ is a Gaussian state, and is hence characterized by its covariance matrix

$$\begin{aligned}\Omega_{ij}^{ab} &= \langle\psi|\left(\hat{\xi}_i^a\hat{\xi}_j^b - \hat{\xi}_j^b\hat{\xi}_i^a\right)|\psi\rangle \\ &= \frac{1}{N}\sum_{\kappa}\begin{pmatrix} 0 & -\cos\left(\kappa(\frac{1}{2}+i-j)\right) \\ \cos\left(\kappa(\frac{1}{2}+j-i)\right) & 0 \end{pmatrix},\end{aligned} \tag{3.83}$$

where $\kappa = \frac{\pi}{N}(2k+1)$ with $k \in \{-\frac{N}{2},\ldots,\frac{N}{2}-1\}$ for even N. In other words, κ belongs to

$$\mathcal{K}^+ = \left\{\frac{\pi}{N} + \frac{2\pi k}{N}\,\middle|\, k\in\mathbb{Z}\,, -\frac{N}{2}\leq k\leq \frac{N}{2}-1\right\}\,. \tag{3.84}$$

Much like in the bosonic case, in (3.83) a and b label the entries of Ω_{ij} for sites i and j of the lattice. Because of this we can write the full covariance matrix as

$$\Omega^{ab} = \frac{1}{N}\sum_{\kappa\in\mathcal{K}^+}\begin{pmatrix} 0 & -\cos\left(\kappa(\frac{1+2N}{2})\right) \\ \cos\left(\kappa(\frac{1-2N}{2})\right) & 0 \end{pmatrix}, \tag{3.85}$$

It is important to mention, however, that when we study fermionic complexity and entanglement of purification in Sec. 5.2.1, Sec. 6.2 and Sec. 6.3, the covariance matrix (3.83) as well as its infinite size limit, *i.e.*, in the continuum limit, $N\to\infty$ given by

$$\Omega_{jk} = \begin{cases} 0 & k=j \\ \frac{(-1)^{k-j}-1}{\pi(k-j)} & k\neq j \end{cases}, \tag{3.86}$$

will be relevant, as they will allow us to study subsystems corresponding to spatial subregions in an efficient manner. At this point we will also return to the discussion of locality and partial traces when computing bipartite entanglement of adjacent and disjoint regions.

From (3.85) we can see that the covariance matrix can be decomposed in 2×2 blocks

$$\Omega = \bigoplus_{k=0}^{N-1}\begin{pmatrix} 0 & \cos(2r_k) \\ -\cos(2r_k) & 0 \end{pmatrix} = \bigoplus_{k=0}^{N-1}\Omega_k\,, \tag{3.87}$$

where here $r_k := (1+2k+N)\pi/4N$. It is important to note that in contrast with the discussion in Sec. 3.2.3 where we focused on two-fermionic state systems, in this case we only have one fermionic state, namely $|J_+\rangle$ at each site of the lattice. If we included the other state $|J_-\rangle$ then we would have a decomposition into 4×4 blocks per site in terms of Majorana modes.

We now want to study the complexity of the ground state with respect to a Gaussian reference state. We will also consider the ground state (3.87) as our target sate, characterized by its complex structure via

$$J_{\mathrm{T}} = \bigoplus_{k=0}^{N-1}\begin{pmatrix} 0 & \cos(2r_k) \\ -\cos(2r_k) & 0 \end{pmatrix}, \tag{3.88}$$

[2] For a detailed discussion see [241] and [240].

In contrast with the bosonic case, the family of reference states that can be considered is highly constrained and in fact, there is only a single spatially unentangled state if we require it to be translational invariant and impose the same parity as the vacuum state $|0\rangle$. In other words, the reference state that we can consider in this case is unique, and is given by

$$J_{\mathrm{R}} = \bigoplus_{k=0}^{N-1} \begin{pmatrix} 0 & 1 \\ -1 & 0 \end{pmatrix} , \tag{3.89}$$

In this case, the relative complex structure $\mathscr{G}^a{}_b = -(J_{\mathrm{T}})^a{}_c (J_{\mathrm{R}})^c{}_b$ is given by

$$\mathscr{G} = \bigoplus_{k=0}^{N-1} \begin{pmatrix} \cos(2r_k) & 0 \\ 0 & \cos(2r_k) \end{pmatrix} = \bigoplus_{k=0}^{N-1} \mathscr{G}^k \ . \tag{3.90}$$

As in the bosonic case, we follow the geometric approach and ask what is the optimal circuit defined via the unitary $\hat{U}$

$$\hat{U} = \overleftarrow{\mathcal{P}} \left\{ e^{\int_0^1 \mathrm{d}t\, \hat{K}(t)} \right\} \ , \tag{3.91}$$

with $\hat{K}(t)$ given by the top expression in (3.22), such that the target state $|J_{\mathrm{T}}\rangle$ (3.88) can be reached/generated from the reference state $|J_{\mathrm{R}}\rangle$ (3.89)

$$|J_{\mathrm{T}}\rangle = \overleftarrow{\mathcal{P}} \left\{ e^{\int_0^1 \mathrm{d}t\, \hat{K}(t)} \right\} |J_{\mathrm{R}}\rangle \ . \tag{3.92}$$

Once again, we choose the L^2 norm [204] defined via the relative covariance matrix (3.90) as it coincides with the geodesic distance on $\mathrm{O}(2N, \mathbb{R})$. It is given by

$$\mathcal{C}_2^{\mathrm{f}}(J_{\mathrm{R}}, J_{\mathrm{T}}) = \frac{1}{2\sqrt{2}} \sqrt{\mathrm{tr}\left(\log(-J_{\mathrm{T}}, J_{\mathrm{R}})^2\right)} = \frac{1}{2\sqrt{2}} \sqrt{\left|\mathrm{tr}\left[(\mathrm{i}\, \log(\mathscr{G}))^2\right]\right|} \ , \tag{3.93}$$

which is given in this case by

$$\mathcal{C}_2^{\mathrm{Ising}}(N) = \frac{1}{2} \sqrt{\left| \sum_{k=0}^{N-1} \log\left(\cos(2r_k)\right)^2 \right|} \ . \tag{3.94}$$

Similarly to the bosonic case (3.60), the cost function (3.93) also arises from a right-invariant metric on the manifold $\mathrm{O}(2N, \mathbb{R})$ constructed in terms of the generators $K \in \mathfrak{so}(2N, \mathbb{R})$ via

$$F_2(K) = \sqrt{\mathrm{tr}\left(K \Omega K^{\intercal} \Omega^{-1}\right)} / \sqrt{2} \tag{3.95}$$

and coincides with the norm induced by the Frobenius inner product $\langle K, \tilde{K} \rangle = \mathrm{tr}\left(K \Omega \tilde{K}^{\intercal} \Omega^{-1}\right)/2$ defined on $\mathfrak{so}(2N, \mathbb{R})$ for an antisymmetric symplectic form Ω, which in this case corresponds to the fermionic covariance matrix.

And as we can see, it is only a function of the size of the system N. From this we can extract the large-N behaviour of $\mathcal{C}_2$, which is given by

$$\mathcal{C}_2^{\mathrm{Ising}}(N) \approx \frac{\pi}{2} N^{1/2} \sim (\mathrm{Vol})^{1/2} \ , \tag{3.96}$$

which shows that in this case the complexity is also proportional to the volume of the system in units of the lattice spacing $\delta = 1$.

If we had both even and odd sectors, then the complexity (3.93) would be given by

$$\mathcal{C}_2(J_{\mathrm{R}}, J_{\mathrm{T}}) = \sqrt{\sum_{k=0}^{N-1} (2r_k)^2} \ , \tag{3.97}$$

since in this case for each site of the lattice we would have both even and odd contributions leading to a 4×4 block decomposition and to a spectrum of $\mathscr{G}$ given by $\{e^{2\mathrm{i}\, r_k}, e^{2\mathrm{i}\, r_k}, e^{-2\mathrm{i}\, r_k}, e^{-2\mathrm{i}\, r_k}\}$. In this case, the large-N behaviour of complexity would also be $\mathcal{C}_2^{\mathrm{Ising}} \sim N^{1/2} = (\mathrm{Vol})^{1/2}$.

3.4. Discussion

One can immediately see the similarities between (3.97) and the behaviour of bosonic complexity for the scalar field in the UV limit, as seen in (3.63), where we also saw a scaling of complexity with $(\mathrm{Vol})^{1/2}$. The exponent in both expressions can be traced back to the choice of norm, namely the F_2 cost function, in (3.58) and (3.93) and the presence of the square root. Analyses of complexity for different choices of norms, such as in [102] show that complexity built from quantum circuits is sensitive to such choices. This inevitably leads to the question of the "correct" choice of norm.

However, as mentioned already in Sec. 3.1.1, one can argue that this question is ill-posed. It is the author's opinion that one should view complexity as a family of *measures* each associated with a different way of measuring "difficulty" of preparing states and accompanied by a number of computational advantages and disadvantages. For example, our choice of cost function is built from a notion of right-invariant metric on the manifold of Gaussian states and coincides with the geodesic distance induced by a natural inner product on the manifold. Mathematically, this is no different from the usual way in which geodesic distances are computed on Riemannian manifolds via integrals of the type

$$\mathcal{D}_2 = \int_0^1 \mathrm{d}\tau \sqrt{\sum_{\mathrm{I,J}} \eta_{\mathrm{IJ}} Y^{\mathrm{I}} Y^{\mathrm{J}}} \ , \tag{3.98}$$

where in our case the metric is simply

$$\eta_{\mathrm{IJ}} = \mathrm{tr}\left(K_{\mathrm{I}} G_{\mathrm{R}} K_{\mathrm{J}}^{\intercal} G_{\mathrm{R}}^{-1}\right)/4 = (1/2)\mathrm{diag}\{1, \ldots, 1\} \ , \tag{3.99}$$

and $Y^{\mathrm{I}} = \mathrm{tr}\left(K G_{\mathrm{T}} K_{\mathrm{I}}^{\intercal} G_{\mathrm{R}}^{-1}\right)/2$. In other words, the metric is computed entirely with respect to the reference state $|J_{\mathrm{R}}\rangle$. Due to the canonical commutation and anti-commutation relations (3.9), this implies that this normalization is independent on the reference state for fermions, but for bosons this implies that the Lie algebra elements $\hat{K}$ are normalized with respect to an equation relating reference and *gate scale*, which we have assumed to be equal in this work. The reader can refer to [102], [101], and [204] for more details.

We can then translate the problem of finding the complexity of a circuit

$$|J_{\mathrm{T}}\rangle = \overleftarrow{\mathcal{P}} \left\{ e^{\int_0^1 \mathrm{d}\tau \sum_{\mathrm{I}} Y^{\mathrm{I}}(\tau)\hat{K}_{\mathrm{I}}} \right\} |J_{\mathrm{R}}\rangle \ , \tag{3.100}$$

to minimizing the cost function (3.98)

$$\mathcal{C}_2 := \min[\mathcal{D}_2] \ , \tag{3.101}$$

i.e., to finding the geodesic distance between the two states. Here the $\hat{K}_{\mathrm{I}}$ are the quadratic operators built from Lie algebra elements, as in (3.22).

As we have mentioned before, the usefulness of the covariance matrix approach lies in the fact that one can study trajectories on the manifold of Gaussian states provided one stays within the class of Gaussian states entirely. One then focuses solely on quantities, such as the relative complex structure, which are invariant under the action of symplectic or orthogonal transformations. In this case one can also make use of the natural inner product notion on the group manifolds to construct a distance function which naturally captures the geodesic distance between two Gaussian states.

As we will discuss in Sec. 5.2.2 and Sec. 5.2.1, the F_2 cost function (3.98) allows for an efficient minimization for Gaussian purifications of mixed Gaussian states in terms of a gradient descent method.

It is also important to note that the approach that we have chosen for our studies of complexity in free bosonic and fermionic theories is to a large extent driven by calculability, since our choice of cost function and the states that we are considering allow for a closed expression of complexity. A natural question is whether these choices are physically well rooted. Regarding the structure of divergences one indeed finds a close resemblance with the holographic complexity proposals, as we have discussed previously. However, one should note that for the study of the time-dependence of complexity, particularly in the case of the thermofield-double (TFD) state [230], one can find shortcuts to circuits when working in momentum space. It therefore seems that the situation is subtle when studying the time-dependence of complexity.

4. Complexity in Non-equilibrium Quantum Dynamics

In this chapter we present and discuss the study of complexity in a time-dependent setting. We do this by considering a smooth quench through a critical point in a $(1+1)$-dimensional Klein–Gordon theory, where the theory becomes critical and described by a conformal field theory. We first describe the solvable quench model in Sec. 4.1 and we find the time-dependent ground state, which is Gaussian. We then analyse the L^2 complexity of the time-dependent ground state with respect to the asymptotic time-independent ground state state defined at $t \to -\infty$ and study the universal scalings in Sec. 4.2 both in the fast (see Sec. 4.2.2) and slow (see Sec. 4.2.1) regimes. We show that the zero-mode contribution to complexity exhibits scalings both in the fast and slow regimes, while the higher-mode contributions exhibit saturation in the slow regimes. These scalings are contrasted with the ones found for other quantities such as entanglement entropy and 1- and 2-point correlation functions. This shows that complexity, like entanglement entropy can be used as a probe of phase transitions in quantum many-body systems providing a foundation for further studies in this direction.

4.1. Quenches in Quantum Field Theories

The physics of phase transitions in condensed matter systems and in general non-equilibrium dynamics in quantum many-body systems are active topics of research with many challenging aspects. The main motivation for their study is that we are surrounded by a myriad of time-dependent physical phenomena; from the formation of galaxies to chemical reactions, time-dependent phenomena are ubiquitous in nature. While statistical methods, such as the macroscopic fluctuation theory [242], have been developed to study non-equilibrium classical states, several new techniques are still being uncovered to understand strongly-coupled quantum many-body systems using the AdS/CFT Correspondence.

A particular topic which attracted the attention over the past decade is the study of *quantum quenches* [243], which describe a particular type of time-dependence in quantum systems that is generated by a time-dependent coupling appearing in the Hamiltonian. The interest in this type of out-of-equilibrium systems arose mainly due to experimental results in cold atom physics [244], which helped develop the field of quantum dynamics over the past decade. One of the areas where such time-dependent models have led to remarkable success include the study of mechanisms underlying thermalization [82, 245–248] as encoded in reduced density matrices [249, 250].

Of particular interest in the study of quantum quenches, are the ones that lead the theory through a *critical point*, allowing a tractable study of phase transitions in interacting systems. Nonetheless, free theories such as the Klein–Gordon model

described in Sec. 3.3.1 are also used as interesting models to study the emergence of universal properties, such as scalings, for interesting observables. For example, if one takes the mass in (3.40) to be time-dependent such that at time t_0 the mass goes to zero, then at this point the theory becomes *critical*, in this case becoming conformally invariant. When the mass is abruptly taken to zero, *e.g.*, via a step-function, this leads to an *instant quench* corresponding to a discontinuous phase transition. If one takes the mass to zero in a smooth way, *i.e.*, with a smooth function $m(t)$, then this type of quench is called *smooth*.

In this case one can also control how fast the theory approaches its critical point. This turns out to be a crucial aspect of the study of smooth quenches since depending how slow or how fast this critical point is reached, it will ultimately lead to different scaling behaviour for observables in the theory. In this regard, one can typically distinguish between two different regimes. One such regime, often called the Kibble–Zurek (KZ) regime [251, 252], occurs when the approach to criticality is done slowly in an attempt to adiabatically evolve the system. This regime attracted a considerable amount of attention in the last decade both in the context of the AdS/CFT correspondence and in quantum field theories [253–257].

On the other hand, one can also evolve the system in a "fast" non-adiabatic way, leading to a different scaling behaviour than the KZ regime. This regime, which has been studied in the AdS/CFT Correspondence [258–262], free field theory [263–266] and lattice spin models [267, 268], also appears to lead to universal scalings present in interacting theories which flow from a conformal field theory [269, 270]. Most of these studies focused on a particular class of one and two point functions, although more recent works also studied the universal scaling of entanglement entropy [271–273] and complexity [274, 275, **CamH03**].

It is worth noting that there are several motivations for studying complexity in the context of quantum quenches. On one hand, it allows to study the time-dependence of complexity in simple yet revealing models bringing its study closer to the original motivation in the AdS/CFT correspondence where, as we saw in Sec. 2.3, the time-dependence of the holographic complexity proposals was crucial to establishing a connection with a notion of complexity. On the other hand it is interesting to determine whether complexity also exhibits universal scalings like entanglement entropy, and to compare them. At the same time, since entanglement entropy is computed for a reduced density matrix corresponding to spatial subsystems and complexity for the full pure state, it is interesting to determine how the physical information of the system undergoing the quench is captured distinctly by complexity and entanglement. In a following chapter, Ch. 5, we will explicitly consider a notion of complexity for spatial subsystems which probes to the same amount of information about the system as entanglement entropy.

We will now describe a particular solvable quench protocol in Sec. 4.1.1 and then proceed to study the universal scalings of circuit complexity of the vacuum state in both regimes in Sec. 4.2. First we will do this for a single bosonic mode,*i.e.*, for a harmonic oscillator and then we will consider a lattice of oscillators, such as in (3.41).

4.1.1. A Solvable Quench Model

We begin by considering a single harmonic oscillator described by the following time-dependent Hamiltonian

$$\hat{H}(t) = \frac{1}{2}\hat{p}^2 + \frac{1}{2}\omega^2(t/\delta t)\hat{q}^2 \ , \tag{4.1}$$

where δt is the *quench rate* or quench parameter and where $\omega(t/\delta t)$ is a time-dependent frequency profile. We introduce this quench parameter in order to have $\omega(t/\delta t)$ varying over one unit of its argument. Here $\hat{\xi} = \{\hat{q}, \hat{p}\}$ are canonical (dimensionless) variables which satisfy $[\hat{q}, \hat{p}] = \mathrm{i}$. Note that in principle one can also choose to work with dimensionful variables by introducing a mass M, although this doesn't alter our analysis of complexity, as such a mass would get adjusted by appropriately choosing a gate scale.

In order to find the time-dependent ground state, we propose a solution of the equations of motion

$$\frac{\mathrm{d}^2\,\hat{q}(t)}{\mathrm{d}t^2} + \omega^2(t/\delta t)\hat{q}(t) = 0 \quad , \quad \hat{p}(t) = \frac{\mathrm{d}\,\hat{q}(t)}{\mathrm{d}t} \ , \tag{4.2}$$

of the form

$$\hat{q}(t) = f(t)\hat{a} + f^*(t)\hat{a}^\dagger \ , \tag{4.3a}$$

$$\hat{p}(t) = \frac{\mathrm{d}\,f(t)}{\mathrm{d}t}\hat{a} + \frac{\mathrm{d}\,f^*(t)}{\mathrm{d}t}\hat{a}^\dagger \ , \tag{4.3b}$$

where $f(t)$ is a time-dependent complex function and where $\{\hat{a}, \hat{a}^\dagger\}$ are annihilation and creation operators respectively, which satisfy $[\hat{a}, \hat{a}^\dagger] = 1$. Here $f^*(t)$ denotes the complex conjugate of $f(t)$. This leads to the following Wronskian constraint for $f(t)$

$$f(t)\frac{\mathrm{d}\,f^*(t)}{\mathrm{d}t} - f^*(t)\frac{\mathrm{d}\,f(t)}{\mathrm{d}t} = \mathrm{i} \ , \tag{4.4}$$

where now $f(t)$ is a solution of the equation of motion

$$\frac{\mathrm{d}^2\,f(t)}{\mathrm{d}t^2} + \omega^2(t/\delta t)f(t) = 0 \ , \tag{4.5}$$

for all t. We choose the asymptotic boundary condition

$$f(t \to -\infty) \to f_{\mathrm{in}}(t) = \frac{1}{\sqrt{2\omega_{\mathrm{in}}}} e^{-\mathrm{i}\,\omega_{\mathrm{in}} t} \ , \tag{4.6}$$

where $\omega_{\mathrm{in}} := \omega(t \to -\infty)$. Even though we do not explicitly write down the dependence on δt, the reader should be aware that the time-dependent function $f(t)$ is in reality a function of the ratio $t/\delta t$. That is, we want our system to start with the "in" vacuum of the asymptotic (time-independent) Hamiltonian at $t \to -\infty$.

We now construct the time-dependent ground state $|\psi_0\rangle$ by imposing that it is annihilated by $\hat{a}$

$$\hat{a}\,|\psi_0\rangle = -\mathrm{i}\left(\frac{\mathrm{d}\,f^*(t)}{\mathrm{d}t}\hat{q} - f^*(t)\hat{p}\right)|\psi_0\rangle = 0 \ . \tag{4.7}$$

In position space this condition becomes the following differential equation for the ground state wavefunction $\psi_0(q,t)$

$$\left(\frac{\mathrm{d}\, f^*(t)}{\mathrm{d}t} q + \mathrm{i}\, f^*(t) \frac{\mathrm{d}}{\mathrm{d}q}\right) \psi_0(q,t) = 0 \ , \tag{4.8}$$

which is solved by

$$\psi_0(q,t) = \left(\frac{1}{2\pi\, f^*(t) f(t)}\right)^{1/4} \exp\left[\mathrm{i}\, \frac{1}{f^*(t)} \frac{\mathrm{d}\, f^*(t)}{\mathrm{d}t} \frac{q^2}{2}\right] \ . \tag{4.9}$$

This is the most general ground state solution to the time-dependent equations of motion for a generic frequency profile $\omega(t/\delta t)$. Of course, we still need to find a solution $f(t)$ to (4.5) for a specific profile, but we have already found the general form of the ground state wavefunction. We can immediately see that this is a Gaussian state, as expected. In particular, we can bring the wavefunction (4.9) to the form (3.13), where now $a(t)$ and $b(t)$ are time-dependent real-valued functions corresponding to the real and imaginary parts of $-\mathrm{i}(1/f^*(t))(\mathrm{d}\, f^*(t)/\mathrm{d}t)$. The precise form of $a(t)$ and $b(t)$ in this case is not particularly revealing, although one can certainly do the algebra to obtain them in terms of the real and imaginary part of $f(t)$ and their time-derivatives. The normalizability condition $a(t) > 0$ is now imposed on the function $f(t)$.

One can also see that at early times the ground state solution is simply given by

$$\psi_0(q, t \to -\infty) = \psi_0^{\mathrm{in}}(q) = \left(\frac{\omega_{\mathrm{in}}}{\pi}\right)^{1/4} \exp\left[-\frac{\omega_{\mathrm{in}}\, q^2}{2}\right] \ , \tag{4.10}$$

which is the "in" vacuum ground state obtained simply by taking (4.6) in (4.9).

What we now need is a particular quench profile $\omega(t/\delta t)$ with the properties that we discussed at the beginning of this chapter; that is, a profile which asymptotes to a constant both at early and late times and which takes the theory through a critical point in the interval $[-\delta t, \delta t]$. One such profile, which has also been used to study the scalings of entanglement entropy [272], is:

$$\omega(t/\delta t) = \omega_0 \left(1 - \frac{1}{\cosh^2\left(\frac{t}{\delta t}\right)}\right)^{1/2} = \omega_0 \tanh\left(\frac{t}{\delta t}\right) \ , \tag{4.11}$$

where ω_0 is a free parameter corresponding to the "in" asymptotic value of the frequency $\omega_0 = \omega_{\mathrm{in}}$. As we can see from Fig. 4.1, the quench parameter δt controls how fast the system approaches the critical point at $t = 0$ where $\omega(0) = 0$. In particular, one can see that for $\delta t \gg \omega_0^{-1}$ the approach to the critical point at $t = 0$ is "slow". This corresponds to the Kibble–Zurek regime, which we already mentioned in the introduction to this chapter. On the other hand for $0 < \delta t < \omega_0^{-1}$, the approach to the critical point is more sudden, corresponding to the "fast" quench regime and which in the limit $\delta t \to 0$ corresponds to a sudden quench. We will return to an analysis these two regimes in Sec. 4.2.1 and Sec. 4.2.2 respectively.

With this profile it is possible solve the equation (4.5) for $\omega(t/\delta)$ given by (4.11), which now takes the form

$$f''(\tau) + w_0^2 \tanh^2(\tau)\, f(\tau) = 0 \ , \tag{4.12}$$

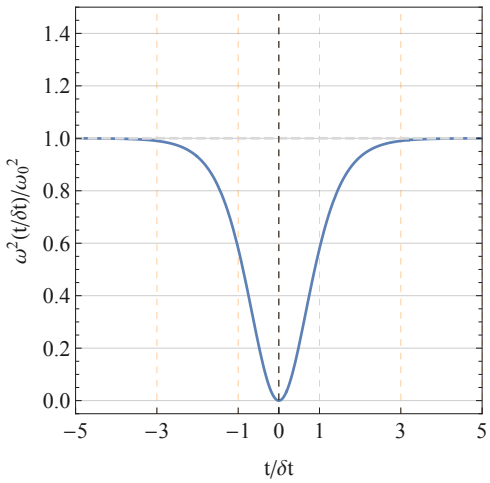

Figure 4.1.: Plot of the quench profile $\omega^2(t/\delta t)/\omega_0^2$ as a function of $t/\delta t$. Note the asymptotic behaviour of the profile $\omega(t \to \pm\infty) = \omega_0$.

where we re-defined for simplicity $\tau = t/\delta t$ and $w_0 = \omega_0 \delta t$ and where $f''(\tau) = d^2 f(\tau)/d\tau^2$. The solution $f(\tau)$ then can be written in terms of hypergeometric functions, or Legendre functions of the first and second kind. A full description of the solution can be found in [272].

It is important to note that a by-product of the time-dependence is that now the covariance matrix of the ground state (4.9) will be given in terms of $f(t)$ and its derivatives rather than simply by $\omega(t/\delta t)$, as in the time-independent case. This will also apply in case of the harmonic chain. We omit a full description of the solution at this point, but the reader should bear in mind that the most relevant feature of this particular quench protocol is that it is solvable analytically.

We can also see how the time-dependent mass parameter influences the energy of the system. Even though we initially start with the "in" ground state of the Hamiltonian (4.1) with constant energy $E_0 = \omega_0$ at early times $t \to -\infty$ given by (4.10), the adiabaticity of the system is lost as we bring it through the critical point at $t = 0$. At the same time, we can see that at early times the system is gapped by $\omega_0 > 0$ but then becomes gapless $\omega(t = 0) = 0$ at the point where the system becomes conformally invariant $m^2(t = 0) = \omega^2(t = 0) = 0$, corresponding to oscillator excitations above the ground state (4.9) as the system evolves in time with (4.1). The mass (or energy) gap of the system $E(t) = m(t) = \omega(t)$ is an important parameter which will be relevant in Sec. 4.2.1 to understand the loss of adiabaticity of the system.

This analysis can be naturally generalized to a harmonic chain of N oscillators; *i.e.*, to a lattice discretization of the Klein–Gordon model in $(1 + 1)$-dimensions, just as in (3.41). A system of two coupled harmonic oscillators with a time-dependent coupling was also used in [109, 111, 272] to study entanglement entropy. Setting the lattice spacing to unity $\delta = 1$ we have the time-dependent Hamiltonian

$$\hat{H}(t) = \frac{1}{2} \sum_{i=0}^{N-1} \left(\hat{\pi}_i^2 + m(t)^2 \hat{\varphi}_i^2 + (\hat{\varphi}_i - \hat{\varphi}_{i+1})^2 \right) , \tag{4.13}$$

where $\hat{\varphi}_i$ and $\hat{\pi}_i$ once again correspond to our choice of canonical variables $\hat{\xi}_i^a = (\hat{\varphi}_i, \hat{\pi}_i)$ for $a = 1, 2$ which satisfy the canonical commutation relations $[\hat{\varphi}_i, \hat{\pi}_j] = \mathrm{i}\,\delta_{i,j}$ and where we also imposed periodic boundary conditions $N + i = i$, $\forall\, i$.

Once again, we can diagonalize the Hamiltonian by introducing a discrete Fourier transform, like in (3.43), with which we obtain the Hamiltonian in momentum space

$$\hat{H}(t) = \frac{1}{2}\sum_{k=0}^{N-1}\left(|\tilde{\pi}_k|^2 + \omega_k^2(t)|\tilde{\varphi}_k|^2\right) \ , \tag{4.14}$$

which also describes a system of N decoupled harmonic oscillators with now time-dependent frequencies:

$$\omega_k(t) = \sqrt{m^2(t) + 4\sin^2\left(\frac{\pi k}{N}\right)} \ . \tag{4.15}$$

and where now the modes $\tilde{\varphi}_k$ satisfy

$$\frac{\mathrm{d}^2\,\tilde{\varphi}_k(t)}{\mathrm{d}t^2} + \left(m^2(t) + 4\sin^2\left(\frac{\pi k}{N}\right)\right)\tilde{\varphi}_k = 0 \ , \tag{4.16}$$

where in this case we simply take the time-dependent mass $m(t)$ to be given by the quench profile $\omega(t/\delta)$ in (4.11).

One can now repeat a similar analysis as in the single harmonic oscillator case, and propose a general solution of the differential equation of the type:

$$\tilde{\varphi}_k(t) = f_k(t)\hat{a}_k + f_k^*(t)\hat{a}_{-k}^\dagger \ , \tag{4.17a}$$

$$\tilde{\pi}_k(t) = \frac{\mathrm{d}\,f_k(t)}{\mathrm{d}t}\hat{a}_k + \frac{\mathrm{d}\,f_k^*(t)}{\mathrm{d}t}\hat{a}_{-k}^\dagger \ , \tag{4.17b}$$

where $f_k(t)$ are time-dependent complex functions for each mode k and where $\{\hat{a}_k, \hat{a}_k^\dagger\}$ are the k-mode annihilation and creation operators respectively, which satisfy $[\hat{a}_k, \hat{a}_{k'}^\dagger] = \delta_{k,k'}$. Here we also have a Wronskian constraint for $f_k(t)$

$$f_k(t)\frac{\mathrm{d}\,f_k^*(t)}{\mathrm{d}t} - f_k^*(t)\frac{\mathrm{d}\,f_k(t)}{\mathrm{d}t} = \mathrm{i} \ , \tag{4.18}$$

and where $f_k(t)$ solves the differential equation

$$\frac{\mathrm{d}^2\,f_k(t)}{\mathrm{d}t^2} + \omega_k^2(t)f_k(t) = 0 \ . \tag{4.19}$$

In this case the asymptotic boundary conditions are given by

$$f_k(t \to -\infty) \to f_k^{\mathrm{in}}(t) = \frac{1}{\sqrt{2\omega_k}}e^{-\mathrm{i}\,\omega_k t} \ , \tag{4.20}$$

where $\omega_k := \omega_k(t \to -\infty) = \left(\omega_0^2 + 4\sin^2(\pi\, k/N)\right)^{1/2}$. This leads to a mode-by-mode decomposition of the time-dependent ground state $|\Psi_0\rangle$, which is annihilated

by $\hat{a}_k |\Psi_0\rangle = 0$ for all k. In the field operator basis, this leads to a differential equation which is solved by the ground state wavefunction given by

$$\Psi_0(\tilde{\varphi}_k, t) = \prod_{k=0}^{N-1} \left(\frac{1}{2\pi f_k^*(t) f_k(t)} \right)^{1/4} \exp\left[\mathrm{i} \frac{\dot{f}_k^*(t)}{f_k^*(t)} \frac{|\tilde{\varphi}_k|^2}{2} \right] = \prod_{k=0}^{N-1} \Psi_0^k(\tilde{\varphi}_k, t) \ , \quad (4.21)$$

and which is also Gaussian, as expected. One can also refer to [272] for the full solution $f_k(t)$ of (4.19), which is also given in terms of hypergeometric functions.

Here, once again, the reader should note that the entries of the covariance matrix corresponding to each individual mode are comprised of combinations of real and imaginary parts of $(\mathrm{i}/f_k^*(t))(\mathrm{d}f_k^*(t)/\mathrm{d}t)$ instead of simply the k-mode frequencies ω_k:

$$G(t) = \bigoplus_{k=0}^{N-1} G_k(t) = \bigoplus_{k=0}^{N-1} \begin{pmatrix} \frac{1}{a_k(t)} & \frac{-b_k(t)}{a_k(t)} \\ \frac{-b_k(t)}{a_k(t)} & \frac{a_k^2(t)+b_k^2(t)}{a_k(t)} \end{pmatrix} \ , \quad (4.22)$$

where $a_k(t)$ and $b_k(t)$ refer to the functions characterizing each of the time-dependent modes, as in (3.13) and (3.15), corresponding to the real and imaginary parts of $-(\mathrm{i}/f_k^*(t))(\mathrm{d}f_k^*(t)/\mathrm{d}t)$. Much like in the time-independent case discussed in Sec. 3.3.1, this mode-by-mode decomposition of the ground state covariance matrix allows for an efficient study of complexity, which will be analysed in the following section.

4.2. The Universal Scalings of Complexity

Having found the time-dependent ground state for the quench protocol (4.11), we are in a position to study the time-dependence of complexity in this model. To do this, we follow the geometric procedure described in Sec. 3.1.1 applied to bosonic Gaussian states in Sec. 3.3.1 and consider that the time-dependent ground state (4.21) with covariance matrix (4.22) corresponds to the target state $|\Psi(t)\rangle$ of the quantum circuit

$$|\Psi(t)\rangle = \hat{U}(t) |\Psi_{\mathrm{R}}\rangle \ , \quad (4.23)$$

where we will take the reference state $|\Psi_{\mathrm{R}}\rangle$ to be the "in" ground state of the Hamiltonian at $t \to -\infty$ with covariance matrix

$$G_{\mathrm{R}}^{\mathrm{in}} = \bigoplus_{k=0}^{N-1} G_k^{\mathrm{in}} = \bigoplus_{k=0}^{N-1} \begin{pmatrix} \frac{1}{\omega_k} & 0 \\ 0 & \omega_k \end{pmatrix} \ , \quad (4.24)$$

where as before $\omega_k := \omega_k(t \to -\infty) = \left(\omega_0^2 + 4\sin^2(\pi\, k/N)\right)^{1/2}$. Note that this is in contrast with our choice for reference state in Sec. 3.3.1, where we took the spatially disentangled state defined by the linear complex structure (3.55) as the reference state. The motivation for this that this choice allows to study the time-dependence of complexity mode-wise allowing at the same time an mode-by-mode analysis of the fast and KZ scalings of complexity. This of course means that in the $t \to -\infty$ limit, both states coincide and $\hat{U}(t \to -\infty) = \hat{\mathbb{1}}$.

The relative complex structure $\mathscr{G}^a{}_b(t) = -(J_{\mathrm{T}}(t))^a{}_c (J_{\mathrm{R}})^c{}_b$ is given in this case by:

$$\mathscr{G}(t) = \bigoplus_{k=0}^{N-1} \mathscr{G}^k(t) = \bigoplus_{k=0}^{N-1} \begin{pmatrix} \frac{\omega_k}{a_k(t)} & -\frac{b_k(t)}{\omega_k a_k(t)} \\ -\frac{\omega_k b_k(t)}{a_k(t)} & \frac{a_k^2(t)+b_k^2(t)}{\omega_k a_k(t)} \end{pmatrix} \ . \quad (4.25)$$

We now address another crucial and distinguishing aspect of the analysis, namely our choice of cost function. We will follow [CamH03], where the choice of norm differs from the geodesic distance defined on the manifold $\mathrm{Sp}(2N,\mathbb{R})$ given by (3.58). The main reason being that in this work we were motivated by generating the target state with the minimal number of gates, which could be achieved by considering a (closed) subgroup of $\mathrm{Sp}(2N,\mathbb{R})$. That is, since we have reduced the problem of computing the complexity for N bosonic modes to the problem of computing complexity for a single mode, we can consider a closed subgroup in $\mathrm{Sp}(2,\mathbb{R})$ with which we can construct a geodesic distance akin to (3.98) providing a notion of distance for each k-mode.

This analysis should also be taken as an example of how different choices for gates ultimately lead to different measures for complexity even when considering the same type of cost-function. Intuitively, one can imagine that having access to fewer gates constrains the "freedom" with which one can build quantum circuits and thus the complexity measure obtained thereof can be considered a bound to other measures of complexity built from a larger set of universal gates.

For each mode, we consider the Lie group $\mathrm{Sp}(2,\mathbb{R})$ as the full set of transformations that allows us to get from the reference state $|\Psi^k_{\mathrm{R}}\rangle$ to the time-evolved target state $|\Psi^k_{\mathrm{T}}(t)\rangle$. From this we will consider a closed subgroup which is *sufficient* to generate the target state as we will describe now. The reader can refer to the supplemental material of [CamH03] for details of this analysis.

The algebra $\mathfrak{sp}(2,\mathbb{R})$ is generated by the quadratic operators

$$\hat{W} = \frac{\mathrm{i}}{2}\left(\hat{q}\hat{p} + \hat{p}\hat{q}\right) \ , \ \hat{V} = \frac{\mathrm{i}}{\sqrt{2}}\hat{q}^2 \ , \ \hat{Z} = \frac{\mathrm{i}}{\sqrt{2}}\hat{p}^2 \ , \tag{4.26}$$

where here $\{\hat{q},\hat{p}\}$ are the dimensionless phase space coordinates considered in (4.1). Note that these correspond to the quadratic operators described in (3.22), and satisfy the commutation relations

$$[\hat{W},\hat{V}] = 2\hat{V} \ , \ [\hat{W},\hat{Z}] = -2\hat{Z} \ , \ [\hat{V},\hat{Z}] = -2\hat{W} \ . \tag{4.27}$$

It can be shown that $\{\hat{V},\hat{W}\}$ form a closed subalgebra which is capable of generating the general Gaussian state (3.15). Hence, in contrast with our analysis in Sec. 3.3.1, we restrict to circuits (4.23) generated by the the submanifold of $\mathrm{Sp}(2,\mathbb{R})$ generated by matrix representations of the form

$$\hat{U} = \exp\left(\alpha(z,y)\hat{W} + \beta(z,y)\hat{V}\right) \to \mathcal{R}(\hat{U}) = \frac{1}{\sqrt{z}}\begin{pmatrix} z & 0 \\ \frac{y}{\sqrt{2}} & 1 \end{pmatrix} \ , \tag{4.28}$$

where $\alpha = -\log(z)/2$ and $\beta = y\log(z)/(2(z-1))$. The matrix representation of this operator can then be used to construct the control functions Y^{I} used to build the F_2 cost function (3.8b), which after a judicious choice of penalty factors leads to the metric of the Poincaré disc

$$\mathrm{d}s^2 = \sum_{\mathrm{IJ}} g_{\mathrm{IJ}} Y^{\mathrm{I}} Y^{\mathrm{J}} = \frac{2\mathrm{d}z^2 + \mathrm{d}y^2}{8z^2} \ , \tag{4.29}$$

i.e., the metric of the 2-dimensional hyperbolic space $\mathbb{H}^2$, for which the geodesic distance is known to be given by:

$$\mathcal{D}_2^{\mathbb{H}^2}(p_0,p_1)=\frac{1}{2}\log\left(\chi(p_0,p_1)+\sqrt{\chi^2(p_0,p_1)-1}\right)\ , \tag{4.30}$$

where $p_0=(z_0,y_0)$ and $p_1=(z_1,y_1)$ parametrize the starting and end points of the geodesic respectively, and where

$$\chi(p_0,p_1)=\frac{2(z_1^2+z_0^2)+(y_1-y_0)^2}{4z_1z_0}\ . \tag{4.31}$$

The reader should note that the fact that the metric obtained (4.29) is the one for the hyperbolic space is a consequence of the choice of gates and penalty factors used to construct the quantum circuit and is not connected with holography or the AdS/CFT correspondence.

The physical information of the reference and target states enter precisely here, for which we have:

$$(z_0,y_0)=(1,0)\ \ ,\ \ (z_1,y_1)=\left(\frac{\omega_k}{a_k(t)},\frac{-\sqrt{2}b_k(t)}{a_k(t)}\right)\ . \tag{4.32}$$

The function (4.31) can be recognized to be related to the trace of the relative covariance matrix, leading to the measure of complexity for the whole harmonic chain given by

$$\mathcal{C}_2^{\mathbb{H}^2}(t)=\left(\sum_{k=0}^{N-1}\left[\frac{1}{2}\log\left(\chi_k(t)+\sqrt{\chi_k^2(t)-1}\right)\right]\right)^{1/2}\ , \tag{4.33}$$

where

$$\chi_k(t):=\frac{1}{2}\mathrm{tr}\left(\mathscr{G}^k(t)\right)=\frac{1}{2}\left(\frac{\omega_k}{a_k(t)}+\frac{a_k^2(t)+b_k^2(t)}{\omega_k a_k(t)}\right)\ , \tag{4.34}$$

and where we constructed the full complexity of the harmonic chain by using the geodesic distance function for each copy of the hyperbolic disc $\mathbb{H}^2$ corresponding to each of the modes.

The description here differs slightly from the analysis present in [**CamH03**], where (4.34) was constructed from the *squeezed* target state covariance matrix. While the form of the squeezed target covariance matrix and relative covariance matrix is different, they do share the same trace and same determinant. It is also worth mentioning that a similar formula recently appeared in a study of the complexity of primordial perturbations in quantum cosmology [276].

As we have already mentioned, in this case the complexity functional is an upper-bound on the complexity cost function constructed by considering the full set of symplectic transformations $\mathrm{Sp}(2N,\mathbb{R})$ (3.58):

$$\mathcal{C}_2^b(t)\leq\mathcal{C}_2^{\mathbb{H}^2}(t)\ , \tag{4.35}$$

since lengths of geodesics in the full manifold of $\mathrm{Sp}(2N,\mathbb{R})$ are bounded from above by the lengths of geodesics in $(\mathbb{H}^2)^{\otimes(N)}$.

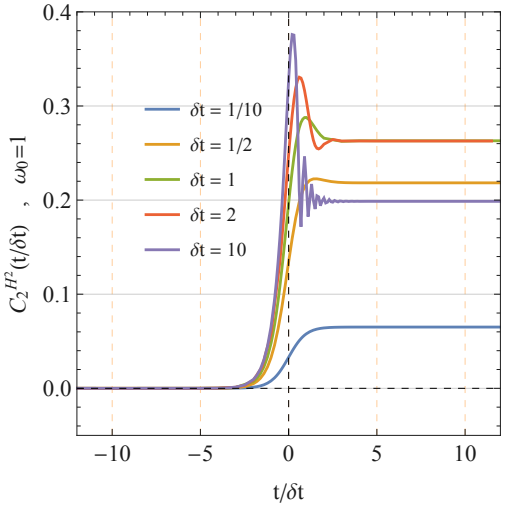

Figure 4.2.: Plot of $\mathcal{C}_2^{\mathbb{H}^2}(t/\delta t)$ for $\omega_0 = 1$ and different values of δt. The oscillations observed for large δt arise from the rapidly oscillating behaviour of the solution (4.21) after passing through the critical point at $t = 0$. Note the saturation of $\mathcal{C}_2^{\mathbb{H}^2}(t/\delta t)$ for large $t/\delta t$, which is due to the choice of reference frequency $\omega_0 = 1$.

The continuum limit of (4.33), which we will use for the analysis of scalings in the following sections, is obtained by integrating over momentum modes:

$$\mathcal{C}_2^{\mathbb{H}^2}(t) = \left(\int_0^{2\pi} \frac{\mathrm{d}k}{2\pi} \left[\frac{1}{2} \log \left(\chi_k(t) + \sqrt{\chi_k^2(t) - 1} \right) \right]^2 \right)^{1/2} , \tag{4.36}$$

where we also now have a k-the mode frequency $\omega_k(t)$ in the continuum given by

$$\omega_k(t) = \sqrt{m^2(t) + 4 \sin^2 \left(\frac{k}{2} \right)} . \tag{4.37}$$

An example of the behaviour of $\mathcal{C}_2^{\mathbb{H}^2}(t, \delta t)$ for different values of δt can be seen in Fig. 4.2.

In order to study the scalings of complexity in the following section, we will evaluate the complexity functional (4.36) at the critical point $t = 0$ as a function of quench parameter δt. We will do this mode-by-mode and for the different regimes in the following sections. To illustrate what the behaviour of the complexity functional (4.33) at $t = 0$, Fig. 4.3 shows a plot of $\mathcal{C}_2^{\mathbb{H}^2}(t = 0, \delta t)$.

4.2.1. "Slow" Kibble–Zurek Regime

As mentioned at the beginning of this chapter, it has been conjectured that observables obey a KZ scaling [251, 252] for slow quenches $\delta t \gg \omega_0$, evidence for which has been found in solvable models and simulations [244, 255]. This type of scalings

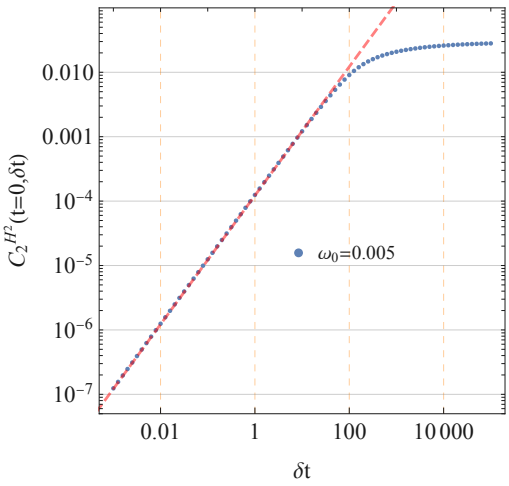

Figure 4.3.: Plot of $\mathcal{C}_2^{\mathbb{H}^2}(t=0,\delta t)$ as a function of δt for $\omega_0 = 0.005$. The dashed red line shows a linear scaling $\propto \delta t$ in the small δt regime.

can be heuristically motivated as follows: one assumes that as soon as the adiabatic evolution of the system starts to break down at some time t_{KZ}, the system enters a "diabatic" phase where energy is no longer conserved. It is at this time that a length scale named the *correlation length* ξ_{KZ} becomes the only characteristic length scale of the system throughout this critical phase. That is, the system is "frozen" at t_{KZ}. At this point, 1-point correlation functions of operators $\hat{O}_\Delta(t)$ scale as $\langle \hat{O}_\Delta(t)\rangle \sim \xi_{KZ}^{-\Delta}$ where Δ denotes the scaling dimension of the operator at the critical point $t = 0$. More detailed analyses [255, 256] reveal a scaling of 1- and 2-point correlation functions of the form

$$\langle \hat{O}_\Delta(t)\rangle \sim \xi_{KZ}^{-\Delta} F(t/t_{KZ}) \,, \tag{4.38a}$$

$$\langle \hat{O}_\Delta(q,t)\hat{O}_\Delta(q',t')\rangle \sim \xi_{KZ}^{-2\Delta} F\left(\frac{|q-q'|}{\xi_{KZ}}, \frac{(t-t')}{t_{KZ}}\right) \,, \tag{4.38b}$$

where F is a function dependent only on the displayed ratios. The loss of adiabaticity of the system starting from the KZ time t_{KZ} can be understood from the Landau criterion [277], which estimates the time scale when the leading adiabatic corrections in perturbation becomes of the same order as the mass gap ω_0 itself:

$$\frac{1}{E(t)^2}\frac{\mathrm{d}E(t)}{\mathrm{d}t}\Big|_{t_{KZ}} = 1 \,, \tag{4.39}$$

where $E(t)$ is in general the time-dependent mass gap from criticality: $E(t) = m(t)$. For the quench profile (4.11) one finds that the correlation length ξ_{kZ} coincides with the KZ time t_{KZ} given in this case by $t_{KZ} \approx \sqrt{\delta t/\omega_0}$, for which we obtain a k-mode frequency given by:

$$\omega_{KZ}(t) = \sqrt{m^2(t_{KZ}) + 4\sin^2\left(\frac{k}{2}\right)} \approx \sqrt{\frac{\omega_0}{\delta t} + 4\sin^2\left(\frac{k}{2}\right)} \,, \tag{4.40}$$

where we used the fact that $m^2(t_{KZ}) \sim \omega_0^2 t_{KZ}^2/\delta t^2$ since in the slow regime we have $\delta t > t_{KZ}$.

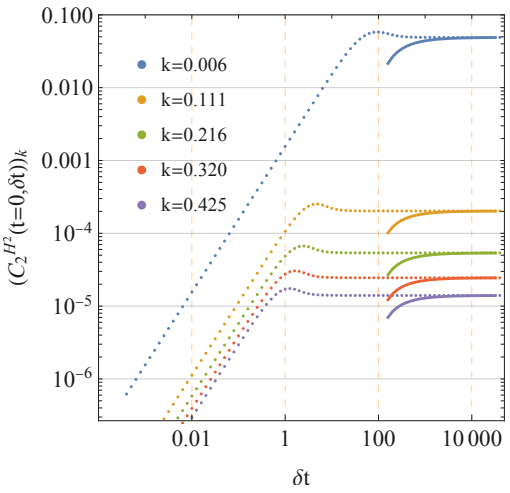

Figure 4.4.: Plot of single-mode contributions to $C_2^{\mathbb{H}^2}(t=0,\delta t)$ as a function of δt for $\omega_0 = 0.005$ and for different values of k. The solid lines show an agreement of the exact (dotted) solutions with the saturation value (4.41) in the large δt KZ regime.

In this case, the KZ scaling of complexity for the k-th mode can be extracted by computing the complexity for the KZ frequency (4.40). In this case we found a KZ scaling in the slow regime for $\delta t < (\omega_0/4)\csc^2(k/2)$. On the other hand, when δt exceeds this value we observed a saturation in the frequency to $2\sin(k/2)$ and of the k-th mode complexity to

$$\mathcal{C}_2^{\text{sat}}(k) = \frac{1}{2}\log\left(\frac{\omega_0^2 + 2 - 2\cos(k)}{2|\sin(k/2)|}\right) \ . \tag{4.41}$$

This saturation value in the large δt regime can be contrasted with the KZ approximation with exact numerical results for different k-modes, which can be seen in Fig. 4.4. From Fig. 4.4 we can see the contributions from individual modes to $\mathcal{C}_2^{\mathbb{H}^2}(t=0,\delta t)$ for $k > 0$. We can see that all modes go to zero in the limit $\delta t \to 0$, whereas there is a mode-dependent saturation in the slow regime $\delta t \to \infty$, consistent with the KZ expectation (4.41). In other words, Fig. 4.4 shows that the non-zero k-modes saturate for large δt and that the KZ expectation (4.41) reproduces the behavior of the respective mode-wise complexity at large δt, which shows that a KZ scaling is present in our measure of complexity.

In this context it is also important to analyse the zero-mode $k = 0$ which, as we saw in Sec. 3.3.1, is the source for a divergence of the two-point function of the ground state (4.21) also in the time-independent case (3.46). Fig. 4.5 shows that unlike higher k-modes, the complexity of the zero mode does not saturate in the KZ regime and furthermore presents logarithmic scaling in this regime. In this case, by analysing the numerical data we find that the zero-mode has the following behaviour in the KZ regime:

$$\mathcal{C}_{KZ}^{k=0}(\delta t) = \frac{1}{4}\log(\delta t) \ . \tag{4.42}$$

By comparing Figs. 4.5 and 4.3, we see that the zero-mode is primarily responsible

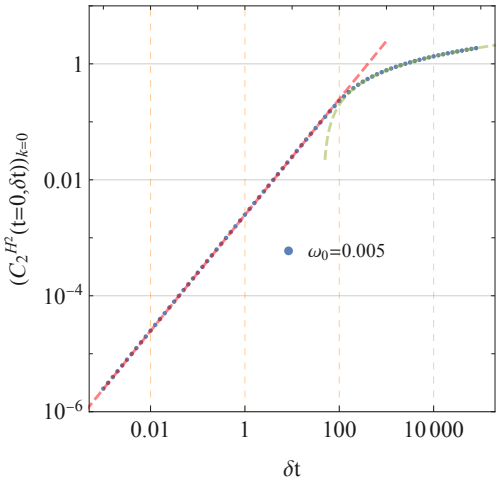

Figure 4.5.: Plot of the zero-mode contribution to complexity $\mathcal{C}^{\mathbb{H}^2}_{2,k=0}(t=0,\delta t)$ as a function of δt for $\omega_0 = 0.005$. The dashed red line shows a linear scaling $\propto \delta t$ in the small δt regime, while the dashed green line shows a logarithmic scaling $\propto (1/4)\log(\delta t)$ in the large δt regime. The transition from the fast to the slow regime occurs at $\omega_0 \delta t \sim 1$, *i.e.*, $\delta t \sim 200$ in this case.

for the large δt behaviour of complexity, which does not exactly show a KZ scaling, due to the contributions from the higher-modes which otherwise tend to saturate the full complexity.

A similar KZ scaling has been observed for entanglement entropy under a similar critical quantum quench where the authors found instead a 1/6 logarithmic coefficient [271, 272].

4.2.2. Fast Regime

A different kind of scaling present in the so-called "fast" regime was originally found in holographic models [259, 260] and subsequently shown to be completely general in relativistic quantum field theories [263–267]. This type of scaling is a consequence of causality and the fact that in this regime one can use linear response to accurately study the behaviour of expectation values. For critical quantum quenches one can furthermore use perturbation theory around the critical Hamiltonian describing the underlying conformal field theory for a perturbation arising from the time-dependent coupling.

In this case, for $\delta t \ll \omega_0$ one finds an expectation value of 1-point functions

$$\langle \hat{O}_\Delta \rangle \sim \delta t^{D-2\Delta}, \tag{4.43}$$

where D is the spacetime dimension and Δ is the scaling dimension of the operator $\hat{O}_\Delta(t)$.

From Fig. 4.5 we can see that not only does the complexity of the zero mode exhibit a logarithmic scaling in the KZ regime, but it also exhibits a linear scaling in the

fast regime

$$\mathcal{C}^{k=0}_{\text{fast}}(\delta t) \propto \delta t \ . \tag{4.44}$$

A transition between these two regimes occurs around $\delta t\, \omega_0 \sim 1$.

Furthermore, in the fast regime $\delta t < \omega_0$, the full state complexity also grows linearly with δt, as can be seen from Fig. 4.3. While these fast scalings are also present for higher modes as well, as in Fig. 4.4, the reader can see that they are confined to increasingly narrow regions of δt for larger values of k.

4.3. Discussion

One natural question to ask at this point is whether the observation of scalings in complexity depends on the choice of norm, namely of our cost function (4.36). Fig. 4.4 shows that as we approach the UV modes, both the exact solution as well as the KZ approximation for non-zero modes (4.41) saturate to smaller values of complexity at lower values of δt. However, as we already mentioned, it is the zero mode 4.5 which dominates the large δt limit. This means that the full complexity, when written in terms of the Fourier (momentum) modes, approximately inherits the scaling behaviour of the zero mode. This in turn implies that for complexity measures arising from F_p cost functions with $p > 2$, we can generically expect that the full state complexity constructed from Fourier modes will be dominated by the zero mode and will also approximately inherit its logarithmic behaviour in the KZ regime.

The exception to this analysis, however, is the F_1 cost function (3.8a) which gives rise to an L^1 norm. In this case it is not entirely clear what universal scalings can be extracted from the full state complexity, since the saturation values for higher k-modes would not be as suppressed as in the other cases. The reason is that the exponent with which the different contributions are summed-over is 1. In this case it is hence not clear how much the scalings of zero-mode contribution to complexity would dominate over the higher-mode contributions.

The reader could also wonder what would happen if we considered the spatially disentangled reference state (3.55) as the reference state, instead of the time-independent ground state. In this case, numerical studies show that only the zero-mode exhibits equivalent scalings in both regimes, as expected, while higher k-modes do not. The difference between this choice and our initial choice of reference state case, is that the non-zero k mode saturations occur at larger values of δt. Thus, in the previous case when the small contributions from higher k-modes are squared and became subdominant in the k-mode sum, in this case they remain relevant. This is also the same mechanism why the F_2 cost function "gets rid" of the non-zero k mode saturations more efficiently than the F_1 cost function. When the individual mode contributions to complexity are risen to higher powers, the non-zero saturations (which are $\ll \omega_0$) essentially become subdominant.

Similar studies were carried out in the context of the relativistic fermionic Ising theory in [275]. In this case, a linear behaviour of complexity was also observed in the instantaneous quench regime $\omega_0 \delta t \ll 1$, as well as a saturation of the higher

modes in the slow quench regime $\delta t < (\omega_0/4)\csc^2(k/2)$. The main difference in this case is that the zero-mode contribution to the complexity vanishes. This is because the Bogoliubov transformation of the zero-mode which is used to determine the contribution is trivial, which is in turn due to the fact that Majorana modes have independent zero modes. Of course, in this case the zero-mode simply refers to the momentum mode with $k = 0$, and does not have any associated IR divergence as in the bosonic case.

Another difference between the work [275] and our analysis is that the former evaluates complexity using the L_1 norm assuming that the shortest circuit minimizes an L_2 complexity. This is a commonly used technique to studying the former case since the minimization of F_1 cost functions are in general a challenging task. Regardless of this, the analysis of the universal scalings fermionic complexity presented in [275] presents strong similarities with the bosonic case. As a consequence, these works provide strong evidence that complexity is a useful quantity to study universal scalings in quantum quenches that take a theory through criticality.

5. Complexity of Purification

In this chapter we present the study of complexity of purification, a measure of complexity which generalizes the notion from pure to mixed quantum states. In Sec. 5.1 we present the basic ideas behind the notion of complexity of purification and apply it to a system of two coupled harmonic oscillators using of our critical quench model presented in the previous chapter. This allows us to study this notion also in a time-dependent scenario while setting the stage for the next section (Sec. 5.2), where we study complexity of purification in the general context of Gaussian mixed bosonic and fermionic states. In this section we study complexity of purification for vacuum subregions of free quantum field theories following Sec. 3.3.1 and Sec. 3.3.2 using the most general Gaussian purifications. We show that complexity of purification captures the divergence structure of pure state complexity, where the size of the full system is replaced by the size of the spatial subregion. This occurs for subsystems consisting of a single interval. In the case of two adjacent intervals, of which our studies are pioneering, we show that complexity of purification exhibits a logarithmic divergence akin to the holographic subregion complexity proposals described in Sec. 2.3.2. We end this chapter by comparing our bosonic complexity of purification results with two other approaches present in the literature. This comparison shows that our method based on a general optimization over Gaussian purifications provide better results as the conformal limit of the massive Klein–Gordon theory is approached.

5.1. The Concept of Complexity of Purification

While we have focused so far on the study of complexity in the context of pure quantum states, the reader may wonder if the same formalism applies directly to mixed states described by a density matrix ρ. The main motivation being that mixed states are also ubiquitous in nature; considering a finite subregion from a larger system described by a pure quantum state irrevocably leads to the consideration of mixed states, which in most cases will have entangled degrees of freedom with its exterior. However, it is not possible to construct mixed states via quantum circuits comprised only of unitary gates [278], rendering our approach to study complexity of pure states in quantum field theory inapplicable to mixed ones in its present form. The reason being that unitary operators map pure states into pure states, while it is not possible to obtain a mixed state by acting on a pure state only with unitary operators, since unitary operators do not change the spectrum of the density operator. As a consequence, it is not possible to change the spectrum of a density matrix via circuits constructed solely of unitary operators.

It should be pointed out, however, that works such as [207] deal with the study of complexity involving non-unitary circuits. In this case, authors study the Euclidean

time evolution of mixed states in the context of $(1+1)$-dimensional CFTs where circuits consist of both Hermitian (Euclidean) and unitary transformations.

A way of circumventing this difficulty would be to consider pure states in an enlarged Hilbert space corresponding to purifications of the mixed states where ancillary degrees of freedom are entangled with the physical degrees of freedom of the mixed state. In this case, one can apply the machinery presented in previous chapters to study the complexity of the purified state. One would then need to find the optimal purification which minimizes the complexity of said state.

This is precisely one of the approaches which authors in [198] proposed in order to tackle the problem of defining complexity for conformal field theory subregions in the context of the AdS/CFT Correspondence. In said work, authors proposed two notions for complexity of mixed states based on a study of subregion complexity in neutral and charged black hole spacetimes. Such notions are the *complexity of purification*, which will be the main focus of this chapter, and spectrum complexity.[1] These notions were also explored further in [279]. The reader should also recall that the study of complexity in dual gravitational theories led to the holographic subregion complexity proposals discussed previously in Sec. 2.3.2 and developed originally in [188, 193–195, 280, 281].

While we will focus on the complexity of purification as a natural extension of complexity for mixed states, it is worth pointing out that there have been other recent approaches [282, 283] which avoid the problem of considering purifications. In particular, authors in [283] consider a geodesic distance in the manifold of mixed Gaussian states arising from the Fisher information metric which agrees with the L^2 norm when restricted to pure states. We will come back to a comparison of the methods presented in this work with this approach in Sec. 5.2.2. It is also important to mention that first efforts to apply complexity of purification to Gaussian states corresponding to vacuum subregions of free quantum field theories was done in [202], albeit with approximations that we will mention in Sec. 5.2.2.

The complexity of purification is a measure of complexity for mixed states which uses the definition of complexity for pure states, where this complexity is minimized with respect to all possible purifications. This includes in principle purifications which contain an arbitrary number of ancillae greater or equal to the number of degrees of freedom in the subsystem. To be precise, given a mixed state characterized by a density matrix ρ_A defined in a Hilbert space $\mathcal{H}_A$, we consider a new Hilbert space

$$\mathcal{H}' = \mathcal{H}_A \otimes \mathcal{H}_{A'} \ , \tag{5.1}$$

where $\mathcal{H}_{A'}$ is the Hilbert space of an ancillary system A'. In this new Hilbert space $\mathcal{H}'$, we consider a purification $|\psi_{\mathrm{T}}\rangle \in \mathcal{H}$ of ρ_A such that $\rho_A = \mathrm{tr}_{\mathcal{H}_{A'}}(|\psi_{\mathrm{T}}\rangle\langle\psi_{\mathrm{T}}|)$. We then define the *complexity of purification* CoP $\mathcal{C}_P$ of ρ_A as the minimum of

[1] Given a mixed state ρ, an reference state $|\psi_{\mathrm{R}}\rangle = |0,\dots,0\rangle$, a set of universal gates $\mathcal{G}$ and a tolerance ϵ, the spectrum complexity $\mathcal{C}_S$ of ρ is defined as the minimum number of unitaries from $\mathcal{G}$ needed to transform the $|\psi_{\mathrm{R}}\rangle$ state plus ancillae into a state $|\psi_{\mathrm{T}}\rangle$ whose partial trace has the same spectrum as ρ and such that all ancilla are entangled with the original system. Since ρ has the same spectrum as itself, in general the spectrum complexity $\mathcal{C}_S$ will be smaller than the complexity of purification $\mathcal{C}_P$.

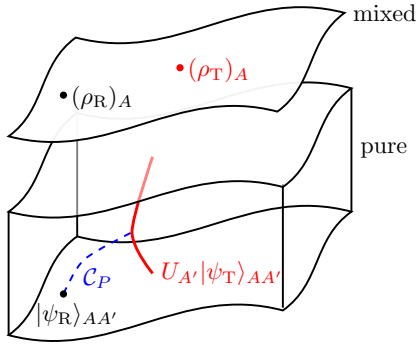

Figure 5.1.: Sketch of how the manifold of mixed states on Hilbert space $\mathcal{H}_A$ is related to the manifold of pure states on the larger Hilbert space $\mathcal{H} = \mathcal{H}_A \otimes \mathcal{H}_{A'}$ taken from [CamH02]. The manifold (solid line) of all possible purifications $|\psi_T\rangle_{AA'}$ related by Gaussian unitaries $U_{A'}$ is also shown. The complexity of purification $\mathcal{C}_P$ is given by the geodesic distance (dashed line) between the purified reference state $|\psi_R\rangle_{AA'}$ and the family of purified target states $\hat{U}_{A'}|\psi_T\rangle_{AA'}$.

a complexity functional $\mathcal{C}$ with respect to a reference state $|\psi_R\rangle$ over all possible purifications $|\psi_T\rangle$

$$\mathcal{C}_P(\rho_A) := \min_{\psi_T \in \mathcal{H}_{A'}} \left[\mathcal{C}\left(|\psi_T\rangle, |\psi_R\rangle\right)\right] . \tag{5.2}$$

Of course the purification $|\psi_T\rangle$ is not unique, but after having found one, any other purification of ρ_A can be found by acting on $|\psi_T\rangle$ with a unitary $\hat{U} = \hat{\mathbb{1}}_A \otimes \hat{U}_{A'}$ where $\hat{U}_{A'}$ is an arbitrary unitary which acts only on the ancilla Hilbert space $\mathcal{H}_{A'}$. In other words

$$\mathcal{C}_P(\rho_A) = \min_{\hat{U}=\hat{\mathbb{1}}_A \otimes \hat{U}_{A'}} \left[\mathcal{C}\left(\hat{U}|\psi_T\rangle, |\psi_R\rangle\right)\right] . \tag{5.3}$$

Fig. 5.1 provides a visualization of how CoP is computed. Essentially CoP incorporates a new minimization on top of the one carried out for complexity in pure states, namely one also must find the minimal distance between a given reference state $|\psi_R\rangle$ to the set of all possible purifications $|\psi_T\rangle$ of the mixed state ρ_A.

It is not a priori clear what the physical interpretation of the purifying Hilbert space $\mathcal{H}_{A'}$ should be. For example, in the case when $\mathcal{H}_A$ corresponds to a local subregion of a quantum field theory, *i.e.*, $\mathcal{H}_{A'}$ may not have a direct physical interpretation. As a consequence, one needs to be be careful when computing CoP in order to meaningfully apply it to arbitrary extended Hilbert spaces $\mathcal{H}' = \mathcal{H}_A \otimes \mathcal{H}_{A'}$ since the reference state $|\psi_R\rangle$ is usually chosen as spatially disentangled with respect to a notion of locality.

Definition (5.2) shows that CoP possesses all the subtleties and characteristics of complexity for pure states, such as the dependence on a choice for cost function which evaluates the lengths of circuits as well as on a reference state $|\psi_R\rangle$. In this sense, there are two minimizations that need to be performed in order to compute CoP for a given mixed state ρ_A. For a given choice of cost function, one does not only need to minimize over all purifications, but for each one of them one must

also solve the problem of finding the optimal circuit. Moreover, one would need in principle to consider purifications with an arbitrary number of ancillae, as there is a priori no reason why *minimal purifications*, *i.e.*, purifications whose ancilla have the same number of degrees of freedom as the reduced density matrix, would be the optimal or even sufficient to minimize complexity.

It is therefore to be expected that the efficient evaluation of CoP is in general a challenging task. The main reason being that generally the minimization procedure must be done numerically, where the dimension of the manifold over which one must perform the minimization grows rapidly with the number of degrees of freedom in $\mathcal{H}_A$. In order to make the study of CoP tractable, we will study CoP for Gaussian purifications of mixed Gaussian states. That is, starting from a Gaussian mixed state ρ_A^{G} we will consider Gaussian purifications $|\psi^{\mathrm{G}}\rangle$ and then perform the minimization only over Gaussian states $\hat{U}^{\mathrm{G}}|\psi^{\mathrm{G}}\rangle$ where $\hat{U}^{\mathrm{G}} = \hat{\mathbb{1}}_A \otimes \hat{U}^{\mathrm{G}}_{A'}$ is a unitary which defines a family of Gaussian states. That is, we will focus on Gaussian complexity of purification

$$\mathcal{C}_P^{\mathrm{G}}(\rho_A^{\mathrm{G}}) = \min_{\hat{U}^{\mathrm{G}}=\hat{\mathbb{1}}_A\otimes\hat{U}^{\mathrm{G}}_{A'}} \left[\mathcal{C}(\hat{U}^{\mathrm{G}}|\psi^{\mathrm{G}}\rangle, |\psi_{\mathrm{R}}\rangle)\right] , \tag{5.4}$$

which satisfies $\mathcal{C}_P(\rho_A^{\mathrm{G}}) \leq \mathcal{C}_P^{\mathrm{G}}(\rho_A^{\mathrm{G}})$. That is, the Gaussian CoP bounds the "true" CoP from above. As we will see in Chap 6, there is numerical evidence that supports the conjectured equality for entanglement of purification $E_P(\rho_A^{\mathrm{G}}) = E_P^{\mathrm{G}}(\rho_A^{\mathrm{G}})$, although this is not straightforward to verify in the case of CoP. However, studying CoP or in general complexity for non-Gaussian states remains a challenge and limited progress has been achieved on this front so far. It is therefore meaningful to restrict to Gaussian purifications of Gaussian mixed states.

In this case we will be able to use the machinery of the covariance matrix and linear complex structure formalism to Gaussian states described in detail in Sec. 3.2. For a mixed Gaussian state ρ_A, its linear complex structure J_A has purely imaginary eigenvalues $\pm \mathrm{i}\, c_i$, where $c_i \in [1,\infty)$ and $c_i \in [0,1]$ for bosons and fermions respectively. A parametrization of these eigenvalues is $c_i = \cosh(2r_i)$ for bosons and $c_i = \cos(2r_i)$ for fermions. As we saw in (3.17), the Gaussian state will be pure in the case in which $c_i = 1$ for all i. The general form of J_A for a mixed Gaussian state ρ_A^{G} in a canonical basis $\hat{\xi}_A^a = \{\hat{q}_A^1, \hat{p}_A^1, \ldots, \hat{q}_A^{N_A}, \hat{p}_A^{N_A}\}$ is given by

$$J_A = \begin{pmatrix} c_1\mathbb{A}_2 & 0 & 0 \\ 0 & \ddots & 0 \\ 0 & 0 & c_{N_A}\mathbb{A}_2 \end{pmatrix} \quad \text{where} \quad \mathbb{A}_2 = \begin{pmatrix} 0 & 1 \\ -1 & 0 \end{pmatrix} , \tag{5.5}$$

or equivalently

$$J_A = \bigoplus_{i=1}^{N_A} \begin{pmatrix} 0 & c_i \\ -c_i & 0 \end{pmatrix} . \tag{5.6}$$

We can always find a basis $\hat{\xi}_{A'}^a = \{\hat{q}_{A'}^1, \hat{p}_{A'}^1, \ldots, \hat{q}_{A'}^{N_{A'}}, \hat{p}_{A'}^{N_{A'}}\}$ such that the complex

structure J of a Gaussian purification $|\psi^{\mathrm{G}}\rangle$ of ρ_A^{G} is given by [224]

$$J = \left(\begin{array}{ccc|ccc|ccc} c_1\mathbb{A}_2 & \cdots & 0 & s_1\mathbb{S}_2 & \cdots & 0 & 0 & \cdots & 0 \\ \vdots & \ddots & \vdots & \vdots & \ddots & \vdots & \vdots & \ddots & \vdots \\ 0 & \cdots & c_{N_A}\mathbb{A}_2 & 0 & \cdots & s_{N_A}\mathbb{S}_2 & 0 & \cdots & 0 \\ \hline \pm s_1\mathbb{S}_2 & \cdots & 0 & c_1\mathbb{A}_2 & \cdots & 0 & 0 & \cdots & 0 \\ \vdots & \ddots & \vdots & \vdots & \ddots & \vdots & \vdots & \ddots & \vdots \\ 0 & \cdots & \pm s_{N_A}\mathbb{S}_2 & 0 & \cdots & c_{N_A}\mathbb{A}_2 & 0 & \cdots & 0 \\ 0 & \cdots & 0 & 0 & \cdots & 0 & \mathbb{A}_2 & \ldots & 0 \\ \vdots & \ddots & \vdots & \vdots & \ddots & \vdots & \vdots & \ddots & \vdots \\ 0 & \cdots & 0 & 0 & \cdots & 0 & 0 & \ldots & \mathbb{A}_2 \end{array}\right), \tag{5.7}$$

where $(+)$ and $s_i = \sqrt{c_i^2 - 1}$ corresponds to bosons and $(-)$ and $s_i = \sqrt{1 - c_i^2}$ to fermions, and where

$$\mathbb{S}_2 = \begin{pmatrix} 0 & 1 \\ 1 & 0 \end{pmatrix} . \tag{5.8}$$

An equivalent parametrization of s_i in terms of r_i, where $s_i = \sinh(2r_i)$ for bosons and $s_i = \sin(2r_i)$ for fermions.

Here we have considered a purification with $N_{A'} = N_A + N_{\mathrm{nm}} \geq N_A$ degrees of freedom, where N_{nm} corresponds to the number of additional ancillary degrees of freedom for a non-minimal purification. From (5.7) we see that in general the form of the linear complex structure J of the general Gaussian purification $|\psi^{\mathrm{G}}\rangle$ is

$$J = \left(\begin{array}{c|c} J_A & J_{AA'} \\ \hline J_{A'A} & J_{A'} \end{array}\right) , \tag{5.9}$$

which is of dimension $(N_A + N_{A'}) \times (N_A + N_{A'}) = (2N_A + N_{\mathrm{nm}}) \times (2N_A + N_{\mathrm{nm}})$. It is important to note that different purifications of ρ_A^{G} only differ by the choice of the basis of the purifying system A', namely $\hat{\xi}^a_{A'}$, for which J takes the *standard form* (5.7). Because of this, the action of the corresponding Lie group $\mathcal{G}_{A'}$ can be used to transform $J \to MJM^{-1}$ with $M = \mathbb{1}_A \oplus M_{A'}$ where $M_{A'} \in \mathcal{G}_{A'}$ is represented by a $(2N_{A'}) \times (2N_{A'})$ matrix.

The next step is to identify the possible reference states $|J_{\mathrm{R}}\rangle$ that can be considered. Two straightforward choices are thermal states and mixed states arising from spatial subsystems. In the latter case, which will be the focus of our approach, we start from a pure Gaussian state $|\psi\rangle \in \mathcal{H} = \mathcal{H}_A \otimes \mathcal{H}_{\bar{A}}$ which is then reduced to a local subsystem $\rho_A = \mathrm{tr}_{\mathcal{H}_{\bar{A}}}(|\psi\rangle\langle\psi|)$. In said subsystem, there is a pure and spatially disentangled Gaussian reference state $|J_{\mathrm{R}}\rangle_A$ which can be extended to the purifying system as $|J_{\mathrm{R}}\rangle = |J_{\mathrm{R}}\rangle_A \otimes |J_{\mathrm{R}}\rangle_{A'} \in \mathcal{H}' = \mathcal{H}_A \otimes \mathcal{H}_{A'}$. In this case, only the target state $|J_{\mathrm{T}}\rangle$ is entangled in $\mathcal{H}' = \mathcal{H}_A \otimes \mathcal{H}_{A'}$, while the reference state is a product state $|J_{\mathrm{R}}\rangle = |J_{\mathrm{R}}\rangle_A \otimes |J_{\mathrm{R}}\rangle_{A'}$. Since there is a priori no physical notion of locality in the ancillary system A', as we mentioned previously, the only requirement is that $|J_{\mathrm{R}}\rangle_A$ is pure and Gaussian. Hence, the natural choices for bosonic and fermionic reference states are:

$$J_{\mathrm{R}} = \bigoplus_{i=1}^{N_A} \begin{pmatrix} 0 & \frac{1}{\mu} \\ -\mu & 0 \end{pmatrix} , \quad \text{(bosons)} \tag{5.10a}$$

$$J_{\mathrm{R}} = \bigoplus_{i=1}^{N_A} \begin{pmatrix} 0 & 1 \\ -1 & 0 \end{pmatrix} \quad , \quad \text{(fermions)} \tag{5.10b}$$

where here i denotes the local sites, and where here μ is the reference state scale or frequency, as in (3.55).

Another consequence of our decision to focus on Gaussian states is that we can choose the L^2 cost function, which is the geodesic distance between Gaussian states $|J_{\mathrm{T}}\rangle$ and $|J_{\mathrm{R}}\rangle$ within the manifold of Gaussian states, as a measure of pure-state complexity in (5.4) and which is given by

$$\mathcal{C}(|J_{\mathrm{T}}\rangle, |J_{\mathrm{R}}\rangle) = \frac{1}{2\sqrt{2}} \sqrt{|\mathrm{tr}\left(\log(\mathscr{G})^2\right)|} = \frac{1}{2\sqrt{2}} \sqrt{|\mathrm{tr}\left(\log(-J_{\mathrm{T}}J_{\mathrm{R}})^2\right)|} \,, \tag{5.11}$$

for $\mathscr{G} = -J_{\mathrm{T}}J_{\mathrm{R}}$, as in (3.58) and (3.93). Note that by construction the complexity functional (5.11) is invariant under the action of a Gaussian unitary $\hat{U}$ acting both on the reference state and target state:

$$\mathcal{C}(|J_{\mathrm{T}}\rangle, |J_{\mathrm{R}}\rangle) = \mathcal{C}(U|J_{\mathrm{T}}\rangle, U|J_{\mathrm{R}}\rangle) \,, \tag{5.12}$$

where U is related to a group transformation $M^a{}_b \in \mathcal{G}$ via $U^\dagger \hat{\xi}^a U = M^a{}_b \hat{\xi}^b$. Consequently, the optimization over all Gaussian purifications in (5.4) can be therefore performed over the reference or target state. As mentioned previously, we will optimize over all Gaussian purifications for the target state; having found one purification $|J_{\mathrm{T}}\rangle$, any other purification is generated by unitaries of the form $(\hat{\mathbb{1}}_A \otimes \hat{U}_{A'})|J_{\mathrm{T}}\rangle$. Hence

$$\begin{aligned} \mathcal{C}_P(|J_{\mathrm{T}}\rangle, |J_{\mathrm{R}}\rangle) &= \min_{\hat{U}_{A'}} \left[\mathcal{C}\left((\hat{\mathbb{1}}_A \otimes \hat{U}_{A'})|J_{\mathrm{T}}\rangle, |J_{\mathrm{R}}\rangle\right)\right] \\ &= \min_{\hat{V}_{A'}} \left[\mathcal{C}\left[(|J_{\mathrm{T}}\rangle, (\hat{\mathbb{1}}_A \otimes \hat{V}_{A'})|J_{\mathrm{R}}\rangle\right)\right] \\ &= \min_{\hat{U}_{A'}, \hat{V}_{A'}} \left[\mathcal{C}\left((\hat{\mathbb{1}}_A \otimes \hat{U}_{A'})|J_{\mathrm{T}}\rangle, (\hat{\mathbb{1}}_A \otimes \hat{V}_{A'})|J_{\mathrm{R}}\rangle\right)\right] \,, \end{aligned} \tag{5.13}$$

where $\hat{U}_{A'}$ and $\hat{V}_{A'}$ are both Gaussian unitaries acting only on the ancillary system A'. This follows from (5.12). As a consequence, we can choose to begin with a basis $\hat{\xi}^a_A$ such that $(J_{\mathrm{T}})_A$ has the form (5.5) and then purify the system with respect to a basis $(\hat{\xi}')^a = (\hat{\xi}^a_A, \hat{\xi}^a_{A'})$ so that J_{T} takes the standard form (5.7) with respect to $(\hat{\xi}')^a$. The purification of the reference state will then have the block diagonal form

$$J_{\mathrm{R}} = (J_{\mathrm{R}})_A \oplus (J_{\mathrm{R}})_{A'} = \left(\begin{array}{c|c} (J_{\mathrm{R}})_A & 0 \\ \hline 0 & (J_{\mathrm{R}})_{A'} \end{array}\right) \,, \tag{5.14}$$

since it is a product state. For $M = \mathbb{1}_A \oplus M_{A'}$ we have $(\hat{\mathbb{1}}_A \otimes \hat{U}_{A'})|J\rangle = |MJM^{-1}\rangle$ so that

$$\mathcal{C}_P(J_{\mathrm{T}}, J_{\mathrm{R}}) = \min_{M = \mathbb{1}_A \oplus M_{A'}} \left[\frac{1}{2\sqrt{2}} \sqrt{\mathrm{tr}\left(\log\left(M J_{\mathrm{T}} M^{-1} J_{\mathrm{R}}\right)^2\right)}\right] \,. \tag{5.15}$$

By the cyclicity of the trace, this transformation on the target state can be equivalently thought of as acting on the reference state via $J_{\mathrm{R}} \to M^{-1} J_{\mathrm{R}} M$. This explicitly

shows our claim that we can choose to perform the optimization over the reference state rather than on the target state. In practical terms, it is actually convenient to do this as the stabilizer group of the reference state is larger, leading to fewer parameters over which one must optimize.

Furthermore, let us emphasize that the L^2 cost function (5.11) allows for a tractable computation of the complexity of purification given that the expressions for the pure-state Gaussian complexity both for bosonic and fermionic states are known as a function of the reference and target states, as we saw in Sec. 3.3 (see (3.61) for bosons and (3.94) for fermions). For other cost functions, *e.g.*, the L^1, even within the realm of Gaussian states, it would be necessary to optimize both over all purifications and over each purification it would be necessary to find the optimal circuit connecting the reference and target states.

Having discussed the details of the Gaussian Cop, in Sec. 5.1.1 we will give an first example of CoP for a system of two coupled harmonic oscillators in the time-dependent setting discussed in the previous chapter, namely that of a smooth quantum quench through a critical point. This will set the stage for Sec. 5.2 where we will study CoP for spatial subregions of vacuum states of the two $(1+1)$-dimensional free fermionic and bosonic quantum field theories that we described in Sec. 3.3.1 and Sec. 3.3.2, namely the Klein–Gordon and Ising CFT theories. In all cases we will also focus on minimal purifications $N_{\rm nm} = 0$, given that a considerable amount of numerical evidence for the cost function (5.15) shows that adding additional ancillae does not lower the value of CoP.

While we do not possess at the moment a concrete mathematical argument in favour of minimal purifications, the reader should note that it is at least in principle possible that adding additional ancilla to general purifications could open the possibility for shorter circuits connecting the purified reference and target states. It would be interesting to explore whether this observation is special to the choice of cost function or if it's a more general statement applicable to a larger class of complexity measures.

5.1.1. A Simple Model: Two Harmonic Oscillators

One of the simplest setups where one can study complexity of purification is the case of a system comprised of two coupled harmonic oscillators. We begin with a pure state describing the ground state of such system, which in position space is characterized by its wavefunction

$$\psi(q_1, q_2) = \frac{\left(a_1 a_2 - a_3^2\right)^{1/4}}{\sqrt{\pi}} \exp\left(-\frac{\omega_1}{2} q_1^2 - \frac{\omega_2}{2} q_2^2 - \omega_3 q_1 q_2\right) , \tag{5.16}$$

where $\omega_i = a_i + \mathrm{i}\, b_i$ and $a_i, b_i \in \mathbb{R}$ such that $a_i > 0$ and $a_1 a_2 > a_3^2$. The covariance matrix of the state (5.16) has the form:

$$G = \left(\begin{array}{c|c} G_{11} & G_{12} \\ \hline G_{21} & G_{22} \end{array}\right) , \tag{5.17}$$

where the blocks G_{12} and G_{21} describe the entanglement between the oscillators labelled by 1 and 2 given by the cross-correlations $\hat{q}^1\hat{p}^2$ and $\hat{q}^2\hat{p}^1$. One can make

a Fourier transform effectively performing a normal mode decomposition of the ground state as in (3.46) arriving at a block diagonal structure of the covariance matrix (5.17). This indeed will be the strategy of Sec. 5.2.2 where we will study CoP of subsystems of N coupled harmonic oscillators corresponding to spatial subregions of the vacuum state of the Klein–Gordon theory. However, it is also interesting for the moment to remain in the basis $\hat{\xi}^a = \{\hat{q}^1, \hat{p}^1, \hat{q}^2, \hat{p}^2\}$ in order to appreciate some further subtleties of CoP. We will thus follow the strategy of [**CamH03**].

From the pure state (5.16) we can obtain two mixed states corresponding to two subsystems; each comprised of a single harmonic oscillator. The reduced density matrix corresponding to the first oscillator obtained simply by tracing out the second oscillator $\rho_1 := \mathrm{tr}_2(|\psi\rangle\langle\psi|)$ in position-space via

$$\rho_1(q_1, \mathfrak{q}_1) = \int_{-\infty}^{+\infty} \mathrm{d}q_2\, \psi^*(q_1, q_2)\, \psi(\mathfrak{q}_1, q_2) \ , \tag{5.18}$$

is given by

$$\rho_1(q_1, \mathfrak{q}_1) = \sqrt{\frac{\alpha_1 - \beta}{\pi}} \exp\left(-\frac{1}{2}\alpha_1(q_1^2 + \mathfrak{q}_1^2) - \frac{\mathrm{i}}{2}\alpha_2(q_1^2 - \mathfrak{q}_1^2) + \beta q_1 \mathfrak{q}_1 \right) \ , \tag{5.19}$$

or equivalently $\rho_1(q_1, \mathfrak{q}_1) = \exp(-q_{ab}\hat{\xi}_1^a\hat{\xi}_1^b - c_0)$ as in (3.19) and where

$$\alpha_1 = a_1 - \frac{a_3^2 - b_3^2}{2a_2} \ , \ \alpha_2 = -b_1 + \frac{a_3 b_3}{a_2} \ , \ \beta = \frac{a_3^2 + b_3^2}{2a_2} \ . \tag{5.20}$$

Here the basis is $\hat{\xi}_1^a = \{q^1, p^1, \mathfrak{q}^1, \mathfrak{p}^1\}$, $c_0 = \log(\pi/(\alpha_1 - \beta))/2$ and

$$q_{ab} = \begin{pmatrix} -(\alpha_1 + \mathrm{i}\,\alpha_2)/2 & \beta/2 \\ \beta/2 & -(\alpha_1 - \mathrm{i}\,\alpha_2)/2 \end{pmatrix} \ . \tag{5.21}$$

The reader should note that the three parameters $\{\alpha_1, \alpha_2, \beta\}$ completely characterize the covariance matrix G_{11}, computed as in (3.18a), and linear complex structure J_1 corresponding to the first harmonic oscillator

$$G_{11} = \begin{pmatrix} \frac{1}{\alpha_1 - \beta} & \frac{\alpha_2}{\alpha_1 - \beta} \\ \frac{\alpha_2}{\alpha_1 - \beta} & \frac{\alpha_1^2 + \alpha_2^2 - \beta^2}{\alpha_1 - \beta} \end{pmatrix} \ , \ J_1 = \begin{pmatrix} \frac{\alpha_2}{\alpha_1 - \beta} & -\frac{1}{\alpha_1 - \beta} \\ \frac{\alpha_1^2 + \alpha_2^2 - \beta^2}{\alpha_1 - \beta} & -\frac{\alpha_2}{\alpha_1 - \beta} \end{pmatrix} \ . \tag{5.22}$$

Note that the parameter β arising purely from the coupling between oscillators 1 and 2 prevents the density matrix (5.19) from describing a pure state, as can be seen by computing the square of its linear complex structure

$$J_1^2 = -\begin{pmatrix} \frac{\alpha_1 + \beta}{\alpha_1 - \beta} & 0 \\ 0 & \frac{\alpha_1 + \beta}{\alpha_1 - \beta} \end{pmatrix} \neq -\mathbb{1}_2 \ . \tag{5.23}$$

This can also be directly seen by noting that the covariance matrix of $\rho_1(q_1, \mathfrak{q}_1)$ (5.22) requires three parameters to be specified, as opposed to two, as would be in the case of a pure state. This extra parameter arises from the entanglement between the two oscillators, namely from β.

We now consider a Gaussian purification of the mixed state (5.19) for which we will be able to minimize the complexity functional (4.33) for a choice of reference state. As the reader can readily note, the wavefunction (5.16) already describes the most general Gaussian purification for a subsystem of comprised of one oscillator. From the six parameters that specify the wavefunction, three are fixed for the subsystem 1 and the optimization of the complexity functional needs to be performed for the other three. Equivalently, one can think of this problem in terms of the covariance matrix (5.17). The block G_{11} corresponding to oscillator 1 is fixed, and the optimization modifies the parameters that characterize the cross-correlations G_{12} and G_{21} as well as the block G_{22}.

The minimization can be done numerically in an efficient manner for a given choice of parameters ω_i, for example in the case of the ground state of the solvable quench model (4.13) studied in Sec. 4.1.1. In this case, it is interesting to consider the complexity with respect to a reference state of a spatially disentangled two-harmonic oscillator system characterized by time-independent constant frequencies $\mu_1 > 0$ and $\mu_2 > 0$

$$G_{\mathrm{R}} = \bigoplus_{i=1}^{2} G_{\mathrm{R}}^{(i)} = \bigoplus_{i=1}^{2} \begin{pmatrix} \frac{1}{\mu_i} & 0 \\ 0 & \mu_i \end{pmatrix} . \tag{5.24}$$

Starting from the time-dependent ground state for a two-harmonic oscillator system, we compute the entries ω_i from (4.21) thus fixing the parameters $\alpha_1, \alpha_2, \beta$ from the data describing the full state. We then perform a minimization of (4.33) for the remaining three parameters in the wavefunction, which are not fixed by the quench solution. By this procedure we obtain the complexity of purification for oscillator 1 at every time t: $\mathcal{C}_P^{(1)}(t) := \mathcal{C}_P(\rho_1(t))$.

We can repeat this process by considering the reduced density matrix for oscillator 2 $\rho_2(q_2, \mathfrak{q}_2)$ in which case the block G_{22} of the covariance matrix (5.17) is now fixed in terms of other parameters akin to (5.20). By minimizing the same complexity functional we obtain the CoP for the second oscillator for all t: $\mathcal{C}_P^{(2)}(t) := \mathcal{C}_P(\rho_2(t))$. Due to the symmetry of the quench solution, in this particular case we have $\mathcal{C}_P^{(1)}(t) = \mathcal{C}_P^{(2)}(t) = \mathcal{C}_P(t)$, which is not in general true. Fig. 5.2 shows a plot of $\mathcal{C}_P(t)$ and $\mathcal{C}(|\psi\rangle)$ for the critical quench model for two different values of δt.

Considering the CoP for each of the subsystems allows us to introduce a concept which will play an important role in the following section, namely *mutual complexity* [203], a quantity akin to mutual information $I(A : B)$ for complexity of subregions. The main motivation is that mutual complexity, usually denoted by $\Delta\mathcal{C}$, is an appropriate quantity for studying subregion complexity as it disposes of (some of) the UV divergences inherent to pure-state complexity. This quantity, much like $I(A : B)$, can be thought of as a "UV-regularised" correlation measure between subsystems. It originally arose in the context of the holographic subregion complexity proposals (see Sec. 2.3.2), where for boundary spatial subregions A and B it is defined as:

$$\Delta\mathcal{C} := \mathcal{C}(A) + \mathcal{C}(B) - \mathcal{C}(A \cup B) . \tag{5.25}$$

From the perspective of quantum field theory, it is clear that this definition requires a notion of complexity for mixed states, such as CoP. It is therefore straightforward

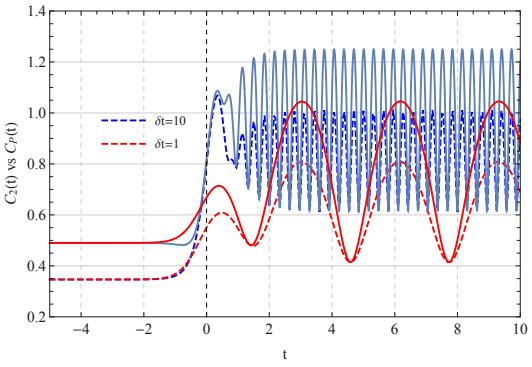

Figure 5.2.: Comparison of complexity of the pure target state $\mathcal{C}(\psi)$ as a function of time t (solid) and the purification $\mathcal{C}_P$ (dashed) for $\delta t = 10$ (blue) and $\delta t = 1$ (red), with $\mu_1 = \mu_2 = 1/2$ for both oscillators, taken from [CamH03].

to apply the notion of CoP to define the mutual complexity in terms of complexity of purification as

$$\Delta\mathcal{C}_P^{(1)} := \mathcal{C}_P(\rho_A) + \mathcal{C}_P(\rho_B) - \mathcal{C}_P(\rho_{A\cup B}) \ , \tag{5.26}$$

where ρ_A and ρ_B are reduced density matrices corresponding to spatial subregions A and B and where here $\mathcal{C}_P(\rho_{A\cup B})$ could be immediately replaced by $\mathcal{C}(|\psi\rangle\langle\psi|)$ in the case in which the union $A\cup B$ coincides with the whole system defined by a pure state $|\psi\rangle$. We will focus on this notion of mutual complexity for the moment, but we will in fact use an alternative one in Sec. 5.2 more adequate to eliminating the UV divergences which arise from an L^2 norm.

It is also worth pointing out that one generally expects CoP to diverge in the continuum limit as circuits acting on spatially disentangled states need to build entanglement on all scales in order to match the features of vacuum states of free quantum field theories, a fact which is also supported by explicit results such as [202]. Therefore, it is meaningful to consider a combination of CoP would cancel such divergences while at the same time allowing to extract relevant physical information from the subsystems.

Again from Fig. 5.2 we can see in this case that , for all t, CoP is smaller than the full complexity but larger than half of it: $\mathcal{C}(|\psi\rangle)/2 \leq \mathcal{C}_P(\rho_{1,2}) \leq \mathcal{C}(|\psi\rangle)$. This inequality can be also be numerically verified for a wide range of parameters independently of the quench solution. The inequality $\mathcal{C}_P(\rho_{1,2}) \leq \mathcal{C}(|\psi\rangle)$ is saturated in the case in which the original target state is already the least complex state among all possible purifications. Meanwhile, the inequality $\mathcal{C}(|\psi\rangle)/2 \leq \mathcal{C}_P(\rho_{1,2})$ is saturated in the case where the original target state is a product state with respect to the chosen bipartition; *i.e.*, if the subsystem of each individual oscillator is actually in a pure state. The previous inequality leads to the conjecture that complexity of purification for spatial subregions satisfies *subadditivity* $\mathcal{C}_P(\rho_1) + \mathcal{C}_P(\rho_2) = 2\,\mathcal{C}_P(\rho_{1,2}) \geq \mathcal{C}(|\psi\rangle)$.[2] In

[2]Subadditivity can in general be defined for real-valued functions or set functions. In the latter case, if R is a set and $f : P(R) \to \mathbb{R}$ is a set function, where $P(R)$ denotes the power set of R, then f is said to be *subadditive* if for any $S, T \subset R$ we have $f(S) + f(T) - f(S \cup T) \geq 0$.

other words,

$$\Delta \mathcal{C}_P^{(1)} \geq 0 \ . \tag{5.27}$$

A striking consequence of this observation is that it contradicts the holographic subregion proposals in Sec. 2.3.2, which are superadditive. We will explore more in detail the connection between these holographic proposals and the field theoretic properties of bosonic and fermionic CoP in the following section.

It is also interesting to compare the complexity of purification $\mathcal{C}_P^{(1)}$ and entanglement entropy $S_1 := -\mathrm{tr}(\rho_1 \log(\rho_1))$ for a single oscillator given by

$$\begin{aligned} S_1(\alpha_1, \beta) = \frac{1}{2}\Bigg[\left(1 - \sqrt{\frac{\alpha_1+\beta}{\alpha_1-\beta}}\right) \log\left|\frac{1}{2}\left(1 - \sqrt{\frac{\alpha_1+\beta}{\alpha_1-\beta}}\right)\right| + \\ \left(1 + \sqrt{\frac{\alpha_1+\beta}{\alpha_1-\beta}}\right) \log\left|\frac{1}{2}\left(1 + \sqrt{\frac{\alpha_1+\beta}{\alpha_1-\beta}}\right)\right| \Bigg] \ . \end{aligned} \tag{5.28}$$

Note that while $\mathcal{C}_P^{(1)}$ depends non-trivially on the parameter α_2 of (5.19), as well as the full state complexity $\mathcal{C}$, S_1 is insensitive to such parameter, which gives a hint as to how different information about the full state is encoded differently in entanglement and complexity. For completeness one can also see that the entanglement entropy S_1 goes to zero as the parameter β which characterizes the entanglement between the two oscillators goes to zero.

Before moving on, the reader may also note how quickly this minimization procedure of the complexity functional can become computationally challenging as we increase the number of degrees of freedom in the subsystem described by a Gaussian reduced density matrix. Already for a subsystem consisting of two harmonic oscillators described by a reduced density matrix one would need to minimize a functional for 10 parameters in the case of a minimal purification.[3] If we are to make statements about CoP in quantum field theory we inevitably have to consider larger subsystems. This presents a challenging problem for which simplifying assumptions have been considered recently, for example approximating the true CoP by a sum of single-mode optimizations of the complexity functional [202] or avoiding purifying the mixed state all together [282, 283]. However, as we have already anticipated, by exploiting the natural structure of Gaussian pure and mixed states we are able to efficiently perform the optimization required to compute CoP in the case of Gaussian purifications. This will be the focus of the next section, Sec. 5.2.

5.2. Vacuum Subregions of free Quantum Field Theories

In this section we will be interested in studying CoP for vacuum subregions of the (1+1)-dimensional Klein–Gordon model (see Sec. 3.3.1) and of the critical transverse Ising model (see Sec. 3.3.2). We will present the results of numerical computations

[3] For a bosonic system or subsystem described by N degrees of freedom, the dimension of the manifold of pure Gaussian states with vanishing one-point functions is $N(N+1)$, while the dimension of the manifold of mixed Gaussian states with vanishing one-point functions is $N(2N+1)$ [221].

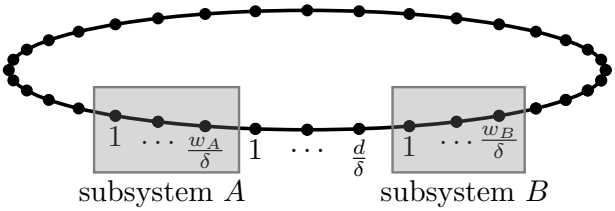

Figure 5.3.: Sketch of the periodic lattice set-up used for the discretized $(1+1)$-dimensional Klein–Gordon and critical transverse Ising models, taken from [CamH02]. The subsystem that defines reduced density matrices for the discretized bosonic and fermionic models in their vacuum state consists of two intervals of a width of w_A/δ and w_B/δ sites and in principle separated by a distance of d/δ sites, where δ is the lattice spacing. When $d = 0$, w_A and w_B will be kept generic. Whenever $d > 0$, we consider for simplicity $w_A = w_B = w$.

for their discretized versions on a periodic lattice or on an infinite lattice. Our computational approach will be based on a gradient descent method tailored for functions, such as CoP (5.15), which take values on the linear complex structure of Gaussian states. The interested reader is referred to the remarkable work [226] for details of this method.

We will consider subsystems consisting of intervals of width w/δ sites and possibly separated by a distance of d/δ where here once again δ is the lattice spacing, as shown in Fig. 5.3. In order to make meaningful statements about the behaviour of CoP in quantum field theories, we need to consider the continuum limit of our discretized models (3.43) and (3.82). That is, we require that the ratios w/L and d/L fixed as the limit $N \to \infty$ is taken, where here $L = N\delta$. That is, we require that the relative sizes of the spatial subregions with respect to the (finite) size of the full system. Note that from the relevant covariance matrices, namely (3.45) and (3.83), we are able to extract the necessary information for subsystems of arbitrary size, or (3.86) in the continuum and infinite size limit. At the same time, one would like to avoid finite size effects that can be relieved by taking an infinite size limit $L \to \infty$, which is accompanied by subtleties, particularly in the bosonic case.

It is worth mentioning that in contrast with entanglement of purification (EoP) which together with reflected entropy will be the focus of the next chapter, Ch. 6, for CoP we will focus on Gaussian mixed states described by reduced density matrices of spatial subregions consisting on single and adjacent intervals both in the bosonic and the fermionic case. There are two main reasons for this.

Firstly, the reader should recall that for bosonic case given by the discretized Klein–Gordon model there is a subtlety arising from the zero-mode, as discussed in Sec. 3.3.1. As mentioned therein, the long-distance physics of mixed states described by reduced density matrices of two spatially disjoint subsystems is dominated by the zero-mode, which implies that in order to reliably study CoP for Gaussian purifications we are constrained in principle to study single, adjacent ($d = 0$) or disjoint intervals sep-

arated by a short distance $d \ll w$. For the latter case, however, we would need to consider subsystem sizes consisting of a large number of lattice sites w/δ of order $> \mathcal{O}(10)$ in order to properly characterize CoP as a function of d/w in the continuum limit while at the same time avoiding finite size effects occurring for small separations $d/\delta \sim \mathcal{O}(1)$. Precise numerical computations for such cases are particularly challenging due to the dimension of the parameter manifold over which the optimization needs to be performed.

To give an example, consider the case for which $d/w \sim \mathcal{O}(1/10)$, which arguably satisfies the condition $d \ll w$. Suppose for example that the separation between the subsystems is $d/\delta \approx \mathcal{O}(3-4)$ lattice sites in order to avoid finite size effects. This implies that the subsystems should have a size of at least $w/\delta \approx \mathcal{O}(30-40)$ lattice sites, implying that the number of degrees of freedom of the reduced density matrix for this subsystem is $N_A = 2w \approx \mathcal{O}(60-80)$, for which the manifold of Gaussian purifications will be of dimension $2N_A(2N_A+1) \approx \mathcal{O}(3660-6480)$ and where the optimization should be performed in principle for a subspace of dimension $N_A(2N_A+1) \approx \mathcal{O}(1830-3240)$.

At the moment, exploratory computations in this regime yield a behaviour of mutual CoP (5.26) in the continuum limit $N \to \infty$ for a small d/w range given by

$$\Delta\mathcal{C}_P^{(1)}(d/w, m/\mu, \mu\delta)\Big|_{d\ll w} \approx f(m/\mu, \mu\delta)\log(d/w) + \cdots \,, \tag{5.29}$$

where the precise form of the function $f(m/\mu, \mu\delta)$ as well as the character of subleading contributions to $(\Delta\mathcal{C}_P^{(1)})_{d\ll w}$ has not been fully determined. As a consequence, we leave the details of the $d > 0$ case for bosonic CoP for the future and outside the scope of the present work.

The second reason is related with the notion of locality in the Ising CFT and the non-Gaussian nature of the reduced density matrix for disjoint subsystems. The basic idea, as discussed already in Sec. 3.3.2, is that there are different notions of locality in the spin and fermion pictures which lead to a different notion of partial trace in lattice systems with a Jordan–Wigner duality [284]. This leads in particular to a different notion of entanglement entropy in the two pictures, a fact has already been recognised in the literature [237, 238, 285–287] and which plays a substantial role when relating the lattice model with the continuum CFT [240]. However, this different notion only affects disjoint subregions, *i.e.*, mixed states whose reduced density matrix describes a subsystem consisting of two non-adjacent intervals. This fact constrains us to consider only single and adjacent intervals $d = 0$ in Fig. 5.3, of the Ising CFT model. In Sec. 6.3, however, we will return to the study of the long-distance behaviour of two quantities of interest, namely of entanglement of purification and reflected entropy.

It would be remiss not to address the CFT limit of both discretized models. In the bosonic case, this limit is naively achieved by taking $m \to 0$ which leads to a conformal field theory with central charge $c = 1$. However to be precise, the massless limit of the Hamiltonian (3.41) actually corresponds to the *decompactification limit* of a one-parameter family of compact free boson conformal field theories arising from the compactification of the bosonic field $\hat{\varphi}$ and which has corresponds to a

different conformal field theory with a different partition function than the modular-invariant $c = 1$ CFT. This difference can be understood by studying the zero-mode contribution to the path-integral. While distinct, we will use our discretized model of a free massive boson as a proxy for extracting the properties of CoP for the modular invariant $c = 1$ free boson conformal field theory in the regimes for which the zero-mode is subdominant namely for single and adjacent intervals. One could also in principle study the regime $d \ll w$ without worrying too much about the zero mode. The reader can refer to [CamH02] where a thorough discussion of the CFT limit of both discretized models is made, as well as of the zero-mode problem and the inequivalent notions of partial trace and tensor product under the Jordan–Wigner duality for lattice spin systems.

As a final comment before proceeding to the following sections, it is worth pointing out that given that our choice of cost function (5.15) is based on an L^2 norm which has a square root, it makes sense to consider a variation of the mutual complexity formula (5.26) more appropriate to dispose of the UV divergencies inherent to complexity, namely (3.63) and (3.96). We propose the L^2 mutual complexity for reduced density matrices ρ_A and ρ_B corresponding to subregions A and B to be defined by

$$\Delta\mathcal{C}_P^{(2)} := \mathcal{C}_P(\rho_A)^2 + \mathcal{C}_P(\rho_B)^2 - \mathcal{C}_P(\rho_{A\cup B})^2 \ , \tag{5.30}$$

where here the (2) on the superscript on the left hand side does not signify a square, but rather simply that it is based on taking the square of individual contributions and then adding them.

5.2.1. Fermionic Complexity of Purification

We begin with the study of the fermionic case as it is far simpler than the bosonic one mainly due to the fact that there are fewer parameters. In particular, there is no reference state scale associated to the reference state. As we mentioned previously, see *e.g.*, the paragraph preceding (3.89), in contrast with the bosonic case, fermionic reference states are highly constrained as there exists only a single spatially unentangled state with the same parity as the vacuum state which is translational invariant.

For a single interval on a line, fermionic CoP can only be a function of the ratio w/δ as the system becomes large $N \to \infty$. In this limit, fermionic CoP behaves as

$$\mathcal{C}_P^2 = e_2 \frac{w}{\delta} + e_1 \log\left(\frac{w}{\delta}\right) + e_0 \ , \tag{5.31}$$

where the e_i are numerical coefficients which can be determined up to the accuracy permitted by the optimization algorithm and which are found to be

$$e_0 = 0.0894 \ , \ e_1 = 0.0544 \ , \ e_2 = 0.103 \ . \tag{5.32}$$

This functional form (5.31) was tested numerically by computing discrete derivatives of $\mathcal{C}_P^2$ with respect to w/δ. Note that in (5.31) we are directly considering the square of the CoP.

Formula (5.31) for fermionic CoP matches the structure of leading divergence for vacuum complexity in free fermionic conformal field theories [204, 205] and also in

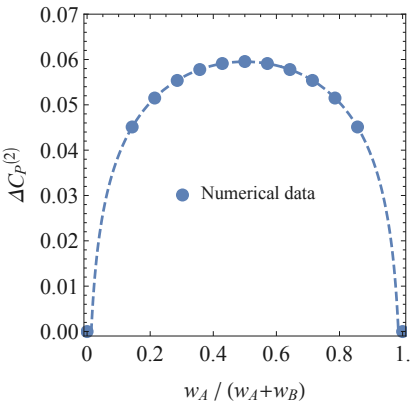

Figure 5.4.: Fermionic CoP for two adjacent ($d = 0$) subsystems. The analytic form (5.33) is plotted as a dashed curve. Here we consider $(w_A+w_B)/\delta = 14$ sites for a total system size of $N = 100(w_A + w_B)/\delta$.

formula (3.96), where in the case of pure state complexity, the role of w is played by the total system size N.

In the case of two adjacent intervals, we find the following behaviour for the L^2 mutual complexity in the $N \to \infty$ limit

$$\Delta\mathcal{C}_P^{(2)} = e_1 \log\left(\frac{w_A w_B}{(w_A + w_B)\delta}\right) + e_0 \ , \tag{5.33}$$

where the coefficients are the same as in (5.32). Note that by considering the L^2 mutual complexity, the leading divergence proportional to w/δ is cancelled by considering this specific combination, thus leaving the logarithmic divergence as the leading one. The form of $\Delta\mathcal{C}_P^{(2)}$ can be seen in Fig. 5.4 in terms of the ratio $w_A/(w_A + w_B)$, where we also show numerical data obtained from the optimization procedure. It can be seen from Fig. 5.4 that $\Delta\mathcal{C}_P^{(2)}$ is positive, which implies the subadditivity of fermionic CoP, in line with the observation (5.27) made for two harmonic oscillators.

Note also the logarithmic divergence in (5.33), which matches the divergence of the holographic mutual complexity for the $\mathrm{CV}_{2.0}$ (2.23c) and CA (2.23b) subregion complexity proposals as in Sec. 2.3.2, but with an opposite sign.

5.2.2. Bosonic Complexity of Purification

Bosonic complexity of purification has arguably a richer structure derived from the interplay of different parameters in the theory such as the mass m of the bosonic field and the reference state frequency μ. Furthermore, given that we consider a small but finite mass m, the continuum limit of the theory on the circle requires keeping the product $mL = m\delta N$ (or m/μ) fixed as we take the limit $N \to \infty$. As mentioned before, different values of this product correspond to different quantum field theories than the modular invariant $c = 1$ bosonic CFT.

Note that from the expression (3.62) for the pure state complexity for our bosonic model that rescaling the reference state frequency by a real number $\mu \to a\mu$ is equivalent to rescaling the mass and lattice spacing by $m \to m/a$ and $\delta \to a\delta$. This can be directly seen by the functional dependence of CoP on such parameters: $\mathcal{C}_P(m/\mu, \mu\delta)$ and means that without loss of generality we can set $\mu = 1$ in the numerical computations and afterwards restore it in the expressions containing m and δ, which are dimensionless and independent.

Via the numerical optimization procedure we find that in the limit $N \to \infty$, the square of bosonic CoP has the form

$$\mathcal{C}_P^2 = f_2(\mu\delta)\frac{w}{\delta} + f_1\left(\frac{m}{\mu}, \mu\delta\right)\log\left(\frac{w}{\delta}\right) + f_0\left(\frac{m}{\mu}, \mu\delta\right) \ , \tag{5.34}$$

where this form of bosonic CoP accurately describes its w/δ for a large range of m/μ and $\mu\delta$, and where behaviour the functions f_i are estimated to be

$$f_0\left(\frac{m}{\mu}, \mu\delta\right) = 0.80\sqrt{\log(\mu\delta)\log\left(\frac{m}{\mu}\right)} + 0.25\log^2\left(\frac{m}{\mu}\right) \ , \tag{5.35a}$$

$$f_1\left(\frac{m}{\mu}, \mu\delta\right) = 0.25 - 0.46\log\left(\frac{m}{\mu}\right) - 0.17\log(\mu\delta) \ , \tag{5.35b}$$

$$f_2(\mu\delta) = 0.22 + 0.25\log^2(\mu\delta) \ , \tag{5.35c}$$

for m/μ, $\mu\delta \ll 1$. In contrast with the fermionic case (5.32), the numerical values here are only given with two digits of accuracy due to the higher number of parameters involved in the numerical fits. The behaviour of f_0 and f_1 was estimated from the set-up of two adjacent intervals, where the linear divergence with coefficient f_2 cancels.

Note that the coefficient f_2 of the leading divergence w/δ in (5.34) does not depend on the mass m/μ. By comparing this expression with the pure-state expectation for the UV modes (3.63), we find an equivalent behaviour to the one we observed for fermionic CoP in Sec. 5.2.1; namely that in such case the role of w is played by the total system size $L = N\delta$. This is once again in line with the observation for the structure of leading divergence for vacuum complexity in free bosonic conformal field theories [101, 102]. The reader should also note that in the case of pure state bosonic complexity, the leading UV expectation is of the form

$$(\mathcal{C}_2^{UV})^2 \sim (1/4)\log^2(1/\mu\delta)(L/\delta) \ , \tag{5.36}$$

which is also insensitive to the mass m of the field. In this case it is clear that this is because the zero mode is subdominant in the UV regime, which has a contribution of the form

$$(\mathcal{C}_2^{k=0})^2 \sim (1/4)\log^2(m/\mu) \ , \tag{5.37}$$

as in (3.65). From this we can see that the fact that the numerically obtained function f_2 does not seem to depend on the mass is related to the fact that the leading divergence, coming from the UV contribution, is insensitive to the zero-mode contribution. On the contrary, the subdominant logarithmic divergence is sensitive to the mass m/μ.

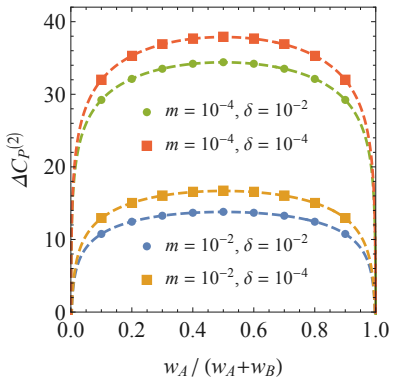

Figure 5.5.: Bosonic CoP for two adjacent ($d = 0$) subsystems in units of the reference state frequency $\mu = 1$. The analytic form (5.38) is plotted as a dashed curve for different values of $m\,\delta$. The numerical data is also shown. Here we consider $(w_A + w_B)/\delta = 20$ sites for a total system size of $N = 100(w_A + w_B)/\delta$.

In the case of two adjacent intervals we use the single interval expression (5.34) to obtain the expression for mutual bosonic CoP

$$\Delta\mathcal{C}_P^{(2)} = f_1\left(\frac{m}{\mu}, \mu\delta\right)\log\left(\frac{w_A w_B}{(w_A + w_B)\delta}\right) + f_0\left(\frac{m}{\mu}, \mu\delta\right) \ , \tag{5.38}$$

from which we can see that the leading divergence cancels, as expected, leaving the logarithmic divergence as the leading one. Furthermore, the coefficients f_0 and f_1 are the same as in the single interval case. Fig. 5.5 shows the behaviour of mutual bosonic CoP in terms of $w_A/(w_A + w_B)$. From Fig. 5.5 the reader can see that as well as in the fermionic case, mutual complexity of purification is subadditive $\Delta\mathcal{C}_P^{(2)} \geq 0$, which is also consistent with our observation (5.27) for two harmonic oscillators.

Finally, note that the logarithmic divergence (5.38) also matches the divergence of the holographic mutual complexity for the $\mathrm{CV}_{2.0}$ (2.23c) and CA (2.23b) subregion complexity proposals as in Sec. 2.3.2, but just as the fermionic CoP result (5.33) it has the opposite sign.

5.2.3. Comparison of bosonic CoP with other methods

In the previous section we presented the results for bosonic complexity of purification which were obtained via an optimization algorithm based on a steepest-descent method using the most general Gaussian purifications for mixed Gaussian states. In order to efficiently perform the minimization of the complexity functional, the natural geometric structure of Gaussian states was crucial, which in the bosonic case arises from the manifold of symplectic transformations $\mathcal{G} = \mathrm{Sp}(2N, \mathbb{R})$.

As we discussed, while this general method provides an accurate result for the resulting CoP, it is not insensitive to computational difficulties associated with considering

subsystems with a large number of degrees of freedom. A natural question which arises in this case is whether we can translate the problem of finding the CoP for a system with N_A degrees of freedom, into the problem of finding CoP for N_A systems with a single degree of freedom.

This is the strategy that authors in [202] used to approximate the complexity of purification for single degrees of freedom of certain Gaussian states using an L^1 norm arising from an F_1 cost function (3.8a) derived originally for similar set-ups in [102]. In this work, authors define two types of L^1 bases with which they perform the minimization of the geodesic distance with respect to an L^2 norm since, as we mentioned in Sec.(3.1.1), it is challenging to minimize the length of a path with respect to a L^1 norm, specially for several modes.

A key feature of subsystems of the Klein–Gordon model consisting several modes is that it is in general not sufficient to optimize over individual modes in order to obtain the true Gaussian CoP. The reason being that it is generally not possible to bring both the $(J_{\mathrm{T}})_A$ of a mixed Gaussian state ρ_A describing a subregion of the vacuum and the $(J_{\mathrm{R}})_A$ of a spatially unentangled product state simultaneously into block-diagonal form. However, there may be cases in which the standard decomposition of the mixed target state also approximately decomposes the reference state into individual modes.

To see this, consider a single bosonic mode in the case of pure Gaussian reference state and a mixed Gaussian target state which do not have $\hat{\varphi}\,\hat{\pi}$ -correlations. This is a more restricted setup compared with the two-harmonic oscillator case that we studied in Sec. 5.1.1 for which we assumed in general non-vanishing $\hat{\varphi}\,\hat{\pi}$ -correlations.

This subsystem can be extended to a subsystem consisting of two bosonic modes $\mathcal{H}' = \mathcal{H}_A \otimes \mathcal{H}_{A'}$ with extended reference state $|J_{\mathrm{R}}\rangle$ and purified target state $|J_{\mathrm{T}}\rangle$ such that their respective linear complex structures are given by

$$J_{\mathrm{T}} = \left(\begin{array}{cc|cc} 0 & \lambda & 0 & \sqrt{\lambda^2-1} \\ -\lambda & 0 & \sqrt{\lambda^2-1} & 0 \\ \hline 0 & \sqrt{\lambda^2-1} & 0 & \lambda \\ \sqrt{\lambda^2-1} & 0 & -\lambda & 0 \end{array}\right), \tag{5.39a}$$

$$J_{\mathrm{R}} = \left(\begin{array}{cc|cc} 0 & \frac{1}{\mu} & 0 & 0 \\ -\mu & 0 & 0 & 0 \\ \hline 0 & 0 & 0 & \frac{1}{\nu} \\ 0 & 0 & -\nu & 0 \end{array}\right), \tag{5.39b}$$

where $\lambda \in [1, \infty)$ is equivalent to the parameters c_i for several degrees of freedom as in (5.6), μ is the reference state frequency for the original single bosonic mode and ν is a parameter for the extender reference state over which the minimization of the complexity functional (5.15) has to be performed. In this case, the L^2 complexity functional has the form

$$\mathcal{C}(\lambda, \mu, \nu) = \frac{1}{2}\sqrt{\log^2\left(\frac{\omega_+}{\mu}\right) + \log^2\left(\frac{\omega_-}{\mu}\right)}\,, \tag{5.40}$$

where here

$$\omega_{\pm} = \frac{\mu}{2}\left[\lambda(\mu+\nu) \pm \sqrt{\lambda^2(\mu+\nu)^2 - 4\mu\nu}\right] \ . \tag{5.41}$$

In this setup,we need to optimize the functional (5.40) with respect to the parameter ν to find the CoP, *i.e.*, $\mathcal{C}_P(\lambda,\mu) := \min_\nu \mathcal{C}(\lambda,\mu,\nu)$. However, in order to do this we need to solve a transcendental equation for ν, which can be done numerically for any choice of λ and μ. Even though in this case there is no closed analytic form for $\mathcal{C}_P$, we have thus effectively reduced the problem of finding the CoP by optimizing over a single parameter for a single mode with vanishing $\hat{\varphi}\,\hat{\pi}$ -correlations in the reference and target state. Note that this is a simplified version of the two-harmonic oscillator set-up presented in Sec. 5.1.1.

The question is now to what extent this procedure can be applied to more subsystems of several modes. For this, consider a mixed state describing a subregion A with N_A degrees of freedom. With respect to a local basis $\hat{\xi}^a_A = (\hat{\varphi}^1_A,\ldots,\hat{\varphi}^{N_A}_A,\hat{\pi}^1_A,\ldots,\hat{\pi}^{N_A}_A)$ the covariance matrix of the reference and target state are of the form

$$(G_{\mathrm{T}})_A = \left(\begin{array}{c|c} G_{\hat{\varphi}\hat{\varphi}} & 0 \\ \hline 0 & G_{\hat{\pi}\hat{\pi}} \end{array}\right) \quad , \quad (G_{\mathrm{R}})_A = \left(\begin{array}{c|c} \frac{1}{\mu}\mathbb{1}_{N_A} & 0 \\ \hline 0 & \mu\mathbb{1}_{N_A} \end{array}\right) \ . \tag{5.42}$$

If $(G_{\mathrm{T}})_A$ is the covariance matrix of a pure Gaussian state, then it is possible to find a symplectic transformation M

$$M = \left(\begin{array}{c|c} O & 0 \\ \hline 0 & O \end{array}\right) \ , \tag{5.43}$$

where O is an orthogonal matrix such that it diagonalizes the target state covariance matrix while preserving the one for the reference state, namely $(\tilde{G}_{\mathrm{T}})_A = M(G_{\mathrm{T}})_A M^{\intercal}$ and $(G_{\mathrm{R}})_A = M(G_{\mathrm{R}})_A M^{\intercal}$. However, if $(G_{\mathrm{T}})_A$ is the covariance matrix of a mixed Gaussian state, then the transformation M that diagonalizes it, will no longer preserve $(G_{\mathrm{R}})_A$, as M will no longer be of the form (5.43). In this case, we could approximate the true matrix M by only diagonalizing $G_{\hat{\varphi}\hat{\varphi}}$ with an orthogonal transformation O, *i.e.*, such that $\tilde{G}_{\hat{\varphi}\hat{\varphi}} = OG_{\hat{\varphi}\hat{\varphi}}O^{\intercal}$ is a diagonal matrix. We would then consider a matrix M of the form (5.43) and consider only the diagonal elements of the matrix $\tilde{G}_{\hat{\pi}\hat{\pi}} = OG_{\hat{\pi}\hat{\pi}}O^{\intercal}$, which in general will be non-diagonal. That is, we neglect the off-diagonal terms, which we assume to be small compared to the diagonal ones. With this assumption, we can the apply the single-mode optimization based on the functional (5.40) for each of the modes, such that

$$\mathcal{C}_P(|J_{\mathrm{T}}\rangle\,,|J_{\mathrm{R}}\rangle) \approx \sqrt{\sum_i \min_{\nu_i}\left[\mathcal{C}(\lambda_i,\mu,\nu_i)\right]} \ , \tag{5.44}$$

and where the information for the λ_i defining each individual mode is extracted from the diagonal entries of $\tilde{G}_{\hat{\varphi}\hat{\varphi}}$ and $\tilde{G}_{\hat{\pi}\hat{\pi}}$. Of course, if $|J_{\mathrm{T}}\rangle$ is a pure state, then (5.44) becomes an equality where now on both sides there is the usual pure-state complexity (5.11).

We can directly compare the results for bosonic CoP of vacuum subregions obtained via the full optimization based on the steepest-descent method [226] and this single-mode approximation. Fig. 5.6 shows a comparison between these two approaches

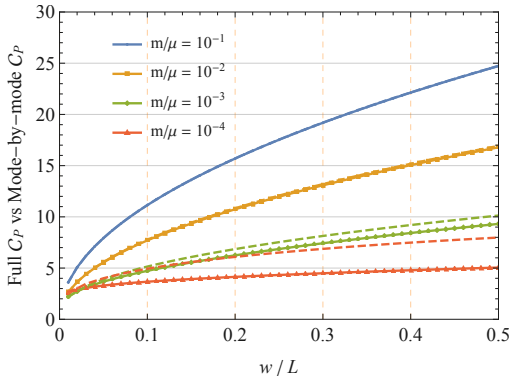

Figure 5.6.: Comparison of the CoP obtained using the full optimization algorithm for the most general Gaussian purification (solid) and the approximate CoP obtained for the single-mode decomposition (dashed), for a single interval as a function of w/L for different values of the mass parameter m/μ in periodic lattice with $N = L/\delta = 100$ sites and for lattice spacing $\mu\delta = 10^{-4}(m/\mu)^{-1}$.

for different values of the mass parameter m/μ. From Fig. 5.6 it can be seen that the single-mode optimization closely matches the full optimization for large values of the mass parameter m/μ, while the former becomes increasingly worse for smaller m/μ. One way to think about this fact is that for large m/μ the reference and target state are to a very good approximation decomposable into a sum of individual modes, whereas for smaller m/μ this approximate decomposition becomes increasingly worse. The reader should note that this observation is starker if one additionally considers $\hat{\varphi}\hat{\pi}$-correlations, as is the case for general mixed states. In this case, as well as for generic subsystems and fermionic systems a full optimization is required to appropriately capture the physics encoded in CoP.

This exercise also allows us to contrast our method with [202], where authors considered a similar single-mode optimization, albeit with respect to a L^1 norm. The main difference being that authors in [202] optimize the complexity functional over a restricted subset of parameters per mode effectively considering a subset of all possible Gaussian purifications.

In a different yet similarly interesting work [283], authors propose a measure for complexity of Gaussian mixed states based on a particular norm called the Fisher–Rao distance function which can be defined on the manifold of $(2N) \times (2N)$ real and positive-definite matrices $\mathbb{P}(N)$. It is worth pointing out that in [283] authors focused on mixed bosonic Gaussian states arising from subsystems on the Hilbert space of harmonic chains, and therefore the proposal (5.45) should be thought of, at least at the moment and until a similar formula is derived for fermions, as only applicable to the bosonic case.

By effectively restricting to such subset of all bosonic Gaussian covariance matrices, the authors are able to propose a measure of complexity for mixed states based entirely on said notion of distance for $\mathbb{P}(N)$. If we consider G_{T} and G_{R} real covari-

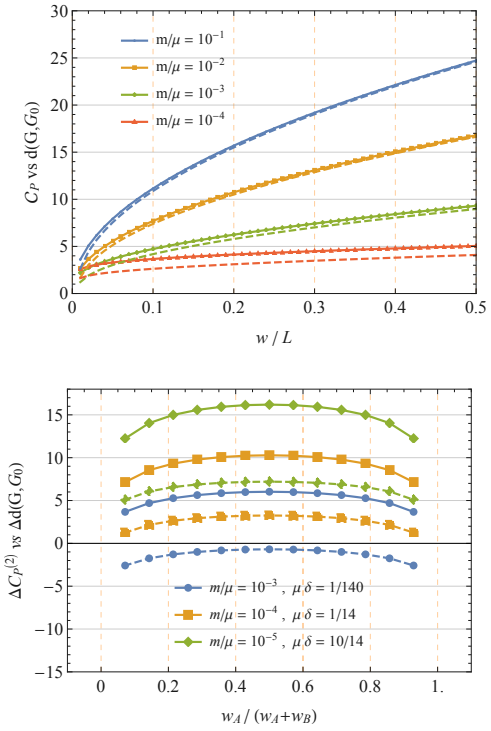

Figure 5.7.: Comparison of CoP obtained using the Gaussian optimization algorithm (solid) and the Fisher–Rao distance function (dashed) for a single interval (top) and two adjacent intervals (bottom). The data for the single interval case were generated for a mass parameter $m/\mu = 10^{-1}, 10^{-2}, 10^{-3}, 10^{-4}$, $N = L/\delta = 100$, and for lattice spacing $\mu\delta = 10^{-4}(m/\mu)^{-1}$, while the data for the adjacent interval case were generated for a mass parameter $m/\mu = 10^{-3}, 10^{-4}, 10^{-5}$, $N = L/\delta = 1400$, $(w_A + w_B) = 14$, and for lattice spacing $\mu\delta = (1/14) \times 10^{-4}(m/\mu)^{-1}$.

ance matrices for mixed target and reference Gaussian states, then the Fisher–Rao distance function

$$d(G_{\mathrm{T}}, G_{\mathrm{R}}) = \frac{1}{2\sqrt{2}} \sqrt{\mathrm{tr}\left(\log^2(G_{\mathrm{T}} G_{\mathrm{R}}^{-1})\right)} \,, \tag{5.45}$$

which measures the geodesic distance between the two matrices is interpreted as the complexity of one state with respect to the other. Fig. 5.7 shows a comparison between the CoP obtained with the full optimization algorithm and the Fisher–Rao distance function (5.45). From it we can see that for the case of a single interval there is both a quantitative and qualitative agreement between both notions, whereas for the two adjacent intervals these deviate notable and significantly although the qualitative behaviour remains comparable.

It is also interesting to note that the single-interval agreement is particularly remarkable, given the fact that these two notions are distances defined on different spaces. While CoP is defined as the geodesic distance between purified reference and target states on an enlarged Hilbert space $\mathcal{H}' = \mathcal{H}_A \otimes \mathcal{H}_{A'}$, as can be seen in Fig. 5.1, the Fisher–Rao distance function is a measure defined entirely on the manifold of mixed

states associated with the Hilbert space $\mathcal{H}_A$, and in principle these needn't even be comparable to each other.

5.3. Discussion

In this Chapter we discussed complexity of purification (CoP) for vacuum subregions of $(1+1)$-dimensional free conformal field theories. We focused on two particular set-ups; one related to the discussion of Chapter 4 of complexity in non-equilibrium quantum dynamics, and one related to the study of CoP in subsystems comprised of single and two adjacent intervals in the vacuum of lattice discretizations of free bosonic and fermionic theories. In both cases we exploited the Gaussian character of the mixed states in consideration to use the full machinery of Gaussian techniques of Chapter 3 in order to study CoP.

In the first set-up, we studied CoP for a subsystem comprised of two harmonic oscillators with a time dependent mass, following Chapter 4. This simple yet revealing set-up allowed us to present the concept of CoP while at the same time providing evidence for the sub-additivity of mutual complexity, a UV-regulated quantity akin to mutual information adequate for studying the CoP for bipartite subsystems. Furthermore, this set-up provided an example to the known claim in the AdS/CFT correspondence that "entanglement entropy is not enough" to capture the full information about a quantum system (which has a gravitational dual). We showed this by comparing the functional dependence of entanglement entropy with the complexity of purification of a single oscillator.

In the second set-up, we studied CoP for vacuum subregions of free CFTs consisting of a single and two adjacent intervals. In the first case, we found that the leading divergence of CoP is a direct generalization of the leading divergence of pure-state complexity, which was studied in Chapter 3. We also found a subleading logarithmic divergence as well as a third term, which in the fermionic case is a simple constant, but in the bosonic case is a logarithmic divergence corresponding to the zero-mode.

For two adjacent intervals, we found a logarithmic divergence of the mutual complexity in both fermionic and bosonic models, which matches the holographic expectation of the subregion complexity CA and $\mathrm{CV}_{2.0}$ proposals, though with the opposite sign. In the fermionic case, we find a simple characterization of the logarithmic divergence with a constant coefficient, while in the bosonic case we find a coefficient with a complex interplay between different parameters such as the mass and reference scales. This contradiction between the subadditive and superadditive behaviours of subregion complexity from QFT and holography has been noticed before (see *e.g.*, [202]), but this is the first time that a full comparison between both quantities has been done for both fermions and bosons, especially using the most general Gaussian purifications.

We also compared our approach and results for bosonic CoP with two recently-developed methods that have been used to study it, namely mode-by-mode purifications and the Fisher–Rao distance proposal. For the first method, we found that our approach based on an optimization over the full Gaussian manifold provides

a better minimization of the complexity functional particularly when the theory is taken closer to criticality. This implies that the mode-by-mode approximation is insufficient to accurately capture the behaviour of CoP in the critical theory. For the second one, we found that while the Fisher–Rao distance function appears to behave similarly to the full CoP, the "mutual Fisher–Rao distance" seems to violate subadditivity in some cases. Furthermore, this mixed-state proposal is only defined for bosonic Gaussian states, as the positive-definiteness of the covariance matrix is necessary for the implementation of the distance measure.

As a consequence, there are two main novelties of the results presented in this Chapter. Firstly, we provided results using a general optimization method for CoP for any Gaussian mixed state in the vacuum of a CFT and showed that the mutual complexity computed via it has an equivalent logarithmic divergence akin to two of the holographic subregion complexity proposals but is subadditive instead of superadditive. We also showed that said method leads to an optimal minimization of complexity which is stable and efficient also near criticality. As a consequence, these studies lay the foundation for a more complete understanding of CoP in free CFTs.

6. Entanglement of Purification and Reflected Entropy

In this chapter we present the study of entanglement of purification (EoP), a correlation measure which generalizes the notion of entanglement entropy to mixed states, and of reflected entropy (RE), another correlation measure built from the so-called canonical purification; both conjectured to be holographically dual to the entanglement wedge cross section (see Sec. 2.2.1). We introduce both notions in Sec. (6.1) and briefly discuss them. In Sec. 6.2.1 we focus entirely on Gaussian EoP, and discuss its behaviour for vacuum subregions of free quantum field theories (QFT) consisting of two adjacent intervals using the most general Gaussian purifications, following Sec. 3.3.1 and Sec. 3.3.2. We show that in both cases Gaussian EoP has a leading behaviour proportional to half the mutual information (MI) in accordance with holographic and CFT expectations. In Sec. 6.2.2 we study bosonic Gaussian EoP for disjoint intervals in the small separation regime, showing an agreement both with holographic and CFT expectations. Then in Sec. 6.3 we study EoP and RE for two largely-separated spherical subregions in the vacuum of a CFT in any dimension with a gape in the operator spectrum. Using general arguments applicable to lattice realizations of said theories, we provide a proof that both quantities present a logarithmic enhancement with respect to the leading power-law divergence in the separation of the subregions, a feature which provides new insights into the large distance behaviour of these correlation measures. Finally, using the $c = 1/2$ Ising CFT as a concrete example of a lattice model, we explicitly compute the overall coefficients for both quantities.

6.1. The Concept of Entanglement of Purification and Reflected Entropy

Quantifying the entanglement properties of quantum many-body systems is a challenging and vast enterprise in quantum information science (see *e.g.*, [288–291]). Of the several entanglement measures which can be defined, however, *entanglement entropy* (EE) stands out as arguably one of the most studied ones in the field of high-energy physics. From quantum field theory (see [86, 228, 292, 293]), to conformal field theory (see [294]) and the AdS/CFT correspondence (see [132, 227, 229]), quantum entanglement and the entropy associated with it has played a key role in the development of the field over the past twenty years. See *e.g.*, [229, 295] for recent reviews.

In essence, EE is a measure of pure state entanglement between a subregion and its complement. Given a system in a pure quantum state described by a density matrix $\rho = |\psi\rangle\langle\psi|$ and a subsystem A with reduced density matrix $\rho_A = \mathrm{tr}_{\bar{A}}(\rho)$, EE is defined as the von Neumann entropy of ρ_A

$$S_A = S(\rho_A) := -\mathrm{tr}_A(\rho_A \log(\rho_A)) \ , \tag{6.1}$$

where $\bar{A}$ denotes the complement of A. One can think of EE as measuring how entangled subsystem A is with its complement $\bar{A}$ in the state ρ. In quantum field theories, EE is an UV-divergent quantity due to correlations at arbitrarily short distances and its computation is in general a difficult task. However, several results are known in a variety of settings such as free theories [221, 296–299], two-dimensional CFTs [85, 300–303], two-dimensional gapped and gapless systems [76, 88] and strongly-coupled holographic QFTs [118, 123, 127, 128].

For subsystems consisting of two components $A \cup B$, *i.e.*, for bipartite Hilbert spaces $\mathcal{H} = \mathcal{H}_A \otimes \mathcal{H}_B$, a quantity known as *mutual information* (MI) defined through EE as

$$I(A:B) := S_A + S_B - S_{A\cup B} \ , \tag{6.2}$$

is used to characterize the correlations between them in a given pure state ρ. MI has the property of being a UV-regulated version of EE in quantum field theories and is therefore adequate for studying the correlations of bipartite spatial subregions. It should also be noted that in conformal field theories, MI is generically non-universal, as it is computed via a 4-point function of twist operators, which is spectrum dependent [86].

Note that the definition of entanglement entropy S_A of a subregion A (6.1) intrinsically requires the knowledge of the pure state $\rho = |\psi\rangle\langle\psi|$ of which the subregion characterized by the reduced density matrix ρ_A is a subsystem of. The natural question then arises: how can we characterize the correlations between different components of a subsystem corresponding to a mixed state characterized by a reduced density matrix?

Of the correlation measures that can be defined for mixed states, two stand out in the context of the AdS/CFT correspondence, namely *entanglement of purification* (EoP) and *reflected entropy* (RE).[1] While EoP can be considered a mixed state generalization of EE measuring the correlations of bipartite subsystems, RE arises from an algebraic construction as the von Neumann entropy of the canonical purification of the mixed state describing the bipartite subsystem. Remarkably, in the case of strongly-interacting QFTs with a holographic dual, both notions have been conjectured to be dual to the same gravitational quantity, namely the *entanglement wedge cross section* E_W (see Sec. 2.2.1). As a consequence, contrasting these two notions in conformal field theories can help elucidate their precise role in the AdS/CFT correspondence and their connection with the entanglement wedge cross section.

In the next sections, Sec. 6.1.1 and Sec. 6.1.2, we define these two correlation measures. In Sec. 6.2.1, we focus on the study of EoP for mixed Gaussian states corresponding to spatial subregions of vacuum states of free bosonic and fermionic theories consisting of two adjacent subsystems. We then study Gaussian EoP in free bosonic theories consisting of two disjoint subsystems in the small separation regime in Sec. 6.2.2. Finally, in Sec. 6.3 we compare EoP and RE for spatial subregions consisting of two disjoint subsystems in the large separation regime, which

[1] There exists indeed a plethora of correlation measures for mixed states and which reduce to EE for pure states; some of which have also been studied in the AdS/CFT correspondence, such as entanglement negativity, entanglement of formation or squashed entanglement.

reveals an interesting enhancement of the leading divergent behaviour that has been extensively studied also for MI.

6.1.1. The Concept of Entanglement of Purification

Entanglement of purification EoP is a measure of total correlations between two subsystems that includes both classical and quantum correlations.[2] It can be regarded as a mixed state generalization of EE [158, 159].

Given a mixed state with reduced density matrix $\rho_{AB} : \mathcal{H}_{AB} \to \mathcal{H}_{AB}$, we consider a purification $|\psi\rangle \in \mathcal{H}$ by extending the Hilbert space $\mathcal{H}_{AB}$ according to

$$\mathcal{H}_{AB} = \mathcal{H}_A \otimes \mathcal{H}_B \to \mathcal{H} := \mathcal{H}_A \otimes \mathcal{H}_B \otimes \mathcal{H}_{A'} \otimes \mathcal{H}_{B'} \ , \tag{6.3}$$

such that $\rho_{AB} = \mathrm{tr}_{A'B'}(|\psi\rangle \langle\psi|)$. EoP, $E_P(\rho_{AB})$, is then defined as the minimum of the entanglement entropy $S(A \cup A') = S_{AA'} = -\mathrm{tr}_{AA'}(\rho_{AA'} \log(\rho_{AA'}))$ for the reduced density matrix $\rho_{AA'} = \mathrm{tr}_{BB'}(|\psi\rangle \langle\psi|)$ over all possible purifications $|\psi\rangle \in \mathcal{H}$. In other words,

$$E_P(\rho_{AB}) := \min_{|\psi\rangle \in \mathcal{H}} [S_{AA'}] \ . \tag{6.4}$$

Note that EoP reduces to the usual entanglement entropy if ρ_{AB} is a pure state $E_P(\rho_{AB}) = S_A = S_B$ and vanishes for product states $E_P(\rho_{AB}) = E_P(\rho_A \otimes \rho_B) = 0$. Furthermore, one should in principle consider a minimization over all possible purifications, including ones with a larger number of ancillary degrees of freedom than in the original Hilbert space $\mathcal{H}_{AB}$, which makes in practice the computation of EoP in general a challenging task.

The operational interpretation of EoP can be explained via a regularized version built from considering n-copies of the reduced density matrix as: $E_{\mathrm{LO}_q}(\rho_{AB}) = E_P^{\infty}(\rho_{AB}) := \lim_{n\to\infty} E_P(\rho_{AB}^{\otimes n})/n$. This version of EoP can be interpreted as counting the number of initial EPR pairs required to create the mixed state ρ_{AB} by local operations and asymptotically vanishing communication [156, 158].

EoP made its appearance in quantum field theories relatively recently due to its conjectured holographic realization in the AdS/CFT correspondence as the dual of the entanglement wedge cross-section:

$$E_W(\rho_{AB}) = \frac{\mathrm{Area}(\Sigma_{AB}^{\min})}{4G_N} \ , \tag{6.5}$$

where $\Sigma_{AB}^{\min}$ is the minimal cross section of the entanglement wedge, as explained in Sec. 2.2.1. That is,

$$E_P^{\mathrm{holo}}(\rho_{AB}) = E_W(\rho_{AB}) \ . \tag{6.6}$$

[2] In general, distinguishing between classical and quantum correlations of subsystems in mixed states, specially in quantum field theories, is a challenging task. This stems from the fact that the decomposition of a mixed state into a combination of pure states is in general not unique, and given the ambiguity of state preparation, it is a priori not clear whether correlations between subsystems arise from classical (local operations and classical communication - LOCC) or quantum (entanglement) interactions.

This connection between holographic E_P and $E_W(\rho_{AB})$ (6.5) was conjectured in [156, 157] based on tensor network interpretations of the AdS/CFT Correspondence, supported by conformal field theory techniques in specific examples [160] and has since been an active topic of research [161–168], which strongly motivated its study in quantum field theories. Note that the first studies in this direction include [304, 305].

It is interesting to compare the definition of EoP (6.4) with CoP (5.2). In contrast with the latter, for which one must solve an intricate minimization problem for the circuit length computed for each purification, EoP requires only one minimization, namely that of the entanglement entropy of the appropriate reduced density matrix of the purification. Furthermore, and as mentioned in Sec. (5.1), there is no need to specify a reference state $|\psi_{\mathrm{R}}\rangle$ in order to compute EoP. In this sense, finding the EoP for a given mixed state is more straightforward than finding the CoP. However, as we said before, it is still a challenging computation which requires a minimization over an infinite number for purifications of the given mixed state.

Given the inherent challenges to the minimization procedure, we must consider scenarios where such task is manageable. One such scenario deals with Gaussian states and is based on the Gaussian techniques that we have discussed in Sec. 3.2 and which we also applied to CoP in Sec. 5.2. By focusing on Gaussian purifications of Gaussian mixed states corresponding to vacuum subregions of free bosonic and fermionic theories, we are able tackle this problem efficiently, particularly in the case of subregions comprised of a single and two adjacent intervals. This is the strategy that we pursue in Sec. 6.2.1 and which allows us to extract the properties of Gaussian EoP for single or adjacent vaccuum subregions of free CFTs. We also tackle the case of two disjoint intervals with a small separations for bosonic theories in Sec. 6.2.2.

The other scenario that we will consider deals with the opposite regime; namely that of vacuum subregions of free CFTs comprised of two disjoint intervals in the large separation limit. In this case, we focus on free fermionic CFTs, for which we are compelled to go beyond the Gaussian Ansatz. This allows us to step into the direction of non-Gaussian states in CFTs, a vastly unexplored territory for many quantum information-theoretic quantities in high energy physics. We will focus on this regime in Sec. 6.3.

6.1.2. The Concept of Reflected Entropy

Given a mixed state there is an infinite number of ways in which we can purify it. However, there exists a unique and special purification called the *canonical purification*. Consider a mixed state with reduced density matrix $\rho_{AB} : \mathcal{H}_{AB} \to \mathcal{H}_{AB}$ and take its decomposition into a basis of eigenstates $\{|\psi_i\rangle\}$ with eigenvalues $\{p_i\}$ as $\rho_{AB} = \sum_i p_i |\psi_i\rangle \langle\psi_i|$ with $\sum_i p_i = 1$ and $p_i \geq 0$. The canonical purification of ρ_{AB} denoted by $|\sqrt{\rho_{AB}}\rangle$ is given by

$$|\sqrt{\rho_{AB}}\rangle = \sum_i \sqrt{p_i} \, |\psi_i\rangle_{AB} \otimes |\psi_i\rangle_{A'B'} \ , \tag{6.7}$$

where $|\psi_i\rangle_{A'B'}$ is a basis of eigenstates on the ancillary Hilbert space $\mathcal{H}_{A'B'} = \mathcal{H}_{A'} \otimes \mathcal{H}_{B'}$ which in this case is equal to the original bipartite Hilbert space $\mathcal{H}_A \otimes \mathcal{H}_B$. That is, $|\sqrt{\rho_{AB}}\rangle$ is the unique purification which is symmetric under the exchange $A \leftrightarrow A'$ and $B \leftrightarrow B'$. Every other purification of ρ_{AB} can be written as $|\psi\rangle = (\hat{\mathbb{1}}_{AB} \otimes \hat{U}_{A'B'})\,|\sqrt{\rho_{AB}}\rangle$ where $\hat{U}_{A'B'}$ is a unitary acting only on $\mathcal{H}_{A'B'}$.

Note the similarity between the canonical purification and the known thermofield double (TFD) state $|\mathrm{TFD}\rangle$ written in an energy eigenbasis $\{|E_n\rangle_{AB}\}$ as

$$|\mathrm{TFD}\rangle = \frac{1}{\sqrt{\mathcal{Z}}} \sum_n e^{-\frac{\beta E_n}{2}} |E_n\rangle_{AB} \otimes |E_n\rangle_{A'B'} \ , \tag{6.8}$$

where $\mathcal{Z} = \mathrm{tr}(e^{-\beta \hat{H}}) = \sum_n e^{-\beta E_n}$ is the partition function in the canonical ensemble. The TFD state is the canonical purification of the thermal density matrix $\rho_\beta := e^{-\beta \hat{H}}/\mathcal{Z} = (1/\mathcal{Z}) \sum_n e^{-\beta E_n} |E_n\rangle_{AB} \langle E_n|$, *i.e.*, $\rho_\beta = \mathrm{tr}_{A'B'}(|\mathrm{TFD}\rangle \langle \mathrm{TFD}|)$. Because of this, the canonical purification is sometimes referred to as the thermofield double (TFD) purification.

The doubling of the Hilbert space $\mathcal{H}_{AB} \to \mathcal{H} = \mathcal{H}_{AB} \otimes \mathcal{H}_{A'B'}$ can be thought of as arising from the Gelfand–Neumark–Segal (GNS) representation [306, 307] of the matrix algebra which acts on the original Hilbert space. For a detailed analysis of the algebraic approach to quantum field theories see [308–310].

Using the canonical purification construction, authors in [169] proposed a "simpler" holographic dual to the entanglement wedge cross section E_W which does not require any minimization like EoP. For a bipartite quantum system $\mathcal{H}_{AB}$, mixed state ρ_{AB} with canonical purification $|\sqrt{\rho_{AB}}\rangle$, the *reflected entropy* (RE) is defined as

$$S_R(\rho_{AB}) := S\left(\mathrm{tr}_{BB'}\left(|\sqrt{\rho_{AB}}\rangle \langle \sqrt{\rho_{AB}}|\right)\right) \ . \tag{6.9}$$

Much like EoP, RE is a measure of correlations between subsystems A and B which contains both classical and quantum contributions. However, unlike E_P, S_R does not seem to have a direct operational interpretation but stands out among other correlation measures as the EE corresponding to the unique canonical purification.

However, note that the canonical purification is in particular one of the purifications over which we optimize in the definition of EoP, leading to the following connection between EoP and RE

$$\begin{aligned} E_P(\rho_{AB}) &= \min_{|\psi\rangle \in \mathcal{H}} \left[S\left(\mathrm{tr}_{BB'}(|\psi\rangle \langle \psi|)\right)\right] \\ &= \min_{\hat{U}_{A'B'}} \left[S\left(\mathrm{tr}_{BB'}\left((\hat{\mathbb{1}}_{AB} \otimes \hat{U}_{A'B'})\,|\sqrt{\rho_{AB}}\rangle \langle \sqrt{\rho_{AB}}|\,(\hat{\mathbb{1}}_{AB} \otimes \hat{U}_{A'B'})^\dagger\right)\right)\right] \\ &\leq S\left(\mathrm{tr}_{BB'}(|\sqrt{\rho_{AB}}\rangle \langle \sqrt{\rho_{AB}}|)\right) = S_R(\rho_{AB}) \ , \end{aligned} \tag{6.10}$$

where $\hat{U}_{A'B'}$ is a unitary acting on $\mathcal{H}_{A'B'}$. *i.e.*, $E_P(\rho_{AB}) \leq S_R(\rho_{AB})$. Note that this is valid for symmetric purifications in which $\dim(\mathcal{H}_{A\cup B}) = \dim(\mathcal{H}_{A'\cup B'})$. In general, one can consider $\dim(\mathcal{H}_{A\cup B}) < \dim(\mathcal{H}_{A'\cup B'})$. The unitary $\hat{U}_{A'B'}$ mentioned previously applies only to the former case, since for RE one has $\dim(\mathcal{H}_{A\cup B}) = \dim(\mathcal{H}_{A'\cup B'})$ by definition.

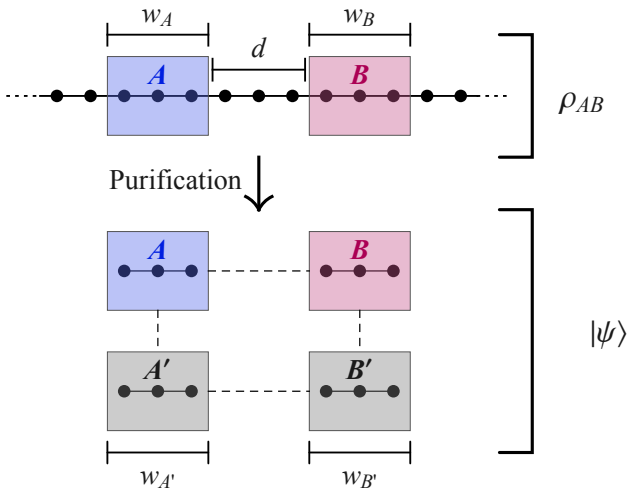

Figure 6.1.: Sketch of entanglement of purification and reflected entropy on an infinite lattice, taken from [CamH01]. The mixed state ρ_{AB} on a subsystem of two disjoint regions $A \cup B$ separated by d/δ sites is purified to a state with auxiliar regions A' and B', taken to be of the same size w_A/δ and w_B/δ as A and B, respectively, where δ is the lattice spacing. We will consider $w_A \neq w_B$ for adjacent intervals ($d = 0$), and $w_A = w_B$ for disjoint intervals ($d \neq 0$).

At the same time, authors in [169] argued that in QFTs with a holographic dual, S_R satisfies the equality

$$S_R^{\text{holo}}(\rho_{AB}) = 2E_W(\rho_{AB}) + \dots \ , \tag{6.11}$$

where the ellipsis denotes quantum corrections to the bulk reflected entropy starting at order $\mathcal{O}(G_N^0)$. This conjecture implies the following relation between EoP and RE for states with a holographic dual

$$E_P^{\text{holo}}(\rho_{AB}) = E_W(\rho_{AB}) = \frac{S_R^{\text{holo}}(\rho_{AB})}{2} \ . \tag{6.12}$$

Note that the holographic expectation (6.12) does not contradict the result (6.10) arising purely from their operatorial definitions. However, for generic states in quantum field theories and in quantum many-body systems one would expect find $E_P \neq S_R/2$, and hence the expectation (6.12) may only be true for a special class of states which includes holographic states with a classical bulk geometry. It is therefore an interesting question from the perspective of quantum field theories, and more specifically from conformal field theories, to study these quantities. We will do this in Sec. 6.3, although we first study Gaussian EoP in Sec. 6.2. Nonetheless in both sections we focus on two-dimensional free CFTs using their lattice approximations (see Sec. 3.3.1 and Sec. 3.3.2). We study the case of two intervals of sizes w_A/δ and w_B/δ (possibly) separated by a distance d (see Fig. 6.1).

6.2. Gaussian Entanglement of Purification

Until very recently, most of the understanding of EoP came from its conjectured holographic realization as the dual of the entanglement wedge cross-section (6.5), a series of results determined by local conformal transformations in CFTs and by studies in free QFTs for subsystems with a small number of degrees of freedom. In this section, based on [**CamH02**], we go beyond the previously known results in the latter case by computing EoP using the most general Gaussian purifications of Gaussian mixed states corresponding to vacuum subregions of free bosonic and fermionic CFTs; that is, essentially using the same models that we used for CoP in Sec. 5.2. This allows us to approach the QFT limit and uncover properties of EoP in this regime.

Starting from a Gaussian mixed state ρ^{G}_{AB}, we consider a Gaussian purification $|\psi^{\mathrm{G}}\rangle \in \mathcal{H}' = \mathcal{H}_{AB} \otimes \mathcal{H}_{A'B'}$ and then perform minimization of the entanglement entropy of the reduced density matrix $\tilde{\rho}^{\mathrm{G}}_{AA'} = \mathrm{tr}_{BB'}(|\psi^{\mathrm{G}}\rangle \langle\psi^{\mathrm{G}}|)$ over Gaussian states of the form $\hat{U}^{\mathrm{G}} |\psi^{\mathrm{G}}\rangle$ where $\hat{U}^{\mathrm{G}} = \hat{\mathbb{1}}_{AB} \otimes \hat{U}^{\mathrm{G}}_{A'B'}$ is a Gaussian unitary. In other words, we focus on *Gaussian entanglement of purification*

$$E^{\mathrm{G}}_P(\rho^{\mathrm{G}}_{AB}) := \min_{\hat{U}^{\mathrm{G}} = \hat{\mathbb{1}}_{AB} \otimes \hat{U}^{\mathrm{G}}_{A'B'}} \left[S\left(\mathrm{tr}_{BB'} \left(\hat{U}^{\mathrm{G}} |\psi^{\mathrm{G}}\rangle \langle\psi^{\mathrm{G}}| (\hat{U}^{\mathrm{G}})^\dagger \right) \right) \right] , \tag{6.13}$$

which in general is expected to satisfy the inequality $E_P(\rho^{\mathrm{G}}_{AB}) \leq E^{\mathrm{G}}_P(\rho^{\mathrm{G}}_{AB})$. That is, Gaussian EoP $E^{\mathrm{G}}_P(\rho^{\mathrm{G}}_{AB})$ bounds the true EoP $E_P(\rho^{\mathrm{G}}_{AB})$ from above. However, as mentioned in Sec. 5.1, there is numerical evidence [226] which supports the conjecture [304] that for Gaussian mixed states this is actually an equality $E_P(\rho^{\mathrm{G}}_{AB}) \equiv E^{\mathrm{G}}_P(\rho^{\mathrm{G}}_{AB})$, meaning that Gaussian purifications of Gaussian mixed states suffice to reach the true minimum over all possible purifications.

Similarly to CoP, we can rephrase this minimization in terms of the complex structure of the Gaussian purification $|J\rangle$ of the Gaussian mixed state ρ_{AB}. In this case, all the necessary information about the purified Gaussian state is encoded in the complex structure J of the state, which can be decomposed similarly to (5.9) as

$$J = \left(\begin{array}{c|c} J_{AB} & J_{ABA'B'} \\ \hline J_{A'B'AB} & J_{A'B'} \end{array} \right) , \tag{6.14}$$

and which is of dimension $(N_{A\cup B} + N_{A'\cup B'}) \times (N_{A\cup B} + N_{A'\cup B'})$. In this case, the (Gaussian) entanglement entropy $S_{AA'}(|J\rangle)$ can be direclty computed via

$$S_{AA'}(|J\rangle) = \begin{cases} \mathrm{tr}_{AA'} \left(\frac{\mathbb{1}_A + \mathrm{i}\, J_{AA'}}{2} \log \left| \frac{\mathbb{1}_A + \mathrm{i}\, J_{AA'}}{2} \right| \right) & , \text{(bosons)} \\ -\mathrm{tr}_{AA'} \left(\frac{\mathbb{1}_A + \mathrm{i}\, J_{AA'}}{2} \log \left(\frac{\mathbb{1}_A + \mathrm{i}\, J_{AA'}}{2} \right) \right) & , \text{(fermions)} \, . \end{cases} \tag{6.15}$$

These analytical expressions for entanglement entropy of Gaussian states were first derived in [296, 297] and rephrased in terms of linear complex structures in [299, 311].

The procedure to compute Gaussian EoP is then straightforward: we start with a matrix representation of the complex structure J_{AB} of the mixed Gaussian state ρ_{AB} in a basis $\hat{\xi}^a = \left(\hat{\xi}^a_A, \hat{\xi}^a_B \right)$ which decomposes J_{AB} to a matrix of the form (5.5).

This basis can be found from the eigenvectors of J_{AB}. With this, we construct a starting purification of the form (5.7), with N_{nm} the number of ancillary degrees of freedom beyond the minimal purification.

In the basis $\hat{\xi}^a = \left(\hat{\xi}^a_A, \hat{\xi}^a_B, \hat{\xi}^a_{A'}, \hat{\xi}^a_{B'}\right)$, the complex structure of the purified state has the block form (6.14), where the diagonal blocks are precisely the complex structures restricted to the mixed states ρ_{AB} and $\rho_{A'B'}$. By varying the block $J_{A'B'}$ and the off-diagonal blocks in a compatible way, we have access different purifications of ρ_{AB}. As a consequence, the Gaussian manifold over which we perform the minimization is parametrized by transformations $M_{A'B'}$ which act solely on the reduced complex structure $J_{A'B}$ and acting on the full complex structure via $M = \mathbb{1}_{AB} \oplus M_{A'B'}$. The minimization can then be iteratively performed by varying $M_{A'B'}$ with the steepest-descent method developed in [226].

In the following section (Sec. 6.2.1) we discuss the numerical results obtained in [**CamH02**] for Gaussian EoP for adjacent intervals for the discretized $(1+1)$ - dimensional Klein–Gordon and critical transverse Ising CFT models using minimal purifications $N_{\mathrm{nm}} = 0$. The reason being that there exists numerical evidence [226] which shows that the minimum of (6.4) is reached when choosing the numbers of degrees of freedom of the purifying systems A' and B' is equal to the respective numbers of degrees of freedom in the original subsystems A and B, *i.e.*, $N_{A'} = N_A$ and $N_{B'} = N_B$.

6.2.1. Adjacent Intervals in Free Conformal Field Theories

The guiding principle for our analysis of Gaussian EoP for adjacent intervals comes from the holographic expectation, represented in terms of the holographic formula (6.6). In particular, studies such as [160] performed analytical computations of EoP based on path-integral optimization (see [104]) for holographic CFTs. In this case, for adjacent subsystems A and B of a boundary CFT it was found that

$$E_W(A:B) = \frac{c}{6} \log\left(\frac{2w_A w_B}{(w_A + w_B)\delta}\right) , \tag{6.16}$$

where here c is the central charge of the boundary CFT, w_A and w_B are the lengths of the spatial boundary intervals A and B and where δ is a UV-regulator.

Starting from an equivalent adjacent interval setting, we applied the steepest descent method to the covariance matrices (3.45) and (3.83) in order to compute the Gaussian EoP using minimal purifications ($N_{\mathrm{nm}} = 0$) according to (6.13) and we found

$$E_P(A:B) = \begin{cases} \frac{1}{6}\log\left(\frac{2w_A w_B}{(w_A+w_B)\delta}\right) & , \text{(bosons)} \\ \frac{1}{12}\log\left(\frac{2w_A w_B}{(w_A+w_B)\delta}\right) & , \text{(fermions)} , \end{cases} \tag{6.17}$$

where here δ is the lattice spacing which acts as a UV regulator. These results are represented in Fig. 6.2 together with numerical data obtained for $(w_A + w_B)/\delta = 12$ sites in chains of $N = 100(w_A + w_B)/\delta$ total sites. From Fig. 6.2 we see a close agreement between the numerical results and the holographic expectation (6.16)

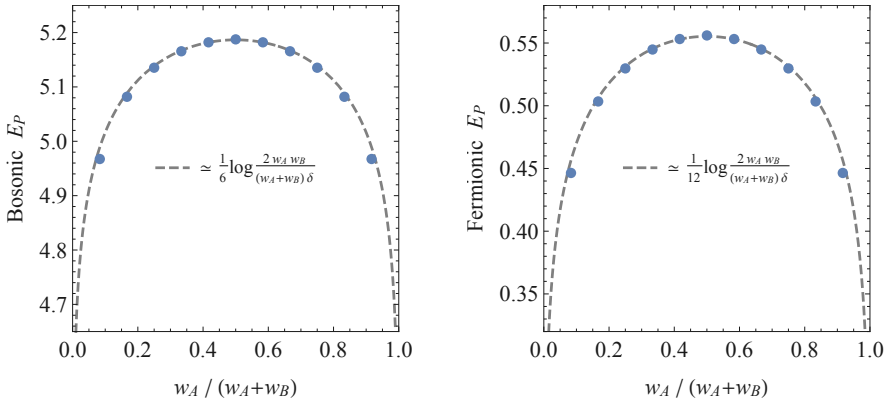

Figure 6.2.: Bosonic ($c = 1$, (left)) and fermionic/Ising spin EoP ($c = \frac{1}{2}$, (right)) for two adjacent ($d = 0$) subsystems A and B on $\frac{w_A+w_B}{\delta} = 12$ sites, with the continuum result for a fitted lattice spacing δ plotted as a dashed curve. Total system size $N = 1200$ and bosonic mass scale $m\,L = 10^{-4}$.

where we simply have $c = 1$ for the discretized KG model, and $c = 1/2$ for the critical transverse Ising model.

At the same time, it is interesting to compare these numerical results with the CFT expectation of mutual information $I(A : B)$ for the same setup, which comes from the computation for entanglement entropy for a single interval originally in [85, 86] and which is given by

$$I(A : B) = \frac{c}{3} \log \left(\frac{w_A w_B}{(w_A + w_B)\delta} \right) , \tag{6.18}$$

and that was also confirmed by numerical computations in [**CamH02**] using the discretized models. Note that in this case EoP and MI are have the same leading divergent behaviour, in agreement with the bound

$$E_P(A : B) \geq \frac{1}{2} I(A : B) , \tag{6.19}$$

found originally in [155] and proven proven for finite Hilbert spaces in [159] based on the sub-additivity of conditional entropy for a composite quantum system of four subsystems. The holographic version of this inequality was proven in [156]. A the same time, we can compare it with the individual entanglement entropies of the subsystems, given by

$$S_{A/B} = \frac{c}{3} \log \left(\frac{w_{A/B}}{\delta} \right) , \tag{6.20}$$

and so EoP (6.17) satisfies also the inequality

$$E_P(A : B) \leq \min \{S_A, S_B\} , \tag{6.21}$$

which is also a property of holographic EoP (6.6), thus showing a complete and remarkable agreement between Gaussian EoP computed numerically with both holographic and CFT expectations.

6.2.2. Small Separations in Free Bosonic CFTs

Here we investigate the behaviour Gaussian EoP for two disjoint intervals for the discretized Klein–Gordon model in the small separation regime. We focus on the bosonic theory since the vacuum state of the critical transverse Ising CFT model is generically non Gaussian for subsystems comprised of two disjoint intervals. We study EoP and RE for this model in the large separation limit in the following section, Sec. 6.3. At the same time, we focus on small separations for the bosonic model, since in this regime we can expect the zero-mode to be sub-dominant with respect to the UV behaviour of EoP that we wish to extract. We comment on the behaviour of bosonic EoP in the large separation limit also in Sec. 6.3.

We can use our Gaussian methods to study bosonic EoP for disjoint subsystems A and B of sizes $w_A = w_B = w$ in the small separation d regime, namely $d \ll w$ (see Fig. 6.1.). In this case, the holographic expectation [156, 157] and path-integral optimization approach [160] predict a behaviour of $E_W(\rho_{AB})$ of the form

$$E_W(A:B)\Big|_{d\ll w} = \frac{c}{6}\log\left(\frac{2w}{d}\right) , \tag{6.22}$$

which is consistent with (6.16) under the simple replacement $\delta = d$ and $w_A = w_B = w$.

Numerical results obtained with the steepest descent method for the discretized Klein–Gordon model for a mass scale $mL = 10^{-3}$ yield a logarithmic dependence of bosonic Gaussian EoP in the $d \ll w$ regime given by

$$E_p(A:B)\Big|_{d\ll w} \approx \frac{1}{6}\log\left(\frac{w}{d}\right) - \frac{1}{2}\log(mL) + c_0 , \tag{6.23}$$

where c_0 is a constant. Note that this result is consistent with the holographic expectation (6.22) for $c = 1$.

At the same time, there exists the following universal result for mutual information at small separations $d \ll w$ [86, 294]

$$I(A:B)\Big|_{d\ll w} \simeq \frac{c}{3}\log\left(\frac{w}{2d}\right) , \tag{6.24}$$

which is corroborated by numerical computations performed on the discretized model and which yield the behaviour in the small d/w regime given by

$$I(A:B)\Big|^{\text{num}}_{d\ll w} \approx a_1\log\left(\frac{w}{d}\right) - \frac{1}{2}\log(mL) + a_0 . \tag{6.25}$$

where a_0 is a constant. The coefficient a_1 can be bound according to $0.27 \lesssim a_1 \lesssim 0.40$ by closely analysing the numerical behaviour of $I(A:B)$ and $S(A\cup B)$ as done in [**CamH02**], suggesting an asymptotic behaviour $a_1 \propto 1/3$ consistent with (6.24) for $c = 1$.

Note the logarithmic mL dependence present in both numerical results for EoP (6.23) and MI (6.25), which is a consequence of the fact that we are considering a massive KG field model with small mass scale mL as a proxy for the modular invariant $c = 1$

bosonic CFT, as explained in Sec. 3.3.1. For MI this logarithmic divergence was first observed in [305].

We therefore also find in this case a remarkable agreement between the numerical results for Gaussian EoP and the CFT and holographic expectations, which relied on a benchmark set by an analysis of MI in this regime.

6.2.3. Large Separations in Free Bosonic CFTs

We now turn to the case of the large separation behaviour of bosonic Gaussian EoP. In this case, numerical computations (see [**CamH02**]) show a behaviour akin to bosonic MI.[3] This observation had already been made for smaller subsystems and smaller separations in [305] and is consistent with the observation that EoP weighs classical and quantum correlations differently at mall distances, when both become relevant. At large separations, both EoP and MI have a zero-mode contribution alongside a sub-polynomial (logarithmic or double-logarithmic) decay. That is, both MI and EoP suffer from an infrared divergence which can be regulated by a $\log(m\,L)/2$ and $\log(\log(m\,L))/2$ term respectively. That is, bosonic EoP behaves in this limit as

$$E_P(A:B)\big|^{\text{bos}}_{w\ll d} \approx d_1 \left(\frac{w}{d}\right)^{d_2} - \frac{1}{2}\log(m\,L) + d_0 \ , \tag{6.26}$$

with $d_2 \lesssim 0.15$ and d_0 a constant, which is consistent with the absence of a long-distance power behavior. On the other hand, bosonic MI behaves as

$$I(A:B)\big|^{\text{bos}}_{w\ll d} \simeq f_{\text{MI}}\left(\frac{d}{w}\right) + \frac{1}{2}\log\left(\log\left(\frac{1}{m\delta}\right)\right) \ , \tag{6.27}$$

where two possibilities for a behaviour of the coefficient f_{MI} explored in [**CamH02**] are given by

$$f_{\text{MI}} \sim \begin{cases} g_0 - g_1\left(\log\left(\frac{d}{w}\right)\right)^{g_2} \ , \\ h_0 - h_1\left(\log\left(\log\left(\frac{d}{w}\right)\right)\right)^{h_2} \ , \end{cases} \tag{6.28}$$

with $g_2 \lesssim 0.1$ and $h_2 \lesssim 1.3$, showing the likelihood of a double-logarithmic decay of bosonic MI in an infinite line set-up.

As opposed to (6.26), in (6.27) the numerical computations were performed on an infinite line, *i.e.*, taking the limit $m\delta \to 0$ only after the limit $N \to \infty$. This analysis differs from the periodic set-up, which was used to find (6.26) and where we considered the limit of a large number of sites N with the mass scale $m\,L = m\,N\delta$ constant and small. In this limit, the mass dependence of both MI and EoP is accurately described by $-\log(m\,L)/2$. The sub-polynomial dependence (6.28) in the infinite line (as well as in the periodic setup) for MI contradicts earlier numerical observations of a power law [312].

[3] Recall that a free scalar field $\phi(\vec{x})$ in D dimensions has a scaling dimension $\Delta = (D-2)/2$, which implies that in $D = 2$ the scalar field operator $\hat{\phi}$ transforms trivially $\hat{\phi} \to \hat{\phi}$ under a scaling transformation $\vec{x} \to \lambda\vec{x}$. Therefore, the formula (6.31) for MI and analysis of the previous section do not apply to the discretized Klein–Gordon model in $(1+1)$-dimensions, which leads to a gapless CFT at criticality $m \to 0$.

6.2.4. Universal Behaviour of Reflected Entropy in 2-dimensional Conformal Field Theories

So far we have discussed the behaviour of EoP in the context of free $(1+1)$-dimensional bosonic and fermionic CFTs. However, the behaviour of reflected entropy (RE) in CFTs has also been explored in [313–315].

In particular, authors in [313] find a universal behaviour of RE across 2-dimensional CFTs corroborated by [314, 315]. Authors compute RE using replica techniques according to [169] yielding an expression of RE determined by conformally invariant cross-ratios $x_{A,B}$, which in the case of two intervals of sizes w_A and w_B separated by a distance d take the form

$$x_{A,B} = \frac{w_A w_B}{(d+w_A)(d+w_B)} \ , \tag{6.29}$$

in such a way that for adjacent intervals $d = 0$ RE has the universal form

$$S_R(A:B) = \frac{c}{3} \log\left(\frac{2w_A w_B}{(w_A+w_B)\delta}\right) \ , \tag{6.30}$$

where here δ is also a UV regulator. From here we can see that EoP and RE of adjacent intervals follow closely the holographic expectation (6.12). We will see in the following section, that generically this is not the case for disjoint intervals that are separated from each other.

6.3. Long Distance Behaviour in Free Conformal Field Theories

In this final section of the Chapter, we present the study of EoP and RE for two spherical subregions far away from each other in the vacuum of a CFT in any dimension, following [**CamH01**]. This simple yet revealing set-up will allow us to extract universal properties of EoP and RE across CFTs which do not rely on intrinsic properties of the states in consideration, such as Gaussianity, or particular properties of the CFT. In particular, we will perform this analysis using quantum many-body techniques and elementary properties of EE without relying on conformal symmetry. We will first present the general arguments which we propose to hold in general for CFTs in any dimension with a gap in the operator spectrum and then provide a concrete example with explicit computations using the $(1+1)$-dimensional $c = 1/2$ Ising CFT in the language of spins and fermions.

The basic setting of interest consists of two spherical regions of equal diameter w separated by a distance d. Fig. 6.1 displays this set-up in the case of a $(1+1)$-dimensional CFT where the spherical subregions correspond to intervals of size w. The starting point for our analysis is the behaviour of MI (6.2) in the large separation regime. Recall that MI is generically a non-universal quantity which is computed from the 4-point function of twist operators, which is spectrum dependent [86]. At large separations between two subregions in a CFT, such that $d/w \gg 1$, MI decays as

$$I(A:B) \simeq \mathcal{N} \frac{\Gamma(3/2)\Gamma(2\Delta+1)}{2^{4\Delta+1}\Gamma(2\Delta+3/2)} \times \epsilon_\Delta^2 + \dots \ , \tag{6.31}$$

where

$$\epsilon_\Delta := \left(\frac{w}{d}\right)^{2\Delta} \ , \tag{6.32}$$

and where Δ corresponds to the scaling dimension of the lowest non-trivial operator(s) in the theory [302, 303], $\mathcal{N}$ is a factor denoting the possible degeneracy of such operators and the ellipsis denotes additional terms with a faster decay in ϵ_Δ [301, 303, 316]. Formula (6.31) applies to CFTs with a gap in the operator spectrum with the lowest one(s) being scalar(s).

6.3.1. General Argument

Our goal in this section is to find and prove an analogous formula to (6.31) for EoP and RE assuming the existence of a gap in the operator spectrum of the CFT. For RE there is in fact recent numerical evidence [314, 315] which shows that in free CFTs

$$S_R \simeq \alpha \epsilon_\Delta^2 \log(\epsilon_\Delta^{-2}) + \dots \ \text{ with } \ \epsilon_\Delta \ll 1 \ , \tag{6.33}$$

where α is a positive constant which depends on the particular theory. We will show that this asymptotic form holds both for EoP and RE in CFTs with a gapped spectrum and which have a lattice realization.

The fundamental assumption that will be the basis for our analysis and which will be valid both for EoP and RE is that the density matrix ρ_{AB} of spherical subregions A and B which are largely separated from each other can be written in the following way

$$\rho_{AB}(\epsilon_\Delta) \simeq \rho_A^{(0)} \otimes \rho_B^{(0)} + \epsilon_\Delta \rho_{AB}^{(1)} + \frac{1}{2}\epsilon_\Delta \rho_{AB}^{(2)} + \cdots \ , \tag{6.34}$$

where the ellipsis denotes terms with higher (non necessarily integer) powers of ϵ_Δ. We also assume that this asymptotic behaviour of the reduced density matrix holds for any sizes of the Hilbert spaces associated with the spherical subregions A and B. Note that terms with negative powers of ϵ_Δ are not allowed as these would contradict the known decay of correlations with the separation d between A and B.

It is important to note that the linear term in ϵ_Δ in (6.34) must be non-vanishing in order to have a power-law scaling of correlations functions which involve the insertions of the operator with the lowest scaling dimension in A and B. We will not assume anything in particular about the term which is quadratic in ϵ_Δ, though we will show that it does not contribute to the leading term in the large distance behaviour of EoP and RE.

The asymptotic behaviour of the reduced density matrix (6.34) can be seen as a consequence of the formal expression of a generic purification $|\psi\rangle_{ABA'B'} \equiv |\psi\rangle \in \mathcal{H}_{ABA'B'}$ with perturbative expansion

$$|\psi\rangle \simeq |\psi^{(0)}\rangle + \epsilon_\Delta |\psi^{(1)}\rangle + \frac{1}{2}\epsilon_\Delta^2 |\psi^{(2)}\rangle + \dots \ , \tag{6.35}$$

where the leading term $|\psi^{(0)}\rangle$ factorizes as

$$|\psi^{(0)}\rangle \equiv |\psi^{(0)}_{AA'}\rangle \otimes |\psi^{(0)}_{BB'}\rangle \ , \tag{6.36}$$

in order to be consistent with the decomposition of $\rho^{(0)}_{AB} = \rho^{(0)}_A \otimes \rho^{(0)}_B$ in (6.34). Furthermore, both the purification $|\psi\rangle$ (6.35) as well as the term responsible for the infinite separation behaviour, namely, $|\psi^{(0)}\rangle$, are normalized

$$\langle\psi|\psi\rangle = 1 \ , \tag{6.37a}$$

$$\langle\psi^{(0)}|\psi^{(0)}\rangle = \langle\psi^{(0)}_{AA'}|\psi^{(0)}_{AA'}\rangle \otimes \langle\psi^{(0)}_{BB'}|\psi^{(0)}_{BB'}\rangle = 1 \ , \tag{6.37b}$$

with $\langle\psi^{(0)}_{AA'}|\psi^{(0)}_{BB'}\rangle = 0$. These normalization conditions, in turn, lead to the following constraints for $|\psi^{(1)}\rangle$ and $|\psi^{(2)}\rangle$

$$\langle\psi^{(0)}|\psi^{(1)}\rangle + \langle\psi^{(1)}|\psi^{(0)}\rangle = 0 \ , \tag{6.38a}$$

$$\langle\psi^{(0)}|\psi^{(2)}\rangle + 2\,\langle\psi^{(1)}|\psi^{(1)}\rangle + \langle\psi^{(2)}|\psi^{(0)}\rangle = 0 \ . \tag{6.38b}$$

From the definitions of EoP and RE, (6.4) and (6.9) respectively, we see that their large separation asymptotics is determined by the behaviour of the eigenvalues $\{\mu_j\}$ of the reduced density matrix

$$\rho_{AA'} := \mathrm{tr}_{BB'}(|\psi\rangle\,\langle\psi|) \ , \tag{6.39}$$

as these determine the EE

$$S_{AA'} := -\mathrm{tr}_{AA'}(\rho_{AA'}\log(\rho_{AA'})) = -\sum_{j\geq 0}\mu_j\log(\mu_j) \ . \tag{6.40}$$

From here we can see that in the infinite separation limit $\epsilon_\Delta \to 0$ the fact that $\rho_{AB}(\epsilon_\Delta \to 0)$ factorizes to $\rho^{(0)}_A \otimes \rho^{(0)}_B$ also implies that in this limit the reduced density matrix $\rho_{AA'}(\epsilon_\Delta \to 0)$ describes a pure state and as a consequence has a single non-zero eigenvalue $\mu_0 = 1$, with $\mu_{j>1} = 0$. Of course, this behaviour is modified by considering a large but finite separation of the spherical subregions.

We can generically expect that the density matrix $\rho_{AA'}$ be well-defined regardless of the sign of ϵ_Δ when viewed as a formal parameter. As a consequence the linear correction to $\mu_{j\geq 0}$ proportional to ϵ_Δ can be expected to vanish and therefore the first *possible* correction to $\mu_{j\geq 0}$ in the large distance expansion must be proportional to ϵ^2_Δ. In other words, we can expect the leading asymptotic behaviour of the eigenvalues of $\rho_{AA'}$ to be given by

$$\mu_0 \sim 1 - \alpha_{\mathrm{tot}}\epsilon^2_\Delta \ , \tag{6.41a}$$

$$\mu_{j>0} \sim \alpha_j\epsilon^2_\Delta \ , \tag{6.41b}$$

where

$$\alpha_{\mathrm{tot}} := \sum_{j>0}\alpha_j \ . \tag{6.42}$$

for $\alpha_{j>0} \geq 0$. We stress that this is not necessarily the case for $\rho_{AA'}$ arising from a generic CFT but that the form (6.41) indeed encapsulates the *possible* leading order asymptotic behaviour. In particular, if $\alpha_j = 0$ for all $j > 0$, then the behaviour (6.41) would simply involve an expression in terms of ϵ^k_Δ for $k > 2$.

Assuming that the eigenvalues $\mu_{j\geq 0}$ of $\rho_{AA'}(\epsilon_\Delta)$ indeed have the asymptotic behaviour (6.41), we directly find the EE (6.43) for *any* purification $|\psi\rangle$ with perturbative expansion (6.35) given by

$$S_{AA'} \simeq \alpha_{\text{tot}} \epsilon_\Delta^2 \log(\epsilon_\Delta^{-2}) + \beta \epsilon_\Delta^2 + \dots \ , \tag{6.43}$$

where

$$\beta := \sum_{j>0} \alpha_j \left(1 - \log(\alpha_j)\right) \ . \tag{6.44}$$

where the ellipsis in (6.43) denotes terms with higher powers in ϵ_Δ^2. Of course, there are additional constraints on the purification (6.35) arising from the definitions of EoP and RE which will determine the precise form of the leading coefficient α_{tot} and offset β, as we will show. However, as we can already see, the form of the EE (6.43) has the same leading order behaviour as the numerical fits obtained in [314, 315] for RE encapsulated by (6.33).

A general guiding principle that we will follow is the observation that $S_{AA'}$ is bounded from below [169] by

$$S_{AA'}(|\psi\rangle) \geq \frac{1}{2} I_{AB}(\rho_{AB}) \ , \tag{6.45}$$

regardless of the purification $|\psi\rangle$ and the long distance asymptotics, as proven in Eq. (6) of [159]. As a consequence, given the asymptotic behaviour of MI (6.31), the bound (6.45) implies that at long distances $S_{AA'}$ *cannot* have a leading behaviour which scales with a higher power than ϵ_Δ^2. This fact combined with the analysis of the eigenvalues μ_j of $\rho_{AA'}$ predicting that the highest power-law factor is exactly ϵ_Δ^2 implies that α_{tot} must be greater than 0. The consequence of this is that the asymptotic behaviour (6.45) necessarily applies to both EoP and RE for any CFT with an operator gap and with a lattice realization.

Furthermore, since $\alpha_{\text{tot}} > 0$ is defined by (6.42) this means that there must exist at least one $\alpha_{j>0} > 0$ which in turn implies that the term in (6.43) containing the offset β must generically appear in such an expression. We remark once again that this is consistent with the results reported in [314, 315] where such a term was also present in RE.

While this general argument only proves that α_{tot} must be greater than zero, we can nevertheless provide more details about the information of the purification $|\psi\rangle$ (6.35) which determines α_{tot}. Indeed, a straightforward way to compute α_{tot} is by calculating the trace of $\rho_{AA'}^2$ which is giving lo leading order by

$$\text{tr}_{AA'}(\rho_{AA'}^2) \simeq 1 - 2\alpha_{\text{tot}} \epsilon_\Delta^2 + \cdots \ . \tag{6.46}$$

Considering the general form of the purification (6.35) and defining

$$|\psi_{AA'}^{(i)}\rangle = \left(\hat{\mathbb{1}}_{AA'} \otimes \langle \psi_{BB'}^{(0)}|\right) |\psi^{(i)}\rangle \ , \tag{6.47a}$$

$$|\psi_{BB'}^{(i)}\rangle = \left(\langle \psi_{AA'}^{(0)}| \otimes \hat{\mathbb{1}}_{BB'}\right) |\psi^{(i)}\rangle \ , \tag{6.47b}$$

for $i \in \{0,1,2\}$, we find that the reduced density matrix $\rho_{AA'}$ is in general given by

$$\begin{aligned}\rho_{AA'} = |\psi^{(0)}_{AA'}\rangle\langle\psi^{(0)}_{AA'}| + \epsilon_\Delta \left(|\psi^{(0)}_{AA'}\rangle\langle\psi^{(1)}_{AA'}| + |\psi^{(1)}_{AA'}\rangle\langle\psi^{(0)}_{AA'}|\right) + \\ + \frac{1}{2}\epsilon^2_\Delta \left(|\psi^{(2)}_{AA'}\rangle\langle\psi^{(0)}_{AA'}| + 2\mathrm{tr}_{BB'}\left(|\psi^{(1)}\rangle\langle\psi^{(1)}|\right) + |\psi^{(0)}_{AA'}\rangle\langle\psi^{(2)}_{AA'}|\right) ,\end{aligned} \tag{6.48}$$

which allows us to directly compute $\mathrm{tr}(\rho^2_{AA'})$. By imposing the constraints (6.38) arising from the normalization conditions (6.37) we find that α_{tot} is given by

$$\alpha_{\mathrm{tot}} = \||\psi^{(1)}\rangle\|^2 + |\langle\psi^{(0)}|\psi^{(1)}\rangle|^2 - \||\psi^{(1)}_{AA'}\rangle\|^2 - \||\psi^{(1)}_{BB'}\rangle\|^2 . \tag{6.49}$$

As claimed in the paragraph below (6.34), from (6.49) we can see that indeed the term proportional to ϵ^2_Δ in ρ_{AB} given by (6.34) *does not* contribute to the leading coefficient α_{tot}. This insight has the potential to provide a way of fixing the the form of α_{tot} for EoP and RE in terms of CFT data in an akin manner as to how (6.31) provides it for the computation of MI.

While for RE obtaining α_{tot} involves a direct computation using the canonical purification of the reduced density matrix ρ_{AB}, for EoP it amounts to solving a minimization problem of the quadratic polynomial (6.49) obtained from the components of $|\psi^{(1)}\rangle$ and subject to the constraint (6.37a) and additional condition

$$\rho^{(1)}_{AB} = \mathrm{tr}_{A'B'}\left(|\psi^{(1)}\rangle\langle\psi^{(0)}| + |\psi^{(0)}\rangle\langle\psi^{(1)}|\right) , \tag{6.50}$$

generally leading to constraints on $|\psi^{(1)}\rangle$. We expect these expressions to have a well-defined minimum based on the arguments that we presented above. At the same time, it is important to note that while α_{tot} does not depend on ρ^2_{AB}, the individual $\alpha_{j>0}$ do, and as a consequence so does the offset β (6.44).

To provide a concrete realization of this analysis we will now consider on the critical Ising model and the closely related fermionic CFT, which have also been the focus of the previous chapter on CoP. We will show how we can obtain the numerical values of the leading coefficient α_{tot} and offset β for EoP and RE and in particular compare with the numerical results for RE appearing in [314, 315].

Consider the $(1+1)$-dimensional critical ($J = J_z = 1$) transverse Ising model on an infinite line with Hamiltonian (3.66) given in terms of generalized Pauli operators $\hat{S}^{x,z}_i$ (see (3.68))

$$\hat{H} = -\sum_{i=-\infty}^{\infty}\left(2\hat{S}^x_i\hat{S}^x_{i+1} + \hat{S}^z_i\right) , \tag{6.51}$$

which defines the $c = 1/2$ Ising CFT. In this case the non-degenerate ($\mathcal{N} = 1$) lightest operator of scaling dimension $\Delta = 1/8$ corresponds to the spin operator $\hat{S}^x_i$, often called the *spin field* and denoted simply by σ.

The Ising model can be mapped to a free fermion theory in terms of Majorana modes using the Jordan–Wigner transformation, as we did in Sec. 3.3.2. It is important to mention, however, that the set-up we are interested in, namely the reduced density

	Free Fermions			Ising Spins		
	α_{tot}	β	Eq.	α_{tot}	β	Eq.
MI	0	$\frac{\log\frac{\pi+2}{\pi-2}}{4\pi} \approx 0.120$	(A.9)	0	$C^2\left(\frac{4\pi^2}{\pi^2-4}+\frac{\pi}{2}\log\frac{4+4\pi+\pi^2}{4-4\pi+\pi^2}\right) \approx 0.298$	(A.31)
EoP	$\frac{1}{8+2\pi^2} \approx 0.036$	$\frac{\log 2e(8+2\pi^2)}{8+2\pi^2} \approx 0.181$	(A.17)	$\frac{4C^2\pi^4}{\pi^4-16} \approx 0.124$	0.440	(A.39)
RE	$\frac{1}{2\pi^2} \approx 0.051$	$\frac{1+\log(4\pi^2)}{2\pi^2} \approx 0.237$	(A.23)	$\frac{4C^2(\pi^2-2)}{\pi^2-4} \approx 0.139$	0.425	(A.44)

Table 6.1.: Summary of analytical and numerical results for the leading coefficient α_{tot} and the offset β obtained for MI, EoP and RE with asymptotic behaviour (6.43) both for Ising spins and free fermions for $w = \delta$. The offset β for EoP and RE of Ising spins were obtained with a numerical fit.

matrix of two disjoint intervals, is genuinely *non-Gaussian* in the spin picture [317–320, **CamH02**]. In the fermoinic case, for which the set-up has a Gaussian representation, there are two $\mathcal{N} = 2$ operators with lowest scaling dimension with $\Delta = 1/2$ which correspond to the fermionic (Majorana) field operators.

Just as described in Chapter 5, an important question in our analysis is to what extend the computations performed on a lattice describe continuum properties of the CFT. As argued many times throughout this thesis, this can generically be expected for large enough subsystem sizes w at fixed values of w/d. However, considering enlarged Hilbert spaces arising from the purifications of mixed states can also lead to computational challenges such as in the case of EoP which requires a minimization of $S_{AA'}$ via α_{tot} (6.49). Ultimately the question is what is the size of the subsystems that we need to consider in order to reach the continuum limit of our computations. In this regard, one key role is played by MI, for which we have a clear expectation encapsulated by (6.31). Our numerical computations show, see the top row of Fig. 6.3, that a close agreement with the CFT expectation can be achieved already for $w = 2\delta$, 3δ afterwards ($\mathcal{O}(10^4)$) value of d/w, and that in fact the smallest possible subsystem size, namely $w = \delta$ already provides a reasonable agreement with the expectation.

Given this fact, in the following subsections we will show the leading coefficient α_{tot} and offset β of MI, EoP and RE in the case where $w = \delta$ both for free fermions and Ising spins. These results are summarized in Table 6.1. The numerical results for the computations of EoP and RE for $w = 2\delta$, 3δ, as well as the analytical predictions for $w = \delta$ that we will discuss in the following subsections can be seen in the middle and bottom plots of Fig. 6.3. Said numerical results are based on the general form of reduced density matrix ρ_{AB} describing disjoint intervals in the both pictures. From these plots we can see a clear indication of the convergence of these quantities to their continuum values and furthermore a clear match with our proven formula for their asymptotic behaviour (6.43).

6.3.2. MI, EoP and RE for Free Fermions and Ising Spins for Single Site Intervals

In this section, we present the results of the analysis of the long-distance behaviour of MI, EoP and RE in the set-up consisting of a subsystem $A \cup B$ comprised of two

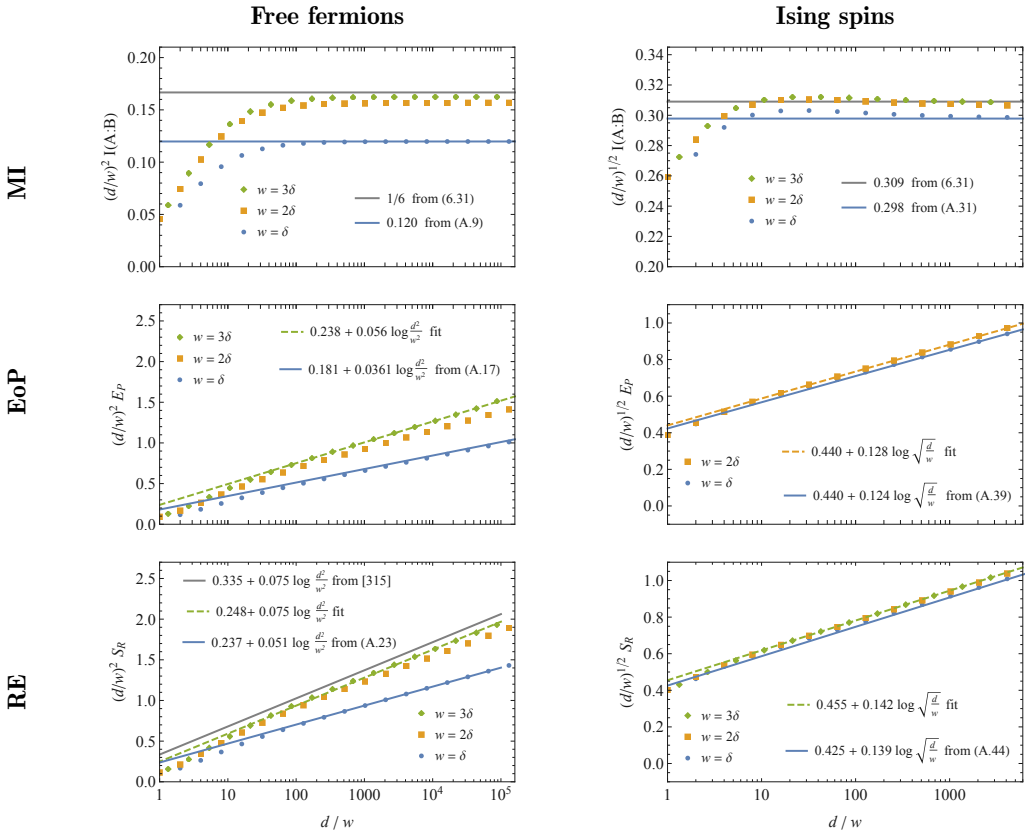

Figure 6.3.: Plots of the long-distance behaviour of mutual information, entanglement of purification and reflected entropy for free fermions and Ising spins, rescaled by the power-law contribution $\epsilon_\Delta^2 = (w/d)^{4\Delta}$ of the respective leading term with $\Delta = 1/2$ for free fermions and $\Delta = 1/8$ for Ising spins. The analytical computations for $w = \delta$ are discussed in the Appendix Sec. A.2 and Sec. A.1 (see also Table 6.1). The analytical comparisons are drawn as solid lines while the numerical fits of the data for EoP and RE at the largest available w appear as dashed ones. The top solid (grey) line in the plot for fermionic RE displayed above the numerical data corresponds to the result reported in [315].

single sites $w/\delta = 1$ separated by d/δ sites in the vacuum state of the critical Ising model (6.51). The details of these computations can be found in App. A.

The MI computed for free fermions and spins is given by

$$I(A:B) = \begin{cases} \frac{\log\left(\frac{\pi+2}{\pi-2}\right)}{4\pi} \cdot \epsilon_{1/2}^2 \approx 0.120 \left(\frac{w}{d}\right)^2 & \text{(fermions)} , \\ \left(\frac{4\pi^2}{\pi^2-4} + \frac{\pi}{2} \log\left(\frac{4+4\pi+\pi^2}{4-4\pi+\pi^2}\right)\right) C^2 \cdot \epsilon_{1/8}^2 \approx 0.298\sqrt{\frac{w}{d}} & \text{(spins)} , \end{cases} \tag{6.52}$$

which is in remarkable agreement with formula (6.31), as can be seen from the first row of Fig. 6.3 and of Table 6.1. This expression shows that the leading coefficient α_{tot} vanishes for MI, only leaving the offset β as expected.

The EoP computed for free fermions and Ising spins, on the other hand, is given by

$$E_P(A:B) = \begin{cases} \left(0.0361 \log\left(\frac{d}{w}\right)^2 + 0.181\right) \left(\frac{w}{d}\right)^2 & \text{(fermions)} , \\ \left(0.124 \log\sqrt{\frac{d}{w}} + 0.440\right) \sqrt{\frac{w}{d}} & \text{(spins)} , \end{cases} \tag{6.53}$$

where the leading coefficient is found to be non-zero thus showing that EoP presents a logarithmic enhancement to the power-law decay of MI. These results can be seen from the second row of Fig. 6.3 and of Table 6.1, together with the numerical results obtained for larger subsystem sizes. The analytical formulas leading to the numerical values of α_{tot} and β can be found in the appendix App. A.

Finally, the fermionic and Ising RE is given by

$$S_R(A:B) = \begin{cases} \left(0.051 \log\left(\frac{d}{w}\right)^2 + 0.237\right) \left(\frac{w}{d}\right)^2 & \text{(fermions)} , \\ \left(0.139 \log\sqrt{\frac{d}{w}} + 0.425\right) \sqrt{\frac{w}{d}} & \text{(spins)} . \end{cases} \tag{6.54}$$

where we also find a non-vanishing leading coefficient α_{tot}, providing a logarithmic enhancement of power-law decay of the long-distance behaviour of RE compared to MI. These results can be seen from the third row of Fig. 6.3 and of Table 6.1, together with the numerical results obtained for larger subsystem sizes as well as to the numerical results obtained in [315].

As a consequence, these results provide a concrete realization of the ideas presented in Sec. 6.3.1 corroborating our expectation (6.43) which we have shown to generically hold for CFTs with a lattice discretization and with a gap in the operator spectrum.

6.4. Discussion

In this Chapter we discussed entanglement of purification (EoP), reflected entropy (RE) and mutual information (MI) for vacuum subregions of free conformal field theories (CFT)s. We focused on subregions with associated bipartite Hilbert spaces in the vacuum of bosonic and fermionic theories and considered the cases where said subregions were adjacent to each other and also separated from each other. This allowed us to distinguish between scenarios where we could exploit the Gaussian

character of the mixed states which describe said subregions, and the scenarios where we needed to go beyond Gaussianity and consider a more general approach. For adjacent subregions, we used the most general Gaussian purifications to study the EoP for adjacent intervals in (1+1)-dimensional lattice models. In this case we found an agreement with the known bound relating EoP and MI, confirming earlier studies performed on subsystems with fewer degrees of freedom. For disjoint intervals, on the other hand, we considered the bosonic and fermionic cases separately as these have different properties at criticality.

In the bosonic case we studied both the small and large separation regimes for disjoint intervals in the vacuum of the massive Klein–Gordon model in $(1 + 1)$-dimensions using Gaussian techniques. The subtlety in this lattice realization of the decompactified free bosonic $c = 1$ CFT is the zero mode, an infrared divergence which affects primarily long-distance physics; *i.e.*, the latter regime. For small separations we found a remarkable agreement between our numerical studies and holographic predictions based on the path-integral optimization approach, where the zero-mode contribution could be isolated from the leading logarithmic divergence in the separation between the intervals. In this case we also found agreement between our numerical methods and known universal results for MI, which we used to benchmark our numerical analysis. For large separations we found a subtle sub-polynomial decay of EoP in the distance, a result which was accompanied by a similar analysis of the decay of MI where a sub-polynomial decay was also found, contradicting previous numerical studies showing a polynomial decay, but tending to the expected analytical results for free bosonic CFTs.

Motivated by the properties of the $c = 1/2$ Ising CFT, we demonstrated a general formula encapsulating the asymptotic behaviour of EoP and RE valid for largely-separated spherical subregions in the vacuum of a CFT in any dimension which has a gap in the operator spectrum. We showed that one can generically expect both quantities to exhibit an enhancement of the power-law decay present in MI by a logarithm of the separation between the spherical subregions. We then showed a concrete realization of this result in the context of the aforementioned $c = 1/2$ Ising CFT in the language of spins and fermions. While this enhancement was observed recently only for RE in $(1 + 1)$-dimensional free theories using Gaussian methods, we showed that EoP is also sensitive to this enhancement. In the spin picture, our results for EoP and RE provide new predictions while for free fermions, our RE result is in remarkable agreement with said earlier studies [314, 315]. Moreover, our general result can be used as a guiding principle to study the leading coefficient in terms of CFT data in an analogous way to the known formula for MI.

There are two main novelties in the study of EoP and RE presented in this Chapter. On one hand we used the most general Gaussian purifications to study the EoP of Gaussian mixed states. This allowed us to manage larger subsystem sizes than were previously considered when studying EoP which in turn enabled us to study its behaviour close to the continuum limit. We were able to surpass the known difficulties associated with the minimization procedure by exploiting the Gaussian properties of the mixed states associated with adjacent spatial intervals of free CFTs. While arising in the context of free theories, the Gaussian states that we studied allowed for a complete characterization of EoP for which we were also able to isolate

the zero-mode contribution in the cas of the CFT obtained from the massive Klein–Gordon model in $(1+1)$-dimensions.

The second novelty is related to the large-distance behaviour of EoP and RE for which we proved a general formula that holds in general for any CFTs in any dimension with a gapped operator spectrum and with a lattice realization. This result by itself opens up a new avenue to study the properties of these quantities from the perspective of CFT data beyond the sector of the stress-energy tensor. It is important to note that the proof of this general formula didn't rely on any particular aspects of the CFT, the dimension or even the free character of the theory, which signals both the generality and realm of applicability of our analysis.

A natural question is precisely in what way is the CFT data encoded in the leading coefficient α_{tot} for EoP and RE. We believe that it would be in general necessary to consider other models where these quantities can be studied, as this would provide a better indication on the relevant data entering α_{tot}. In order to do compute the long distance behaviour of EoP and RE for more complicated models, a possibility would be to consider tensor network techniques to compute the reduced density matrices of the largely-separated spatial subregions. Of course, operating on states beyond the Gaussian realm presents stark computational challenges associated with the size of the parameter space over which one would need to perform the computations and in particular the optimization procedure associated with EoP. Nevertheless, it may be possible to represent purifications of the form (6.35) using tensor networks and building upon earlier works such as [157, 321].

7. Summary and Outlook

In this thesis we explored various aspects of complexity and entanglement for pure and mixed states in quantum field theory (QFT) inspired by the AdS/CFT correspondence. We focused primarily on three aspects of these quantities: the time-dependence of complexity in the context of non-equilibrium quantum dynamics realised through a solvable quantum quench model studied in detail in Chapter 4, the universal quantum information-theoretic properties of Gaussian mixed states encapsulated by vacuum subregions of free CFTs and the long distance behaviour of correlations in general bipartite subregions in any CFT with a gap in the operator spectrum studied in Chapters 5 and 6.

Our study of non-equilibrium dynamics in Chap. 4 was based on a solvable quench model through a critical point applied to a $(1+1)$-dimensional Klein–Gordon theory and was based on [**CamH03**]. Here we found that the complexity of the time-dependent ground state exhibits universal scalings which are dependent on the rate of the quantum quench δt. In order to make our computations tractable, we considered a lattice discretization of the theory which led us to consider the behaviour of complexity in terms of the Fourier (momentum) mode decomposition of the ground state. Then, by using the L_2 norm of the circuit complexity constructed from unitary circuits built from gates belonging to a closed subalgebra of the 2-dimensional symplectic algebra $\mathfrak{sp}(2,\mathbb{R})$, we found that the full state complexity exhibits universal scalings as the theory goes through the critical point.

The Fuourier mode decomposition of the ground state allowed us to decompose the complexity of the full state in terms of the complexity of the individual momentum modes. We observed that both in the fast $\omega_0\delta t \ll 1$ and slow Kibble–Zurek (KZ) $\omega_0\delta t \gg 1$ regimes the zero-mode of the ground state dominates over higher momentum modes and thus determines the overall scaling behaviour of complexity. The zero mode was found to have a logarithmic scaling in the slow regime and a linear one in the fast. The finding in the slow regime is particularly interesting since it was also observed that entanglement entropy (EE) exhibits an equivalent scaling albeit with a different coefficient. In the case of a slow quantum quench, we showed that the higher momentum modes saturate, a feature which prevents the full complexity from exhibiting a clear scaling in this regime.

As we mentioned in Sec. 4.3, similar studies were carried out in the context of the relativistic fermionic Ising theory in [275]. In this case, a linear behaviour of complexity was also observed in the sudden quench regime $\omega_0\delta t \to 0$, as well as a saturation of the higher modes in the slow quench regime $\delta t < (\omega_0/4)\csc^2(k/2)$. The main difference in this case is that the zero-mode contribution to the complexity vanishes. This is because the Bogoliubov transformation of the zero-mode which is used to determine the contribution is trivial, which is in turn due to the fact that Majorana modes have independent zero-modes. Of course, in this case the zero-

mode simply refers to the momentum mode with $k = 0$, and does not have any associated IR divergence as in the bosonic case.

Another difference between the work [275] and our results from Chapter 4 is that the former evaluates complexity using the L_1 norm assuming that the shortest circuit minimizes an L_2 complexity. This is a commonly used technique to studying the former case since the minimization of F_1 cost functions are in general a challenging task. Regardless of this, the analysis of the universal scalings fermionic complexity presented in [275] presents strong similarities with the bosonic case. These works therefore provide strong evidence that complexity, much like correlation functions or EE, is a useful quantity to study universal scalings in quantum quenches that take a theory through criticality.

A natural question which stems from this analysis is whether complexity is sensitive to other kinds of phase transitions in quantum many-body systems out of equilibrium. An example of an interesting question would be whether complexity is sensitive to topological phase transitions. This has been studied recently in [322, 323] where it was found that complexity can be used used to detect equilibrium and dynamical topological phase transitions by the presence of non-analyticity. An outstanding question is then whether complexity can be used for defining topological order. Certain authors [324] claim that this is not the case, since complexity is an extensive quantity on the size of the system, and is thus inadequate for defining topological order. It would be interesting to understand to what complexity can play a role in the definition of topological order. A long-term goal would be to understand the role of complexity in more general models in condensed matter physics both in and out of equilibrium.

As we also mentioned previously, complexity has also entered the realm of cosmology through the study of primordial perturbations [276]. It has also been used to study chaotic quantum systems [325–331]. It will be interesting to study whether complexity can bring new insights in other areas of physics. Whether it be in other interesting quantum many-body models, or to offer a new perspective on phenomena seemingly unrelated to quantum information.

In the context of complexity of purification (CoP) discussed in Chapter 5 and based on [**CamH03**, **CamH02**] we showed that our results obtained from Gaussian mixed states corresponding to vacuum subregions of free CFTs (Sec. 5.2) are in remarkable agreement with holographic expectations (2.19). To be precise, we showed that the leading divergences of CoP obtained for a single and two adjacent intervals in the vacuum of Ising ($c = 1/2$) and bosonic ($c = 1$) CFTs match the divergences of the dual holographic computations carried out in AdS_3. In the case of subregions consisting of two compontents, as is the case for the adjacent intervals, we showed that mutual complexity is a appropriate quantity which disposes of the leading divergence both in the fermionic and bosonic case. We also showed how an effective method for computing the Gaussian CoP based on the steepest-descent method allows for an effective method which does not require any further assumptions and simplifications about the purifications of the mixed Gaussian states.

We also showed in the case of a two-harmonic oscillator system how the notions of pure state complexity, CoP and EE capture different information about the state

as encoded in its covariance matrix. The claim that complexity of the pure state is sensitive to more information about the state than EE is not surprising, however it remains to be determined what is the connection between complexity of subregions, as captured *e.g.*, by CoP, and EE. In order to determine this, it is likely that we would need to go beyond states which are Gaussian and hence completely characterised by their 2-point functions.

This naturally leads to the question whether one goes beyond Gaussian states in free theories and beyond scenarios in CFTs governed by the stress tensor sector. In the former case it would be interesting to study cases where the Gaussian Ansatz of the quantum state in consideration, whether it be pure or mixed, does not apply as this would be the case in interacting theories. In this regard there would be both conceptual and computational challenges that one would need to overcome.

One of the main challenges would be how to properly choose a universal gate set of unitaries with which one can construct the quantum circuit relating the (potentially) non-Gaussian reference and target states. For Hilbert spaces of a sufficiently small dimension this may not be too difficult and one can imagine having a universal gate set from which certain unitaries can be constructed. However the main difficulty would arise when asking about the *optimal* circuit which takes the reference state to the target state. Assuming that one would work using an F_2 cost function (3.8b) the challenge here would be how to find the geodesic distance. Computationally speaking, this is the biggest challenge that one needs to overcome in order to define a notion of circuit complexity for non-Gaussian states.

An approach which could be useful in this case can be drawn from the work [332], where authors quantify the non-Gaussian character of a (bosonic) quantum state by introducing a non-Gaussianity measure based on the Hilbert–Schmidt distance between the state under examination and a reference Gaussian state. It his worth noting that this definition applies to mixed states. This construction has been used to define a notion of non-Gaussianity in continuous-variable systems naturally appearing in quantum information [333].

In the context of complexity, these ideas could perhaps be applied to construct a notion of complexity for non-Gaussian states. A general strategy would be the following: We first choose pure non-Gaussian target state τ and a Gaussian reference state ρ. We then construct a mixed Gaussian "intermediate" state σ such that its 1- and 2-point functions match the ones for ρ. This is because a non-Gaussian pure state will always define a mixed Gaussian reference state. In other words, only a pure Gaussian state has 1- and 2-point functions of a pure Gaussian state, while non-Gaussian states have 1- and 2-point functions that can only be matched to a mixed Gaussian state. We then compute the Gaussian notion of complexity $\mathcal{C}^{\mathrm{G}}(\rho, \sigma)$ between ρ and σ using complexity of purification (5.4) or the Fisher–Rao distance function (5.45) as in [283]. We then construct the non-Gaussian complexity $\mathcal{C}^{\mathrm{nG}}(\sigma, \tau)$ by using the Hilbert–Schmidt distance between σ and τ. Having computed both complexities, we could need to compute the "total" complexity $\mathcal{C}^{\mathrm{tot}}$ using a weighted sum of the individual complexities.

Conceptually, we would be solving the problem of defining non-Gaussian complexity by incorporating the standard Gaussian methods and a simple non-Gaussian

method. This definition has furthermore have some desirable properties: If the non-Gaussian target state τ is taken to be close to a Gaussian state, the previous definition will reduce to the usual Gaussian definition. More importantly, this might be a computable notion of non-Gaussian complexity. This notion, however, should perhaps be interpreted as a first order non-Gaussian approximation of a potentially more complicated definition of non-Gaussian complexity.

An example of a scenario were we could apply this ideas could be the case of two spins located in two separated sites in the vacuum of the critical Ising model considered in Chapters 5 and 6 of this thesis. This set-up, as we thoroughly discussed in Sec. 6.3, is genuinely non-Gaussian and could potentially lead to a tractable implementation of these ideas. Essentially, the goal would be to arrive at a meaningful notion of complexity which we could use in interacting theories in order to bring the study of complexity in QFTs on similar footing to the status that EE has in the AdS/CFT correspondence: with well-defined computable notions on both sides of the holographic duality. Ultimately we would like to understand how exactly is the information about the interior of AdS black holes encoded in complexity.

Returning to the context of Gaussian states corresponding to vacuum subregions of free CFTs in $(1+1)$-dimensions, we performed analogous computations for entanglement of purification (EoP) based on [**CamH02**] where we were also able to find the leading divergent behaviour in agreement with holographic expectations obtained with the path-integral optimization method and with known bounds involving mutual information (MI) in for finite size Hilbert spaces in quantum information.

Of course, one can also wonder whether the computations that we have done for free theories have some counterpart in a genuine string theory dual, based on the AdS/CFT correspondence. This is because following the discussion in the Introduction 1, one can also wonder if by taking the opposite limit which leads to the strong/weak duality, *i.e.*, the limit of small λ (1.7), one could arrive at a complementary weak/strong duality. That is, a strongly-interacting quantum gravity theory is dual to a weakly-coupled CFT. On this regard there are proposals in the context of AdS4 holography [334], with a non-trivial test that triggered many developments in [335], and more recently in [336].

Insofar as the AdS/CFT correspondence provides a dynamical equivalence between these theories for any values of the parameters which defines them it is to be expected, at least in principle, that the free theory computations that we have discussed both in the context of quantum quenches and of vacuum subregions of free CFTs have a counterpart at the level of the strongly-interacting string theory. This of course, is an exceptionally difficult statement to prove, as string duals are notoriously hard to work with.

Finally, in our study of the long-distance behaviour of EoP and reflected entropy (RE) presented in Sec. 6.3 and based on [**CamH01**] we proved a general formula which applies to any CFT with a gap in the operator spectrum and for any dimensions. The main assumption in this case being that the reduced density matrix defining the set-up of two spherical subregions of diameter w largely separated from each other $(d/w \gg 1)$ has a formal expansion in terms of the parameter $\epsilon_\Delta = (w/d)^{2\Delta}$ around the infinite separation limit, where we expect the state to be described by a product

state. Following these assumptions and assuming that the CFTs in question have a gap in the operator spectrum and a realization as lattice models, we prove that EoP and RE have a logarithmic enhancement with respect to the known power-law decay of MI. This result opens the avenue for studying these quantities in a set-up within CFTs which is beyond the stress-energy tensor.

Understanding the way that the CFT data is encoded in these quantities can bridge the gap between our understanding of their conjectured realizations in the AdS/CFT correspondence via the entanglement wedge cross-section, and their behaviour in CFTs. Given the relevance that the entanglement wedge has in the reconstruction of bulk regions associated with spatial boundary subregions, it is therefore necessary to have a better understanding of these quantities from this perspective and our results set the stage for this enterprise.

In conclusion, the results that we discussed in this thesis set the stage for a better understanding of complexity and entanglement in QFTs. This is paramount for elucidating the mechanism which connects gravity and quantum theories within the AdS/CFT correspondence. As a consequence, we believe that these can lead to a better understanding of quantum gravity and quite possible to new tools in the study of quantum many-body systems.

A. Appendices

A. Long-Distance Behaviour of MI, EoP and RE

In this appendix we review the details of the computations of MI, EoP and RE in the set-up consisting of a subsystem comprised of two single sites $w/\delta = 1$ in the vacuum state of the critical Ising model as discussed in Chap 6, Sec. 6.3.

A.1. Free Fermions

The starting point of our analysis of MI, EoP and RE is the set-up shown in Fig. A.1.

The first step for computing the MI involves the computation of the covariance matrix and reduced density matrix corresponding to the subsystem consisting of $1+1$ sites separated by $d/w = d/\delta$ sites from the fermionic perspective, *i.e.*, using the Majorana modes γ_i (3.75). In this case $\Delta = 1/2$, $\epsilon_\Delta = (w/d)^{2\Delta}$ corresponds simply to $\epsilon_{1/2} = w/d$. The fermionic covariance matrix is fully determined by restricting the general expression of the infinite-size covariance matrix (3.86) to the aforementioned number of sites and is given by

$$\Omega_{AB}^{\text{ferm}} = \begin{pmatrix} & -\frac{2}{\pi} & & -\frac{2}{(2d/w+3)\pi} \\ \frac{2}{\pi} & & -\frac{2}{(2d/w+3)\pi} & \\ & \frac{2}{(2d/w+3)\pi} & & -\frac{2}{\pi} \\ \frac{2}{(2d/w+3)\pi} & & \frac{2}{\pi} & 0 \end{pmatrix} . \tag{A.1}$$

Note that the anti-diagonal terms in (A.1) can be rewritten in terms of $\epsilon_{1/2}$ as $2\epsilon_{1/2}/(2\pi + 3\pi\epsilon_{1/2})$. The reduced density matrix ρ_{AB} associated to this mixed state with asymptotic behaviour (6.34) given by

$$\rho_{AB}^{\text{ferm}} \simeq \rho_A^{(0)} \otimes \rho_B^{(0)} + \epsilon_{1/2}\rho_{AB}^{(1)} + \dots , \tag{A.2}$$

can be computed explicitly with respect to the basis of $\mathcal{H}_{AB}$ given by $\{|\downarrow\downarrow\rangle, |\uparrow\downarrow\rangle, |\downarrow\uparrow\rangle, |\uparrow\uparrow\rangle\}$ and is given by

$$\rho_{AB}^{\text{ferm}} \simeq \begin{pmatrix} D & & & \frac{1}{2\pi}\epsilon_{1/2} \\ & E & & \\ & & E & \\ \frac{1}{2\pi}\epsilon_{1/2} & & & F \end{pmatrix} , \tag{A.3}$$

where

$$D = \frac{1}{4} + \frac{1}{\pi} + \frac{1}{\pi^2} , \; E = \frac{1}{4} - \frac{1}{\pi^2} , \; F = \frac{1}{4} - \frac{1}{\pi} + \frac{1}{\pi^2} . \tag{A.4}$$

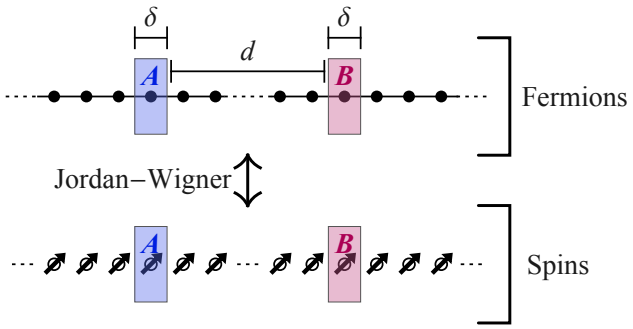

Figure A.1.: Visualization of the Jordan–Wigner transform in a one-dimensional lattice with subsystems consisting of two disjoint lattice sites, taken from [CamH01]. Subsystem setup in the fermionic picture (top) and spin picture (bottom). The subsystem $A \cup B$ consists of two single sites A and B, $w_A/\delta = 1 = w_B/\delta$ separated by d/δ sites.

In other words, the basis states of $\mathcal{H}_{AB}$ are given by $|i\,j\rangle = |i\rangle_A \otimes |j\rangle_B$ for $i, j \in \{0, 1\}$ with $\uparrow = 1$ and $\downarrow = 0$. By further restricting the reduced density matrix (A.3) to a single site, the fermionic covariance matrix and reduced density matrix become

$$\Omega_A^{\text{ferm}} = \begin{pmatrix} & -\frac{2}{\pi} \\ \frac{2}{\pi} & \end{pmatrix} , \quad \rho_A^{\text{ferm}} = \begin{pmatrix} \frac{1}{2} - \frac{1}{\pi} & \\ & \frac{1}{2} + \frac{1}{\pi} \end{pmatrix} , \tag{A.5}$$

where ρ_A^{ferm} is written with respect to the basis $\{|\downarrow\rangle, |\uparrow\rangle\}$.

We now compute the von Neumann entropies of the subsystems $A, B, A \cup B$. These EE can be directly computed from the symplectic eigenvalues of the fermionic covariance matrices of each individual site (A.5) and of both sites (A.1). Recall that in general the von Neumann entropy of a Gaussian mixed state ρ with covariance matrix Ω can be computed via

$$S(\rho) = -\sum_i \left(\frac{1+\lambda_i}{2} \log\left(\frac{1+\lambda_i}{2}\right) + \frac{1-\lambda_i}{2} \log\left(\frac{1-\lambda_i}{2}\right) \right) , \tag{A.6}$$

where $\pm \mathrm{i}\lambda$ are the purely-imaginary eigenvalues of Ω. Applying this formula directly to the covariance matrices (A.5) and (A.1) leads to

$$S_A = -\frac{\pi+2}{2\pi} \log\left(\frac{\pi+2}{2\pi}\right) - \frac{\pi-2}{2\pi} \log\left(\frac{\pi-2}{2\pi}\right) \approx 0.476 , \tag{A.7a}$$

$$S_{AB}^{\text{ferm}} = -\sum_{k=1}^{2} \left(\frac{1+\lambda_k}{2} \log\left(\frac{1+\lambda_k}{2}\right) + \frac{1-\lambda_k}{2} \log\left(\frac{1-\lambda_k}{2}\right) \right) , \tag{A.7b}$$

where the eigenvalues λ_k of $\Omega_{AB}^{\text{ferm}}$ are

$$\lambda_\pm = \frac{1}{\pi} \left(2 \pm \frac{3}{4} \epsilon_{1/2}^2 + \dots \right) . \tag{A.8}$$

Note that the expression for the entanglement entropy of the individual sites (A.7a) applies to the spin case, since the EE of connected regions are invariant under a

Jordan–Wigner transformation. This implies a similar expansion for S_{AB} (A.7b) which leads to a behaviour of the MI for $w = \delta$ given by

$$I^{\text{ferm}}(A:B) \simeq \frac{\log\left(\frac{\pi+2}{\pi-2}\right)}{4\pi}\epsilon_{1/2}^2 + \cdots \simeq 0.120\left(\frac{w}{d}\right)^2 , \tag{A.9}$$

which reproduces the correct power law of fermionic MI in the continuum limit, but with a smaller coefficient than the continuum value (6.31). Note that this result also matches the long distance expansion of results known for Dirac fermions [337]

$$I^{\text{Dirac}}(A:B) = \frac{c}{3}\log\left(\frac{(d+w)^2}{d(2w+d)}\right) = \frac{1}{6}\epsilon_{1/2}^2 = \frac{1}{6}\left(\frac{w}{d}\right)^2 , \tag{A.10}$$

computed for two intervals of equal and arbitrary size w.

We use a similar perturbative expansion of the fermionic covariance matrix for two disjoint intervals akin to (A.2) in terms of $\epsilon_{1/2}$ in order to compute the fermionic EoP. For subsystems comprised of a single lattice site, the large separation expansion $w = \delta \ll d$ of a purification of $\Omega_{AB}^{\text{ferm}}$ (A.1) is

$$\Omega \simeq \Omega^{(0)} + \epsilon_{1/2}\Omega^{(1)} + \frac{1}{2}\epsilon_{1/2}^2\Omega^{(2)} + \dots , \tag{A.11}$$

obtained in the limit $\epsilon_{1/2} \to 0$ and where

$$\Omega^{(0)} = \left(\begin{array}{cccc|cccc} & -G & & & & L & & \\ G & & & & L & & & \\ & & -G & & & & L & \\ & & & G & & & & L \\ \hline & -L & & & & -G & & \\ -L & & & & G & & & \\ & & -L & & & & -G & \\ & & & -L & & & G & \end{array}\right) , \tag{A.12}$$

is the purification of Ω_{AB} in the infinite separation limit $d/\delta \to \infty$ in the Hilbert space $\mathcal{H}_{AB} \otimes \mathcal{H}_{A'B'}$ with $G = 2/\pi$ and $L = \sqrt{1-G^2}$.

By further imposing the constraint that Ω represents a pure sate $\Omega^2 = -\mathbb{1}$ together with constraints for $\Omega_{AB}^{(1)}$ and $\Omega_{AB}^{(2)}$ arising from (6.38), one can find $\Omega^{(0)}$ and $\Omega^{(1)}$ in an iterative manner, first by solving $\Omega^{(1)}$ in terms of $\Omega^{(0)}$ and then $\Omega^{(2)}$ in terms of $\Omega^{(0)}$ and $\Omega^{(1)}$.

In order to determine the asymptotic behaviour of the symplectic eigenvalues λ_i of $\Omega_{AA'}$, we use the strategy mentioned in Sec. 6.3.1 which relies on computing $\text{tr}(\Omega_{AA'}^2)$. In this case we have $\text{tr}(\Omega_{AA'}^2) = -2(\lambda_1^2 + \lambda_2^2)$ and $\text{tr}(\Omega_{AA'}^4) = 2(\lambda_1^4 + \lambda_2^4)$, which allows us to obtain the asymptotic behaviour of the eigenvalues λ_i given in the limit $\epsilon_{1/2} \to 0$ by

$$\lambda_1 = \lambda_2 \sim 1 - \alpha_{\text{tot}}\,\epsilon_{1/2}^2 , \tag{A.13}$$

where α_{tot} depends on parameters found in $\Omega^{(1)}$ and $\Omega^{(2)}$. With this computation we directly find

$$\begin{aligned}\alpha_{\text{tot}} = \frac{x_{14}a_{23} - x_{13}x_{24} + \pi^{-2}}{2} + \frac{G(x_{14} - x_{23})\pi^{-1}}{2L} \\ + \frac{(x_{14} - x_{23})^2 + (x_{13} + x_{24})^2}{4L^2} \,,\end{aligned} \tag{A.14}$$

where the parameters x_{ij} correspond to the unconstrained entries in the term $\Omega^{(1)}$ appearing in the expansion (A.11). In order to find the EoP, given by the the minimum of $S_{AA'}$, we need to minimize α_{tot} over the x_{ij}. Given that (A.14) is quadratic in x_{ij}, its minimum value can be computed analytically leading to

$$\alpha_{\text{tot}} = \frac{1}{8 + 2\pi^2} \approx 0.03605\,. \tag{A.15}$$

Similarly to MI, we can expand $S_{AA'} \sim \sum_i (\log 2 - \frac{\lambda_i}{2})$ via the eigenvalues λ_i up to second order in $\epsilon_{1/2}$. In this way, we find both α_{tot} the offset β analytically leading to

$$S_{AA'} \simeq \epsilon_{1/2}^2 \left(\alpha_{\text{tot}} \log(\epsilon_{1/2}^{-2}) + \alpha_{\text{tot}} \log \frac{2e}{\alpha_{\text{tot}}} \right) \,. \tag{A.16}$$

Combining this expression with (A.15) yields the asymptotic behaviour of fermionic EoP given by

$$\begin{aligned}E_P^{\text{ferm}}(A:B) &\simeq \left(\frac{1}{8 + 2\pi^2} \log(\epsilon_{\frac{1}{2}}^{-2}) + \frac{\log 2e(8 + 2\pi^2)}{8 + 2\pi^2} \right) \epsilon_{\frac{1}{2}}^2 \\ &\simeq \left(0.0361 \log \left(\frac{d}{w} \right)^2 + 0.181 \right) \left(\frac{w}{d} \right)^2 \,,\end{aligned} \tag{A.17}$$

which agrees with the expected behaviour (6.43).

On the other hand, in order to compute the fermionic RE, we need to construct the canonical purification of (A.3) via

$$|\sqrt{\rho_{AB}}\rangle = \sum_i \sqrt{e_i}\, |e_i\rangle \otimes |e_i\rangle = |\psi^{(0)}\rangle + \epsilon_{1/2}\, |\psi^{(1)}\rangle + \dots \,, \tag{A.18}$$

where $\rho_{AB}\, |e_i\rangle = e_i\, |e_i\rangle$. Note that we can construct the canonical purification $|\sqrt{\rho_{AB}}\rangle$ exactly for the given form of the initial reduced density matrix ρ_{AB} and hence we do not need to phrase our computation of RE in terms of covariance matrices as in the case of MI and EoP.

The term $|\psi^{(1)}\rangle$ can be computed directly using (A.18), leading to

$$|\psi^{(1)}\rangle = \tfrac{1}{2\pi}(|\phi_4\rangle + |\phi_{13}\rangle)\,, \tag{A.19}$$

with the states $|\phi_i\rangle$ forming the basis of $\mathcal{H}_{ABA'B'}$ ordered as $\{|\downarrow\downarrow\downarrow\downarrow\rangle\,, |\uparrow\downarrow\downarrow\downarrow\rangle\,, |\downarrow\uparrow\downarrow\downarrow\rangle\,, |\uparrow\uparrow\downarrow\downarrow\rangle\,, \dots, |\uparrow\uparrow\uparrow\uparrow\rangle\}$. From the density matrix of the canonical purification $\rho := |\sqrt{\rho_{AB}}\rangle\, \langle\sqrt{\rho_{AB}}|$ we restrict ourselves to the subsystems AA' given by the reduced

density matrix $\rho_{AA'} = \mathrm{tr}_{BB'}(\rho)$ and which has the asymptotic behaviour $\rho_{AA'} = \rho_A^{(0)} \otimes \rho_{A'}^{(0)} + \epsilon_{1/2}^2 \rho_{AA'}^{(2)}/2$ explicitly given by

$$\rho_{AA'} \simeq \rho_{AA'}^{(0)} + \frac{1}{2}\epsilon_{1/2}^2 \rho_{AA'}^{(2)} = \begin{pmatrix} \tilde{G}_1 & & & \tilde{H} \\ & \tilde{J} & & \\ & & \tilde{J} & \\ \tilde{H} & & & \tilde{G}_1 - \frac{2}{\pi} \end{pmatrix} , \tag{A.20}$$

where

$$\tilde{G}_1 = \frac{\pi+2}{2\pi} - \frac{\epsilon_{1/2}^2}{4\pi^2} , \quad \tilde{H} = \frac{\sqrt{\pi^2-4}}{2\pi} - \frac{\sqrt{\pi^2-4}\epsilon_{1/2}^2}{4\pi(\pi^2-4)} , \quad \tilde{J} = \frac{\epsilon_{1/2}^2}{4\pi^2} . \tag{A.21}$$

We follow the same strategy as for EoP and compute the trace of the square of (A.20) from which we obtain

$$\alpha_{\mathrm{tot}} = \frac{1}{2\pi^2} \approx 0.051 . \tag{A.22}$$

This shows that the fermionic RE, $S_R(\rho_{AB}) = S_{AA'}(\rho)$, exhibits the following asymptotic behaviour

$$\begin{aligned} S_R^{\mathrm{ferm}}(A:B) &\simeq \left(\frac{1}{2\pi^2} \log \epsilon_{1/2}^{-2} + \frac{1+\log(4\pi^2)}{2\pi^2} \right) \epsilon_{1/2}^2 \\ &= \left(0.051 \log \left(\frac{d}{w} \right)^2 + 0.237 \right) \left(\frac{w}{d} \right)^2 , \end{aligned} \tag{A.23}$$

where the offset β in (A.23) was computed from the eigenvalues of (A.20) according to (6.44).

A.2. Ising Spins

The reduced density matrix of the Ising vacuum subregion of two disjoint sites written in terms of spin operators $\rho_{AB}^{\mathrm{spin}}$ is genuinely non-Gaussian. However, following [319] we can still use Gaussian techniques to deduce its asymptotic behaviour in the limit $d/w \to \infty$, or equivalently $\epsilon_{1/8} \to 0$. In this case, the reduced density matrix in the spin picture written with respect to the basis $\{|\uparrow\uparrow\rangle, |\downarrow\uparrow\rangle, |\uparrow\downarrow\rangle, |\downarrow\downarrow\rangle\}$ consistent with an asymptotic behaviour

$$\rho_{AB}^{\mathrm{spin}} \simeq \rho_A^{(0)} \otimes \rho_B^{(0)} + \epsilon_{1/8} \rho_{AB}^{(1)} + \dots , \tag{A.24}$$

is given by

$$\rho_{AB}^{\mathrm{spin}} \simeq \begin{pmatrix} D & & & C \cdot \epsilon_{1/8} \\ & E & C \cdot \epsilon_{1/8} & \\ & C \cdot \epsilon_{1/8} & E & \\ C \cdot \epsilon_{1/8} & & & F \end{pmatrix} \tag{A.25}$$

with D, E, F given by (A.4). As mentioned previously, in this case the lowest lying operator corresponds to the spin field σ with scaling dimension $\Delta = 1/8$ and as such

we have $\epsilon_\Delta = (w/d)^{2\Delta}$ is given by $\epsilon_{1/8} = (w/d)^{1/4}$. The constant C is associated with the expectation value of a non-local fermionic operator computed from

$$C = \lim_{n\to\infty} \left(\frac{2}{\pi}\right)^n \frac{n^{1/4}}{4} \det(M^n) \ , \tag{A.26}$$

where M^n is an $n \times n$ matrix defined via

$$(M^n)_{jk} = \begin{cases} \frac{(-1)^{k-j}}{2(k-j)+1} & j \leq k \ , \\ \frac{(-1)^{j-k+1}}{2(j-k)-1} & j > k \ , \end{cases} \tag{A.27}$$

from which we obtain

$$C = \frac{e^{(3\zeta'(-1))}}{2^{23/12}} \approx 0.1612 \ , \tag{A.28}$$

with $\zeta'(s)$ the derivative of the Riemann zeta function [338]. The anti-diagonal terms $C\,\epsilon_{1/8}$ in (A.25) encode long distance correlations between $\hat{S}_i^x$ at the two sites.

In order to compute the EE we and consequently the spin MI we compute the eigenvalues of the reduced density matrix (A.25), which are given by

$$\mu_{1,2} \simeq \frac{1}{4} - \frac{1}{\pi} \pm C \cdot \epsilon_{1/8} + \dots \ , \tag{A.29a}$$

$$\mu_{3,4} \simeq \frac{1}{4} - \frac{1}{\pi} \pm \sqrt{\frac{1}{\pi^2} + C^2 \cdot \epsilon_{1/8}^2} + \dots \ , \tag{A.29b}$$

from which we can directly compute the EE via

$$S_{AB}^{\text{spin}} = -\sum_{j=1}^{4} \mu_j \log(\mu_j) \ , \tag{A.30}$$

which leads to the following behaviour of the spin MI

$$\begin{aligned} I^{\text{spin}}(A:B) &\simeq \left(\frac{4\pi^2}{\pi^2-4} + \frac{\pi}{2}\log\left(\frac{4+4\pi+\pi^2}{4-4\pi+\pi^2}\right)\right) C^2 \cdot \epsilon_{1/8}^2 + \dots \\ &\approx 0.298\sqrt{\frac{w}{d}} \ , \end{aligned} \tag{A.31}$$

and which matches the power-law behaviour of the analytical CFT formula (6.31), and whose coefficient is off by 3.6% with respect to the continuum value ≈ 0.309. Recall that (A.7a) is also the EE of the individual sites in the spin picture and hence we used this expression to compute (A.31).

In order to compute spin EoP (6.4), we purify the mixed state (A.25). In the infinite separation limit between the two single sites, a minimal purification $|\psi^{(0)}\rangle$ of ρ_{AB} is given by

$$|\psi^{(0)}\rangle = \sqrt{D}\,|\downarrow\downarrow\downarrow\downarrow\rangle + \sqrt{E}\,(|\uparrow\downarrow\uparrow\downarrow\rangle + |\downarrow\uparrow\downarrow\uparrow\rangle) + \sqrt{F}\,|\uparrow\uparrow\uparrow\uparrow\rangle \ , \tag{A.32}$$

where here D, E, F are also given by (A.4). Just as we have done before, we supplement this minimal purification with corrections up to second order in $\epsilon_{1/8}$ such that the full purification has the asymptotic expression

$$|\psi\rangle \simeq |\psi^{(0)}\rangle + \epsilon_{1/8}\,|\psi^{(1)}\rangle + \frac{1}{2}\epsilon_{1/8}^2\,|\psi^{(2)}\rangle \ , \tag{A.33}$$

where we impose the normalization constraint $\langle\psi|\psi\rangle = 1$ order by order in $\epsilon_{1/8}$. The idea is then to optimize over $|\psi^{(1)}\rangle$ and $|\psi^{(2)}\rangle$ subject to this constraint as well to the requirement that the reduced density matrices $\rho^{(1)} := |\psi^{(0)}\rangle\langle\psi^{(1)}| + |\psi^{(1)}\rangle\langle\psi^{(0)}|$ and $\rho^{(2)} := |\psi^{(0)}\rangle\langle\psi^{(2)}| + |\psi^{(2)}\rangle\langle\psi^{(0)}| + 2|\psi^{(1)}\rangle\langle\psi^{(1)}|$ satisfy the constraints

$$\rho^{(1)}_{AB} = \begin{pmatrix} 0 & 0 & 0 & C \\ 0 & 0 & C & 0 \\ 0 & C & 0 & 0 \\ C & 0 & 0 & 0 \end{pmatrix} \ , \ \rho^{(2)}_{AB} = 0 \ , \tag{A.34}$$

which are a consequence of the form of (A.25). The normalization constraint on $|\psi\rangle$ as well as (A.34) allows us to eliminate free parameters in $|\psi^{(1)}\rangle$ and $|\psi^{(2)}\rangle$.

At the same time, in order to compute $S_{AA'} = \mathrm{tr}_{AA'}(\rho_{AA'}\log(\rho_{AA'}))$, the quantity that we need to optimize over in order to find the EoP (6.4), we need to find the four eigenvalues of the reduced density matrix

$$\rho_{AA'} \simeq \rho^{(0)}_{AA'} + \epsilon_{1/8}\rho^{(1)}_{AA'} + \frac{1}{2}\epsilon^2_{1/8}\rho^{(2)}_{AA'} \ , \tag{A.35}$$

with leading order behaviour

$$\mu_0 \simeq 1 - \alpha_{\mathrm{tot}}\epsilon^2_{1/8} \ , \ \mu_{j>0} \simeq \alpha_j\epsilon^2_{1/8} \ . \tag{A.36}$$

Expanding the first order correction $|\psi^{(1)}\rangle$ in terms of basis elements $|\phi_i\rangle$ of $\mathcal{H} = \mathcal{H}_{AB}\otimes\mathcal{H}_{A'B'}$ as $|\psi^{(1)}\rangle = \sum_i y_i|\phi_i\rangle$, we can find a formula for α_{tot} of the form

$$\frac{\alpha_{\mathrm{tot}}}{C^2} = F(y_i) \ , \tag{A.37}$$

where $F(y_i)$ is a function of the parameters y_i, which can be determined exactly, and which arises from the expansion of $\mathrm{tr}_{AA'}(\rho^2_{AA'}) = \sum_j \mu_j^2 \simeq 1 - 2\alpha_{\mathrm{tot}}\epsilon^2_{1/8}$.

The minimization of $S_{AA'}$ for parameters λ_i used to find the smallest α_{tot} can be done analytically leading to

$$\alpha_{\mathrm{tot}} = \frac{4\pi^4C^2}{\pi^4 - 16} \approx 0.12445 \ , \tag{A.38}$$

which shows that the resulting EoP resulting from (6.43) behaves as

$$\begin{aligned} E_P^{\mathrm{spin}}(A:B) &\simeq \left(\frac{4\pi^4C^2}{\pi^4-16}\log(\epsilon^{-2}_{1/8}) + \beta\right)\epsilon^2_{\frac{1}{8}} \\ &= \left(0.124\log\sqrt{\frac{d}{w}} + 0.440\right)\sqrt{\frac{w}{d}} \ , \end{aligned} \tag{A.39}$$

where we determined the offset β numerically.

Finally, we describe the computation of spin RE. Our starting point here is once again the reduced density matrix for a spin system of $1+1$ sites in the large d limit (A.25). Similarly to the fermionic case, we construct the canonical purification

of (A.25) via $|\sqrt{\rho_{AB}}\rangle = \sum_i \sqrt{e_i}\,|e_i\rangle \otimes |e_i\rangle = |\psi^{(0)}\rangle + \epsilon_{1/8}\,|\psi^{(1)}\rangle$ for $\rho_{AB}\,|e_i\rangle = e_i\,|e_i\rangle$. The first order perturbation $|\psi^{(1)}\rangle$ is found to be

$$|\psi^{(1)}\rangle = \tfrac{\pi}{\sqrt{\pi^2-4}}(|\phi_7\rangle + |\phi_{10}\rangle) + |\phi_4\rangle + |\phi_{13}\rangle \ , \tag{A.40}$$

where the states $|\phi_i\rangle$ are the same for the fermionic case. From the canonical purification's density matrix $\rho := |\sqrt{\rho_{AB}}\rangle\,\langle\sqrt{\rho_{AB}}|$ we consider a restriction to AA' given by the reduced density matrix $\rho_{AA'} = \mathrm{tr}_{BB'}(\rho)$ which has the asymptotic behaviour $\rho_{AA'} = \mathrm{tr}_{BB'}(|\psi^{(0)}\rangle\,\langle\psi^{(0)}|) + \epsilon_{1/8}^2(2\mathrm{tr}_{BB'}(|\psi^{(1)}\rangle\,\langle\psi^{(1)}|))/2$ given by

$$\rho_{AA'} \simeq \rho^{(0)}_{AA'} + \tfrac{1}{2}\epsilon^2_{1/8}\rho^{(2)}_{AA'} = \begin{pmatrix} \tilde{A}_1 & & & \tilde{F} \\ & \tilde{B} & \tilde{E} & \\ & \tilde{E} & \tilde{B} & \\ \tilde{F} & & & \tilde{A}_1 - \frac{2}{\pi} \end{pmatrix} , \tag{A.41}$$

where

$$\begin{aligned} \tilde{A}_1 &= \frac{\pi+2}{2\pi} - \frac{2(\pi^2-2)C^2\epsilon^2_{1/8}}{\pi^2-4} \ , \ \tilde{B} = \frac{2(\pi^2-2)C^2\epsilon^2_{1/8}}{(\pi^2-4)} \ , \\ \tilde{E} &= \frac{2\pi C^2\epsilon^2_{1/8}}{\sqrt{\pi^2-4}} \ , \ \tilde{F} = \frac{\sqrt{\pi^2-4}}{2\pi} - \frac{2\pi(\pi^2-2)C^2\epsilon^2_{1/8}}{(\pi^2-4)^{3/2}} \ , \end{aligned} \tag{A.42}$$

where the constant C is the same as in (A.28). By computing the trace of the the square of (A.41) we find a value of α_{tot} given by

$$\alpha_{\mathrm{tot}} = \frac{4C^2(\pi^2-2)}{\pi^2-4} \approx 0.139 \ , \tag{A.43}$$

leading to a reflected entropy S_R of the Ising subsystem for $w = \delta$ of

$$\begin{aligned} S_R^{\mathrm{spin}}(A:B) &\simeq \left(\frac{4C^2\pi^4}{\pi^4-16}\log\epsilon^{-2}_{1/8} + \mathrm{const}\right)\epsilon^2_{1/8} \\ &= \left(0.139\log\sqrt{\frac{d}{w}} + 0.425\right)\sqrt{\frac{w}{d}} \ , \end{aligned} \tag{A.44}$$

where the offset β was determined numerically.

Bibliography

[1] G. Aad *et al.*, "Observation of a new particle in the search for the Standard Model Higgs boson with the ATLAS detector at the LHC," *Phys. Lett. B*, vol. 716, pp. 1–29, 2012.

[2] S. Chatrchyan *et al.*, "Observation of a New Boson at a Mass of 125 GeV with the CMS Experiment at the LHC," *Phys. Lett. B*, vol. 716, pp. 30–61, 2012.

[3] F. Englert and R. Brout, "Broken Symmetry and the Mass of Gauge Vector Mesons," *Phys. Rev. Lett.*, vol. 13, pp. 321–323, 1964.

[4] P. W. Higgs, "Broken symmetries, massless particles and gauge fields," *Phys. Lett.*, vol. 12, pp. 132–133, 1964.

[5] B. P. Abbott *et al.*, "Observation of Gravitational Waves from a Binary Black Hole Merger," *Phys. Rev. Lett.*, vol. 116, no. 6, p. 061102, 2016.

[6] B. P. Abbott *et al.*, "Astrophysical Implications of the Binary Black-Hole Merger GW150914," *Astrophys. J. Lett.*, vol. 818, no. 2, p. L22, 2016.

[7] A. Einstein, "Über gravitationswellen," *Sitzungsberichte der Königlich Preußischen Akademie der Wissenschaften (Berlin)*, pp. 154–167, 1918.

[8] K. Akiyama *et al.*, "First M87 Event Horizon Telescope Results. I. The Shadow of the Supermassive Black Hole," *Astrophys. J. Lett.*, vol. 875, p. L1, 2019.

[9] M. Srednicki, *Quantum field theory*. Cambridge University Press, 1 2007.

[10] M. D. Schwartz, *Quantum Field Theory and the Standard Model*. Cambridge University Press, 3 2014.

[11] S. W. Hawking and G. F. R. Ellis, *The Large Scale Structure of Space-Time*. Cambridge Monographs on Mathematical Physics, Cambridge University Press, 2 2011.

[12] C. W. Misner, K. S. Thorne, and J. A. Wheeler, *Gravitation*. San Francisco: W. H. Freeman, 1973.

[13] R. M. Wald, *General Relativity*. Chicago, USA: Chicago Univ. Pr., 1984.

[14] J. D. Bekenstein, "Black holes and the second law," *Lett. Nuovo Cim.*, vol. 4, pp. 737–740, 1972.

[15] J. M. Bardeen, B. Carter, and S. W. Hawking, "The Four laws of black hole mechanics," *Commun. Math. Phys.*, vol. 31, pp. 161–170, 1973.

[16] S. W. Hawking, "Black hole explosions?," *Nature*, vol. 248, pp. 30–31, 1974.

[17] S. W. Hawking, "Particle Creation by Black Holes," *Commun. Math. Phys.*, vol. 43, pp. 199–220, 1975. [Erratum: Commun.Math.Phys. 46, 206 (1976)].

[18] G. Penington, "Entanglement Wedge Reconstruction and the Information Paradox," *JHEP*, vol. 09, p. 002, 2020.

[19] A. Almheiri, N. Engelhardt, D. Marolf, and H. Maxfield, "The entropy of bulk quantum fields and the entanglement wedge of an evaporating black hole," *JHEP*, vol. 12, p. 063, 2019.

[20] D. N. Page, "Information in black hole radiation," *Phys. Rev. Lett.*, vol. 71, pp. 3743–3746, 1993.

[21] D. N. Page, "Time Dependence of Hawking Radiation Entropy," *JCAP*, vol. 09, p. 028, 2013.

[22] A. Almheiri, T. Hartman, J. Maldacena, E. Shaghoulian, and A. Tajdini, "The entropy of Hawking radiation," *arXiv:2006.06872 [hep-th]*, 6 2020.

[23] N. D. Birrell and P. C. W. Davies, *Quantum Fields in Curved Space*. Cambridge Monographs on Mathematical Physics, Cambridge, UK: Cambridge Univ. Press, 2 1984.

[24] R. M. Wald, *Quantum Field Theory in Curved Space-Time and Black Hole Thermodynamics*. Chicago Lectures in Physics, Chicago, IL: University of Chicago Press, 1995.

[25] A. Almheiri, D. Marolf, J. Polchinski, and J. Sully, "Black Holes: Complementarity or Firewalls?," *JHEP*, vol. 02, p. 062, 2013.

[26] A. Y. Kitaev, A. H. Shen, and M. N. Vyalyi, *Classical and Quantum Computation*. Graduate Studies in Mathematics, American Mathematical Society, 2006.

[27] I. Bengtsson and K. Zyczkowski, *Geometry of Quantum States: An Introduction to Quantum Entanglement*. Cambridge University Press, 2006.

[28] M. A. Nielsen and I. L. Chuang, *Quantum Computation and Quantum Information: 10th Anniversary Edition*. Cambridge University Press, 2010.

[29] O. Aharony, S. S. Gubser, J. M. Maldacena, H. Ooguri, and Y. Oz, "Large N field theories, string theory and gravity," *Phys. Rept.*, vol. 323, pp. 183–386, 2000.

[30] J. McGreevy, "Holographic duality with a view toward many-body physics," *Adv. High Energy Phys.*, vol. 2010, p. 723105, 2010.

[31] M. Ammon and J. Erdmenger, *Gauge/gravity duality: Foundations and applications*. Cambridge: Cambridge University Press, 4 2015.

[32] D. Lust and S. Theisen, *Lectures on string theory*, vol. 346 of *Lecture Notes in Physics*. Springer-Verlag Berlin Heidelberg, 1989.

[33] J. Polchinski, *String theory. Vol. 1: An introduction to the bosonic string*. Cambridge Monographs on Mathematical Physics, Cambridge University Press, 12 2007.

[34] J. Polchinski, *String theory. Vol. 2: Superstring theory and beyond*. Cambridge Monographs on Mathematical Physics, Cambridge University Press, 12 2007.

[35] M. B. Green, J. H. Schwarz, and E. Witten, *Superstring Theory Vol. 1: 25th Anniversary Edition*. Cambridge Monographs on Mathematical Physics, Cambridge University Press, 11 2012.

[36] M. B. Green, J. H. Schwarz, and E. Witten, *Superstring Theory Vol. 2: 25th Anniversary Edition*. Cambridge Monographs on Mathematical Physics, Cambridge University Press, 11 2012.

[37] R. Blumenhagen, D. Lüst, and S. Theisen, *Basic concepts of string theory*. Theoretical and Mathematical Physics, Heidelberg, Germany: Springer, 2013.

[38] J. M. Maldacena, "The Large N limit of superconformal field theories and supergravity," *Int. J. Theor. Phys.*, vol. 38, pp. 1113–1133, 1999.

[39] G. 't Hooft, "Dimensional reduction in quantum gravity," *Conf. Proc. C*, vol. 930308, pp. 284–296, 1993.

[40] L. Susskind, "The World as a hologram," *J. Math. Phys.*, vol. 36, pp. 6377–6396, 1995.

[41] R. Bousso, "The Holographic principle," *Rev. Mod. Phys.*, vol. 74, pp. 825–874, 2002.

[42] J. D. Bekenstein, "Black holes and entropy," *Phys. Rev. D*, vol. 7, pp. 2333–2346, 1973.

[43] J. D. Bekenstein, "Generalized second law of thermodynamics in black hole physics," *Phys. Rev. D*, vol. 9, pp. 3292–3300, 1974.

[44] J. D. Bekenstein, "A Universal Upper Bound on the Entropy to Energy Ratio for Bounded Systems," *Phys. Rev. D*, vol. 23, p. 287, 1981.

[45] H. Casini, "Relative entropy and the Bekenstein bound," *Class. Quant. Grav.*, vol. 25, p. 205021, 2008.

[46] R. Bousso, "A Covariant entropy conjecture," *JHEP*, vol. 07, p. 004, 1999.

[47] G. 't Hooft, "A Planar Diagram Theory for Strong Interactions," *Nucl. Phys. B*, vol. 72, p. 461, 1974.

[48] G. Policastro, D. T. Son, and A. O. Starinets, "The Shear viscosity of strongly coupled N=4 supersymmetric Yang-Mills plasma," *Phys. Rev. Lett.*, vol. 87, p. 081601, 2001.

[49] P. Kovtun, D. T. Son, and A. O. Starinets, "Viscosity in strongly interacting quantum field theories from black hole physics," *Phys. Rev. Lett.*, vol. 94, p. 111601, 2005.

[50] J. D. Brown and M. Henneaux, "Central Charges in the Canonical Realization of Asymptotic Symmetries: An Example from Three-Dimensional Gravity," *Commun. Math. Phys.*, vol. 104, pp. 207–226, 1986.

[51] S. S. Gubser, I. R. Klebanov, and A. M. Polyakov, "Gauge theory correlators from noncritical string theory," *Phys. Lett. B*, vol. 428, pp. 105–114, 1998.

[52] E. Witten, "Anti-de Sitter space and holography," *Adv. Theor. Math. Phys.*, vol. 2, pp. 253–291, 1998.

[53] T. De Jonckheere, "Modave lectures on bulk reconstruction in AdS/CFT," *PoS*, vol. Modave2017, p. 005, 2018.

[54] D. Harlow, "TASI Lectures on the Emergence of Bulk Physics in AdS/CFT," *PoS*, vol. TASI2017, p. 002, 2018.

[55] N. Beisert *et al.*, "Review of AdS/CFT Integrability: An Overview," *Lett. Math. Phys.*, vol. 99, pp. 3–32, 2012.

[56] D. Serban, "Integrability and the AdS/CFT correspondence," *J. Phys. A*, vol. 44, p. 124001, 2011.

[57] A. Sfondrini, "Towards integrability for $\mathrm{AdS}_{\mathbf{3}}/\mathrm{CFT}_{\mathbf{2}}$," *J. Phys. A*, vol. 48, no. 2, p. 023001, 2015.

[58] S. A. Hartnoll, "Lectures on holographic methods for condensed matter physics," *Class. Quant. Grav.*, vol. 26, p. 224002, 2009.

[59] J. Zaanen, Y.-W. Sun, Y. Liu, and K. Schalm, *Holographic Duality in Condensed Matter Physics*. Cambridge Univ. Press, 2015.

[60] S. A. Hartnoll, A. Lucas, and S. Sachdev, *Holographic quantum matter*. The MIT Press, 12 2016.

[61] J. Casalderrey-Solana, H. Liu, D. Mateos, K. Rajagopal, and U. A. Wiedemann, *Gauge/String Duality, Hot QCD and Heavy Ion Collisions*. Cambridge University Press, 2014.

[62] N. Brambilla *et al.*, "QCD and Strongly Coupled Gauge Theories: Challenges and Perspectives," *Eur. Phys. J. C*, vol. 74, no. 10, p. 2981, 2014.

[63] M. Baggioli, *Applied Holography: A Practical Mini-Course*. SpringerBriefs in Physics, Springer, 2019.

[64] S. J. Devitt, W. J. Munro, and K. Nemoto, "Quantum error correction for beginners," *Reports on Progress in Physics*, vol. 76, p. 076001, Jun 2013.

[65] B. M. Terhal, "Quantum error correction for quantum memories," *Reviews of Modern Physics*, vol. 87, p. 307–346, Apr 2015.

[66] R. Orús, "Tensor networks for complex quantum systems," *APS Physics*, vol. 1, pp. 538–550, 2019.

[67] A. Jahn and J. Eisert, "Holographic tensor network models and quantum error correction: A topical review," *arXiv:2102.02619 [quant-ph]*, 2 2021.

[68] R. Penrose, "Applications of negative dimensional tensors," in *Combinatorial mathematics and its applications* (D. J. A. Welsh, ed.), Proceedings of a Conference held at the Mathematical Institute, Oxford, from 7-10 July, (London-New York), Academic Press, 1971.

[69] R. Penrose, "Angular momentum: an approach to combinatorial space-time," in *Quantum Theory and Beyond* (T. Bastin, ed.), (Cambridge), pp. 151–180, Cambridge University Press, 1971.

[70] C. Rovelli and L. Smolin, "Spin networks and quantum gravity," *Phys. Rev. D*, vol. 52, pp. 5743–5759, 1995.

[71] C. Rovelli, "Loop quantum gravity," *Living Rev. Rel.*, vol. 1, p. 1, 1998.

[72] S. R. White, "Density matrix formulation for quantum renormalization groups," *Phys. Rev. Lett.*, vol. 69, pp. 2863–2866, 1992.

[73] S. R. White, "Density-matrix algorithms for quantum renormalization groups," *Phys. Rev. B*, vol. 48, pp. 10345–10356, 1993.

[74] S. Östlund and S. Rommer, "Thermodynamic limit of density matrix renormalization," *Physical Review Letters*, vol. 75, p. 3537–3540, Nov 1995.

[75] J. Dukelsky, M. A. Martín-Delgado, T. Nishino, and G. Sierra, "Equivalence of the variational matrix product method and the density matrix renormalization group applied to spin chains," *Europhysics Letters (EPL)*, vol. 43, p. 457–462, Aug 1998.

[76] M. B. Hastings, "An area law for one-dimensional quantum systems," *J. Stat. Mech.*, vol. 0708, p. P08024, 2007.

[77] F. Verstraete and J. I. Cirac, "Matrix product states represent ground states faithfully," *Physical Review B*, vol. 73, Mar 2006.

[78] D. Perez-Garcia, F. Verstraete, M. M. Wolf, and J. I. Cirac, "Matrix Product State Representations," *arXiv e-prints*, pp. quant–ph/0608197, Aug. 2006.

[79] A. Weichselbaum, F. Verstraete, U. Schollwöck, J. I. Cirac, and J. von Delft, "Variational matrix-product-state approach to quantum impurity models," *Physical Review B*, vol. 80, Oct 2009.

[80] M. B. Hastings and T. Koma, "Spectral gap and exponential decay of correlations," *Commun. Math. Phys.*, vol. 265, pp. 781–804, 2006.

[81] M. Cramer, J. Eisert, M. B. Plenio, and J. Dreissig, "An Entanglement-area law for general bosonic harmonic lattice systems," *Phys. Rev. A*, vol. 73, p. 012309, 2006.

[82] M. Srednicki, "Chaos and quantum thermalization," *Physical Review E*, vol. 50, p. 888–901, Aug 1994.

[83] J. Eisert, M. Cramer, and M. B. Plenio, "Area laws for the entanglement entropy - a review," *Rev. Mod. Phys.*, vol. 82, pp. 277–306, 2010.

[84] J. L. Cardy and I. Peschel, "Finite Size Dependence of the Free Energy in Two-dimensional Critical Systems," *Nucl. Phys. B*, vol. 300, pp. 377–392, 1988.

[85] C. Holzhey, F. Larsen, and F. Wilczek, "Geometric and renormalized entropy in conformal field theory," *Nucl. Phys. B*, vol. 424, pp. 443–467, 1994.

[86] P. Calabrese and J. L. Cardy, "Entanglement entropy and quantum field theory," *J. Stat. Mech.*, vol. 0406, p. P06002, 2004.

[87] G. Vidal, "Entanglement Renormalization," *Phys. Rev. Lett.*, vol. 99, no. 22, p. 220405, 2007.

[88] G. Vidal, "Class of Quantum Many-Body States That Can Be Efficiently Simulated," *Phys. Rev. Lett.*, vol. 101, p. 110501, 2008.

[89] B. Swingle, "Entanglement Renormalization and Holography," *Phys. Rev. D*, vol. 86, p. 065007, 2012.

[90] N. Bao, C. Cao, S. M. Carroll, A. Chatwin-Davies, N. Hunter-Jones, J. Pollack, and G. N. Remmen, "Consistency conditions for an AdS multiscale entanglement renormalization ansatz correspondence," *Phys. Rev. D*, vol. 91, no. 12, p. 125036, 2015.

[91] A. Milsted and G. Vidal, "Geometric interpretation of the multi-scale entanglement renormalization ansatz," *arXiv:1812.00529 [hep-th]*, 2018.

[92] C. Beny, "Causal structure of the entanglement renormalization ansatz," *New J. Phys.*, vol. 15, p. 023020, 2013.

[93] B. Czech, L. Lamprou, S. McCandlish, and J. Sully, "Tensor Networks from Kinematic Space," *JHEP*, vol. 07, p. 100, 2016.

[94] F. Pastawski, B. Yoshida, D. Harlow, and J. Preskill, "Holographic quantum error-correcting codes: Toy models for the bulk/boundary correspondence," *JHEP*, vol. 06, p. 149, 2015.

[95] J. Haegeman, T. J. Osborne, H. Verschelde, and F. Verstraete, "Entanglement Renormalization for Quantum Fields in Real Space," *Phys. Rev. Lett.*, vol. 110, no. 10, p. 100402, 2013.

[96] F. Verstraete and J. I. Cirac, "Continuous Matrix Product States for Quantum Fields," *Phys. Rev. Lett.*, vol. 104, p. 190405, 2010.

[97] M. Nozaki, S. Ryu, and T. Takayanagi, "Holographic Geometry of Entanglement Renormalization in Quantum Field Theories," *JHEP*, vol. 10, p. 193, 2012.

[98] A. Mollabashi, M. Nozaki, S. Ryu, and T. Takayanagi, "Holographic Geometry of cMERA for Quantum Quenches and Finite Temperature," *JHEP*, vol. 03, p. 098, 2014.

[99] J. S. Cotler, M. Reza Mohammadi Mozaffar, A. Mollabashi, and A. Naseh, "Entanglement renormalization for weakly interacting fields," *Phys. Rev. D*, vol. 99, no. 8, p. 085005, 2019.

[100] J. Cotler, M. R. Mohammadi Mozaffar, A. Mollabashi, and A. Naseh, "Renormalization Group Circuits for Weakly Interacting Continuum Field Theories," *Fortsch. Phys.*, vol. 67, no. 10, p. 1900038, 2019.

[101] S. Chapman, M. P. Heller, H. Marrochio, and F. Pastawski, "Toward a Definition of Complexity for Quantum Field Theory States," *Phys. Rev. Lett.*, vol. 120, no. 12, p. 121602, 2018.

[102] R. Jefferson and R. C. Myers, "Circuit complexity in quantum field theory," *JHEP*, vol. 10, p. 107, 2017.

[103] P. Caputa, N. Kundu, M. Miyaji, T. Takayanagi, and K. Watanabe, "Anti-de Sitter Space from Optimization of Path Integrals in Conformal Field Theories," *Phys. Rev. Lett.*, vol. 119, no. 7, p. 071602, 2017.

[104] P. Caputa, N. Kundu, M. Miyaji, T. Takayanagi, and K. Watanabe, "Liouville Action as Path-Integral Complexity: From Continuous Tensor Networks to AdS/CFT," *JHEP*, vol. 11, p. 097, 2017.

[105] N. Bao, G. Penington, J. Sorce, and A. C. Wall, "Beyond Toy Models: Distilling Tensor Networks in Full AdS/CFT," *JHEP*, vol. 11, p. 069, 2019.

[106] N. Bao, G. Penington, J. Sorce, and A. C. Wall, "Holographic Tensor Networks in Full AdS/CFT," *arXiv:1902.10157 [hep-th]*, 2 2019.

[107] P. Caputa, J. Kruthoff, and O. Parrikar, "Building Tensor Networks for Holographic States," *JHEP*, vol. 05, p. 009, 2021.

[108] G. 't Hooft, "On the Quantum Structure of a Black Hole," *Nucl. Phys. B*, vol. 256, pp. 727–745, 1985.

[109] L. Bombelli, R. K. Koul, J. Lee, and R. D. Sorkin, "A Quantum Source of Entropy for Black Holes," *Phys. Rev. D*, vol. 34, pp. 373–383, 1986.

[110] L. Susskind, "Some speculations about black hole entropy in string theory," in *The Black Hole, 25 Years After* (C. Teitelboim and J. Zanelli, eds.), pp. 118–131, World Scientific, 10 1993.

[111] M. Srednicki, "Entropy and area," *Phys. Rev. Lett.*, vol. 71, pp. 666–669, 1993.

[112] C. G. Callan, Jr. and F. Wilczek, "On geometric entropy," *Phys. Lett. B*, vol. 333, pp. 55–61, 1994.

[113] P. Calabrese and J. L. Cardy, "Evolution of entanglement entropy in one-dimensional systems," *J. Stat. Mech.*, vol. 0504, p. P04010, 2005.

[114] M. B. Hastings, "Solving gapped hamiltonians locally," *Physical Review B*, vol. 73, Feb 2006.

[115] A. Kitaev and J. Preskill, "Topological entanglement entropy," *Phys. Rev. Lett.*, vol. 96, p. 110404, 2006.

[116] M. Levin and X.-G. Wen, "Detecting topological order in a ground state wave function," *Physical Review Letters*, vol. 96, Mar 2006.

[117] H. Li and F. D. M. Haldane, "Entanglement spectrum as a generalization of entanglement entropy: Identification of topological order in non-abelian fractional quantum hall effect states," *Physical Review Letters*, vol. 101, Jul 2008.

[118] S. Ryu and T. Takayanagi, "Holographic derivation of entanglement entropy from AdS/CFT," *Phys. Rev. Lett.*, vol. 96, p. 181602, 2006.

[119] S. Ryu and T. Takayanagi, "Aspects of Holographic Entanglement Entropy," *JHEP*, vol. 08, p. 045, 2006.

[120] M. Headrick and T. Takayanagi, "A Holographic proof of the strong subadditivity of entanglement entropy," *Phys. Rev. D*, vol. 76, p. 106013, 2007.

[121] M. Headrick, "General properties of holographic entanglement entropy," *JHEP*, vol. 03, p. 085, 2014.

[122] P. Hayden, M. Headrick, and A. Maloney, "Holographic Mutual Information is Monogamous," *Phys. Rev. D*, vol. 87, no. 4, p. 046003, 2013.

[123] V. E. Hubeny, M. Rangamani, and T. Takayanagi, "A Covariant holographic entanglement entropy proposal," *JHEP*, vol. 07, p. 062, 2007.

[124] A. C. Wall, "Maximin Surfaces, and the Strong Subadditivity of the Covariant Holographic Entanglement Entropy," *Class. Quant. Grav.*, vol. 31, no. 22, p. 225007, 2014.

[125] T. Faulkner, "The Entanglement Renyi Entropies of Disjoint Intervals in AdS/CFT," *arXiv:1303.7221 [hep-th]*, 3 2013.

[126] T. Hartman, "Entanglement Entropy at Large Central Charge," *arXiv:1303.6955 [hep-th]*, 3 2013.

[127] A. Lewkowycz and J. Maldacena, "Generalized gravitational entropy," *JHEP*, vol. 08, p. 090, 2013.

[128] X. Dong, A. Lewkowycz, and M. Rangamani, "Deriving covariant holographic entanglement," *JHEP*, vol. 11, p. 028, 2016.

[129] J. S. Schwinger, "Brownian motion of a quantum oscillator," *J. Math. Phys.*, vol. 2, pp. 407–432, 1961.

[130] L. V. Keldysh, "Diagram technique for nonequilibrium processes," *Zh. Eksp. Teor. Fiz.*, vol. 47, pp. 1515–1527, 1964.

[131] C. P. Herzog and D. T. Son, "Schwinger-Keldysh propagators from AdS/CFT correspondence," *JHEP*, vol. 03, p. 046, 2003.

[132] H. Casini, M. Huerta, and R. C. Myers, "Towards a derivation of holographic entanglement entropy," *JHEP*, vol. 05, p. 036, 2011.

[133] X. Dong, "Holographic Entanglement Entropy for General Higher Derivative Gravity," *JHEP*, vol. 01, p. 044, 2014.

[134] J. de Boer, M. Kulaxizi, and A. Parnachev, "Holographic Entanglement Entropy in Lovelock Gravities," *JHEP*, vol. 07, p. 109, 2011.

[135] L.-Y. Hung, R. C. Myers, and M. Smolkin, "On Holographic Entanglement Entropy and Higher Curvature Gravity," *JHEP*, vol. 04, p. 025, 2011.

[136] J. de Boer and J. I. Jottar, "Entanglement Entropy and Higher Spin Holography in AdS_3," *JHEP*, vol. 04, p. 089, 2014.

[137] M. Ammon, A. Castro, and N. Iqbal, "Wilson Lines and Entanglement Entropy in Higher Spin Gravity," *JHEP*, vol. 10, p. 110, 2013.

[138] T. Faulkner, A. Lewkowycz, and J. Maldacena, "Quantum corrections to holographic entanglement entropy," *JHEP*, vol. 11, p. 074, 2013.

[139] N. Engelhardt and A. C. Wall, "Quantum Extremal Surfaces: Holographic Entanglement Entropy beyond the Classical Regime," *JHEP*, vol. 01, p. 073, 2015.

[140] A. Almheiri, R. Mahajan, J. Maldacena, and Y. Zhao, "The Page curve of Hawking radiation from semiclassical geometry," *JHEP*, vol. 03, p. 149, 2020.

[141] M. Van Raamsdonk, "Building up spacetime with quantum entanglement," *Gen. Rel. Grav.*, vol. 42, pp. 2323–2329, 2010.

[142] J. M. Maldacena, "Eternal black holes in anti-de Sitter," *JHEP*, vol. 04, p. 021, 2003.

[143] M. Headrick, "Entanglement Renyi entropies in holographic theories," *Phys. Rev. D*, vol. 82, p. 126010, 2010.

[144] J. Molina-Vilaplana, "An Operator Product Expansion for the Mutual Information in AdS/CFT," *Nucl. Phys. B*, vol. 888, pp. 1–16, 2014.

[145] M. M. Wolf, F. Verstraete, M. B. Hastings, and J. I. Cirac, "Area Laws in Quantum Systems: Mutual Information and Correlations," *Phys. Rev. Lett.*, vol. 100, no. 7, p. 070502, 2008.

[146] J. Maldacena and L. Susskind, "Cool horizons for entangled black holes," *Fortsch. Phys.*, vol. 61, pp. 781–811, 2013.

[147] B. Czech, J. L. Karczmarek, F. Nogueira, and M. Van Raamsdonk, "Rindler Quantum Gravity," *Class. Quant. Grav.*, vol. 29, p. 235025, 2012.

[148] B. Czech, J. L. Karczmarek, F. Nogueira, and M. Van Raamsdonk, "The Gravity Dual of a Density Matrix," *Class. Quant. Grav.*, vol. 29, p. 155009, 2012.

[149] M. Headrick, V. E. Hubeny, A. Lawrence, and M. Rangamani, "Causality & holographic entanglement entropy," *JHEP*, vol. 12, p. 162, 2014.

[150] X. Dong, D. Harlow, and A. C. Wall, "Reconstruction of Bulk Operators within the Entanglement Wedge in Gauge-Gravity Duality," *Phys. Rev. Lett.*, vol. 117, no. 2, p. 021601, 2016.

[151] A. Hamilton, D. N. Kabat, G. Lifschytz, and D. A. Lowe, "Holographic representation of local bulk operators," *Phys. Rev. D*, vol. 74, p. 066009, 2006.

[152] D. L. Jafferis, A. Lewkowycz, J. Maldacena, and S. J. Suh, "Relative entropy equals bulk relative entropy," *JHEP*, vol. 06, p. 004, 2016.

[153] V. E. Hubeny and M. Rangamani, "Causal Holographic Information," *JHEP*, vol. 06, p. 114, 2012.

[154] A. Almheiri, X. Dong, and D. Harlow, "Bulk Locality and Quantum Error Correction in AdS/CFT," *JHEP*, vol. 04, p. 163, 2015.

[155] M. Freedman and M. Headrick, "Bit threads and holographic entanglement," *Commun. Math. Phys.*, vol. 352, no. 1, pp. 407–438, 2017.

[156] T. Takayanagi and K. Umemoto, "Entanglement of purification through holographic duality," *Nature Phys.*, vol. 14, no. 6, pp. 573–577, 2018.

[157] P. Nguyen, T. Devakul, M. G. Halbasch, M. P. Zaletel, and B. Swingle, "Entanglement of purification: from spin chains to holography," *JHEP*, vol. 01, p. 098, 2018.

[158] B. M. Terhal, M. Horodecki, D. W. Leung, and D. P. DiVincenzo, "The entanglement of purification," *Journal of Mathematical Physics*, vol. 43, p. 4286–4298, Sep 2002.

[159] S. Bagchi and A. K. Pati, "Monogamy, polygamy, and other properties of entanglement of purification," *Physical Review A*, vol. 91, Apr 2015.

[160] P. Caputa, M. Miyaji, T. Takayanagi, and K. Umemoto, "Holographic Entanglement of Purification from Conformal Field Theories," *Phys. Rev. Lett.*, vol. 122, no. 11, p. 111601, 2019.

[161] N. Bao and I. F. Halpern, "Holographic Inequalities and Entanglement of Purification," *JHEP*, vol. 03, p. 006, 2018.

[162] H. Hirai, K. Tamaoka, and T. Yokoya, "Towards Entanglement of Purification for Conformal Field Theories," *PTEP*, vol. 2018, no. 6, p. 063B03, 2018.

[163] R. Espíndola, A. Guijosa, and J. F. Pedraza, "Entanglement Wedge Reconstruction and Entanglement of Purification," *Eur. Phys. J. C*, vol. 78, no. 8, p. 646, 2018.

[164] K. Umemoto and Y. Zhou, "Entanglement of Purification for Multipartite States and its Holographic Dual," *JHEP*, vol. 10, p. 152, 2018.

[165] R.-Q. Yang, C.-Y. Zhang, and W.-M. Li, "Holographic entanglement of purification for thermofield double states and thermal quench," *JHEP*, vol. 01, p. 114, 2019.

[166] N. Bao, A. Chatwin-Davies, and G. N. Remmen, "Entanglement of Purification and Multiboundary Wormhole Geometries," *JHEP*, vol. 02, p. 110, 2019.

[167] N. Bao, A. Chatwin-Davies, J. Pollack, and G. N. Remmen, "Towards a Bit Threads Derivation of Holographic Entanglement of Purification," *JHEP*, vol. 07, p. 152, 2019.

[168] W.-Z. Guo, "Entanglement of purification and projection operator in conformal field theories," *Phys. Lett. B*, vol. 797, p. 134934, 2019.

[169] S. Dutta and T. Faulkner, "A canonical purification for the entanglement wedge cross-section," *JHEP*, vol. 03, p. 178, 2021.

[170] L. Susskind, "Computational Complexity and Black Hole Horizons," *Fortsch. Phys.*, vol. 64, pp. 24–43, 2016. [Addendum: Fortsch.Phys. 64, 44–48 (2016)].

[171] L. Susskind, "Entanglement is not enough," *Fortsch. Phys.*, vol. 64, pp. 49–71, 2016.

[172] L. Susskind, "ER=EPR, GHZ, and the consistency of quantum measurements," *Fortsch. Phys.*, vol. 64, pp. 72–83, 2016.

[173] D. Stanford and L. Susskind, "Complexity and Shock Wave Geometries," *Phys. Rev. D*, vol. 90, no. 12, p. 126007, 2014.

[174] A. R. Brown and L. Susskind, "Second law of quantum complexity," *Phys. Rev. D*, vol. 97, no. 8, p. 086015, 2018.

[175] P. Bocchieri and A. Loinger, "Quantum recurrence theorem," *Phys. Rev.*, vol. 107, pp. 337–338, Jul 1957.

[176] J. Haferkamp, P. Faist, N. B. T. Kothakonda, J. Eisert, and N. Y. Halpern, "Linear growth of quantum circuit complexity," *arXiv:2106.05305 [quant-ph]*, 6 2021.

[177] J. Couch, S. Eccles, T. Jacobson, and P. Nguyen, "Holographic Complexity and Volume," *JHEP*, vol. 11, p. 044, 2018.

[178] A. R. Brown, D. A. Roberts, L. Susskind, B. Swingle, and Y. Zhao, "Holographic Complexity Equals Bulk Action?," *Phys. Rev. Lett.*, vol. 116, no. 19, p. 191301, 2016.

[179] A. R. Brown, D. A. Roberts, L. Susskind, B. Swingle, and Y. Zhao, "Complexity, action, and black holes," *Phys. Rev. D*, vol. 93, no. 8, p. 086006, 2016.

[180] S. Lloyd, "Ultimate physical limits to computation," *Nature*, vol. 406, p. 1047–1054, Aug 2000.

[181] S. Chapman, H. Marrochio, and R. C. Myers, "Complexity of Formation in Holography," *JHEP*, vol. 01, p. 062, 2017.

[182] L. Lehner, R. C. Myers, E. Poisson, and R. D. Sorkin, "Gravitational action with null boundaries," *Phys. Rev. D*, vol. 94, no. 8, p. 084046, 2016.

[183] A. Reynolds and S. F. Ross, "Divergences in Holographic Complexity," *Class. Quant. Grav.*, vol. 34, no. 10, p. 105004, 2017.

[184] G. Hayward, "Gravitational action for space-times with nonsmooth boundaries," *Phys. Rev. D*, vol. 47, pp. 3275–3280, 1993.

[185] D. Brill and G. Hayward, "Is the gravitational action additive?," *Phys. Rev. D*, vol. 50, pp. 4914–4919, 1994.

[186] J. Couch, W. Fischler, and P. H. Nguyen, "Noether charge, black hole volume, and complexity," *JHEP*, vol. 03, p. 119, 2017.

[187] B. Swingle and Y. Wang, "Holographic Complexity of Einstein-Maxwell-Dilaton Gravity," *JHEP*, vol. 09, p. 106, 2018.

[188] D. Carmi, S. Chapman, H. Marrochio, R. C. Myers, and S. Sugishita, "On the Time Dependence of Holographic Complexity," *JHEP*, vol. 11, p. 188, 2017.

[189] S. Chapman, H. Marrochio, and R. C. Myers, "Holographic complexity in Vaidya spacetimes. Part I," *JHEP*, vol. 06, p. 046, 2018.

[190] K. Goto, H. Marrochio, R. C. Myers, L. Queimada, and B. Yoshida, "Holographic Complexity Equals Which Action?," *JHEP*, vol. 02, p. 160, 2019.

[191] S. Chapman, H. Marrochio, and R. C. Myers, "Holographic complexity in Vaidya spacetimes. Part II," *JHEP*, vol. 06, p. 114, 2018.

[192] A. R. Brown, H. Gharibyan, H. W. Lin, L. Susskind, L. Thorlacius, and Y. Zhao, "Complexity of Jackiw-Teitelboim gravity," *Phys. Rev. D*, vol. 99, no. 4, p. 046016, 2019.

[193] M. Alishahiha, "Holographic Complexity," *Phys. Rev. D*, vol. 92, no. 12, p. 126009, 2015.

[194] D. Carmi, R. C. Myers, and P. Rath, "Comments on Holographic Complexity," *JHEP*, vol. 03, p. 118, 2017.

[195] O. Ben-Ami and D. Carmi, "On Volumes of Subregions in Holography and Complexity," *JHEP*, vol. 11, p. 129, 2016.

[196] R. Abt, J. Erdmenger, H. Hinrichsen, C. M. Melby-Thompson, R. Meyer, C. Northe, and I. A. Reyes, "Topological Complexity in AdS_3/CFT_2," *Fortsch. Phys.*, vol. 66, no. 6, p. 1800034, 2018.

[197] S. Chapman, D. Ge, and G. Policastro, "Holographic Complexity for Defects Distinguishes Action from Volume," *JHEP*, vol. 05, p. 049, 2019.

[198] C. A. Agón, M. Headrick, and B. Swingle, "Subsystem Complexity and Holography," *JHEP*, vol. 02, p. 145, 2019.

[199] A. Bhattacharya, K. T. Grosvenor, and S. Roy, "Entanglement Entropy and Subregion Complexity in Thermal Perturbations around Pure-AdS Spacetime," *Phys. Rev. D*, vol. 100, no. 12, p. 126004, 2019.

[200] R. Abt, J. Erdmenger, M. Gerbershagen, C. M. Melby-Thompson, and C. Northe, "Holographic Subregion Complexity from Kinematic Space," *JHEP*, vol. 01, p. 012, 2019.

[201] R. Auzzi, S. Baiguera, A. Legramandi, G. Nardelli, P. Roy, and N. Zenoni, "On subregion action complexity in AdS_3 and in the BTZ black hole," *JHEP*, vol. 01, p. 066, 2020.

[202] E. Caceres, S. Chapman, J. D. Couch, J. P. Hernandez, R. C. Myers, and S.-M. Ruan, "Complexity of Mixed States in QFT and Holography," *JHEP*, vol. 03, p. 012, 2020.

[203] M. Alishahiha, K. Babaei Velni, and M. R. Mohammadi Mozaffar, "Black hole subregion action and complexity," *Phys. Rev. D*, vol. 99, no. 12, p. 126016, 2019.

[204] L. Hackl and R. C. Myers, "Circuit complexity for free fermions," *JHEP*, vol. 07, p. 139, 2018.

[205] R. Khan, C. Krishnan, and S. Sharma, "Circuit Complexity in Fermionic Field Theory," *Phys. Rev. D*, vol. 98, no. 12, p. 126001, 2018.

[206] P. Caputa and J. M. Magan, "Quantum Computation as Gravity," *Phys. Rev. Lett.*, vol. 122, no. 23, p. 231302, 2019.

[207] H. A. Camargo, M. P. Heller, R. Jefferson, and J. Knaute, "Path integral optimization as circuit complexity," *Phys. Rev. Lett.*, vol. 123, no. 1, p. 011601, 2019.

[208] M. Flory and M. P. Heller, "Geometry of Complexity in Conformal Field Theory," *Phys. Rev. Res.*, vol. 2, no. 4, p. 043438, 2020.

[209] M. Flory and M. P. Heller, "Conformal field theory complexity from Euler-Arnold equations," *JHEP*, vol. 12, p. 091, 2020.

[210] A. R. Brown and L. Susskind, "Complexity geometry of a single qubit," *Phys. Rev. D*, vol. 100, no. 4, p. 046020, 2019.

[211] J. Watrous, "Quantum computational complexity," in *Encyclopedia of Complexity and Systems Science* (R. A. Meyers, ed.), (New York, NY), pp. 7174–7201, Springer New York, 2009.

[212] S. Aaronson, "The Complexity of Quantum States and Transformations: From Quantum Money to Black Holes," *arXiv:1607.05256 [quant-ph]*, 7 2016.

[213] M. A. Nielsen, "A geometric approach to quantum circuit lower bounds," *arXiv:quant-ph/0502070*, 02 2005.

[214] M. A. Nielsen, M. R. Dowling, M. Gu, and A. C. Doherty, "Quantum computation as geometry," *Science*, vol. 311, no. 5764, pp. 1133–1135, 2006.

[215] M. R. Dowling and M. A. Nielsen, "The geometry of quantum computation," *arXiv:quant-ph/0701004*, vol. 8, p. 861–899, 11 2008.

[216] R. J. Gordon and S. A. Rice, "Active control of the dynamics of atoms and molecules," *Annual review of physical chemistry*, vol. 48, no. 1, pp. 601–641, 1997.

[217] H. Rabitz, R. de Vivie-Riedle, M. Motzkus, and K. Kompa, "Whither the future of controlling quantum phenomena?," *Science*, vol. 288, no. 5467, pp. 824–828, 2000.

[218] M. Shapiro and P. Brumer, *Quantum Control of Molecular Processes*. John Wiley & Sons, Ltd, 2012.

[219] D. Bao and Z. Chern, S.-S.and Shen, *An Introduction to Riemann-Finsler Geometry*. New York, NY: Springer New York, 2000.

[220] P. H. Ginsparg, "Applied Conformal Field Theory," in *Les Houches Summer School in Theoretical Physics: Fields, Strings, Critical Phenomena Les Houches, France, June 28-August 5, 1988*, pp. 1–168, 9 1988.

[221] L. Hackl and E. Bianchi, "Bosonic and fermionic Gaussian states from Kähler structures," *arXiv:2010.15518 [quant-ph]*, 10 2020.

[222] J. Eisert and M. B. Plenio, "Introduction to the basics of entanglement theory in continuous-variable systems," *International Journal of Quantum Information*, vol. 01, no. 04, pp. 479–506, 2003.

[223] C. Weedbrook, S. Pirandola, R. García-Patrón, N. J. Cerf, T. C. Ralph, J. H. Shapiro, and S. Lloyd, "Gaussian quantum information," *Reviews of Modern Physics*, vol. 84, p. 621–669, May 2012.

[224] L. Hackl and R. H. Jonsson, "Minimal energy cost of entanglement extraction," *Quantum*, vol. 3, p. 165, 2019.

[225] G. Adesso, S. Ragy, and A. R. Lee, "Continuous variable quantum information: Gaussian states and beyond," *Open Systems & Information Dynamics*, vol. 21, no. 01n02, p. 1440001, 2014.

[226] B. Windt, A. Jahn, J. Eisert, and L. Hackl, "Local optimization on pure Gaussian state manifolds," *SciPost Phys.*, vol. 10, p. 066, 2021.

[227] T. Nishioka, S. Ryu, and T. Takayanagi, "Holographic Entanglement Entropy: An Overview," *J. Phys. A*, vol. 42, p. 504008, 2009.

[228] H. Casini and M. Huerta, "Entanglement entropy in free quantum field theory," *J. Phys. A*, vol. 42, p. 504007, 2009.

[229] M. Rangamani and T. Takayanagi, *Holographic Entanglement Entropy*, vol. 931. Springer, 2017.

[230] S. Chapman, J. Eisert, L. Hackl, M. P. Heller, R. Jefferson, H. Marrochio, and R. C. Myers, "Complexity and entanglement for thermofield double states," *SciPost Phys.*, vol. 6, no. 3, p. 034, 2019.

[231] N. Chagnet, S. Chapman, J. de Boer, and C. Zukowski, "Complexity for Conformal Field Theories in General Dimensions," *arXiv:2103.06920 [hep-th]*, 3 2021.

[232] P. Di Francesco, P. Mathieu, and D. Senechal, *Conformal Field Theory*. Graduate Texts in Contemporary Physics, New York: Springer-Verlag, 1997.

[233] P. Pfeuty, "The one-dimensional ising model with a transverse field," *ANNALS of Physics*, vol. 57, no. 1, pp. 79–90, 1970.

[234] S. Katsura, "Statistical mechanics of the anisotropic linear heisenberg model," *Physical Review*, vol. 127, no. 5, p. 1508, 1962.

[235] P. Jordan and E. P. Wigner, "Über das paulische äquivalenzverbot," in *The Collected Works of Eugene Paul Wigner*, pp. 109–129, Springer, 1993.

[236] P. Coleman, *Introduction to Many-Body Physics*. Cambridge University Press, 2015.

[237] D. Radičević, "Entanglement Entropy and Duality," *JHEP*, vol. 11, p. 130, 2016.

[238] J. Lin and D. Radičević, "Comments on defining entanglement entropy," *Nucl. Phys. B*, vol. 958, p. 115118, 2020.

[239] D. Radičević, "Spin Structures and Exact Dualities in Low Dimensions," *arXiv:1809.07757 [hep-th]*, 9 2018.

[240] D. Radičević, "The Lattice-Continuum Correspondence in the Ising Model," *arXiv:1912.13462 [hep-th]*, 12 2019.

[241] L. Hackl, L. Vidmar, M. Rigol, and E. Bianchi, "Average eigenstate entanglement entropy of the XY chain in a transverse field and its universality for translationally invariant quadratic fermionic models," *Phys. Rev. B*, vol. 99, no. 7, p. 075123, 2019.

[242] L. Bertini, A. De Sole, D. Gabrielli, G. Jona-Lasinio, and C. Landim, "Macroscopic fluctuation theory," *Reviews of Modern Physics*, vol. 87, p. 593–636, Jun 2015.

[243] A. K. Chandra, A. Das, and B. K. Chakrabarti, *Quantum Quenching, Annealing and Computation*. Lect. Notes in Physics, Springer-Verlag Berlin Heidelberg 2010, 2010.

[244] A. Polkovnikov, K. Sengupta, A. Silva, and M. Vengalattore, "Nonequilibrium dynamics of closed interacting quantum systems," *Rev. Mod. Phys.*, vol. 83, p. 863, 2011.

[245] J. M. Deutsch, "Quantum statistical mechanics in a closed system," *Phys. Rev. A*, vol. 43, pp. 2046–2049, Feb 1991.

[246] L. D'Alessio, Y. Kafri, A. Polkovnikov, and M. Rigol, "From quantum chaos and eigenstate thermalization to statistical mechanics and thermodynamics," *Adv. Phys.*, vol. 65, no. 3, pp. 239–362, 2016.

[247] C. Gogolin and J. Eisert, "Equilibration, thermalisation, and the emergence of statistical mechanics in closed quantum systems," *Rept. Prog. Phys.*, vol. 79, no. 5, p. 056001, 2016.

[248] J. M. Deutsch, "Eigenstate thermalization hypothesis," *Reports on Progress in Physics*, vol. 81, p. 082001, Jul 2018.

[249] M. Rigol, V. Dunjko, and M. Olshanii, "Thermalization and its mechanism for generic isolated quantum systems," *Nature*, vol. 452, p. 854–858, Apr 2008.

[250] T. Langen, T. Gasenzer, and J. Schmiedmayer, "Prethermalization and universal dynamics in near-integrable quantum systems," *J. Stat. Mech.*, vol. 1606, no. 6, p. 064009, 2016.

[251] T. W. B. Kibble, "Topology of Cosmic Domains and Strings," *J. Phys. A*, vol. 9, pp. 1387–1398, 1976.

[252] W. H. Zurek, "Cosmological Experiments in Superfluid Helium?," *Nature*, vol. 317, pp. 505–508, 1985.

[253] V. Gritsev and A. Polkovnikov, "Universal Dynamics Near Quantum Critical Points," in *Developments in Quantum Phase Transitions* (L. D. Carr, ed.), 10 2009.

[254] S. Mondal, D. Sen, and K. Sengupta, *Non-equilibrium Dynamics of Quantum Systems: Order Parameter Evolution, Defect Generation, and Qubit Transfer*, pp. 21–56. Berlin, Heidelberg: Springer Berlin Heidelberg, 2010.

[255] J. Dziarmaga, "Dynamics of a quantum phase transition and relaxation to a steady state," *Advances in Physics*, vol. 59, no. 6, pp. 1063–1189, 2010.

[256] A. Chandran, A. Erez, S. S. Gubser, and S. L. Sondhi, "Kibble-zurek problem: Universality and the scaling limit," *Physical Review B*, vol. 86, Aug 2012.

[257] K. Levin, A. Fetter, and D. Stamper-Kurn, *Ultracold Bosonic and Fermionic Gases*. Contemporary Conecpts of Condensed Matter Science, Elsevier, 2012.

[258] A. Buchel, L. Lehner, and R. C. Myers, "Thermal quenches in N=2* plasmas," *JHEP*, vol. 08, p. 049, 2012.

[259] A. Buchel, R. C. Myers, and A. van Niekerk, "Universality of Abrupt Holographic Quenches," *Phys. Rev. Lett.*, vol. 111, p. 201602, 2013.

[260] A. Buchel, L. Lehner, R. C. Myers, and A. van Niekerk, "Quantum quenches of holographic plasmas," *JHEP*, vol. 05, p. 067, 2013.

[261] M. Nozaki, T. Numasawa, and T. Takayanagi, "Holographic Local Quenches and Entanglement Density," *JHEP*, vol. 05, p. 080, 2013.

[262] Y. Kusuki and K. Tamaoka, "Entanglement Wedge Cross Section from CFT: Dynamics of Local Operator Quench," *JHEP*, vol. 02, p. 017, 2020.

[263] S. R. Das, D. A. Galante, and R. C. Myers, "Universal scaling in fast quantum quenches in conformal field theories," *Phys. Rev. Lett.*, vol. 112, p. 171601, 2014.

[264] S. R. Das, D. A. Galante, and R. C. Myers, "Universality in fast quantum quenches," *JHEP*, vol. 02, p. 167, 2015.

[265] S. R. Das, "Old and New Scaling Laws in Quantum Quench," *PTEP*, vol. 2016, no. 12, p. 12C107, 2016.

[266] S. R. Das, D. A. Galante, and R. C. Myers, "Quantum Quenches in Free Field Theory: Universal Scaling at Any Rate," *JHEP*, vol. 05, p. 164, 2016.

[267] D. Das, S. R. Das, D. A. Galante, R. C. Myers, and K. Sengupta, "An exactly solvable quench protocol for integrable spin models," *JHEP*, vol. 11, p. 157, 2017.

[268] M. Goykhman, T. Shachar, and M. Smolkin, "On fast quenches and spinning correlators," *JHEP*, vol. 06, p. 168, 2018.

[269] A. Dymarsky and M. Smolkin, "Universality of fast quenches from the conformal perturbation theory," *JHEP*, vol. 01, p. 112, 2018.

[270] P. Caputa, T. Numasawa, T. Shimaji, T. Takayanagi, and Z. Wei, "Double Local Quenches in 2D CFTs and Gravitational Force," *JHEP*, vol. 09, p. 018, 2019.

[271] M. Nishida, M. Nozaki, Y. Sugimoto, and A. Tomiya, "Entanglement Spreading and Oscillation," *J. Stat. Mech.*, vol. 1905, no. 5, p. 053102, 2019.

[272] P. Caputa, S. R. Das, M. Nozaki, and A. Tomiya, "Quantum Quench and Scaling of Entanglement Entropy," *Phys. Lett. B*, vol. 772, pp. 53–57, 2017.

[273] A. Bhattacharyya, T. Takayanagi, and K. Umemoto, "Universal Local Operator Quenches and Entanglement Entropy," *JHEP*, vol. 11, p. 107, 2019.

[274] D. W. F. Alves and G. Camilo, "Evolution of complexity following a quantum quench in free field theory," *JHEP*, vol. 06, p. 029, 2018.

[275] S. Liu, "Complexity and scaling in quantum quench in $1 + 1$ dimensional fermionic field theories," *JHEP*, vol. 07, p. 104, 2019.

[276] J.-L. Lehners and J. Quintin, "Quantum Circuit Complexity of Primordial Perturbations," *Phys. Rev. D*, vol. 103, no. 6, p. 063527, 2021.

[277] L. D. Landau, "9 - a theory of energy transfer. ii," in *Collected Papers of L.D. Landau* (D. TER HAAR, ed.), pp. 63–66, Pergamon, 1965.

[278] D. Aharonov, A. Kitaev, and N. Nisan, "Quantum circuits with mixed states," in *Proceedings of the Thirtieth Annual ACM Symposium on Theory of Computing*, STOC '98, (New York, NY, USA), p. 20–30, Association for Computing Machinery, 1998.

[279] H. Stoltenberg, "Properties of the (Un)Complexity of Subsystems," *Phys. Rev. D*, vol. 98, no. 12, p. 126012, 2018.

[280] N. S. Mazhari, D. Momeni, S. Bahamonde, M. Faizal, and R. Myrzakulov, "Holographic Complexity and Fidelity Susceptibility as Holographic Information Dual to Different Volumes in AdS," *Phys. Lett. B*, vol. 766, pp. 94–101, 2017.

[281] Y. Zhao, "Uncomplexity and Black Hole Geometry," *Phys. Rev. D*, vol. 97, no. 12, p. 126007, 2018.

[282] S.-M. Ruan, "Purification Complexity without Purifications," *JHEP*, vol. 01, p. 092, 2021.

[283] G. Di Giulio and E. Tonni, "Complexity of mixed Gaussian states from Fisher information geometry," *JHEP*, vol. 12, p. 101, 2020.

[284] A. Coser, E. Tonni, and P. Calabrese, "Spin structures and entanglement of two disjoint intervals in conformal field theories," *J. Stat. Mech.*, vol. 1605, no. 5, p. 053109, 2016.

[285] P. Caban, K. Podlaski, J. Rembielinski, K. A. Smolinski, and Z. Walczak, "Entanglement and tensor product decomposition for two fermions," *Journal of Physics A: Mathematical and General*, vol. 38, no. 6, p. L79, 2005.

[286] M.-C. Banuls, J. I. Cirac, and M. M. Wolf, "Entanglement in fermionic systems," *Physical Review A*, vol. 76, no. 2, p. 022311, 2007.

[287] N. Friis, A. R. Lee, and D. E. Bruschi, "Fermionic-mode entanglement in quantum information," *Physical Review A*, vol. 87, no. 2, p. 022338, 2013.

[288] J. Eisert and M. B. Plenio, "A Comparison of entanglement measures," *J. Mod. Opt.*, vol. 46, pp. 145–154, 1999.

[289] M. J. Donald, M. Horodecki, and O. Rudolph, "The uniqueness theorem for entanglement measures," *Journal of Mathematical Physics*, vol. 43, p. 4252–4272, Sep 2002.

[290] L. Amico, R. Fazio, A. Osterloh, and V. Vedral, "Entanglement in many-body systems," *Rev. Mod. Phys.*, vol. 80, pp. 517–576, 2008.

[291] R. Horodecki, P. Horodecki, M. Horodecki, and K. Horodecki, "Quantum entanglement," *Rev. Mod. Phys.*, vol. 81, pp. 865–942, 2009.

[292] H. Casini and M. Huerta, "A Finite entanglement entropy and the c-theorem," *Phys. Lett. B*, vol. 600, pp. 142–150, 2004.

[293] P. Calabrese and J. L. Cardy, "Entanglement entropy and quantum field theory: A Non-technical introduc3tion," *Int. J. Quant. Inf.*, vol. 4, p. 429, 2006.

[294] P. Calabrese and J. Cardy, "Entanglement entropy and conformal field theory," *J. Phys. A*, vol. 42, p. 504005, 2009.

[295] M. Headrick, "Lectures on entanglement entropy in field theory and holography," *arXiv:1907.08126 [hep-th]*, 7 2019.

[296] R. D. Sorkin, "On the entropy of the vacuum outside a horizon," in *Tenth International Conference on General Relativity and Gravitation (held in Padova, 4-9 July, 1983), Contributed Papers*, vol. 2, pp. 734–736, 1983.

[297] I. Peschel, "Calculation of reduced density matrices from correlation functions," *Journal of Physics A: Mathematical and General*, vol. 36, no. 14, p. L205, 2003.

[298] C. Weedbrook, S. Pirandola, R. García-Patrón, N. J. Cerf, T. C. Ralph, J. H. Shapiro, and S. Lloyd, "Gaussian quantum information," *Reviews of Modern Physics*, vol. 84, pp. 621–669, may 2012.

[299] E. Bianchi, L. Hackl, and N. Yokomizo, "Entanglement entropy of squeezed vacua on a lattice," *Phys. Rev. D*, vol. 92, no. 8, p. 085045, 2015.

[300] P. Calabrese, J. Cardy, and E. Tonni, "Entanglement entropy of two disjoint intervals in conformal field theory," *J. Stat. Mech.*, vol. 0911, p. P11001, 2009.

[301] P. Calabrese, J. Cardy, and E. Tonni, "Entanglement entropy of two disjoint intervals in conformal field theory II," *J. Stat. Mech.*, vol. 1101, p. P01021, 2011.

[302] J. Cardy, "Some results on the mutual information of disjoint regions in higher dimensions," *J. Phys.*, vol. A46, p. 285402, 2013.

[303] T. Ugajin, "Mutual information of excited states and relative entropy of two disjoint subsystems in CFT," *JHEP*, vol. 10, p. 184, 2017.

[304] A. Bhattacharyya, T. Takayanagi, and K. Umemoto, "Entanglement of Purification in Free Scalar Field Theories," *JHEP*, vol. 04, p. 132, 2018.

[305] A. Bhattacharyya, A. Jahn, T. Takayanagi, and K. Umemoto, "Entanglement of Purification in Many Body Systems and Symmetry Breaking," *Phys. Rev. Lett.*, vol. 122, no. 20, p. 201601, 2019.

[306] I. Gelfand and M. Neumark, "On the imbedding of normed rings into the ring of operators in hilbert space," *Rec. Math. [Mat. Sbornik] N.S.*, vol. 12 (54), pp. 197–217, 1943.

[307] I. E. Segal, "Irreducible representations of operator algebras," *Bull. Amer. Math. Soc.*, vol. 53, pp. 73–88, 1947.

[308] R. Haag, *Local Quantum Physics*. Texts and Monographs in Physics, Germany: Springer-Verlag, Berlin, Heidelberg, 1996.

[309] H. Araki, *Mathematical Theory of Quantum Fields*. International Series of Monographs on Physics, New York: Oxford University Press, 2007.

[310] V. Moretti, *Spectral Theory and Quantum Mechanics*. UNITEXT, Italy: Springer International Publishing AG, 2017.

[311] L. Vidmar, L. Hackl, E. Bianchi, and M. Rigol, "Entanglement Entropy of Eigenstates of Quadratic Fermionic Hamiltonians," *Phys. Rev. Lett.*, vol. 119, no. 2, p. 020601, 2017.

[312] S. Marcovitch, A. Retzker, M. Plenio, and B. Reznik, "Critical and noncritical long-range entanglement in Klein-Gordon fields," *Phys. Rev. A*, vol. 80, no. 1, p. 012325, 2009.

[313] J. Kudler-Flam, Y. Kusuki, and S. Ryu, "Correlation measures and the entanglement wedge cross-section after quantum quenches in two-dimensional conformal field theories," *JHEP*, vol. 04, p. 074, 2020.

[314] P. Bueno and H. Casini, "Reflected entropy for free scalars," *JHEP*, vol. 11, p. 148, 2020.

[315] P. Bueno and H. Casini, "Reflected entropy, symmetries and free fermions," *JHEP*, vol. 05, p. 103, 2020.

[316] C. Agón and T. Faulkner, "Quantum Corrections to Holographic Mutual Information," *JHEP*, vol. 08, p. 118, 2016.

[317] F. Iglói and I. Peschel, "On reduced density matrices for disjoint subsystems," *EPL (Europhysics Letters)*, vol. 89, p. 40001, Feb 2010.

[318] M. Fagotti and P. Calabrese, "Entanglement entropy of two disjoint blocks in XY chains," *J. Stat. Mech.*, vol. 1004, p. P04016, 2010.

[319] A. Coser, E. Tonni, and P. Calabrese, "Partial transpose of two disjoint blocks in XY spin chains," *J. Stat. Mech.*, vol. 1508, no. 8, p. P08005, 2015.

[320] A. Coser, E. Tonni, and P. Calabrese, "Spin structures and entanglement of two disjoint intervals in conformal field theories," *Journal of Statistical Mechanics: Theory and Experiment*, vol. 2016, no. 5, p. 053109, 2016.

[321] J. Hauschild, E. Leviatan, J. H. Bardarson, E. Altman, M. P. Zaletel, and F. Pollmann, "Finding purifications with minimal entanglement," *Physical Review B*, vol. 98, Dec 2018.

[322] F. Liu, S. Whitsitt, J. B. Curtis, R. Lundgren, P. Titum, Z.-C. Yang, J. R. Garrison, and A. V. Gorshkov, "Circuit complexity across a topological phase transition," *Phys. Rev. Res.*, vol. 2, no. 1, p. 013323, 2020.

[323] Z. Xiong, D.-X. Yao, and Z. Yan, "Nonanalyticity of circuit complexity across topological phase transitions," *Phys. Rev. B*, vol. 101, no. 17, p. 174305, 2020.

[324] A. Jamadagni and H. Weimer, "An Operational Definition of Topological Order," *arXiv:2005.06501 [cond-mat.str-el]*, 5 2020.

[325] J. Cotler, N. Hunter-Jones, J. Liu, and B. Yoshida, "Chaos, Complexity, and Random Matrices," *JHEP*, vol. 11, p. 048, 2017.

[326] J. M. Magán, "Black holes, complexity and quantum chaos," *JHEP*, vol. 09, p. 043, 2018.

[327] P. D. Bergamasco, G. G. Carlo, and A. M. F. Rivas, "OTOC, complexity and entropy in bi-partite systems," *Phys. Rev. Research.*, vol. 1, p. 033044, 2019.

[328] V. Balasubramanian, M. Decross, A. Kar, and O. Parrikar, "Quantum Complexity of Time Evolution with Chaotic Hamiltonians," *JHEP*, vol. 01, p. 134, 2020.

[329] T. Ali, A. Bhattacharyya, S. S. Haque, E. H. Kim, N. Moynihan, and J. Murugan, "Chaos and Complexity in Quantum Mechanics," *Phys. Rev. D*, vol. 101, no. 2, p. 026021, 2020.

[330] B. Bertini, P. Kos, and T. Prosen, "Operator Entanglement in Local Quantum Circuits I: Chaotic Dual-Unitary Circuits," *SciPost Phys.*, vol. 8, no. 4, p. 067, 2020.

[331] A. Bhattacharyya, W. Chemissany, S. S. Haque, J. Murugan, and B. Yan, "The Multi-faceted Inverted Harmonic Oscillator: Chaos and Complexity," *SciPost Phys. Core*, vol. 4, p. 002, 2021.

[332] M. G. Genoni, M. G. A. Paris, and K. Banaszek, "Measure of the non-gaussian character of a quantum state," *Physical Review A*, vol. 76, Oct 2007.

[333] M. G. Genoni and M. G. A. Paris, "Quantifying non-gaussianity for quantum information," *Physical Review A*, vol. 82, Nov 2010.

[334] I. R. Klebanov and A. M. Polyakov, "AdS dual of the critical O(N) vector model," *Phys. Lett. B*, vol. 550, pp. 213–219, 2002.

[335] S. Giombi and X. Yin, "Higher Spin Gauge Theory and Holography: The Three-Point Functions," *JHEP*, vol. 09, p. 115, 2010.

[336] M. R. Gaberdiel and R. Gopakumar, "The String Dual to Free $\mathcal{N} = 4$ Super Yang-Mills," *arXiv:2104.08263 [hep-th]*, 4 2021.

[337] H. Casini, C. D. Fosco, and M. Huerta, "Entanglement and alpha entropies for a massive Dirac field in two dimensions," *J. Stat. Mech.*, vol. 0507, p. P07007, 2005.

[338] B. McCoy, "Ising model: exact results," *Scholarpedia*, vol. 5, no. 7, p. 10313, 2010. revision #137428.